Regulators of Lipoprotein Uptake and Transport by Endothelial and Clear-Cell Renal Cell Carcinoma Cells

---

Dissertation

zur

Erlangung der naturwissenschaftlichen Doktorwürde

(Dr. sc. nat.)

vorgelegt der

Mathematisch-naturwissenschaftlichen Fakultät

der

Universität Zürich

von

Srividya Velagapudi

von

India

Promotionskommission

Prof. Dr. med. Arnold von Eckardstein (Vorsitz, Leitung der Dissertation)

Prof. Dr. Urs Greber

Prof. Dr. Zhihong Yang

Dr. Lucia Rohrer

Zurich, 2018

Table of Contents

Abstract

Atherosclerosis is the leading cause of cardiovascular disease related deaths world-wide. Accumulation of lipoprotein-derived cholesterol in the arterial wall leads to both initiation and progression of the disease. To reach the arterial wall, pro-atherogenic low-density lipoprotein (LDL) and anti-atherogenic high-density lipoprotein (HDL) are known to pass through the intact endothelial cell monolayer. It has been previously shown that endothelial cells transcytose HDL involving ATP binding cassette transporter G1 (ABCG1), scavenger receptor BI (SR-BI), endothelial lipase (EL) as well as ectopic β-ATPase. The transport of LDL through the endothelial cells was evidenced to be mediated by SR-BI and activin like kinase 1 (ALK1). Although a few protein interactors for the lipoprotein endothelial uptake were identified, the role of signaling kinases in regulating the lipoprotein uptake has not been well understood. This thesis focused on identifying the molecular interactors involved in regulating the HDL and LDL uptake and transport through the endothelial cells.

In the present thesis based on a hypothesis or candidate driven approach, the role of sphingosine-1-phosphate and its cognate receptors known to regulate the endothelial barrier function have been investigated with respect to their effect on the transendothelial transport of HDL and LDL. We used pharmacological inhibitors and agonists against S1P1 and S1P3, which are the two S1P receptors mainly expressed in the human aortic endothelial cells (HAECs). The treatment of the endothelial cells with either S1P1 or S1P3 agonist increased the cellular binding, uptake and transport of HDL by up-regulating the translocation of SR-BI from cytosol to the plasma membrane. In contrast, the treatment of cells with either S1P1 or S1P3 agonist decreased the LDL transport through HAECs. However, treatment with either S1P1 or S1P3 inhibitor increased the transport of LDL across the HAECs involving different mechanisms. Inhibition of S1P1 increased the transport of LDL through fluid-phase whereas the S1P3 increased the LDL transport through an unknown candidate. Therefore, through this study we identified that S1P1 and S1P3 regulate the transport of HDL and LDL through HAECs in an antagonistic manner.

Next, using a hypothesis-free approach we focused on investigating the role of signaling kinases in regulating the uptake of HDL and LDL by HAECs. We performed a microscopy based high-content screening in HAECs with 141 kinase inhibitor small compound drugs. The screen identified the limiting role of vascular endothelial growth factor (VEGFR) in regulating the uptake of HDL but not LDL through HAECs. Interestingly, the biochemical validation studies have not only confirmed the involvement of VEGFR2 in the transport of HDL but also identified that vascular endothelial growth factor (VEGF) is required for the localization of SR-BI to the plasma membrane. The presence of VEGF was also found to affect the cellular binding, uptake and transport of HDL through downstream signaling kinases PI3K/Akt and p38 MAPK.

Lastly, we validated the role of VEGF on the uptake of lipoproteins through clear-cell renal cell carcinoma (ccRCC), which is a major form of renal cancer driven by increased VEGF activity. To understand the pathogenetic basis of cholesterol accumulation and hence the histological appearance of ccRCC, we investigated the expression of (apo)lipoproteins and receptors in tumors as well as the uptake of HDL and LDL by cultivated RCC cells. Interestingly, the ccRCC cell line showed enhanced uptake of both HDL and LDL via SR-BI into a non-degrading compartment in response to the increased VEGF activity.

Currently, lipid-lowering strategies are implemented widely for the prevention and treatment of atherosclerotic vascular diseases. The data of our work point to the regulation of lipoprotein uptake and transport through endothelial and tumor cells as additional potential targets for treatment or prevention of atherosclerosis and cancer, respectively.

Zusammenfassung

Atherosklerose, die häufigste Todesursache weltweit, ist eine chronische, entzündliche Gefässkrankheit. Charakteristisch für diese Erkrankung ist die Einlagerung von Cholesterin aus Lipoproteinen in die Arterienwand. Sowohl die pro-atherogenen Low Density Lipoproteine (LDL) als auch die anti-atherogenen High Density Lipoproteine (HDL) passieren die intakte innerste Schicht der Blutgefässe, das Endothelial. Am Transport von HDL durch das Endothel sind mehrere Proteine beteiligt: der ATP binding cassette transporter G1 (ABCG1), der Scavenger Rezeptor BI (SR-BI), die Endotheliale Lipase (EL) sowie die ektopisch exprimierte β-ATPase. Am Transport von LDL ist neben SR-BI auch Activin Like Kinase 1 (ALK1) beteiligt. In dieser Arbeit wurde untersucht wie Aufnahme und Transport von HDL und LDL durch reguliert wird.

In einem ersten Teil wurde die Rolle von Sphingosine-1-Phosphate (S1P) im transendothelialen Transport von HDL und LDL analysiert. S1P ist ein wichtiger Modulator der Barrierenfunktion des Endothels. Die aus menschlicher Aorta isolierten Endothelzellen (HAEC) exprimieren zwei der fünf bekannten S1P Rezeptoren, S1P1 und S1P3. Mit Hilfe von spezifischen pharmakologischen Inhibitoren und Agonisten wurde deren Beitrag zur Regulation von Aufnahme und Transport von HDL und LDL durch Endothelzellen analysiert. Die Zugabe von spezifische Agonisten für S1P1 und S1P3 verstärkte die Bindung, Internalisierung sowie den Transport von HDL. Weitere Untersuchungen zeigten, dass die S1P Agonisten die Expression von SR-BI in der Zellmembran verstärkt und dadurch die Bindung und Aufnahme von HDL verstärkt. Bindung, Aufnahme und Transport von LDL wurde durch die Zugabe von spezifischen S1P1 oder S1P3 Agonisten verringert und durch Inhibitoren von S1P1 oder S1P3 verstärkt. Durch die Blockierung von S1P1 erfolgte die LDL-Aufnahme via *fluid-phase* Endozytose. Die Blockierung von S1P3 resultierte in einem erhöhten LDL Transport, jedoch unabhängig von fluid-phase Endozytose oder SR-BI. Insgesamt zeigten die Untersuchungen, dass S1P1 und S1P3 den transendothelialen Transport von HDL und LDL antagonistisch regulieren.

Im einem zweiten Teil wurde untersucht, welche Kinase-Signalwege an der Aufnahme von HDL und LDL in HAEC beteiligt sind. In einem Hochdurchsatz-Screen mit vollautomatischen Mikroskopen wurde die Aufnahme von Fluoreszenz markierten HDL und LDL in Gegenwart von Kinase Inhibitoren in primären HAEC untersucht. Die Wirkung von 141 klein-molekularen Kinase Inhibitoren wurde bei 7 verschiedenen Konzentrationen analysiert. Diese Untersuchungen identifizierten den Vascular Endothelial Growth Factor Receptor (VEGFR) als wichtigen Regulator für die Aufnahme von HDL aber nicht LDL in HAEC. In den biochemischen Validierungsexperimenten wurde gezeigt, dass von den drei VEGF-Rezeptoren (nur VEGFR2 für die Regulation der HDL Aufnahme wichtig ist. Durch Aktiiverung von VEGFR2 stimuliert VEGF die Translokalisation von SR-BI aus dem Zytosol in die Plasmamembran. Weiter wurde gezeigt, dass VEGF via die Signalkinasen PI3K/Akt und p38 MAPK, HDL Bindung, Internalisation sowie Transport reguliert.

Im letzten Teil wurde die Rolle von VEGF in der Lipoprotein Aufnahme im klarzelligen Nierenkarzinom (clear-cell renal cell carcinoma (ccRCC)) untersucht. Diese häufigste Form des Nierenkrebs ist sehr häufig durch somatische Mutationen im Von-Hippel-Lindau-Gen verursacht, welche zu einer unkontrollierten Produktion von VEGF führen. Das namengebende Charakteristikum des ccRCC ist die Akkumulation von Cholesterin ist dieser Zellen, deren Ursprung aber nicht bekannt ist. Unsere Untersuchungen zeigten eine Akkumulation von ApoA-I und ApoB sowie eine starke Expression von SR-BI in ccRCC. In Zellkultur, internalisieren ccRCC Zellen HDL und LDL via SR-BI. Auch in diesen Zellen stimuliert VEGF die Translokalisation von SR-BI vom Zytoplasma an die Zelloberfläche und so die Aufnahme von Lipoproteinen. Weitere Analysen zeigten, dass die

Tumorzellen die aufgenommenen Lipoproteine weder abbauen noch ausscheiden können. In Kombination erklären diese Befunde die Lipidakkumulation im ccRCC.

Lipidsenkende Strategien werden bereits im grossen Umfang für die Prävention und Behandlung von atherosklerotischen Gefässkrankheiten eingesetzt. Die Ergebnisse dieser Arbeit weisen darauf hin, dass auch die Aufnahme und der Transport von Lipoproteinen durch das Endothel und Karzinomzellen interessante therapeutische Ziele sind.

Abbreviations

ABC transporter: ATP binding cassette transporter

AJ: Adherens junction

Akt: Protein Kinase B

ALK1: Activin like kinase 1

apoA-I: Apolipoprotein A-I

apoB: Apolipoprotein B

ccRCC: Clear-cell renal cell carcinoma

CE: Cholesterol ester

CETP: Cholesteryl ester transfer protein

CVD: Cardiovascular disease

EC: Endothelial cells

EL: Endothelial lipase

eNOS: Endothelial nitric oxide synthase

ERK: Extracellular signal-related kinases

FITC: Fluorescein isothiocyanate

GLUT: Glucose transporter

GPCR: G protein-coupled receptor

HAEC: Human aortic endothelial cells

HDL: High-density lipoprotein

HL: Hepatic lipase

HIF-α: Hypoxia-inducible factor

IDL: Intermediate-density lipoprotein

IDOL: Inducible degrader of the LDL receptor

kDa: Kilo daltons

LCAT: Lecithin-cholesterol acyl transferase

LDL: Low-density lipoprotein

LDLR: Low-density lipoprotein receptor

LRP: LDL receptor related protein

MAPK: Mitogen-activated protein kinase

MEK: Mitogen-activated protein kinase kinase

NO: Nitric oxide

NPCL1: Niemann-Pick C1-like 1

NRP1: Neuropilin 1

NS control: Non-silencing control

PCSK9: Proprotein convertase subtilisin/kexin type 9

PDZK1: PDZ domain containing 1

PI3K: Phosphatidylinositol-4,5-bisphosphate 3-kinase

PLTP: Phospholipid transfer protein

p38 MAPK: p38 mitogen-activated protein kinase

S1P: Sphingosine-1-phosphate

S1PR: Sphingosine-1-phosphate receptor

SREBP: Sterol regulatory element binding protein

SR-BI: Scavenger receptor class B type 1

VEGF: Vascular endothelial growth factor

VEGFR: Vascular endothelial growth factor receptor

VHL: von-Hippel Lindau

VLDL: Very low-density lipoprotein

1. Introduction

1.1 Cholesterol Metabolism

Biological significance of cholesterol

The name cholesterol originates from Greek words *chole* (bile) and *stereos* (solid) and the suffix –*ol* for alcohol (Figure 1). Cholesterol was discovered by François Poulletier de la Salle in bile and gallstones in the year 1769 [1]. Since then, it has been connected to numerous human diseases such as atherosclerosis, Alzheimer's disease and diverse malformative syndromes. At a cellular level, cholesterol is found in membranes, where it increases both bilayer stiffness and impermeability for water and ions. Furthermore, cholesterol is integrated into specialized lipid-protein membrane microdomains with critical topographical and signaling functions. At an organismal level, cholesterol is the precursor for all steroid hormones, including gluco- and mineralo-corticoids, sex hormones and vitamin D, all of which regulate carbohydrate, sodium, reproductive and bone homeostasis, respectively. This sterol is also the precursor for bile acids, which are important for intestinal absorption of dietary lipids as well as energy and glucose metabolic regulation [2]. The undisputed biomedical importance of cholesterol continuous to fuel the molecular and cell biological research into this molecule.

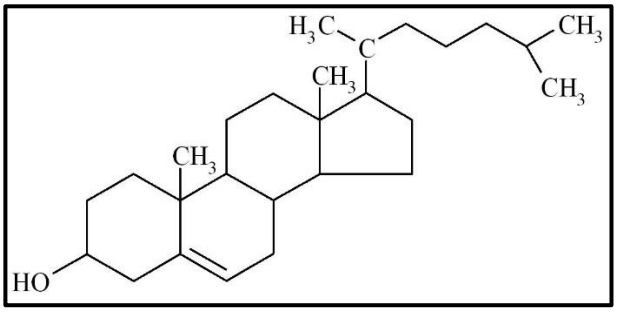

Figure 1: Two-dimensional chemical structure of cholesterol. (Source: PubChem)

Sources of cellular cholesterol

In humans, the body cholesterol is derived from two sources – diet and *de novo* synthesis. The contribution of *de novo* cholesterol synthesis versus dietary intake for total body cholesterol has been estimated as a ratio of ~70:30. In principle, this probably varies considerably between individuals, depending both on the genetic constitution (effectiveness of cholesterol production versus absorption) and dietary cholesterol supply [3].

De novo synthesis of cholesterol

The elucidation of cholesterol's structure and synthesis was determined through the works of Nobel laureates H.O Wieland (1927), L. Ruzicka (1939), R. Robinson (1947), K. Bloch and F. Lynen (1964) and J. W. Cornforth (1975) [4, 5].

Cholesterol is synthesized in the endoplasmic reticulum (ER) by the action of more than 30 enzymes. The first part of this pathway involves four fundamental steps (Figure 2): 1) condensation of three acetyl-CoA units to form 3-hydroxy-3-methylglutaryl-CoA (HMG-CoA); 2) HMG-CoA reduction mediated by NADPH to generate mevalonate (a 30-carbon linear molecule); 3) conversion of mevalonate into activated isoprenoids 3-isopentenyl pyrophosphate and dimethylallyl pyrophosphate; and 4) polymerization of six isoprenoids units into squalene. Next, linear squalene undergoes series of oxygenation and cyclization steps to form lanosterol, and finally, lanosterol is converted to cholesterol by sequential oxidative demethylations and double bond isomerizations and reductions. The rate-limiting reaction in cholesterol biosynthesis is the conversion of HMG-CoA into mevalonate catalyzed by HMG-CoA reductase (HMG-CoA-R). This enzyme is tightly regulated at both transcriptional and

post-translational levels and is the pharmacological target of statins, currently, the most widely used cholesterol lowering agents[5].

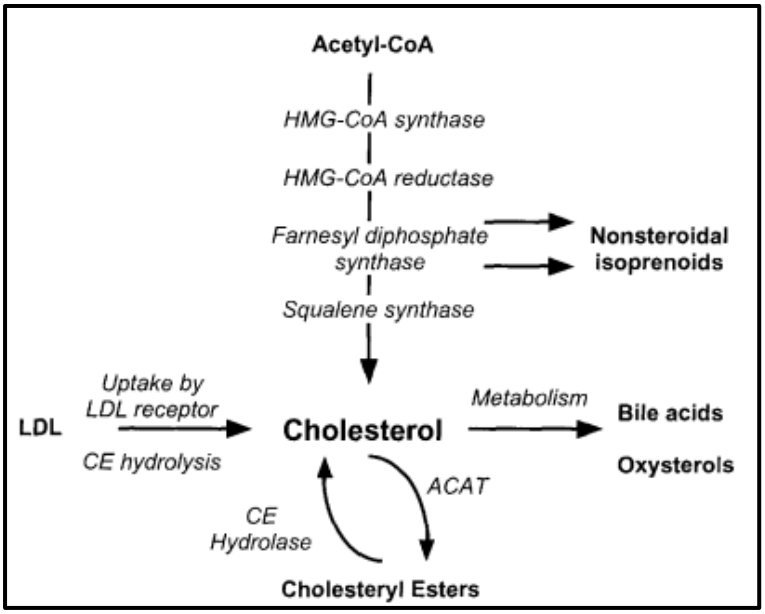

Figure 2: Overview of the metabolic and transport pathways that control cholesterol levels in mammalian cells. Cholesterol is synthesized from acetyl-CoA and four key enzymes that regulate cholesterol synthesis are indicated. Cells also obtain cholesterol by uptake and hydrolysis of LDL (low-density lipoprotein) cholesteryl esters (CE). End products derived from cholesterol or intermediates in this pathway include bile acids, oxysterols, cholesteryl esters and non-steroidal isoprenoids. ACAT: acyl-CoA:cholesterol acyltransferase.

Regulation of cholesterol homeostasis

Cholesterol may be deleterious or even lethal for cells and many protective mechanisms have evolved to prevent this cellular toxicity. The underlying causes of cholesterol's cytotoxicity are not completely clear, but may include: 1) abnormalities in the conformational plasticity of membrane proteins, 2) increased production of oxysterols by oxidative stress, 3) intracellular cholesterol crystallization leading to mechanical membrane disruption, and 4) increased apoptosis [6]. Cellular cholesterol is kept within homeostatic levels by the concerted action of both transcriptional and post-transcriptional mechanisms. At the transcriptional level (Figure 3), sterol regulatory element binding protein (SREBP), a membrane bound member of the basic helix-loop-helix family of transcription factors, controls the gene expression of multiple genes of the mevalonate pathway [7]. SREBP-cleavage activating protein (SCAP), a multi-spanning ER membrane protein, directly binds cholesterol and interacts with SREBP and other ER proteins to regulate SREBP activation. Specifically, when ER cholesterol levels are high, SCAP physically interacts with insulin-induced genes 1 and 2 (INSIG1 and INSIG2) and the SCAP/SREBP complex is retained in the ER preventing its translocation towards the golgi [8, 9]. In contrast, when cholesterol levels are low, the SCAP-INSIGs interaction is abolished, and the SCAP/SREBP complex is transported into the golgi, where SREBP is released from the membrane by the sequential action of site-1 and site-2 proteases (S1P and S2P, respectively). This mature membrane-free SREBP is translocated into the nucleus where it binds to sterol responsive element (SRE) sequences of target genes, activating their transcription [10].

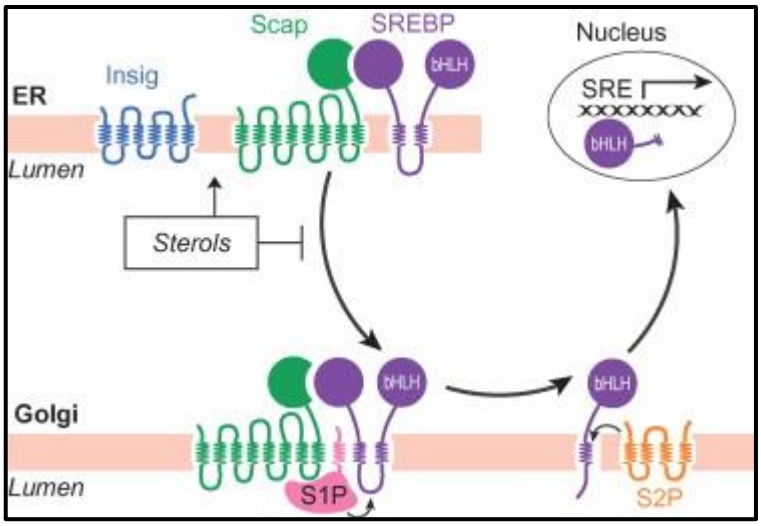

Figure 3: The SREBP pathway. When mammalian cells are deprived of cholesterol, SCAP escorts SREBPs from ER to Golgi. Two Golgi proteases (S1P and S2P) then sequentially cleave SREBP, releasing the active NH2-terminal transcription factor domain, which travels to the nucleus and activates genes involved in the cholesterol synthesis and uptake. High sterol levels trigger the binding of SCAP to an ER retention protein, INSIG. Transport of SREBP to Golgi and subsequent transcriptional activation is then blocked [11].

Further, the acetylation (increased by p300 [12], and reduced by sirtuin 1 (SIRT1)) prevents the rapid degradation of SREBPs[13].Deacetylation of SREBPs facilitates the action of ubiquitin ligases, thus resulting in proteosomal degradation [14, 15]. Small ubiquitin-like modifier 1 (SUMO-1) mediates degradation of SREBPs independently of the 26S proteasome [16]. The transcription of SREBPs also stimulates the expression of intronic micro-RNAs -33a and -33b, which lie within the genomic sequence of *Srebf-2* and *Srebf-1*. Array of the targets of miRNA 33a suppresses the translation of ATP binding cassette transporter A1 (ABCA1) and thereby limiting the efflux of cholesterol from the cell. This response ensures that newly synthesized cholesterol remains within the cell, rather than effluxed to extracellular acceptors. Indeed, a number of microRNA sequences are involved in the regulation of cholesterol homoeostasis, either directly, by repressing the expression of genes and proteins involved in cholesterol synthesis and transport, or indirectly, by modulating the lipid metabolism and energy status of the cell [17].

HMG-CoA reductase is additionally regulated at the post-translational level. When cholesterol concentration in the endoplasmic reticulum is high, HMG-CoA reductase directly binds to cholesterol and to a membrane ubiquitin ligase, gp78. This interaction results in HMG-CoA reductase polyubiquitination and subsequent 26S proteasome-mediated degradation. Conversely, when the cholesterol levels are low in the ER, turnover of HMG-CoA reductase protein is reduced because of decreased polyubiquitination and proteosomal degradation [9, 18]. The activity of HMG-CoA reductase is also controlled by 5′-AMP-activated protein kinase (AMPK), that senses the energy status of the cell, and suppresses sterol synthesis following increases in the AMP/ATP ratio [19].

Cholesterol transfer between tissues

Like other lipids, cholesterol is hydrophobic and mostly insoluble in blood. Therefore, it requires transport within lipoproteins, which possess amphipathic surface proteins (apolipoproteins) that together with phosphatidyl cholines mediate the solubilization of lipids in the aqueous phase and are cofactors and ligands for lipid-processing enzymes. Lipoproteins are classified (Table I) by size and density. The differences in their densities arise from two circumstances [20].

1. Lipids are lighter than protein. Within the particles, proteins are found only at the surface, whereas the interior contains only lipids; therefore, the fractional content of protein is lower with larger particles than with smaller ones. Chylomicrons are the largest and least dense lipoprotein species.
2. Triacylglycerol is lighter, but cholesterol is heavier than water. Accordingly, a high content of cholesterol in the lipid fraction will also increase the overall density.

Lipoprotein	Density (kg/L)	Diameter (nm)	% proteins	Predominant apolipoproteins
Chylomicron	< 0.95	100-1000	< 2	A-I & II, B_{48}, C-I, II, III, E, H
VLDL	0.95-1-006	30-80	10	B_{100}, C-I, C-II, C-III, E
IDL	1.006-1.019	25-50	18	B_{100}, C-II, C-III, E
LDL	1.019-1.063	18-28	25	B_{100}
HDL	> 1.063	5-15	33	A-I, A-II, A-IV, C-I, C-II, C-III, C-IV, D, E, F, H, J, L-I, M

Table I: Classification of lipoproteins based on their density, diameter, protein percentage and apolipoprotein composition.

1.2 Lipoprotein metabolism

Lipoprotein metabolism is differentiated into the exogenous or endogenous pathways, depending whether the particles transport lipids of dietary or hepatic origin.

Exogenous (dietary) lipid metabolism

Triglycerides are the major lipids found in the human diet, contributing to 90-95% of energy provided by dietary fat, and the remaining are phospholipids, free fatty acids, cholesterol and fat-soluble vitamins [21]. Triglycerides from the diet are digested in the gastrointestinal tract to form monoglycerides and free fatty acids through various processes, including bile emulsification, gastric lipase, and pancreatic lipase [22]. Similarly, cholesterol esters from the diet undergo a process of de-esterification to form cholesterol and free fatty acids. Monoglycerides, free fatty acids and cholesterol are soluble in the bile acid micelles and can be absorbed from the chymus into the enterocytes by specific transporters (NPCL1, CD36, FABP). Inside the enterocytes, lipids are re-esterified into triglycerides, cholesterol esters and phospholipids. The microsome triglyceride transfer protein helps to assemble the lipids with Apolipoprotein B-48 to form chylomicrons. Chylomicrons are associated with other apolipoproteins ApoA-II and Apo-C's and then secreted into the lymph of the thoracic duct. Thereby they reach the vena cava superior and hence the blood circulation [23].

In the capillaries of adipose and muscle tissue, apolipoprotein C-II (apo C-II) on the chylomicron activates lipoprotein lipase (LPL) to convert 90% of chylomicron triglycerides to fatty acids and glycerol, which are taken up by adipocytes and muscle cells for energy storage [24]. Glycosylphosphatidylinositol-anchored high-density lipoprotein-binding protein 1 (GPIHBP1) is an endothelial cell protein that is needed for basolateral to apical transport of LPL[25]. Depleted of triglycerides and enriched in cholesterol, chylomicron remnants are transported to the liver to be cleared from the body. Apolipoprotein E (apo E) serves as a ligand of multiple receptors LDLR [26], VLDLR [27], syndecan-1 (HSPG) [28] , LRP1, LRP5 [29] and SR-BI [30].

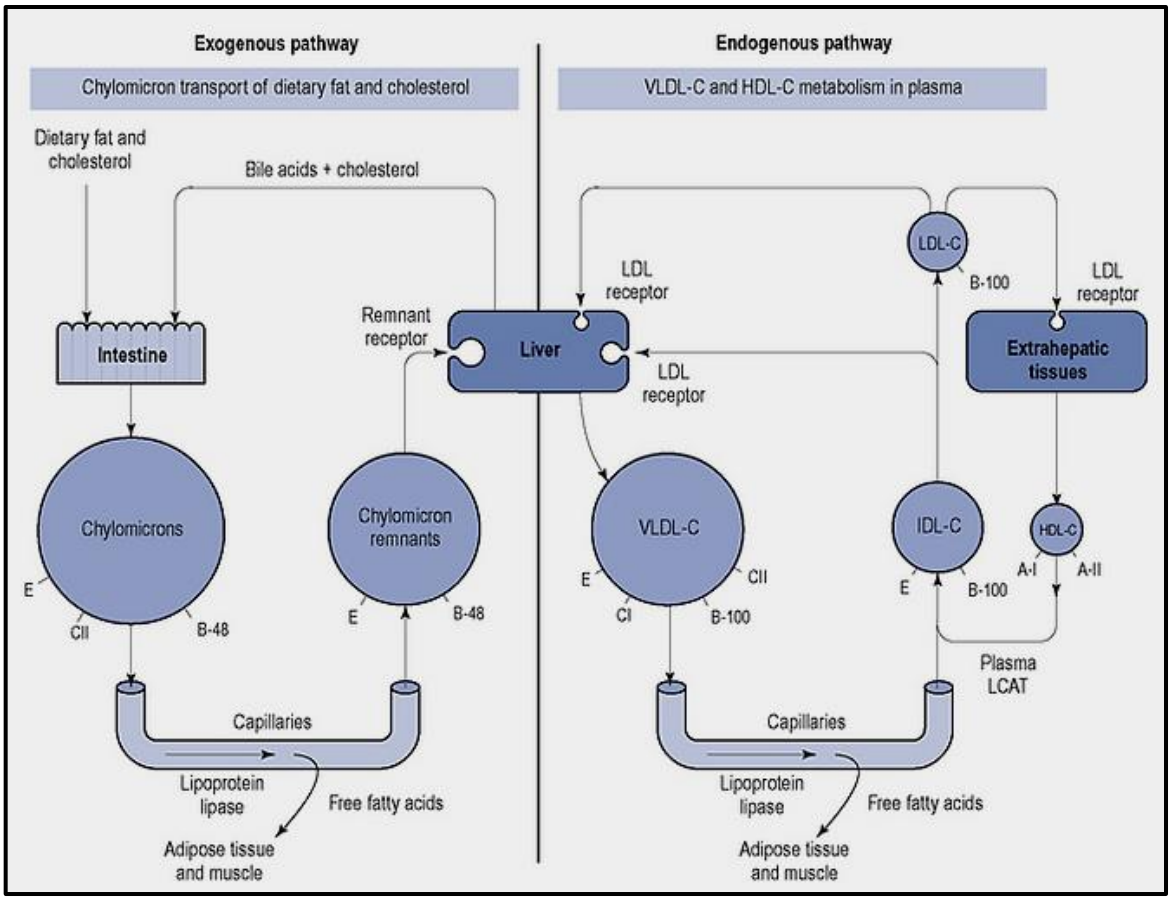

Figure 4: Schematic representation of exogenous and endogenous lipoprotein metabolism pathways. Cholesterol in the circulation will originate either from the exogenous or endogenous pathway. Dietary cholesterol and fat are transported in the exogenous pathway. All cholesterol will be packaged into lipoprotein particles as part of their metabolism pathway and covered with a specific complement of apolipoproteins. As part of the endogenous pathway, the liver is responsible for the packaging of VLDL particles which are hydrolyzed by IDL, returned to the liver so that they may be repackaged as LDL then taken from the circulation by peripheral tissues. (Soure: Walker.R and Williams H, Dyslipidaemia, Chapter 24, Clinical gate)

Endogenous lipid metabolism

Lipoproteins synthesized by the liver transport endogenously synthesized triglycerides and cholesterol. VLDL circulate through the blood continuously until the triglycerides are cleared by peripheral tissues or the lipoproteins themselves are cleared by the liver. Factors that stimulate hepatic lipoprotein synthesis generally lead to elevated plasma cholesterol and triglycerides levels.

Very-low-density lipoproteins (VLDL) contain apoprotein B-100 (apo B), are synthesized in the liver, and transport triglycerides to peripheral tissues. Microsomal triglyceride transfer protein (MTP) is an intracellular lipid-transfer protein found in the endoplasmic reticulum. It is essential for the transfer of the lipid molecules (principally triglycerides) onto apolipoprotein (apo) B 100 [31]. VLDL is the way the liver exports excess triglycerides that are endogenously synthesized or taken up from plasma as albumin bound free fatty acids or chylomicron remnants; VLDL synthesis increases with increase in intrahepatic free fatty acids, for example due to high-fat diets or excess adipose tissue release of free fatty acids directly into the circulation (eg, in obesity, uncontrolled diabetes mellitus). Apo C-II on the VLDL surface activates LPL in the capillaries of adipose tissue or muscle tissue to break down triglycerides into free fatty acids and glycerol, which are taken up by cells [32].

Intermediate-density lipoproteins (IDL) are the product of LPL-mediated processing of VLDL. IDL are rich in cholesterol and either cleared by the liver or metabolized by hepatic lipase into LDL.

Low-density lipoproteins (LDL), are the final products of VLDL and IDL metabolism and the most cholesterol-rich of all lipoproteins. LDL particles contain a core of cholesterol esters, lesser amounts of triglyceride, and apolipoprotein B-100, which is the ligand for binding to the LDL receptor [33]. About 90% of all LDL are cleared by the liver in a process mediated by apo B and hepatic LDL receptors. The rest are taken up by either hepatic LDL or nonhepatic non-LDL (scavenger) receptors. After binding to the LDL receptor on the surface of the hepatocyte, LDL particles are internalized through clathrin-coated pits, in a process dependent on the presence of an NPXY sequence in the cytoplasmic tail of LDLR [34]. Upon fusion of these vesicles with early endosomes, the decrease in pH induces the dissociation of LDL from their receptor [35, 36]. LDLR is either recycled back to the cell surface. However, when proprotein convertase subtilisin/kexin type 9 (PCSK9) binds to the LDLR, PCSK9 prevents the conformational change of the receptor-ligand complex. This inhibition redirects the LDLR to the lysosome instead of recyling [37]. The LDL particle then is targeted to lysosomes where cholesterol is made available again by hydrolysis of the cholesteryl esters. LDLR expression is transcriptionally regulated in response to intracellular cholesterol concentrations. When cholesterol levels are low, membrane-bound precursors of sterol regulatory element-binding proteins (SREBPs) are transported from the ER to the Golgi [38, 39]. Following a two-step proteolytic cleavage event, SREBPs are released from the Golgi membrane and translocated to the nucleus where they activate the transcription of genes, including the LDLR and HMG-CoA reductase, the ratelimiting enzyme in cholesterol biosynthesis. When cholesterol levels are elevated, ER-to-Golgi transport of SREBP is prevented. The cholesterol-sensing chaperone SCAP (for SREBP cleavage-activating protein) that escorts SREBPs towards the Golgi plays a key role in this regulation mechanism [40]. Additionally, elevated levels of cellular cholesterol activates the sterol-sensing nuclear, liver X receptors, and transcriptional induction of one of their target gene, inducible degrader of the LDL receptor (*IDOL*) [41, 42]. IDOL is an E3-ubiquitin ligase that binds to the LDLR, promotes its poly-K63-linked ubiquitylation, and ultimately leads to lysosomal degradation of the receptor [43, 44]. Thus, the LXR-IDOL-LDLR axis offers cells an efficient mechanism, which circumvents the SREBP transcriptional pathway and the long half-life of the LDLR, to limit cholesterol uptake [45].

The size of LDL particles varies from large and buoyant to small and dense. Small, dense LDL is especially rich in cholesterol esters, is associated with metabolic disturbances such as hypertriglyceridemia and insulin resistance, and is especially atherogenic. The increased atherogenicity of small, dense LDL derives from less efficient hepatic LDL receptor binding, leading to prolonged circulation and exposure to endothelium and increased oxidation [46].Nonhepatic scavenger receptors, most notably on macrophages, take up excess modified LDL not processed by hepatic receptors. Macrophages then take up modified LDL and form foam cells within atherosclerotic plaques [47].

Lipoprotein (a) [Lp(a)] Lp(a) is a specialized form of LDL that is assembled extracellularly from apolipoprotein (a) and LDL [48]. Apo(a) links to apolipoprotein B-100 on the surface of LDL by disulfide bridges. The formation of apo(a):apo B complexes requires an LDL particle of a certain morphology and composition. The apo(a) chain contains domains known as kringles IV and V that are homologous with the fibrin-binding domains of plasminogen. Through this structural similarity to plasminogen, Lp(a) interferes with fibrinolysis by competing with plasminogen binding to plasminogen receptors, fibrinogen, and fibrin. The net effect is impaired plasminogen activation and plasmin generation at the thrombus surface, leading to decreased thrombolysis. Lp(a) can also bind to macrophages via a high-affinity receptor, possibly promoting foam cell formation and localization of Lp(a) at atherosclerotic plaques [49, 50]. Studies have shown that scavenger receptor BI binds and promotes cellular uptake of Lp(a), in particular selective lipid uptake of cholesteryl esters from Lp(a) [51].

High-density lipoproteins (HDL) are initially cholesterol-free lipoproteins that are synthesized by both enterocytes and hepatocytes. The role of HDL is to obtain cholesterol from peripheral tissues and other lipoproteins and transport it to where it is needed most—other cells, other lipoproteins (using cholesteryl ester transfer protein [CETP]), and the liver (for clearance) in a process called reverse cholesterol transport (Figure 5). Efflux of free cholesterol from cells is mediated by ATP-binding cassette transporter A1 (ABCA1) and converts lipid-free apoprotein A-I (apo A-I) into nascent discoidal HDL [52]. Nascent HDL acquires additional cholesterol and phospholipids via ABCA1 and ABCG1 mediated efflux [53]. Free cholesterol in nascent HDL is then esterified by the enzyme lecithin-cholesterol acyl transferase (LCAT), producing mature HDL[54]. The phospholipid transfer protein (PLTP) mediates the phospholipid transfer from triglyceride-rich lipoproteins (chylomicrons and VLDL) to HDL [55]. Hepatic lipase (HL) and endothelial lipase (EL) remodel HDL by hydrolysing triglycerides and phospholipids [56]. HDL cholesterol is delivered back to the liver via interaction with scavenger receptor BI (SR-BI) which results in selective uptake of lipids [57] or via the CETP which mediates the exchange of cholesteryl esters from the core of HDL against triglycerides from apoB-containing lipoproteins (LDL, IDL, VLDL, and chylomicrons) [54]. Cholesteryl esters from LDL are delivered to the liver via the LDL receptor. The cholesteryl esters are hydrolyzed in the hepatocytes to cholesterol, which are either recycled back entering the ABCA1 pathway, secreted in the bile as bile acids, or reassembled into lipoproteins that are secreted into the circulation [58].

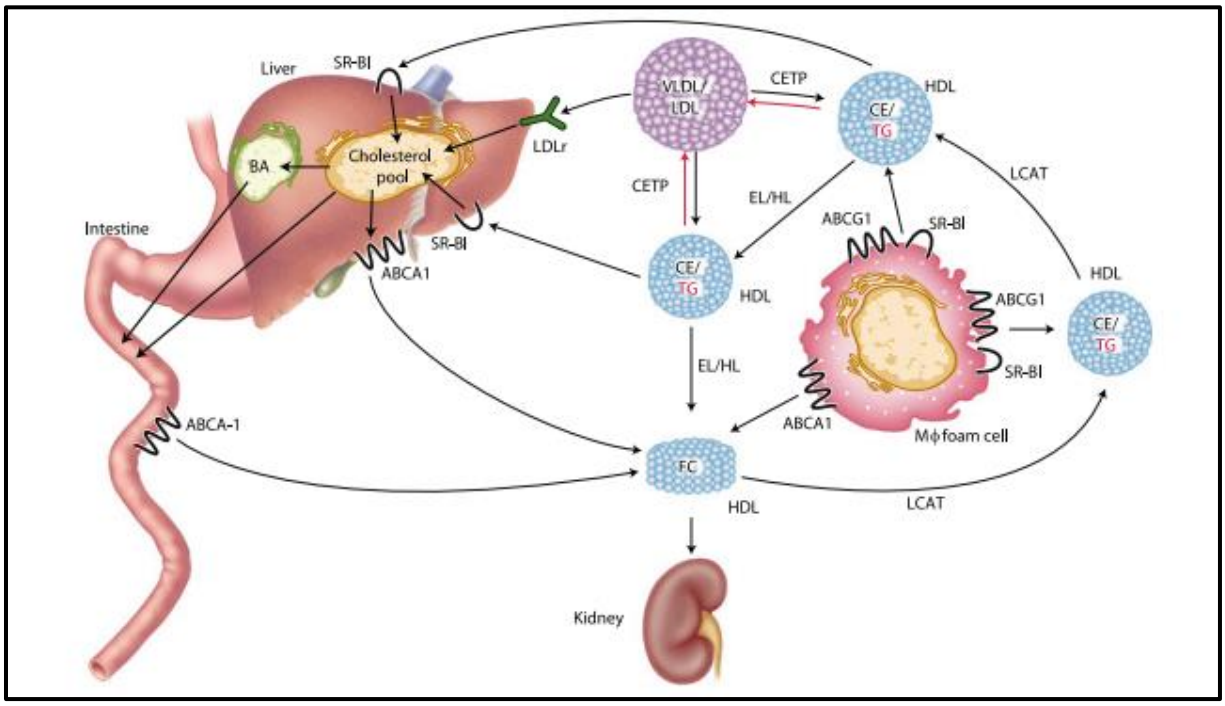

Figure 5: Schematic overview of HDL metabolism. Small discoidal high-density lipoprotein (HDL) particles are generated by the liver and intestine. Free cholesterol (FC) from macrophage foam cells is effluxed to these particles by ATP-binding cassette transporter A1 (ABCA1). Through the action of lecithin:cholesterol acyltransferase (LCAT), these particles mature and become spherical; ABCG1 and scavenger receptor class B type I (SR-BI) add more cholesterol onto these larger HDL. EL and HL hydrolyze HDL phospholipids and phospholipids/triglycerides (TG), respectively, thereby destabilizing the particle, resulting in shedding of poorly lipidated apolipoprotein (apo) A-I that is subject to clearance by the kidneys. Cholesteryl ester from these HDL particles becomes more susceptible towards SR-BI—mediated selective uptake. In turn, selective uptake is also required for HDL remodeling by these lipases to continue. Via SR-BI, HDL cholesterol enters the hepatic cholesterol pool and can either be directly secreted as free cholesterol into bile and feces or after metabolic conversion into bile acids. Cholesteryl ester transfer protein (CETP), mediates the hetero-exchange of cholesteryl ester (CE) originating from HDL with triglycerides originating from apoB-containing lipoproteins. On the other hand, cholesterol transferred to apoB-containing lipoproteins can be taken up into the liver via low-density lipoprotein receptors (LDLR) and then enters the hepatic cholesterol pool [59].

1.3 Arterial wall and atherogenesis

The normal artery contains three layers (Figure 6) namely, intima, media and outer adventitia. The inner layer closest to the arterial lumen, the tunica intima, is lined by a monolayer of endothelial cells that is in contact with blood and overlies a basement membrane. The endothelium functions as an active metabolic barrier between blood and the arterial wall. In contrast to many animal species used for atherosclerosis experiments, the human intima contains resident smooth muscle cells (SMCs). The intima also consists of connective tissue which is composed of a matrix of collagen, proteoglycans and elastin. The middle layer, or tunica media, contains SMCs embedded in a complex extracellular matrix with contractile and synthetic function. As for the contractile function, SMCs enable vasoconstriction and vasodilatation. The arteries often studied in experimental atherosclerosis are elastic arteries, which have clearly demarcated laminae in the tunica media, where layers of elastin lie between strata of SMCs. The adventitia, the outer layer of arteries, contains fibroblasts, mast cells, nerve endings and vasa vasorum[60]. There is a constant dynamic interchange between the arterial wall and its cellular components and the surrounding extracellular matrix. By understanding the physiology of this dynamic interchange and the function of each cellular component, the dysfunction of these cellular components leading to atherogenesis can be better understood.

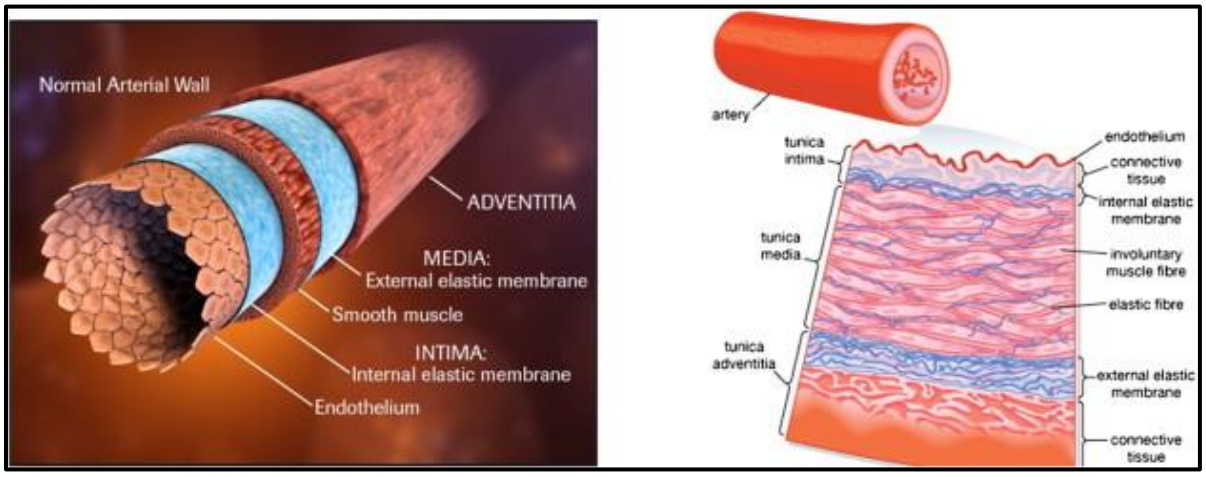

Figure 6: Schematic representation of distinct layers of arterial wall. Left image depicts the top-view of layers of the artery and the right image depicts the cross-sectional view of layers in artery [61].

Lipoproteins and atherosclerosis

Atherosclerotic disease is the major cause of cardiovascular death worldwide, and although it is a complex process in which various environmental and genetic factors are involved, the deposition of lipoprotein-derived cholesterol in the arterial wall is the priming condition necessary for more advanced lesions [62]. Atherogenesis can be divided into five key steps (Figure 7), which are 1) endothelial dysfunction, 2) formation of lipid layer or fatty streak within the intima, 3) migration of leukocytes and smooth muscle cells into the vessel wall, 4) foam cell formation and 5) degradation of extracellular matrix.

The earliest readily visible atherosclerotic lesion is the *fatty streak* that forms within the subendothelial space [63].Arterial endothelial cells, which normally resist to the attachment of the circulating blood cells, express adhesion molecules that capture leukocytes on their surfaces when subjected to irritative stimuli such as dyslipidaemia, hypertension or pro-inflammatory mediators [64, 65]. Parallel changes in endothelial permeability and the composition of the extracellular matrix beneath the endothelium promote the entry and retention of cholesterol-containing LDL particles in the artery wall [66]. This critical initiating event

sparks an inflammatory response leading to monocyte recruitment into the intima, where they differentiate into macrophages and internalize native and modified lipoproteins, resulting in foam cell formation [67, 68].

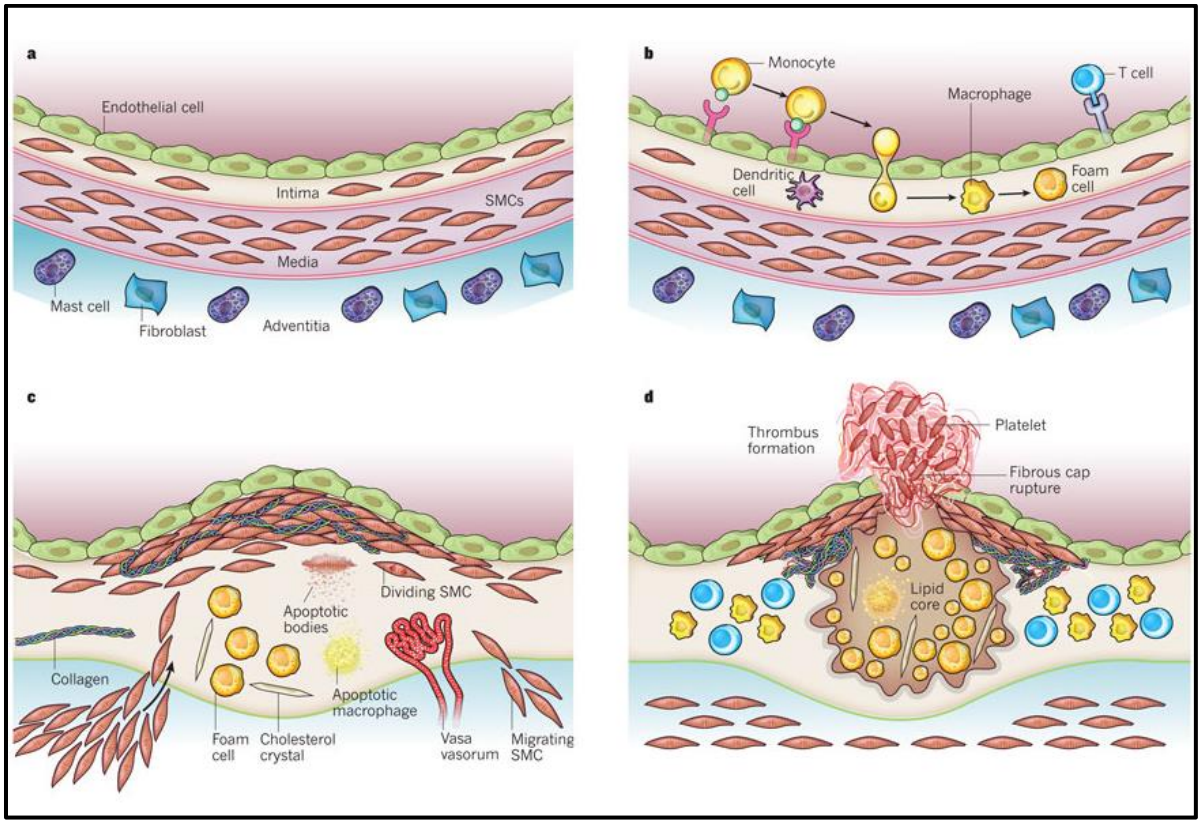

Figure 7: Stages in the development of atherosclerotic lesions. The normal muscular artery and the cell changes that occur during disease progression to thrombosis are shown. **a**, The normal artery contains three layers. The inner layer, the tunica intima, is lined by a monolayer of endothelial cells that is in contact with blood overlying a basement membrane. In contrast to many animal species used for atherosclerosis experiments, the human intima contains resident smooth muscle cells (SMCs). The middle layer, or tunica media, contains SMCs embedded in a complex extracellular matrix. Arteries affected by obstructive atherosclerosis generally have the structure of muscular arteries. The arteries often studied in experimental atherosclerosis are elastic arteries, which have clearly demarcated laminae in the tunica media, where layers of elastin lie between strata of SMCs. The adventitia, the outer layer of arteries, contains mast cells, nerve endings and microvessels. **b**, The initial steps of atherosclerosis include adhesion of blood leukocytes to the activated endothelial monolayer, directed migration of the bound leukocytes into the intima, maturation of monocytes (the most numerous of the leukocytes recruited) into macrophages, and their uptake of lipid, yielding foam cells. **c**, Lesion progression involves the migration of SMCs from the media to the intima, the proliferation of resident intimal SMCs and media-derived SMCs, and the heightened synthesis of extracellular matrix macromolecules such as collagen, elastin and proteoglycans. Plaque macrophages and SMCs can die in advancing lesions, some by apoptosis. Extracellular lipid derived from dead and dying cells can accumulate in the central region of a plaque, often denoted the lipid or necrotic core. Advancing plaques also contain cholesterol crystals and microvessels. **d**, Thrombosis, the ultimate complication of atherosclerosis, often complicates a physical disruption of the atherosclerotic plaque. Shown is a fracture of the plaque's fibrous cap, which has enabled blood coagulation components to come into contact with tissue factors in the plaque's interior, triggering the thrombus that extends into the vessel lumen, where it can impede blood flow [69].

Internalization of the apoB containing lipoproteins by macrophages promotes foam cell formation, which is the hallmark of the fatty streak phase of atherosclerosis [70, 71]. Macrophage inflammation results in enhanced oxidative stress and chemokine secretion, causing more LDL oxidation, endothelial cell activation, monocyte recruitment, and foam cell formation [68, 72]. More recently, uptake of cholesterol crystals has been linked to inflammation via the activation of the NLRP3 inflammasome, which might favour the amplification of a local and systemic immune-inflammatory response[73] characterized by the

production of several proinflammatory cytokines; among them, Interleukin-6 (IL-6) and interleukin-1 (IL-1) are well-established markers of inflammation and their possible causal role in atherosclerosis has been widely investigated [74, 75]. Macrophage inflammatory chemoattractants stimulate proliferation and migration of smooth muscle cells infiltration into intima. Smooth muscle cells produce the extracellular matrix providing a stable fibrous barrier between plaque and the endothelium [76, 77]. Eventually the apoptosis and defective efferocytosis of apoptotic cells results in the formation of necrotic core and increased smooth cell death, decreased extracellular matrix production, and collagen degradation by macrophage proteases. Rupture of the thinning fibrous cap promotes thrombus formation resulting in myocardial infarction, sudden cardiac death and stroke [78].

Lipid-lowering strategy as a treatment for atherosclerosis

The determination of the LDL pathway and the subsequent development of drug inhibitors of HMG-CoA reductase, collectively known as statins, are conspicuous victories of cardiovascular science and medicine [79]. But even in patients treated with statins, a considerable residual burden of cardiovascular risk remains [80]. More than 20% of patients will have a recurrent event within 30 months of an acute coronary syndrome, despite receiving high-dose statin treatment [81]. These findings indicate that treatments to decrease LDL-cholesterol levels even further, beyond the targets currently mandated by various national guidelines, could provide further clinical benefit. Unfortunately, at least one-quarter of high-risk patients who receive intensive statin therapy have LDL-cholesterol levels above current guideline-mandated goals[82]. New biological targets have emerged that may yield incremental lowering of LDL levels to a greater degree than that achieved by high-dose statin therapy.

Ezetimibe, by inhibiting Niemann-Pick C1-Like 1 (NPC1L1), reduces the intestinal absorption of cholesterol and is utilized in clinical practice as monotherapy or when added to statins (Sudhop et al., 2009), and has been extensively studied for the ability not only to decrease plasma LDL-C levels but also to improve the overall cardiovascular outcome. Two pooled analyses of randomized clinical trials, showed significant decrease in the LDL-C levels upon treatment with ezetimibe [83, 84].

Genetic studies have shown that loss-of-function mutations in the gene that encodes the enzyme proprotein convertase subtilisin/kexin type 9 (PCSK9) augment LDL receptor levels on cell surfaces, boosting LDL clearance and yielding lower LDL concentrations in the blood [85]. PCSK9 has emerged as an attractive target for lowering LDL-C levels to reduce the risk of coronary heart disease. Two anti-PCSK9 monoclonal antibodies (alirocumab, evolocumab) subcutaneously administered either biweekly or monthly are currently being studied in phase III trials with large patient populations. By sequestering PCSK9, PCSK9 inhibitors block the binding of PCSK9 protein to LDLRs, preventing LDLR catabolism. In turn, this preserves LDLR recycling and increases receptor density on the hepatocyte surface [86]. Both evolocumab and alirocumab lowered the LDL-cholesterol levels by 60% [87-90]. Further Cardiovascular Outcome Research with PCSK9 Inhibition in subjects with Elevated Risk (FOURIER) clinical trial program showed that inhibition of PCSK9 with evolocumab on a background of statin therapy, lowered LDL cholesterol levels to a median of 30 mg per deciliter and reduced the risk of cardiovascular events [91]. Furthermore, the phase I trial of Inclisiran (Alnylam Pharmaceuticals, Inc, Cambridge, MA), a long-acting RNA interference (RNAi) agent targeting the synthesis of PCSK9, showed no major adverse events as well as reductions of 75% and 51% in PCSK9 and LDL-C concentrations, respectively [92, 93]. Thus, PCSK9 inhibitors are a promising therapeutic strategy to address additional reductions in LDL-C concentrations to reduce CVD in high-risk populations [94, 95].

Plasma levels of Lp(a) are primarily genetically determined by variations in the *LPA* gene coding for Apo(a) [96]. Because of the expanding evidence that high levels of Lp(a) are associated with the

cardiovascular disease risk, antisense oligonucleotide drugs targeting Apo(a) have emerged as a promising approach to reduce Lp(a) levels by 80% in the clinical setting [97]. ApoB is the backbone of all lipoproteins of the VLDL pathway. Interference with the transcription of the *APOB* gene was considered an attractive approach to decrease VLDL production and reduce the number of pro-atherogenic LDL particles [98]. These agents were identified to be very effective, but unfortunately were also associated with side effects and increased risk of liver steatosis in a significant proportion of treated patients [99]. PCSK9 as well as CETP inhibitors lower Lp(a) levels by 30% through an unknown mechanism [100, 101].

Consistent evidence has shown that HDL-C concentration is an independent inverse predictor of the risk for developing a cardiovascular event [102]. Numerous approaches to increase HDL exist or are in development. Apolipoprotein A-I (Apo-AI), the major protein component of HDL, has received much attention as a possible therapeutic target for atherosclerosis [103-105]. Several emerging therapeutic agents are also being designed to target HDL particles, not solely to increase HDL-C levels. These include intravenous infusions of HDL peptide mimetics. Three fully human HDL mimetic compounds are currently being evaluated in proof-of-concept clinical studies. Upon infusion, these drugs are expected to increase cholesterol efflux capacity[106]. Because of the heterogeneity in HDL particles, the complicated pathways of cholesterol flux mediated by HDL and the association of HDL with many proteins that may modify atherosclerosis, the steady-state levels of HDL cholesterol in blood reflect HDL function poorly [107]. In addition to mediating reverse cholesterol transport, HDL can exert anti-inflammatory properties both *in vitro* and *in vivo* [107]. HDL particles carry dozens of proteins and hundreds of lipid species, many with biological activities that have relevance to atherogenesis [108]. The lipid content of HDL particles can be remodeled for example by the plasma protein cholesteryl ester transfer protein (CETP) facilitates the exchange of cholesteryl esters in HDL for triglycerides from apolipoprotein-B-containing lipoproteins[109, 110]. The protein content of HDL particles can also be remodeled for example, when plasma levels of the acute-phase reactant serum amyloid A increase during inflammatory states [111]. Typical clinical assays for HDL do not reflect this high degree of heterogeneity of the particles that influence plaque biology [112].Thus, the mere increase in HDL levels in response to some interventions may not necessarily confer clinical benefit, owing to qualitative changes in the particles.

Of the approaches to increase HDL under study, the potential of CETP inhibition could be a novel therapeutic option for CVD. The CETP inhibitor torcetrapib failed in the clinic, probably owing to off-target effects [113-115] and other CETP inhibitors, dalcetrapib, evacetrapib and anacetrapib, have entered clinical evaluation. In phase 2 studies, dalcetrapib increased HDL-C levels without any effects on LDL-C levels [116]. However, clinical evaluation of dalcetrapib was halted because of the compromised efficacy of the drug treatment. Similarly, evacetrapib was discontinued due to lack of efficacy even though the drug treatment increased HDL-C levels and decreased LDL-C levels [117]. The safety of anacetrapib was recently affirmed by a phase III clinical trial, which provided evidence for reduced clinical events [118, 119]. Finally, TA-8995 (Amgen Inc, Thousand Oaks, CA) is a new promising CETP inhibitor. In the phase II trial in patients with mild dyslipidaemia (TULIP), treatment with TA-8995 showed significant reduction in the LDL-C and ApoB levels, whereas HDL-C and ApoA-I levels were significantly increased. Moreover, TA-8995 was well tolerated without any safety concerns or apparent adverse effects on the liver and muscle. In summary, CETP inhibitors exert beneficial effects on lipid parameters in patients with dyslipidemia [101]. However, the potential of CETP inhibition to improve overall cardiovascular outcome appears to be moderate only.

1.4 Endothelium and lipoproteins

The vascular endothelium lines the inner surface of blood vessels and serves as the first interface for circulating blood components to interact with cells of the vascular wall and surrounding extravascular tissues. In addition to regulating blood delivery and perfusion, a major function of the vascular

endothelium is to provide a semipermeable barrier that controls blood–tissue exchange of fluids, nutrients, and metabolic wastes while preventing pathogens or harmful materials in the circulation from entering into tissues. Thereby, the endothelium has multiple roles including regulation of nitric oxide synthesis, monocyte diapedesis, lipid metabolism, and vessel growth and remodeling, thrombogenesis, platelet activation and inflammation [120-122]. Endothelial cells are involved in all stages of the atherogenic process and their dysfunction is a key early event in the atherosclerotic plaque formation [123]. Therefore, maintenance of endothelial layer is crucial as dysfunction of the endothelium leads to severe pathological conditions.

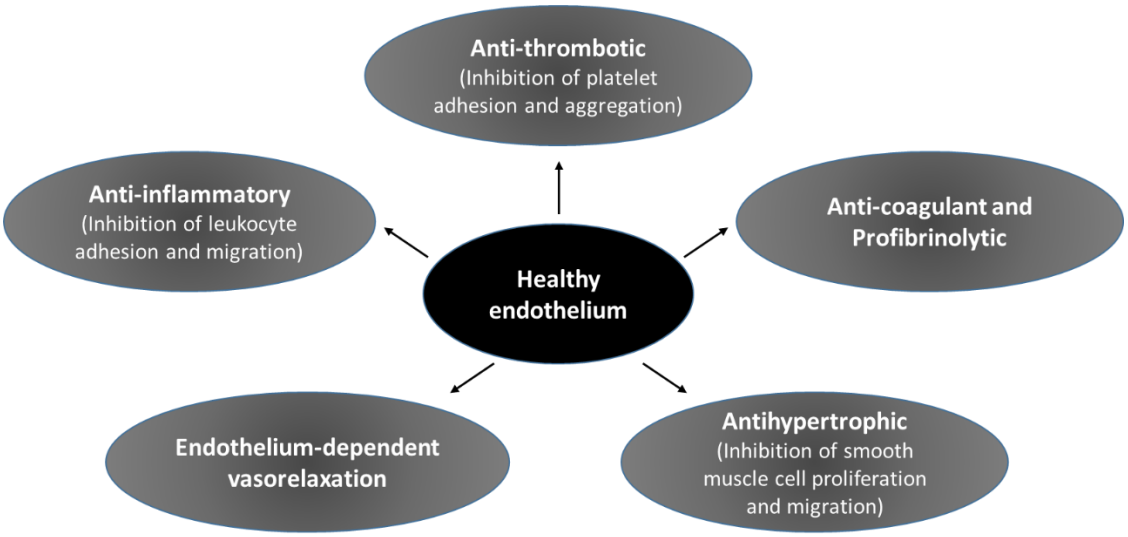

Figure 8: Functions of healthy endothelium. The healthy endothelium mediates endothelium-dependent vasodilation, actively suppresses thrombosis, vascular inflammation, and hypertrophy. Adapted from [124]

Both lipoproteins and endothelium play critical roles in the initiation and progression of atherosclerosis. The endothelial transport and accumulation of pro-atherogenic LDL into the subendothelial space is followed by their modification, which leads to the activation of endothelial cells, upregulation of endothelial adhesion molecules, increase of oxygen radicals, effects on cell viability and apoptosis and to a cascade of events associated with the accumulation of cholesterol in the intima and progression of atherosclerosis [125]. Therefore, removal of cholesterol from the subendothelial space by cholesterol efflux and subsequent reverse cholesterol transport confers protection against atherosclerosis [126]. Recently, much emphasis has been placed on oxidised-LDL (ox-LDL) as a major toxic lipoprotein which is recognised by LOX-1 expressed on endothelial cells and facilitates the internalization and transcytosis through the endothelium [127]. Activation of LOX-1 by oxLDL induces endothelial dysfunction and apoptosis [128] and deletion of LOX-1was found to improve endothelial function leading to reduction in atherogenesis by decreasing proinflammatory and prooxidant signals [129]. Furthermore, LOX-1 was shown to be expressed in atherosclerotic lesions, including endothelial cells [130].

It has been documented that HDLs and their major protein constituent, apolipoprotein (ApoA-I), cross endothelial cells to reach subendothelial space to accept cholesterol from lipid-laden macrophages and re-enter the bloodstream to deliver cholesterol to the liver. The endothelial barrier is thus crossed twice in this process, making the endothelium a key player in the RCT process [131, 132]. While mediating the transendothelial transport of ApoA-I and HDL particles, endothelial cells also efficiently efflux cholesterol to these acceptors [133, 134]. There are four distinct cholesterol efflux pathways which have been described by which HDL and their apolipoproteins remove cholesterol from the cells, *i.e.*, cholesterol transport mediated by ATP-binding cassette transporter A1 (ABCA1), ABCG1 and scavenger receptor class B type I (SR-B1) [135], and by passive cholesterol diffusion following a cholesterol concentration

gradient between the plasma membrane and HDL [136]. The fact that all these receptors also mediate transcytosis indicated that the two processes happen together in the endothelial cells.

Lipoprotein transport through endothelium

Plasma lipoproteins pass the endothelial barrier several times during their metabolic turnover, from the site of their synthesis to the blood, further to the extravascular tissues, and then back into circulation (through vasa vasorum or lymphatic vessels) and finally to the catabolizing organs (liver). The lipoprotein transport through the endothelium was shown to play a major role in the pathogenesis of atherosclerosis. Imbalance between influx and efflux of pro-atherogenic and anti-atherogenic lipoproteins through the arterial wall seems as an important factor for the disease susceptibility [66, 137]. The endothelium is highly permeable to water and small molecules, which are with a diameter below 6nm and nearly impermeable to larger molecules. This relative impermeability of endothelium to macromolecules is a prerequisite for the maintenance of a fluid equilibrium between plasma and interstitium according to the classical Starling principle [138]. However, the macromolecules are known to pass the endothelial barrier in a regulated manner and two major pathways have been identified in the endothelial cells (Figure 9): the paracellular pathway regulates transport through interendothelial junctions whereas the transcellular pathway regulates transport through the cell[139].

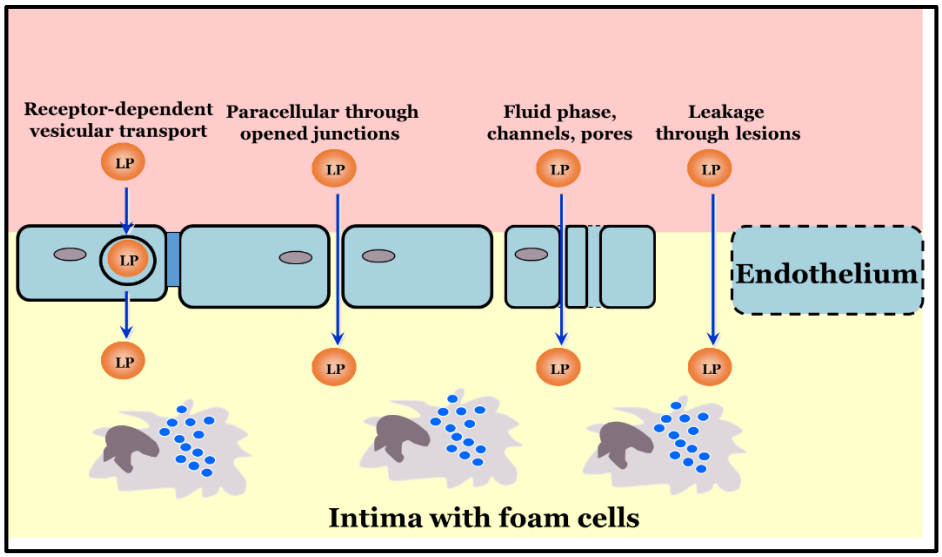

Figure 9: Possible pathways for lipoprotein transport through endothelium. The paracellular transport is performed by opening interendothelial junctions (IEJ). The transcellular pathway is either through receptor-dependent vesicular transport or through fluid-phase uptake in the endothelium.

The paracellular permeability of the endothelial barrier is maintained by the interendothelial junctions, the structures that connect adjacent endothelial cells into a monolayer and restrict the movement of plasma macromolecules from the luminal side to the basolateral side of the vessel [140]. Two types of interendothelial junctions are present in the endothelium, tight junctions (TJ) and adherens junctions (AJ), both contributing to the maintenance of the endothelial barrier. Therefore, paracellular transport requires opening and closing of these junctions, which is a tightly regulated process. Mediators that induce endothelial barrier enhancement and attenuate the response to permeability-increasing mediators are also required for regulation of endothelial permeability. They are present in blood plasma or enriched in the interstitium and provide continuous support for vascular integrity. Suppression of their signaling leads to severe impairment of the endothelial barrier and loss of vessel integrity [141, 142]. Interestingly, sphingosine-1-phosphate (S1P) mediates endothelial barrier enhancement through activation of the G_i protein–coupled $S1P_1$ receptor and protects the lung microvasculature from inflammation-induced injury [143]. Genetic disruption of $S1P_1$ resulted in embryonic lethality due to defects in the development

of the vascular system [144]. Paracrine S1P signaling was also shown to induce AJ assembly [145]. Since, HDL is known to carry more than 50% of plasma S1P and S1P is a regulator of endothelial barrier integrity[146, 147]; it is probable that HDL is transported through transcellular rather than paracellular pathway.

Electron microscopy studies of rat aortas perfused with LDL showed its internalization into cellular vesicles and delivery either to the lysosomes or the basolateral membrane of the cell [148]. The size of LDL precludes paracellular passage without the opening of inter-endothelial junctions, yet an intact endothelium is observed overlying early atherosclerotic lesions [149-151]. Thus, a number of studies have suggested that LDL crosses the endothelium by transcytosis [152-155]. Others have instead suggested that LDL exits the vasculature at areas of damaged or dividing endothelium, implicating the paracellular route. However, the rate of endothelial mitosis is extremely low (<0.05%), and there is scant to no *in vivo* evidence of endothelial apoptosis in human atherosclerosis [151, 156-158].

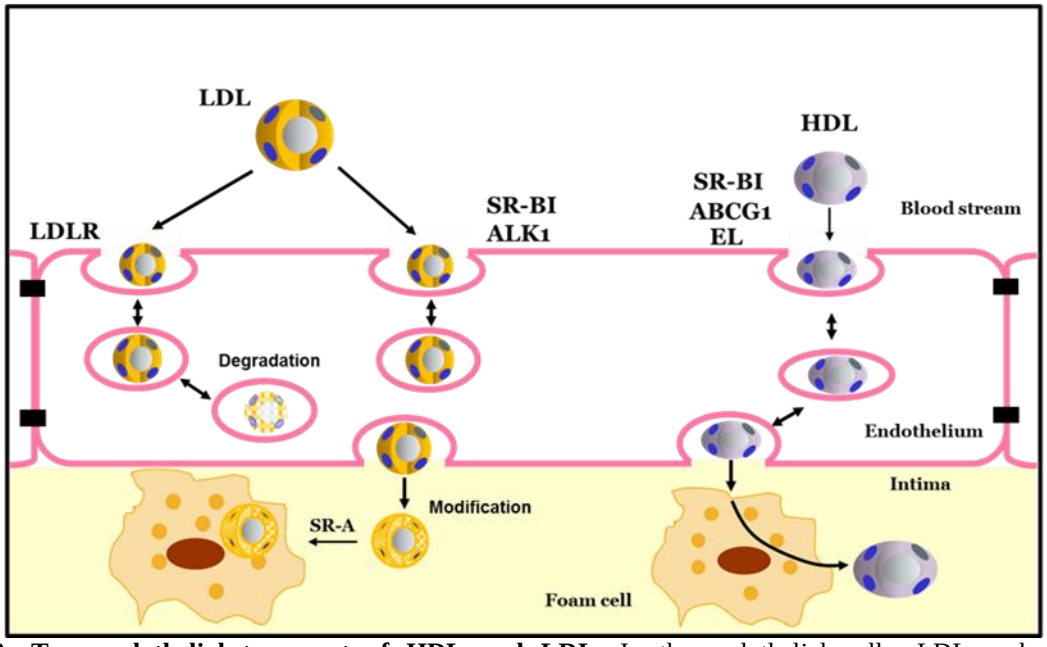

Figure 10: Transendothelial transport of HDL and LDL. In the endothelial cells, LDL undergoes internalization dependent on LDLR, which leads to the degradation of LDL. But the transendothelial transport is modulated by SR-BI and ALK1. On reaching the intima, LDL undergoes modification and is taken up by macrophages through scavenger receptor A (SR-A) to form foam cells. The transport of mature HDL is mediated by SR-BI, ABCG1 and endothelial lipase (EL) to reach the intima and scavenge excess cholesterol from the foam cells. Adapted from [155, 159-163]

The transcellular pathway is the dominant pathway of transporting macromolecules in endothelial cells [139] which can be receptor-independent through fluid-phase uptake or receptor-dependent involving clathrin-coated pits or caveolae [164]. The classical LDL internalization through LDL-receptor was shown to be dependent on clathrin-coated pits. However, the LDL uptake was reduced by endothelial cells from the caveolin-1 knockout mice, which suggests that transendothelial transport of LDL involves caveolae rather than clathrin-coated pits [152]. Immunohistochemical studies showed colocalization of fluorescent and gold-labeled HDL with caveolin-1 in bovine aortic endothelial cells [165]. Recent studies have shown that LDL transport through the endothelial cells to be modulated by SR-BI and activin-like kinase 1(ALK1)[159 155]. Previous *in vitro* data from our group showed that aortic endothelial cells are able to specifically bind, internalize and transport HDL in a saturable and temperature-dependent manner. We also demonstrated that transendothelial transport of mature HDL to be modulated by ABCG1, SR-BI, and endothelial lipase (Figure 10) [160, 161]. Recently our lab showed also that HDL was not colocalized with clathrin or caveolin-1, and blocking of Na^+/H^+-channels essential for any fluid phase transport by Amiloride and/or EIPA even at high concentrations did not change HDL uptake. Neither any co-

localization of fl-HDL with fluorescently labelled 40 kDa Dextran was found, which is taken up by cells through fluid phase endocytosis. Thus, this study demonstrated a possibility of non-classical endocytic route involving dynamin and cytosketal networks for HDL transport through endothelial cells where HDL were found in atypical large vesicles [166].

1.5 Endothelial regulators of HDL transport

Endothelial cells express several genes involved in the reverse cholesterol transport, such as ABCA1, ABCG1, ectopic β-ATPase, SR-BI and endothelial lipase, which were previously shown to promote HDL uptake into the endothelial cells.

ATP-binding cassette transporters

The ATP-binding cassette (ABC) transporters are ubiquitous membrane proteins that couple the hydrolysis of ATP to the transport of diverse substrates across cellular membranes. ABCs are grouped into seven subclasses labeled from ABCA to ABCG [167]. The basic domain organization of ABC transporters consists of two transmembrane domains (TMDs) that provide the passage for the cargo and two cytoplasmic nucleotide-binding domains (NBDs) that bind and hydrolyze ATP. Structurally, ABCs fall into two groups: 1) Full transporters having two similar structural units encoded as a single gene product and 2) half-transporters of single structural units that form active heterodimers or homodimers. ABCA1 and ABCA7 are full transporters, whereas ABCG1 and ABCG4 are homodimeric half transporters [167].

ATP-binding cassette A1

ABCA1 is a member of the ABCA subfamily that plays a central role in HDL metabolism and lipid clearance from cells. ABCA1 mediates the transport of cholesterol, phospholipids and other lipophilic molecules across cellular membranes to lipid-poor HDL apolipoproteins. ABCA1 is broadly expressed with high levels in macrophages, liver cells, intestinal cells, adrenal gland, endothelial cells and placental trophoblast cells[168 169].

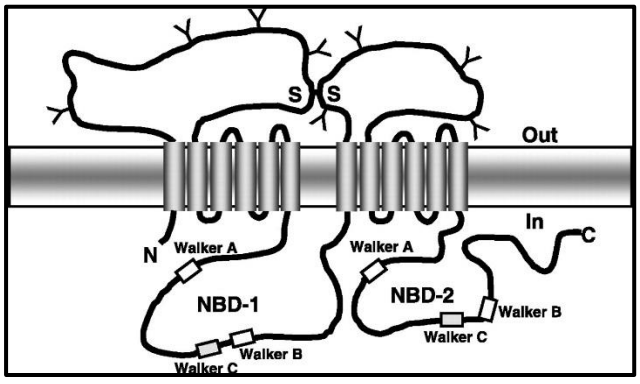

Figure 11: Topological model of ABCA1. The model is based on domain studies of ABCA1. Y indicates approximate glycosylation sites and S-S indicates one predicted disulfide bond. NBD-1 and NBD-2 are the nucleotide binding domains that contain the highly conserves Walker A and Walker B domains and the Walker C signature motif [58].

ABCA1 is a 2,261-amino-acid integral membrane protein that comprises two halves of similar structure (Figure 11). Each half has a transmembrane domain containing six helices and a nucleotide binding domain (NBD) containing two conserved peptide motifs known as Walker A and Walker B, which are present in many proteins that utilize ATP, and a Walker C signature unique to ABC transporters. ABCA1 is predicted to have an NH_2 terminus oriented into the cytosol and two large extracellular loops that are highly glycosylated and linked by one or more cysteine bonds [167, 170]. Binding and hydrolysis of ATP by the two cytoplasmic, nucleotide-binding domains control the conformation of the transmembrane

domains so that the extrusion pocket is available to translocate substrate from the cytoplasmic leaflet to the exofacial leaflet of the bilayer membrane. ABCA1 actively transports phosphatidylcholine, phosphatidylserine, and sphingomyelin with a preference for phosphatidylcholine [171] and this phospholipid translocase activity of ABCA1 leads to the simultaneous efflux of phospholipid and free-cholesterol to lipid-free apoA-I. This protein therefore represents the first and rate-controlling step in the reverse cholesterol transport pathway [172]. The cellular free-cholesterol released to apoA-I originates from both the plasma membrane and the endosomal compartments. This phenomenon occurs because plasma membrane constituents are internalized and recycled via endocytic compartments to the cell surface on a timescale of minutes [173, 174]. Its homology with other better-characterized ABC transporters suggests that ABCA1 forms a channel in the membrane that promotes flipping of lipids from the inner to outer membrane leaflet by an ATPase-dependent process [175].

Mutations in ABCA1 cause a severe HDL deficiency syndrome called Tangier disease (TD) [176]. Lipid-free apoA-I is unable to remove cholesterol and phospholipids from fibroblasts isolated from TD patients, consistent with a defective ABCA1 [177]. Patients with TD experience large yellow-orange tonsils, peripheral neuropathy, splenomegaly, hepatomegaly, ocular abnormalities, hypocholesterolemia, and accelerated atherosclerosis [178]. The ability of HDL to preserve endothelial function is thought to contribute to its overall anti-atherogenic role. In humans, HDL-C levels correlate with endothelium-dependent vasodilation in atherosclerotic coronary arteries and infusion of cholesterol-poor reconstituted HDL improves forearm blood flow in subjects with heterozygous ABCA1 deficiency and reduced HDL levels [179]. Similarly, adenoviral overexpression of ABCA1 in the wild-type mice liver showed increased plasma HDL levels, whereas liver-specific ABCA1 ablation showed 90% decrease in HDL as well as apoA-I levels in the plasma [180]. Studies with transgenic mice expressing human ABCA1 showed increase in HDL-C levels and eNOS mRNA levels in the aorta. The transgenic mice fed on high fat, high cholesterol diet showed 40% increase in plasma HDL and 40% decrease in the aortic lesions compared to the control mice. The hABCA1 transgenic mice also showed decreased expression of genes involved in the endothelial inflammation and apoptosis. Recent studies showed that deficiency of ABCA1 in endothelial cells was associated with decreased eNOS activity, enhanced endothelial cell inflammation, monocyte adhesion and monocyte infiltration into the atherosclerotic plaques [181]. Thus, endothelial expression of ABCA1 plays an important role in the complex interrelationship between endothelial dysfunction, low HDL-C and atherosclerosis [182].

ATP-binding cassette G1

The ATP-binding cassette sub-family G member 1 (ABCG1) is a transmembrane half transporter that exports cellular lipids to extracellular acceptors [183, 184]. The primary function of ABCG1 is to efflux cholesterol to HDL particles [185, 186]. ABCG1 also effluxes cholesterol to LDL, liposomes and cyclodextrin and exports sphingomyelin, phosphatidylcholine and oxysterols to HDL [187, 188]. ABCG1 is ubiquitously expressed, with relatively high expression in the spleen, lung, brain and kidneys and is also highly expressed in the macrophages where it can be upregulated by liver X receptor (LXR) agonists [189].

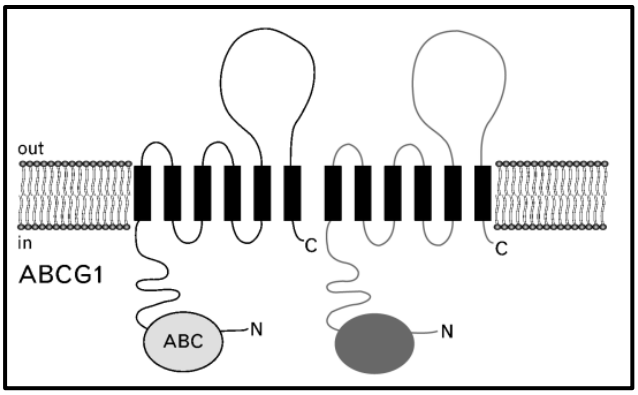

Figure 12: Structure of ABCG1. ABCG1 is a half-transporter with six-transmembrane domains and a single large intracellular region containing one ABC domain. The functional transporter represented in gray, might dimerize with related half-transporters to function [190].

ABCG1 consists of six transmembrane alpha helices and one nucleotide binding domain at the N-terminus (Figure 12). ABCG1 undergoes dimerization to function [191]. Recent studies have shown that ABCG1 forms heterodimers with ABCG4, however, ABCG1 was not found to limit cholesterol efflux [192]. There has been significant debate about the cellular localization and function of ABCG1. A number of studies have reported that ABCG1 is localized and functions in lipid rafts in the plasma membrane and in endosomes that recycle to the cell surface where they efflux cholesterol [186, 193, 194]. However, other reports have suggested that ABCG1 is restricted to the endosomes and functions intracellularly [195]. Recent studies using TIRF microscopy identified ABCG1 in two distinct cellular pools that are located in the endoplasmic reticulum and plasma membrane. Treatment of cells with cholesterol was shown to increase plasma membrane associated ABCG1 levels indicating that ABCG1 cycles between the intracellular and plasma membrane pools based on cellular cholesterol levels. In addition to regulating ABCG1 localization, cholesterol was also seen to regulate ABCG1 levels via inhibition of ubiquitination and subsequent degradation. Further systematic experiments with the cell membrane sheet preparation showed that cell-surface ABCG1 was associated with actin cytoskeleton and loading of cells with cholesterol significantly increased the organization of ABCG1 in the cell membrane into filamentous structures[196].

Mice lacking ABCG1 accumulate lipids in macrophages and hepatocytes, and show significant reduction of plasma HDL-C levels after fed with the high cholesterol diet [197 189]. Transgenic mice over-expressing human *ABCG1* gene are protected against dietary fat-induced lipid accumulation in the liver and lungs [189]. Moreover, over-expression of ABCG1 in macrophages significantly increases macrophage RCT in vivo, whereas knockdown or knockout of ABCG1 expression markedly decreases macrophage RCT in vivo [198]. The ability of ABCG1 to preserve endothelial function was shown by its role in promoting efflux of oxysterol 7-ketocholesterol (7-KC) to HDL, whose delayed clearance is associated with decreased eNOS activity and increased coronary heart disease risk [199]. Atheroprotective effects of vascular ABCG1 were suggested by transplantation of *ABCG1*$^{+/+}$ bone marrow into mice with whole body *Abcg1* deficiency on the *Ldlr*$^{-/-}$ background [200]. Aortic endothelial cells from the ABCG1 knock-out mice have shown increased production of chemokines, increased surface expression of the adhesion molecules ICAM-1 and E-selectin that promote monocyte adhesion, leading to pro-inflammatory endothelial phenotype [201]. Along with ABCA1, recent studies also showed that cholesterol efflux pathway mediated by ABCG1 in endothelial cells is anti-atherogenic through increasing eNOS activity and decreasing endothelial inflammation. In endothelial cells, not only combined *Abca1/g1* deficiency showed accelerated atherosclerosis, but also single *Abca1* and *Abcg1* deficiency promoted atherosclerosis. These studies add to the understanding of the atheroprotective effects of ABCA1 and ABCG1 in the endothelium and provide a link between endothelial cell cholesterol accumulation, inflammation and atherosclerosis [181].

Endothelial lipase

Endothelial lipase (EL) is a member of the triglyceride lipase family, which includes lipoprotein lipase and hepatic lipase. In principle, EL is a phospholipase, with insignificant triglyceride hydrolase activity [202, 203]. EL is synthesized by endothelial cells and hydrolyses phospholipids in HDL much more efficiently than in other lipoproteins [204, 205]. EL contains 482 amino acids with a considerable molecular homology with lipoprotein lipase (LPL) and hepatic lipase (HL). Although alignment of EL with the human LPL and HL amino acid sequences revealed conservation of the catalytic triads, EL has a minimal homology in the lid domain which is known to be critical in determining substrate specificity [202].

After secretion, EL binds to cell surface proteoglycans where it exerts its action. EL acts as bridge between circulating HDL and endothelial cells thus promoting lipoprotein incorporation [206]. EL-mediated hydrolysis of HDL particles determines the plasma levels of HDL-cholesterol, which was established in animal experiments using both overexpression as well as loss-of-function models. Transgenic expression of human EL in mice resulted in a reduction in plasma HDL-cholesterol levels compared with wild-type control animals [207]. Consistent with this finding, adenovirus-mediated over-expression of human EL in LDL receptor-deficient mice lead to significantly decreased plasma concentrations of HDL-cholesterol [203]. Also, inhibition of EL using a polyclonal antimurine antibody in mice resulted in a significant increase in HDL-C and phospholipid levels as well as an increased HDL particle size [208]. HDL-induced angiogenesis in aortic rings from EL-deficient mice was markedly decreased compared with wild-type controls. In cell culture, small interfering RNA–mediated knockdown of EL also reduced HDL-promoted endothelial cell migration, tube formation and phosphorylation of eNOS and Akt, indicating that EL modulates HDL-dependent signaling responses [209].

Atherosclerosis is an inflammatory process and cytokines are thought to have an important role in initiating the expression of a variety of genes that promote cell adhesion and other processes that are required for disease progression [210]. Two cytokines that have received the most attention in this regard are TNF-α and IL-1β. Thus, the expression of EL by these cytokines in endothelial cells was determined by Quertermous and colleagues [211]. When cultured human endothelial cells were treated with IL-1β or TNFα, there was a significant increase in EL mRNA levels. Our group has shown that treatment of cells with IL-6 increased transcytosis of HDL through the endothelial cells via increase in the EL expression, marking the importance of endothelial lipase in the first step of RCT [160]. Many studies have been performed to understand the role of EL in RCT and identified that EL works both as a promoting and inhibiting agent [212 213, 214].

In a cohort of healthy subjects with a family history of premature coronary heart disease, increased human plasma EL concentrations were shown to be significantly associated with the metabolic syndrome and subclinical coronary heart disease event [215]. Given the strong association between plasma HDL-cholesterol levels and cardiovascular disease risk in humans, many studies expected that alteration in plasma HDL levels by EL in experimental animals might affect the progression of atherosclerosis. Studies dedicated to this hypothesis have suggested 2 different opinions, where Ishida et al reported that the inactivation of EL was associated with an approximately 70% decrease in atherosclerotic disease area in apoE knockout mice compared with controls despite the presence of a proatherogenic lipid profile [216]. Conversely, Ko et al found that although EL modulated the lipoprotein profile in mice, there was no effect of EL inactivation on atherosclerosis development in hyperlipidemic atherosclerosis-prone mice models [217]. The single-nucleotide polymorphism of *LIPG* Asn396Ser increased plasma HDL-C levels, but did not reduce the risk of myocardial infarction [218]. This discrepancy supports the concept that changes in HDL-cholesterol levels are not a surrogate for atheroprotection.

Scavenger receptor class B type I (SR-BI)

SR-BI mainly functions as a receptor for HDL was first isolated and identified by Calvo et.al [219]. The sequence of SR-BI is closely related to CD36 and LIMPII analogous-1 and the gene, now called *SCARB1*, was initially named CLA-1. SR-BI is primarily expressed in the liver and nonplacental steroidogenic tissues, but is also expressed in macrophages and endothelial cells, where it functions to reduce atherosclerosis[220]. Acton and colleagues demonstrated that SR-BI binds HDL with high affinity and mediates the selective uptake of HDL cholesteryl ester into the liver. SR-BI also mediates the bidirectional flux of free cholesterol between cells and HDL [221-223]. SR-BI mediated influx of HDL cholesteryl esters and free cholesterol are trafficked to bile and is a major route of delivery of peripheral cholesterol to the liver for excretion in both mice and humans [224-227].

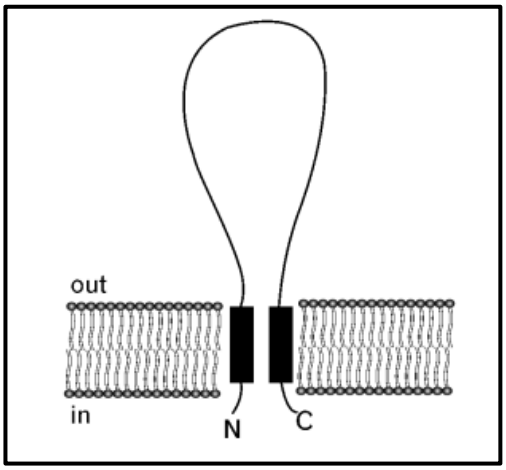

Figure 13: Structure of SR-BI: SR-BI has a single, large and highly glycosylated extracellular loop that is anchored by two transmembrane domains with short cytoplasmic extensions [190].

SR-BI is a hairpin-looped structure with two short transmembrane domains, two cytoplasmic tails and a large extracellular loop (Figure 13). Studies using SR-BI/CD36 chimeric receptors demonstrated that the extracellular domain binds to multiple ligands and is critical for both selective cholesteryl esters uptake and bi-directional flux of free cholesterol [228]. Binding of HDL to the extracellular loop is not necessary for cholesterol efflux, however, subdomains of the N-terminal half of the extracellular domain are required for cholesterol efflux and organization of the plasma membrane cholesterol domains. Binding of HDL to the subdomains of C-terminal half of the extracellular domain are important for the selective cholesteryl ester uptake [229]. Lysosomal integral membrane protein type-2 is a CD36 family member, which shares structural protein homology with SR-BI and was crystallized for high-resolution analysis. According to this model, a large cavity traverses the entire length of the SR-BI molecules and mutagenesis of SR-BI showed that the cavity is a lipophilic tunnel through which cholesteryl esters are delivered from the bound lipoprotein to the outer leaflet of the plasma membrane [230]. Using fluorescence resonance energy transfer, it has been shown that SR-BI forms oligomers at the C-terminal region of the extracellular domain [231]. In addition, a glycine dimerization motif in the N-terminal transmembrane domain is critical to SR-BI oligomerization and cholesteryl ester transport, which is proportional to the degree of oligomerization [232]. The C-terminal cytoplasmic and transmembrane domains are critical to SR-BI signaling. The C-terminal cytoplasmic domain contains a PDZ-binding domain that interacts with the adaptor protein PDZK1. In endothelial cells, activation of eNOS involves interaction of SR-BI with Src and then activation of Src further leads to the activation of phosphoinositide 3-kinase (PI3K), Akt and eNOS. However, PDZK1 interaction with SR-BI is not required for Src interaction with SR-BI [233]. In macrophages, PDZK1 is also required for the HDL and SR-BI induced activation of Akt signaling [234]. In hepatocytes, PDZK1 interaction maintains steady-state levels of SR-BI by preventing its degradation [235]. SR-BI acts as a membrane cholesterol sensor and the C-terminal transmembrane domain

binds to the cholesterol. Using a SR-BI C-terminal transmembrane point mutation Q445A, which showed reduced interaction with cholesterol, it has been demonstrated that SR-BI interaction with membrane cholesterol is not critical for interaction with Src or PDZK1 but is required for activation of the Src signaling pathway [236, 237].

Inflammatory events are critical to the progression of fatty streaks to advanced atherosclerotic lesions and studies suggest that SR-BI protects against atherosclerosis by regulating the inflammatory response. Compared with $LDLR^{-/-}$ mice, SR-BI/LDLR double-knockout mice fed an atherogenic diet have increased plasma levels of proinflammatory interleukin-6 (IL-6) and tumor necrosis factor alpha (TNF-α) [238]. As the main pathway of hepatic removal of HDL cholesterol in mice, SR-BI is critical for the delivery of cholesterol to bile and the preservation of HDL functions. Hepatic SR-BI is also crucial in the clearance of remnant lipoproteins and atherogenic lipoprotein (a) in mice [51]. In addition, HDL interaction with SR-BI reduces the inflammatory response to lipopolysaccharide in human macrophages by markedly reducing NF-κB activation [239]. Furthermore, recent studies have shown that the interaction of macrophage SR-BI with apoptotic cells activates PI3K/Akt signaling and induces the expression of anti-inflammatory cytokines [240]. In addition, HDL activates PI3K/Akt signaling in macrophages, which is mediated by SR-BI and involves interaction with its adaptor protein PDZK1 and activation of sphingosine 1-phosphate (S1P) receptor 1 (S1PR1) signaling [234]. Thus, SR-BI regulates inflammation by activating Akt phosphorylation and reducing NF-κB activation.

Recent studies suggest that endothelial cell SR-BI functions in reducing atherosclerotic lesion foam cell formation. Specific overexpression of SR-BI in endothelial cells decreased atherosclerosis in both $apoE^{-/-}$ and WT mice [241]. Studies by our group and others have shown that a major portion of the endothelial cell transcytosis of HDL from the apical to the basolateral side is mediated by SR-BI, suggesting that SR-BI provides HDL to the subendothelium to promote cholesterol efflux from macrophages [161, 241]. Furthermore, recent studies have shown that endothelial cell SR-BI mediates the uptake and transcytosis of HDL in lymphatic vessels to effectively remove cholesterol from peripheral tissue, thereby raising the possibility that lymphatic SR-BI also reduces foam cell formation in atherosclerotic lesions [242]. Limiting endothelial cell inflammation is critical to reducing monocyte adhesion and recruitment into intima and thereby preventing lesion progression. SR-BI interaction with HDL prevents endothelial cell inflammation by controlling eNOS activation and expression of the antioxidant enzyme 3-beta-hydroxysteroid-delta 24-reductase (DHCR24) [243, 244]. SR-BI-mediated production of nitric oxide (NO) and DHCR24 leads to less TNF-α-stimulated NF-κB activation resulting in reduced endothelial cell expression of inflammatory monocyte adherence proteins and chemokines, thereby reducing monocyte recruitment into the intima [245]. Taking these findings together, SR-BI is a multifunctional receptor against atherosclerosis making it a viable therapeutic target. Identification of the detailed mechanism by which SR-BI functions, including its adaptor proteins, signaling molecules, and transcriptional regulators, will be important to provide the basis for new therapeutic approaches for atherosclerosis [227].

Ectopic β–chain of F_0F_1-ATPase

Ectopic F_0F_1-ATPase is a mitochondrial complex that was shown to play role in the endocytosis of apoA-I and HDL in hepatocytes and endothelial cells [162, 246]. The F_0 domain is an integral membrane domain that contains a transmembrane channel for protons and the F_1 domain is a peripheral membrane protein complex containing binding sites for ATP and ADP, and the catalytic site for ATP synthesis or hydrolysis [247, 248]. The F_1 ATPase domain was found ectopically expressed on the plasma membrane of hepatocytes, endothelial cells, adipocytes and tumor cells [249-252].

On endothelial cells, binding of apoA-I to ecto-F_1-ATPase stimulates the hydrolysis of extracellular ATP into ADP and phosphate. The ADP released transduces this enzymatic activity into cellular effects

through the activation of ADP-responsive P2Y receptors and trigger the transendothelial transport of both lipid-free apoA-I and HDL. Of the two P2Y receptors preferentially activated by ADP and expressed by endothelial cells ($P2Y_1$ and $P2Y_{12}$), it was shown that apoA-I/HDL transcytosis was mediated by $P2Y_{12}$, as this process could be reduced with the $P2Y_{12}$ inhibitor 2-MeSAMP [162]. Moreover, binding of apoA-I to the ectopic- F_1-ATPase stimulates downstream signaling pathways, which subsequently promote endothelial cell proliferation and reduce apoptosis. These effects of apoA-I on endothelial cell survival were strictly limited to ecto-F_1-ATPase activity because they persisted when other HDL/apoA-I receptors, such as SR-BI and ABCA1, were inhibited but were impaired when treated with F_1-ATPase inhibitors[162, 253]. In addition, it has been recently reported that ecto-F_1-ATPase was expressed at the plasma membrane of human endothelial progenitor cells (EPC) and was involved in the effect of apoA-I in the proliferation and angiogenic capacity of early EPCs [254].

In conclusion, these data support a role of the ecto-F_1-ATPase/$P2Y_{12}$ axis in controlling apoA-I/HDL crossing from the plasma compartment into the sub-endothelial space where they are in the close vicinity of foam cells. Further studies are needed to interpret the physiological and pathological relevance of ecto-F_1-ATPase/$P2Y_{12}$ axis in affecting atheroma formation even at an early stage of the disease when endothelial dysfunction occurs.

1.6 Endothelial regulators of LDL transport

As a first step in the pathogenesis of atherosclerosis, LDL crosses the endothelium to accumulate in the intima. Several studies have shown that LDL can cross intact endothelial cell layer by transcytosis.

Low-density lipoprotein receptor

The low-density lipoprotein receptor (LDLR) is a cell-surface glycoprotein that plays a critical role in the homeostatic control of blood cholesterol by mediating the removal of cholesterol-containing lipoprotein particles from the circulation. Brown & Goldstein originally identified the LDLR in 1973 during their search for the molecular basis of familial hypercholesterolemia (FH), which is one of the most common human inborn errors of metabolism and is caused by loss of function mutations of the gene encoding LDLR [33].

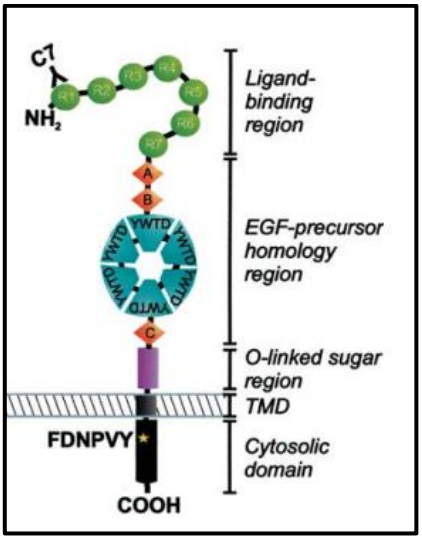

Figure 14: Schematic representation of the regional composition of the LDLR. The LDLR has five functionally distinct regions: an N-terminal ligand-binding region, an epidermal growth factor (EGF)-precursor homology region, a region containing O-linked sugars, a transmembrane domain and a C-terminal cytosolic domain [255].

The human LDLR is encoded by a gene of ~45 kb located on chromosome 19p13.1–13.3. The 18 exons of the gene are translated into an 860-amino acid type I transmembrane protein including a signal sequence of 21 amino acids, which is cleaved during translocation into the endoplasmic reticulum [256]. The exons act as functionally independent modules in the protein domain organization [256]. The LDLR has five functionally distinct regions: an N-terminal ligand-binding region, an epidermal growth factor (EGF)-precursor homology region, a region containing O-linked sugars, a transmembrane domain and a C-terminal cytosolic domain (Figure 14). The ligand-binding region consists of seven cysteine rich repeats (R1-R7) of approximately 40 amino acids, called as LDLR class A repeats. This region also consists of a conserved sequence of acidic amino acids present in the C-terminal part of each LDL-A repeat, which is proposed to mediate interaction with basic amino acid residues of apoB-100 and ApoE. At neutral plasma pH, LDLR binds to the LDL via a 550-kDa apoB-100, which is the sole protein of LDL [257, 258]. Studies using monoclonal antibodies to identify specific apoB-100 epitopes on the surface of LDL particles by electron microscopy suggest that apoB-100 is distributed over the surface of the LDL particle like a ribbon, with a bow contributed by the C-terminal end [259]. The LDL receptor also binds tightly to lipoproteins that contain multiple copies of to ApoE, a 34kDa protein found in beta migrating forms of VLDL or certain intermediate and high-density lipoproteins [260, 261].

Endocytosis and intracellular transport of the LDLR are regulated through its cytoplasmic domain. Mutational analysis has revealed a dominant role for the FDNPVY sequence (NPXY motif) in recruitment of the LDLR to clathrin-coated pits on the cell surface [262-265]. The NPXY motif adopts a tight hairpin conformation that serves as a binding site for a variety of adaptor proteins and signaling molecules. The autosomal recessive hypercholesterolemia (ARH) gene encodes an adaptor protein that binds via its N-terminal phosphotyrosine binding (PBD) domain to the FDNPVY motif of the LDLR [266]. Via a canonical clathrin box sequence (LLDLE) in its C-terminal domain, ARH binds directly to clathrin, whereas a conserved 27-amino acid sequence interacts with the β2- subunit of the clathrin-binding AP-2 adaptor complex [267]. Mutations in the ARH gene lead to reduced internalization of the LDLR and a clinical phenotype indistinguishable from FH [268, 269]. The β-arrestin-2 adaptor protein was shown to mediate clathrin-dependent internalization of the LDLR but not of a mutant LDLR with a Y-to-A substitution in the FDNPVY motif [270]. Another clathrin- and AP-2 binding protein, Disabled-2 (Dab-2), binds peptides corresponding to the FDNPXY motif and co-localizes with the LDLR in clathrin-coated pits [255, 271, 272].

Upon binding, the LDL-LDLR complex is taken up by the cells via clathrin-mediated endocytosis. In endosomes the ligand dissociates from the receptor due to the local low pH. The LDL receptor is subsequently returned to the cell surface in a process called receptor recycling [36, 273]. In contrast to the internalization process, little is known about proteins involved in intracellular LDLR trafficking. Sorting nexin-17, a protein located in early endosomes, binds the LDLR NPXY motif, but its precise role in intracellular trafficking remains unclear [274] [255]. Recent studies have shown that show that the COMMD/CCDC22/CCDC93 (CCC) and the Wiskott–Aldrich syndrome protein and SCAR homologue (WASH) complexes are both crucial for endosomal sorting of LDLR and for its function. Inactivation of both these complexes has been shown to cause LDLR mislocalization, increased lysosomal degradation of LDLR and impaired LDL uptake [275]. However, in endothelial cells receptor-mediated endocytosis of LDL by LDLR is shown to be dependent on caveolae-mediated pathway. Caveolae are 50- to 100-nm cell surface flask-shaped invaginated structures that are highly abundant and play an important role in the cholesterol transport, endocytosis, transcytosis, and signal transduction in the endothelial cells [276]. Caveolin-1 (Cav-1) is the major coat protein of endothelial caveolae and is necessary for caveolae assembly [277]. Studies of the aortic rings from caveolin-1 knockout mice revealed reduced LDL internalization, while *cav1*$^{-/-}$ */ApoE*$^{-/-}$ mice were protected from atherosclerosis despite having increased plasma LDL levels. These data are also consistent with those obtained by Fernández-Hernando et al., who showed that endothelial caveolin-1 could regulate LDL entry into the arterial wall

by showing that the permeability of the aorta to 1^{25}I-LDL is reduced in caveolin-1-deficient mice [278-280]. Interestingly, PCSK9-mediated LDLR degradation did not impair the transcytosis, indicating that LDLR is not required for the LDL endothelial transcytosis [155].

Electron microscopy studies have demonstrated that physiological levels of LDL particles can be internalized by two pathways; LDLR dependent and LDLR independent pathways[148]. The LDLR-mediated pathway promotes LDL degradation and is downregulated at the higher concentrations of LDL while the additional studies have shown that at least 50% of the LDL that is endocytosed by the endothelium traverses the cells to reach the basolateral side via an unknown active LDLR independent transport mechanism [138, 281].

SR-BI

Previous studies have shown that SR-BI binds native LDL [282] with high affinity and is capable of performing bona fide receptor-mediated endocytosis [283]. The findings showed a partial colocalization of LDL with SR-BI and overexpression of SR-BI increased LDL transcytosis, whereas knockdown of SR-BI using RNA interference significantly decreased LDL endothelial transcytosis. Further it was also shown that HDL and LDL compete for binding to SR-BI in the endothelial cells [155 161].

Activin-like kinase 1 (ALK1)

Recent studies using genome-wide RNAi approach in the endothelial cell line (EA.hy926) identified ALK1 as a novel low-affinity, high –capacity receptor for LDL transcytosis in endothelial cells. ALK1 is a TGF-β-type 1 receptor which binds the bone morphogenetic proteins (BMP) 9 and 10 ligands with high affinity. ALK1 is highly expressed in primary human endothelial cells compared to the hepatocytes.

ALK1 is one of the seven activin-like kinase receptors that shares a similar homology in the intracellular domain but very low homology with the extracellular amino terminal domain. The amino-terminal domain is responsible for the ligand binding but only ALK1 is shown to specifically bind LDL. Studies have shown that both LDLR and ALK1 bind to different sites on LDL. The uptake of LDL by ALK1 was shown to be independent of its kinase activity. Experiments using total internal reflectance microscopy (TIRF) in primary human endothelial cells showed that knockdown of ALK1 decreased transcytosis of LDL from the apical to the basolateral membrane. LDL uptake was significantly reduced into the arterial wall of the mice with endothelial specific Acvrl1$^{-/-}$ and LDL $^{-/-}$ double knock-out mouse. Taken together, the data point at the role of ALK1 on LDL uptake and transcytosis through the endothelial cells [159].

1.7 Aim and outline of the thesis

From the previously mentioned chapter, it is clear that endothelial cells facilitate the uptake and transcytosis of HDL and LDL through specific protein interactions. The overall aim of the research summarized in this thesis was to provide more insight into the identification of novel protein interactors that are involved in regulating the endothelial uptake and transcytosis of HDL and LDL, which is crucial for targeting cardiovascular disease progression.

We used both hypothesis/candidate driven and hypothesis-free approach. In the hypothesis driven approach we investigated the role of S1P, which is a well-known regulator of endothelial barrier integrity (Chapter 2). For the hypothesis-free approach, we performed kinase inhibitor screen. This identified VEGF as a crucial regulator of endothelial HDL uptake and transendothelial HDL transport (Chapter 3). Finally, we validated the role of VEGF for lipoprotein endocytosis in clear-cell renal cell carcinoma, which is a well-known VEGF-driven disease (Chapter 4).

Lastly, Chapter 5 summarizes and discusses the most relevant findings described in the thesis and concludes with implications for future research.

1.8 References

1. Olson RE. Discovery of the lipoproteins, their role in fat transport and their significance as risk factors. *J Nutr* 1998;**128**:439S-443S.
2. Ikonen E. Cellular cholesterol trafficking and compartmentalization. *Nat Rev Mol Cell Biol* 2008;**9**:125-138.
3. Grundy SM. Absorption and metabolism of dietary cholesterol. *Annu Rev Nutr* 1983;**3**:71-96.
4. Bloch K. The biological synthesis of cholesterol. *Science* 1965;**150**:19-28.
5. Goldstein JL, Brown MS. Regulation of the mevalonate pathway. *Nature* 1990;**343**:425-430.
6. Tabas I. Consequences of cellular cholesterol accumulation: basic concepts and physiological implications. *J Clin Invest* 2002;**110**:905-911.
7. Ye J, DeBose-Boyd RA. Regulation of cholesterol and fatty acid synthesis. *Cold Spring Harb Perspect Biol* 2011;**3**.
8. Shao W, Espenshade PJ. Sterol regulatory element-binding protein (SREBP) cleavage regulates Golgi-to-endoplasmic reticulum recycling of SREBP cleavage-activating protein (SCAP). *J Biol Chem* 2014;**289**:7547-7557.
9. Goldstein JL, DeBose-Boyd RA, Brown MS. Protein sensors for membrane sterols. *Cell* 2006;**124**:35-46.
10. Engelking LJ, Liang G, Hammer RE, Takaishi K, Kuriyama H, Evers BM, et al. Schoenheimer effect explained--feedback regulation of cholesterol synthesis in mice mediated by Insig proteins. *J Clin Invest* 2005;**115**:2489-2498.
11. Radhakrishnan A, Sun L-P, Espenshade PJ, Goldstein JL, Brown MS. The SREBP Pathway: Gene Regulation through Sterol Sensing and Gated Protein Trafficking. *Regulation of Organelle and Cell Compartment Signaling: Cell Signaling Collection* 2011:355.
12. Giandomenico V, Simonsson M, Gronroos E, Ericsson J. Coactivator-dependent acetylation stabilizes members of the SREBP family of transcription factors. *Mol Cell Biol* 2003;**23**:2587-2599.
13. Walker AK, Yang F, Jiang K, Ji JY, Watts JL, Purushotham A, et al. Conserved role of SIRT1 orthologs in fasting-dependent inhibition of the lipid/cholesterol regulator SREBP. *Genes Dev* 2010;**24**:1403-1417.
14. Stohr R, Mavilio M, Marino A, Casagrande V, Kappel B, Mollmann J, et al. ITCH modulates SIRT6 and SREBP2 to influence lipid metabolism and atherosclerosis in ApoE null mice. *Sci Rep* 2015;**5**:9023.
15. Hirano Y, Yoshida M, Shimizu M, Sato R. Direct demonstration of rapid degradation of nuclear sterol regulatory element-binding proteins by the ubiquitin-proteasome pathway. *J Biol Chem* 2001;**276**:36431-36437.
16. Hirano Y, Murata S, Tanaka K, Shimizu M, Sato R. Sterol regulatory element-binding proteins are negatively regulated through SUMO-1 modification independent of the ubiquitin/26 S proteasome pathway. *J Biol Chem* 2003;**278**:16809-16819.
17. Jeon TI, Osborne TF. miRNA and cholesterol homeostasis. *Biochim Biophys Acta* 2016;**1861**:2041-2046.
18. Horton JD, Goldstein JL, Brown MS. SREBPs: activators of the complete program of cholesterol and fatty acid synthesis in the liver. *J Clin Invest* 2002;**109**:1125-1131.
19. Mihaylova MM, Shaw RJ. The AMPK signalling pathway coordinates cell growth, autophagy and metabolism. *Nat Cell Biol* 2011;**13**:1016-1023.
20. Rosenson RS, Brewer HB, Jr., Chapman MJ, Fazio S, Hussain MM, Kontush A, et al. HDL measures, particle heterogeneity, proposed nomenclature, and relation to atherosclerotic cardiovascular events. *Clin Chem* 2011;**57**:392-410.
21. Carey MC, Small DM, Bliss CM. Lipid digestion and absorption. *Annu Rev Physiol* 1983;**45**:651-677.
22. Miled N, Canaan S, Dupuis L, Roussel A, Riviere M, Carriere F, et al. Digestive lipases: from three-dimensional structure to physiology. *Biochimie* 2000;**82**:973-986.
23. Hussain MM. Intestinal lipid absorption and lipoprotein formation. *Curr Opin Lipidol* 2014;**25**:200-206.
24. Wang H, Eckel RH. Lipoprotein lipase: from gene to obesity. *Am J Physiol Endocrinol Metab* 2009;**297**:E271-288.
25. Young SG, Davies BS, Voss CV, Gin P, Weinstein MM, Tontonoz P, et al. GPIHBP1, an endothelial cell transporter for lipoprotein lipase. *J Lipid Res* 2011;**52**:1869-1884.

26. Ishibashi S, Perrey S, Chen Z, Osuga J, Shimada M, Ohashi K, et al. Role of the low density lipoprotein (LDL) receptor pathway in the metabolism of chylomicron remnants. A quantitative study in knockout mice lacking the LDL receptor, apolipoprotein E, or both. *J Biol Chem* 1996;**271**:22422-22427.
27. Goudriaan JR, Espirito Santo SM, Voshol PJ, Teusink B, van Dijk KW, van Vlijmen BJ, et al. The VLDL receptor plays a major role in chylomicron metabolism by enhancing LPL-mediated triglyceride hydrolysis. *J Lipid Res* 2004;**45**:1475-1481.
28. Stanford KI, Bishop JR, Foley EM, Gonzales JC, Niesman IR, Witztum JL, et al. Syndecan-1 is the primary heparan sulfate proteoglycan mediating hepatic clearance of triglyceride-rich lipoproteins in mice. *J Clin Invest* 2009;**119**:3236-3245.
29. Martins IJ, Hone E, Chi C, Seydel U, Martins RN, Redgrave TG. Relative roles of LDLr and LRP in the metabolism of chylomicron remnants in genetically manipulated mice. *J Lipid Res* 2000;**41**:205-213.
30. Van Eck M, Hoekstra M, Out R, Bos IS, Kruijt JK, Hildebrand RB, et al. Scavenger receptor BI facilitates the metabolism of VLDL lipoproteins in vivo. *J Lipid Res* 2008;**49**:136-146.
31. Raabe M, Veniant MM, Sullivan MA, Zlot CH, Bjorkegren J, Nielsen LB, et al. Analysis of the role of microsomal triglyceride transfer protein in the liver of tissue-specific knockout mice. *J Clin Invest* 1999;**103**:1287-1298.
32. Bisgaier CL, Glickman RM. Intestinal synthesis, secretion, and transport of lipoproteins. *Annu Rev Physiol* 1983;**45**:625-636.
33. Goldstein JL, Brown MS. The LDL receptor. *Arterioscler Thromb Vasc Biol* 2009;**29**:431-438.
34. Chen WJ, Goldstein JL, Brown MS. NPXY, a sequence often found in cytoplasmic tails, is required for coated pit-mediated internalization of the low density lipoprotein receptor. *J Biol Chem* 1990;**265**:3116-3123.
35. Rudenko G, Henry L, Henderson K, Ichtchenko K, Brown MS, Goldstein JL, et al. Structure of the LDL receptor extracellular domain at endosomal pH. *Science* 2002;**298**:2353-2358.
36. Davis CG, Goldstein JL, Sudhof TC, Anderson RG, Russell DW, Brown MS. Acid-dependent ligand dissociation and recycling of LDL receptor mediated by growth factor homology region. *Nature* 1987;**326**:760-765.
37. Zhang DW, Lagace TA, Garuti R, Zhao Z, McDonald M, Horton JD, et al. Binding of proprotein convertase subtilisin/kexin type 9 to epidermal growth factor-like repeat A of low density lipoprotein receptor decreases receptor recycling and increases degradation. *J Biol Chem* 2007;**282**:18602-18612.
38. Brown MS, Goldstein JL. A proteolytic pathway that controls the cholesterol content of membranes, cells, and blood. *Proc Natl Acad Sci U S A* 1999;**96**:11041-11048.
39. Rawson RB. The SREBP pathway--insights from Insigs and insects. *Nat Rev Mol Cell Biol* 2003;**4**:631-640.
40. Nohturfft A, Yabe D, Goldstein JL, Brown MS, Espenshade PJ. Regulated step in cholesterol feedback localized to budding of SCAP from ER membranes. *Cell* 2000;**102**:315-323.
41. Zelcer N, Tontonoz P. Liver X receptors as integrators of metabolic and inflammatory signaling. *J Clin Invest* 2006;**116**:607-614.
42. Zelcer N, Hong C, Boyadjian R, Tontonoz P. LXR regulates cholesterol uptake through Idol-dependent ubiquitination of the LDL receptor. *Science* 2009;**325**:100-104.
43. Sorrentino V, Scheer L, Santos A, Reits E, Bleijlevens B, Zelcer N. Distinct functional domains contribute to degradation of the low density lipoprotein receptor (LDLR) by the E3 ubiquitin ligase inducible Degrader of the LDLR (IDOL). *J Biol Chem* 2011;**286**:30190-30199.
44. Sorrentino V, Zelcer N. Post-transcriptional regulation of lipoprotein receptors by the E3-ubiquitin ligase inducible degrader of the low-density lipoprotein receptor. *Curr Opin Lipidol* 2012;**23**:213-219.
45. Sorrentino V, Nelson JK, Maspero E, Marques AR, Scheer L, Polo S, et al. The LXR-IDOL axis defines a clathrin-, caveolae-, and dynamin-independent endocytic route for LDLR internalization and lysosomal degradation. *J Lipid Res* 2013;**54**:2174-2184.
46. Ehara S, Ueda M, Naruko T, Haze K, Itoh A, Otsuka M, et al. Elevated levels of oxidized low density lipoprotein show a positive relationship with the severity of acute coronary syndromes. *Circulation* 2001;**103**:1955-1960.
47. Palinski W, Rosenfeld ME, Yla-Herttuala S, Gurtner GC, Socher SS, Butler SW, et al. Low density lipoprotein undergoes oxidative modification in vivo. *Proc Natl Acad Sci U S A* 1989;**86**:1372-1376.
48. Loscalzo J, Weinfeld M, Fless GM, Scanu AM. Lipoprotein(a), fibrin binding, and plasminogen activation. *Arteriosclerosis* 1990;**10**:240-245.
49. Kurt B, Soufi M, Sattler A, Schaefer JR. Lipoprotein(a)-clinical aspects and future challenges. *Clin Res Cardiol Suppl* 2015;**10**:26-32.
50. Hoover-Plow J, Huang M. Lipoprotein(a) metabolism: potential sites for therapeutic targets. *Metabolism* 2013;**62**:479-491.
51. Yang XP, Amar MJ, Vaisman B, Bocharov AV, Vishnyakova TG, Freeman LA, et al. Scavenger receptor-BI is a receptor for lipoprotein(a). *J Lipid Res* 2013;**54**:2450-2457.

52. Brunham LR, Kruit JK, Iqbal J, Fievet C, Timmins JM, Pape TD, et al. Intestinal ABCA1 directly contributes to HDL biogenesis in vivo. *J Clin Invest* 2006;**116**:1052-1062.
53. Hersberger M, von Eckardstein A. Low high-density lipoprotein cholesterol: physiological background, clinical importance and drug treatment. *Drugs* 2003;**63**:1907-1945.
54. Santamarina-Fojo S, Lambert G, Hoeg JM, Brewer HB, Jr. Lecithin-cholesterol acyltransferase: role in lipoprotein metabolism, reverse cholesterol transport and atherosclerosis. *Curr Opin Lipidol* 2000;**11**:267-275.
55. van Tol A. Phospholipid transfer protein. *Curr Opin Lipidol* 2002;**13**:135-139.
56. Strauss JG, Zimmermann R, Hrzenjak A, Zhou Y, Kratky D, Levak-Frank S, et al. Endothelial cell-derived lipase mediates uptake and binding of high-density lipoprotein (HDL) particles and the selective uptake of HDL-associated cholesterol esters independent of its enzymic activity. *Biochem J* 2002;**368**:69-79.
57. Silver DL, Wang N, Xiao X, Tall AR. High density lipoprotein (HDL) particle uptake mediated by scavenger receptor class B type 1 results in selective sorting of HDL cholesterol from protein and polarized cholesterol secretion. *J Biol Chem* 2001;**276**:25287-25293.
58. Oram JF, Heinecke JW. ATP-binding cassette transporter A1: a cell cholesterol exporter that protects against cardiovascular disease. *Physiol Rev* 2005;**85**:1343-1372.
59. Annema W, Tietge UJ. Role of hepatic lipase and endothelial lipase in high-density lipoprotein-mediated reverse cholesterol transport. *Curr Atheroscler Rep* 2011;**13**:257-265.
60. Ross R, Agius L. The process of atherogenesis--cellular and molecular interaction: from experimental animal models to humans. *Diabetologia* 1992;**35 Suppl 2**:S34-40.
61. Fortier A, Gullapalli V, Mirshams RA. Review of biomechanical studies of arteries and their effect on stent performance. *IJC Heart & Vessels* 2014;**4**:12-18.
62. Writing Group M, Mozaffarian D, Benjamin EJ, Go AS, Arnett DK, Blaha MJ, et al. Executive Summary: Heart Disease and Stroke Statistics--2016 Update: A Report From the American Heart Association. *Circulation* 2016;**133**:447-454.
63. Glass CK, Witztum JL. Atherosclerosis. the road ahead. *Cell* 2001;**104**:503-516.
64. Luscher TF, Dohi Y, Tanner FC, Boulanger C. Endothelium-dependent control of vascular tone: effects of age, hypertension and lipids. *Basic Res Cardiol* 1991;**86 Suppl 2**:143-158.
65. Gimbrone MA, Jr., Garcia-Cardena G. Vascular endothelium, hemodynamics, and the pathobiology of atherosclerosis. *Cardiovasc Pathol* 2013;**22**:9-15.
66. Schwenke DC, Carew TE. Initiation of atherosclerotic lesions in cholesterol-fed rabbits. II. Selective retention of LDL vs. selective increases in LDL permeability in susceptible sites of arteries. *Arteriosclerosis* 1989;**9**:908-918.
67. Libby P. Vascular biology of atherosclerosis: overview and state of the art. *Am J Cardiol* 2003;**91**:3A-6A.
68. Gimbrone MA, Jr., Garcia-Cardena G. Endothelial Cell Dysfunction and the Pathobiology of Atherosclerosis. *Circ Res* 2016;**118**:620-636.
69. Brown MS, Goldstein JL, Krieger M, Ho YK, Anderson RG. Reversible accumulation of cholesteryl esters in macrophages incubated with acetylated lipoproteins. *J Cell Biol* 1979;**82**:597-613.
70. Brown MS, Goldstein JL. Lipoprotein metabolism in the macrophage: implications for cholesterol deposition in atherosclerosis. *Annu Rev Biochem* 1983;**52**:223-261.
71. Torzewski M, Lackner KJ. Initiation and progression of atherosclerosis--enzymatic or oxidative modification of low-density lipoprotein? *Clin Chem Lab Med* 2006;**44**:1389-1394.
72. Tabas I, Bornfeldt KE. Macrophage Phenotype and Function in Different Stages of Atherosclerosis. *Circ Res* 2016;**118**:653-667.
73. Ridker PM. From C-Reactive Protein to Interleukin-6 to Interleukin-1: Moving Upstream To Identify Novel Targets for Atheroprotection. *Circ Res* 2016;**118**:145-156.
74. Ridker PM, Cannon CP, Morrow D, Rifai N, Rose LM, McCabe CH, et al. C-reactive protein levels and outcomes after statin therapy. *N Engl J Med* 2005;**352**:20-28.
75. Tabas I. Macrophage death and defective inflammation resolution in atherosclerosis. *Nat Rev Immunol* 2010;**10**:36-46.
76. Majesky MW. Developmental basis of vascular smooth muscle diversity. *Arterioscler Thromb Vasc Biol* 2007;**27**:1248-1258.
77. Libby P. Molecular and cellular mechanisms of the thrombotic complications of atherosclerosis. *Journal of lipid research* 2009;**50**:S352-S357.
78. Libby P, Ridker PM, Hansson GK. Progress and challenges in translating the biology of atherosclerosis. *Nature* 2011;**473**:317-325.
79. Brown MS, Goldstein JL. Heart attacks: gone with the century? *Science* 1996;**272**:629.
80. Libby P. The forgotten majority: unfinished business in cardiovascular risk reduction. *J Am Coll Cardiol* 2005;**46**:1225-1228.

81. Cannon CP, Braunwald E, McCabe CH, Rader DJ, Rouleau JL, Belder R, et al. Intensive versus moderate lipid lowering with statins after acute coronary syndromes. *N Engl J Med* 2004;**350**:1495-1504.
82. Nissen SE, Nicholls SJ, Sipahi I, Libby P, Raichlen JS, Ballantyne CM, et al. Effect of very high-intensity statin therapy on regression of coronary atherosclerosis: the ASTEROID trial. *JAMA* 2006;**295**:1556-1565.
83. Pearson TA, Ballantyne CM, Veltri E, Shah A, Bird S, Lin J, et al. Pooled analyses of effects on C-reactive protein and low density lipoprotein cholesterol in placebo-controlled trials of ezetimibe monotherapy or ezetimibe added to baseline statin therapy. *Am J Cardiol* 2009;**103**:369-374.
84. Cannon CP, Blazing MA, Giugliano RP, McCagg A, White JA, Theroux P, et al. Ezetimibe Added to Statin Therapy after Acute Coronary Syndromes. *N Engl J Med* 2015;**372**:2387-2397.
85. Lambert G, Sjouke B, Choque B, Kastelein JJ, Hovingh GK. The PCSK9 decade. *J Lipid Res* 2012;**53**:2515-2524.
86. Lepor NE, Kereiakes DJ. The PCSK9 Inhibitors: A Novel Therapeutic Target Enters Clinical Practice. *Am Health Drug Benefits* 2015;**8**:483-489.
87. Colhoun HM, Robinson JG, Farnier M, Cariou B, Blom D, Kereiakes DJ, et al. Efficacy and safety of alirocumab, a fully human PCSK9 monoclonal antibody, in high cardiovascular risk patients with poorly controlled hypercholesterolemia on maximally tolerated doses of statins: rationale and design of the ODYSSEY COMBO I and II trials. *BMC Cardiovasc Disord* 2014;**14**:121.
88. Kastelein JJ, Ginsberg HN, Langslet G, Hovingh GK, Ceska R, Dufour R, et al. ODYSSEY FH I and FH II: 78 week results with alirocumab treatment in 735 patients with heterozygous familial hypercholesterolaemia. *Eur Heart J* 2015;**36**:2996-3003.
89. Moriarty PM, Jacobson TA, Bruckert E, Thompson PD, Guyton JR, Baccara-Dinet MT, et al. Efficacy and safety of alirocumab, a monoclonal antibody to PCSK9, in statin-intolerant patients: design and rationale of ODYSSEY ALTERNATIVE, a randomized phase 3 trial. *J Clin Lipidol* 2014;**8**:554-561.
90. Schwartz GG, Bessac L, Berdan LG, Bhatt DL, Bittner V, Diaz R, et al. Effect of alirocumab, a monoclonal antibody to PCSK9, on long-term cardiovascular outcomes following acute coronary syndromes: rationale and design of the ODYSSEY outcomes trial. *Am Heart J* 2014;**168**:682-689.
91. Sabatine MS, Giugliano RP, Keech AC, Honarpour N, Wiviott SD, Murphy SA, et al. Evolocumab and Clinical Outcomes in Patients with Cardiovascular Disease. *N Engl J Med* 2017;**376**:1713-1722.
92. Fitzgerald K, Frank-Kamenetsky M, Shulga-Morskaya S, Liebow A, Bettencourt BR, Sutherland JE, et al. Effect of an RNA interference drug on the synthesis of proprotein convertase subtilisin/kexin type 9 (PCSK9) and the concentration of serum LDL cholesterol in healthy volunteers: a randomised, single-blind, placebo-controlled, phase 1 trial. *Lancet* 2014;**383**:60-68.
93. Fitzgerald K, White S, Borodovsky A, Bettencourt BR, Strahs A, Clausen V, et al. A Highly Durable RNAi Therapeutic Inhibitor of PCSK9. *N Engl J Med* 2017;**376**:41-51.
94. Anderson TJ, Gregoire J, Pearson GJ, Barry AR, Couture P, Dawes M, et al. 2016 Canadian Cardiovascular Society Guidelines for the Management of Dyslipidemia for the Prevention of Cardiovascular Disease in the Adult. *Can J Cardiol* 2016;**32**:1263-1282.
95. Mancini GB, Baker S, Bergeron J, Fitchett D, Frohlich J, Genest J, et al. Diagnosis, Prevention, and Management of Statin Adverse Effects and Intolerance: Canadian Consensus Working Group Update (2016). *Can J Cardiol* 2016;**32**:S35-65.
96. Kronenberg F, Utermann G. Lipoprotein(a): resurrected by genetics. *J Intern Med* 2013;**273**:6-30.
97. Jansen AC, van Aalst-Cohen ES, Tanck MW, Trip MD, Lansberg PJ, Liem AH, et al. The contribution of classical risk factors to cardiovascular disease in familial hypercholesterolaemia: data in 2400 patients. *J Intern Med* 2004;**256**:482-490.
98. Panta R, Dahal K, Kunwar S. Efficacy and safety of mipomersen in treatment of dyslipidemia: a meta-analysis of randomized controlled trials. *J Clin Lipidol* 2015;**9**:217-225.
99. Hashemi N, Odze RD, McGowan MP, Santos RD, Stroes ES, Cohen DE. Liver histology during Mipomersen therapy for severe hypercholesterolemia. *J Clin Lipidol* 2014;**8**:606-611.
100. Raal FJ, Giugliano RP, Sabatine MS, Koren MJ, Langslet G, Bays H, et al. Reduction in lipoprotein(a) with PCSK9 monoclonal antibody evolocumab (AMG 145): a pooled analysis of more than 1,300 patients in 4 phase II trials. *J Am Coll Cardiol* 2014;**63**:1278-1288.
101. Hovingh GK, Kastelein JJ, van Deventer SJ, Round P, Ford J, Saleheen D, et al. Cholesterol ester transfer protein inhibition by TA-8995 in patients with mild dyslipidaemia (TULIP): a randomised, double-blind, placebo-controlled phase 2 trial. *Lancet* 2015;**386**:452-460.
102. Emerging Risk Factors C, Di Angelantonio E, Sarwar N, Perry P, Kaptoge S, Ray KK, et al. Major lipids, apolipoproteins, and risk of vascular disease. *JAMA* 2009;**302**:1993-2000.
103. Nissen SE, Tsunoda T, Tuzcu EM, Schoenhagen P, Cooper CJ, Yasin M, et al. Effect of recombinant ApoA-I Milano on coronary atherosclerosis in patients with acute coronary syndromes: a randomized controlled trial. *JAMA* 2003;**290**:2292-2300.

104. Tardif JC, Gregoire J, L'Allier PL, Ibrahim R, Lesperance J, Heinonen TM, et al. Effects of reconstituted high-density lipoprotein infusions on coronary atherosclerosis: a randomized controlled trial. *JAMA* 2007;**297**:1675-1682.
105. Navab M, Anantharamaiah GM, Reddy ST, Van Lenten BJ, Hough G, Wagner A, et al. Human apolipoprotein AI mimetic peptides for the treatment of atherosclerosis. *Curr Opin Investig Drugs* 2003;**4**:1100-1104.
106. Degoma EM, Rader DJ. Novel HDL-directed pharmacotherapeutic strategies. *Nat Rev Cardiol* 2011;**8**:266-277.
107. Rye KA, Bursill CA, Lambert G, Tabet F, Barter PJ. The metabolism and anti-atherogenic properties of HDL. *J Lipid Res* 2009;**50 Suppl**:S195-200.
108. Vaisar T, Pennathur S, Green PS, Gharib SA, Hoofnagle AN, Cheung MC, et al. Shotgun proteomics implicates protease inhibition and complement activation in the antiinflammatory properties of HDL. *J Clin Invest* 2007;**117**:746-756.
109. Brewer HB, Jr. High-density lipoproteins: a new potential therapeutic target for the prevention of cardiovascular disease. *Arterioscler Thromb Vasc Biol* 2004;**24**:387-391.
110. Chapman MJ, Le Goff W, Guerin M, Kontush A. Cholesteryl ester transfer protein: at the heart of the action of lipid-modulating therapy with statins, fibrates, niacin, and cholesteryl ester transfer protein inhibitors. *Eur Heart J* 2010;**31**:149-164.
111. Jahangiri A, de Beer MC, Noffsinger V, Tannock LR, Ramaiah C, Webb NR, et al. HDL remodeling during the acute phase response. *Arterioscler Thromb Vasc Biol* 2009;**29**:261-267.
112. Asztalos BF, de la Llera-Moya M, Dallal GE, Horvath KV, Schaefer EJ, Rothblat GH. Differential effects of HDL subpopulations on cellular ABCA1- and SR-BI-mediated cholesterol efflux. *J Lipid Res* 2005;**46**:2246-2253.
113. Tall AR, Yvan-Charvet L, Terasaka N, Pagler T, Wang N. HDL, ABC transporters, and cholesterol efflux: implications for the treatment of atherosclerosis. *Cell Metab* 2008;**7**:365-375.
114. Barter PJ, Caulfield M, Eriksson M, Grundy SM, Kastelein JJ, Komajda M, et al. Effects of torcetrapib in patients at high risk for coronary events. *N Engl J Med* 2007;**357**:2109-2122.
115. Barter PJ, Kastelein JJ. Targeting cholesteryl ester transfer protein for the prevention and management of cardiovascular disease. *J Am Coll Cardiol* 2006;**47**:492-499.
116. Schwartz GG, Olsson AG, Abt M, Ballantyne CM, Barter PJ, Brumm J, et al. Effects of dalcetrapib in patients with a recent acute coronary syndrome. *N Engl J Med* 2012;**367**:2089-2099.
117. Lincoff AM, Nicholls SJ, Riesmeyer JS, Barter PJ, Brewer HB, Fox KAA, et al. Evacetrapib and Cardiovascular Outcomes in High-Risk Vascular Disease. *N Engl J Med* 2017;**376**:1933-1942.
118. Cannon CP, Shah S, Dansky HM, Davidson M, Brinton EA, Gotto AM, et al. Safety of anacetrapib in patients with or at high risk for coronary heart disease. *N Engl J Med* 2010;**363**:2406-2415.
119. Group HTRC. Effects of Anacetrapib in Patients with Atherosclerotic Vascular Disease. *N Engl J Med* 2017.
120. Furchgott RF, Zawadzki JV. The obligatory role of endothelial cells in the relaxation of arterial smooth muscle by acetylcholine. *Nature* 1980;**288**:373-376.
121. Celermajer DS. Endothelial dysfunction: does it matter? Is it reversible? *J Am Coll Cardiol* 1997;**30**:325-333.
122. Dzau VJ, Gibbons GH, Cooke JP, Omoigui N. Vascular biology and medicine in the 1990s: scope, concepts, potentials, and perspectives. *Circulation* 1993;**87**:705-719.
123. Simionescu M. Implications of early structural-functional changes in the endothelium for vascular disease. *Arterioscler Thromb Vasc Biol* 2007;**27**:266-274.
124. Landmesser U, Hornig B, Drexler H. Endothelial function: a critical determinant in atherosclerosis? *Circulation* 2004;**109**:II27-33.
125. Rader DJ, Dugi KA. The endothelium and lipoproteins: insights from recent cell biology and animal studies. *Semin Thromb Hemost* 2000;**26**:521-528.
126. Gleissner CA, Leitinger N, Ley K. Effects of native and modified low-density lipoproteins on monocyte recruitment in atherosclerosis. *Hypertension* 2007;**50**:276-283.
127. Sawamura T, Kume N, Aoyama T, Moriwaki H, Hoshikawa H, Aiba Y, et al. An endothelial receptor for oxidized low-density lipoprotein. *Nature* 1997;**386**:73-77.
128. Chen J, Mehta JL, Haider N, Zhang X, Narula J, Li D. Role of caspases in Ox-LDL-induced apoptotic cascade in human coronary artery endothelial cells. *Circ Res* 2004;**94**:370-376.
129. Mehta JL, Sanada N, Hu CP, Chen J, Dandapat A, Sugawara F, et al. Deletion of LOX-1 reduces atherogenesis in LDLR knockout mice fed high cholesterol diet. *Circ Res* 2007;**100**:1634-1642.
130. Li DY, Chen HJ, Staples ED, Ozaki K, Annex B, Singh BK, et al. Oxidized low-density lipoprotein receptor LOX-1 and apoptosis in human atherosclerotic lesions. *J Cardiovasc Pharmacol Ther* 2002;**7**:147-153.

131. Glomset JA, Janssen ET, Kennedy R, Dobbins J. Role of plasma lecithin:cholesterol acyltransferase in the metabolism of high density lipoproteins. *J Lipid Res* 1966;**7**:638-648.
132. Rader DJ, Alexander ET, Weibel GL, Billheimer J, Rothblat GH. The role of reverse cholesterol transport in animals and humans and relationship to atherosclerosis. *J Lipid Res* 2009;**50 Suppl**:S189-194.
133. Yancey PG, Bortnick AE, Kellner-Weibel G, de la Llera-Moya M, Phillips MC, Rothblat GH. Importance of different pathways of cellular cholesterol efflux. *Arterioscler Thromb Vasc Biol* 2003;**23**:712-719.
134. O'Connell BJ, Denis M, Genest J. Cellular physiology of cholesterol efflux in vascular endothelial cells. *Circulation* 2004;**110**:2881-2888.
135. Miao L, Okoro EU, Cao Z, Yang H, Motley-Johnson E, Guo Z. High-density lipoprotein-mediated transcellular cholesterol transport in mouse aortic endothelial cells. *Biochem Biophys Res Commun* 2015;**465**:256-261.
136. Tall AR. Cholesterol efflux pathways and other potential mechanisms involved in the athero-protective effect of high density lipoproteins. *J Intern Med* 2008;**263**:256-273.
137. Tabas I, Williams KJ, Boren J. Subendothelial lipoprotein retention as the initiating process in atherosclerosis: update and therapeutic implications. *Circulation* 2007;**116**:1832-1844.
138. Rippe B, Rosengren BI, Carlsson O, Venturoli D. Transendothelial transport: the vesicle controversy. *J Vasc Res* 2002;**39**:375-390.
139. Komarova Y, Malik AB. Regulation of endothelial permeability via paracellular and transcellular transport pathways. *Annu Rev Physiol* 2010;**72**:463-493.
140. Bazzoni G, Dejana E. Endothelial cell-to-cell junctions: molecular organization and role in vascular homeostasis. *Physiol Rev* 2004;**84**:869-901.
141. Thurston G, Suri C, Smith K, McClain J, Sato TN, Yancopoulos GD, et al. Leakage-resistant blood vessels in mice transgenically overexpressing angiopoietin-1. *Science* 1999;**286**:2511-2514.
142. Rosen H, Gonzalez-Cabrera PJ, Sanna MG, Brown S. Sphingosine 1-phosphate receptor signaling. *Annu Rev Biochem* 2009;**78**:743-768.
143. Tauseef M, Kini V, Knezevic N, Brannan M, Ramchandaran R, Fyrst H, et al. Activation of sphingosine kinase-1 reverses the increase in lung vascular permeability through sphingosine-1-phosphate receptor signaling in endothelial cells. *Circ Res* 2008;**103**:1164-1172.
144. Liu Y, Wada R, Yamashita T, Mi Y, Deng CX, Hobson JP, et al. Edg-1, the G protein-coupled receptor for sphingosine-1-phosphate, is essential for vascular maturation. *J Clin Invest* 2000;**106**:951-961.
145. Lee MJ, Thangada S, Claffey KP, Ancellin N, Liu CH, Kluk M, et al. Vascular endothelial cell adherens junction assembly and morphogenesis induced by sphingosine-1-phosphate. *Cell* 1999;**99**:301-312.
146. Murata N, Sato K, Kon J, Tomura H, Yanagita M, Kuwabara A, et al. Interaction of sphingosine 1-phosphate with plasma components, including lipoproteins, regulates the lipid receptor-mediated actions. *Biochem J* 2000;**352 Pt 3**:809-815.
147. Christoffersen C, Obinata H, Kumaraswamy SB, Galvani S, Ahnstrom J, Sevvana M, et al. Endothelium-protective sphingosine-1-phosphate provided by HDL-associated apolipoprotein M. *Proc Natl Acad Sci U S A* 2011;**108**:9613-9618.
148. Vasile E, Simionescu M, Simionescu N. Visualization of the binding, endocytosis, and transcytosis of low-density lipoprotein in the arterial endothelium in situ. *J Cell Biol* 1983;**96**:1677-1689.
149. Bhalodkar NC, Blum S, Rana T, Kitchappa R, Bhalodkar AN, Enas EA. Comparison of high-density and low-density lipoprotein cholesterol subclasses and sizes in Asian Indian women with Caucasian women from the Framingham Offspring Study. *Clin Cardiol* 2005;**28**:247-251.
150. von Eckardstein A, Rohrer L. Transendothelial lipoprotein transport and regulation of endothelial permeability and integrity by lipoproteins. *Curr Opin Lipidol* 2009;**20**:197-205.
151. Williams KJ, Tabas I. The response-to-retention hypothesis of early atherogenesis. *Arterioscler Thromb Vasc Biol* 1995;**15**:551-561.
152. Frank PG, Pavlides S, Cheung MW, Daumer K, Lisanti MP. Role of caveolin-1 in the regulation of lipoprotein metabolism. *Am J Physiol Cell Physiol* 2008;**295**:C242-248.
153. Bian F, Yang X, Zhou F, Wu PH, Xing S, Xu G, et al. C-reactive protein promotes atherosclerosis by increasing LDL transcytosis across endothelial cells. *Br J Pharmacol* 2014;**171**:2671-2684.
154. Quest AF, Leyton L, Parraga M. Caveolins, caveolae, and lipid rafts in cellular transport, signaling, and disease. *Biochem Cell Biol* 2004;**82**:129-144.
155. Armstrong SM, Sugiyama MG, Fung KY, Gao Y, Wang C, Levy AS, et al. A novel assay uncovers an unexpected role for SR-BI in LDL transcytosis. *Cardiovasc Res* 2015;**108**:268-277.
156. Cancel LM, Tarbell JM. The role of mitosis in LDL transport through cultured endothelial cell monolayers. *Am J Physiol Heart Circ Physiol* 2011;**300**:H769-776.

157. Lin SJ, Jan KM, Chien S. Role of dying endothelial cells in transendothelial macromolecular transport. *Arteriosclerosis* 1990;**10**:703-709.
158. Cancel LM, Fitting A, Tarbell JM. In vitro study of LDL transport under pressurized (convective) conditions. *Am J Physiol Heart Circ Physiol* 2007;**293**:H126-132.
159. Kraehling JR, Chidlow JH, Rajagopal C, Sugiyama MG, Fowler JW, Lee MY, et al. Genome-wide RNAi screen reveals ALK1 mediates LDL uptake and transcytosis in endothelial cells. *Nat Commun* 2016;**7**:13516.
160. Robert J, Lehner M, Frank S, Perisa D, von Eckardstein A, Rohrer L. Interleukin 6 stimulates endothelial binding and transport of high-density lipoprotein through induction of endothelial lipase. *Arterioscler Thromb Vasc Biol* 2013;**33**:2699-2706.
161. Rohrer L, Ohnsorg PM, Lehner M, Landolt F, Rinninger F, von Eckardstein A. High-density lipoprotein transport through aortic endothelial cells involves scavenger receptor BI and ATP-binding cassette transporter G1. *Circ Res* 2009;**104**:1142-1150.
162. Cavelier C, Ohnsorg PM, Rohrer L, von Eckardstein A. The beta-chain of cell surface F(0)F(1) ATPase modulates apoA-I and HDL transcytosis through aortic endothelial cells. *Arterioscler Thromb Vasc Biol* 2012;**32**:131-139.
163. Cavelier C, Rohrer L, von Eckardstein A. ATP-Binding cassette transporter A1 modulates apolipoprotein A-I transcytosis through aortic endothelial cells. *Circ Res* 2006;**99**:1060-1066.
164. Mehta D, Malik AB. Signaling mechanisms regulating endothelial permeability. *Physiol Rev* 2006;**86**:279-367.
165. Chao WT, Fan SS, Chen JK, Yang VC. Visualizing caveolin-1 and HDL in cholesterol-loaded aortic endothelial cells. *J Lipid Res* 2003;**44**:1094-1099.
166. Perisa D, Rohrer L, Kaech A, von Eckardstein A. Itinerary of high density lipoproteins in endothelial cells. *Biochim Biophys Acta* 2016;**1861**:98-107.
167. Dean M, Hamon Y, Chimini G. The human ATP-binding cassette (ABC) transporter superfamily. *J Lipid Res* 2001;**42**:1007-1017.
168. Aiello RJ, Brees D, Francone OL. ABCA1-deficient mice: insights into the role of monocyte lipid efflux in HDL formation and inflammation. *Arterioscler Thromb Vasc Biol* 2003;**23**:972-980.
169. Tang C, Oram JF. The cell cholesterol exporter ABCA1 as a protector from cardiovascular disease and diabetes. *Biochim Biophys Acta* 2009;**1791**:563-572.
170. Fitzgerald ML, Mendez AJ, Moore KJ, Andersson LP, Panjeton HA, Freeman MW. ATP-binding cassette transporter A1 contains an NH2-terminal signal anchor sequence that translocates the protein's first hydrophilic domain to the exoplasmic space. *J Biol Chem* 2001;**276**:15137-15145.
171. Quazi F, Molday RS. Differential phospholipid substrates and directional transport by ATP-binding cassette proteins ABCA1, ABCA7, and ABCA4 and disease-causing mutants. *J Biol Chem* 2013;**288**:34414-34426.
172. Oram JF, Yokoyama S. Apolipoprotein-mediated removal of cellular cholesterol and phospholipids. *J Lipid Res* 1996;**37**:2473-2491.
173. Smith JD, Le Goff W, Settle M, Brubaker G, Waelde C, Horwitz A, et al. ABCA1 mediates concurrent cholesterol and phospholipid efflux to apolipoprotein A-I. *J Lipid Res* 2004;**45**:635-644.
174. Chen W, Sun Y, Welch C, Gorelik A, Leventhal AR, Tabas I, et al. Preferential ATP-binding cassette transporter A1-mediated cholesterol efflux from late endosomes/lysosomes. *J Biol Chem* 2001;**276**:43564-43569.
175. Oram JF. HDL apolipoproteins and ABCA1: partners in the removal of excess cellular cholesterol. *Arterioscler Thromb Vasc Biol* 2003;**23**:720-727.
176. Marcil M, Brooks-Wilson A, Clee SM, Roomp K, Zhang LH, Yu L, et al. Mutations in the ABC1 gene in familial HDL deficiency with defective cholesterol efflux. *Lancet* 1999;**354**:1341-1346.
177. Francis GA, Knopp RH, Oram JF. Defective removal of cellular cholesterol and phospholipids by apolipoprotein A-I in Tangier Disease. *J Clin Invest* 1995;**96**:78-87.
178. Assmann G, von Eckardstein A, Brewer H. Familial high density lipoprotein deficiency: Tangier disease. *The metabolic and molecular bases of inherited disease* 1995:2053-2072.
179. Bisoendial RJ, Hovingh GK, Levels JH, Lerch PG, Andresen I, Hayden MR, et al. Restoration of endothelial function by increasing high-density lipoprotein in subjects with isolated low high-density lipoprotein. *Circulation* 2003;**107**:2944-2948.
180. Wellington CL, Brunham LR, Zhou S, Singaraja RR, Visscher H, Gelfer A, et al. Alterations of plasma lipids in mice via adenoviral-mediated hepatic overexpression of human ABCA1. *J Lipid Res* 2003;**44**:1470-1480.
181. Westerterp M, Tsuchiya K, Tattersall IW, Fotakis P, Bochem AE, Molusky MM, et al. Deficiency of ATP-Binding Cassette Transporters A1 and G1 in Endothelial Cells Accelerates Atherosclerosis in Mice. *Arterioscler Thromb Vasc Biol* 2016;**36**:1328-1337.

182. Vaisman BL, Demosky SJ, Stonik JA, Ghias M, Knapper CL, Sampson ML, et al. Endothelial expression of human ABCA1 in mice increases plasma HDL cholesterol and reduces diet-induced atherosclerosis. *J Lipid Res* 2012;**53**:158-167.
183. Gelissen IC, Cartland S, Brown AJ, Sandoval C, Kim M, Dinnes DL, et al. Expression and stability of two isoforms of ABCG1 in human vascular cells. *Atherosclerosis* 2010;**208**:75-82.
184. Klucken J, Buchler C, Orso E, Kaminski WE, Porsch-Ozcurumez M, Liebisch G, et al. ABCG1 (ABC8), the human homolog of the Drosophila white gene, is a regulator of macrophage cholesterol and phospholipid transport. *Proc Natl Acad Sci U S A* 2000;**97**:817-822.
185. Wang N, Lan D, Chen W, Matsuura F, Tall AR. ATP-binding cassette transporters G1 and G4 mediate cellular cholesterol efflux to high-density lipoproteins. *Proc Natl Acad Sci U S A* 2004;**101**:9774-9779.
186. Vaughan AM, Oram JF. ABCG1 redistributes cell cholesterol to domains removable by high density lipoprotein but not by lipid-depleted apolipoproteins. *J Biol Chem* 2005;**280**:30150-30157.
187. Kobayashi A, Takanezawa Y, Hirata T, Shimizu Y, Misasa K, Kioka N, et al. Efflux of sphingomyelin, cholesterol, and phosphatidylcholine by ABCG1. *J Lipid Res* 2006;**47**:1791-1802.
188. Xu M, Zhou H, Tan KC, Guo R, Shiu SW, Wong Y. ABCG1 mediated oxidized LDL-derived oxysterol efflux from macrophages. *Biochem Biophys Res Commun* 2009;**390**:1349-1354.
189. Kennedy MA, Barrera GC, Nakamura K, Baldan A, Tarr P, Fishbein MC, et al. ABCG1 has a critical role in mediating cholesterol efflux to HDL and preventing cellular lipid accumulation. *Cell Metab* 2005;**1**:121-131.
190. Jessup W, Gelissen IC, Gaus K, Kritharides L. Roles of ATP binding cassette transporters A1 and G1, scavenger receptor BI and membrane lipid domains in cholesterol export from macrophages. *Curr Opin Lipidol* 2006;**17**:247-257.
191. Kerr ID, Haider AJ, Gelissen IC. The ABCG family of membrane-associated transporters: you don't have to be big to be mighty. *Br J Pharmacol* 2011;**164**:1767-1779.
192. Hegyi Z, Homolya L. Functional Cooperativity between ABCG4 and ABCG1 Isoforms. *PLoS One* 2016;**11**:e0156516.
193. Wang N, Ranalletta M, Matsuura F, Peng F, Tall AR. LXR-induced redistribution of ABCG1 to plasma membrane in macrophages enhances cholesterol mass efflux to HDL. *Arterioscler Thromb Vasc Biol* 2006;**26**:1310-1316.
194. Neufeld EB, O'Brien K, Walts AD, Stonik JA, Demosky SJ, Malide D, et al. Cellular Localization and Trafficking of the Human ABCG1 Transporter. *Biology (Basel)* 2014;**3**:781-800.
195. Tarling EJ, Edwards PA. ATP binding cassette transporter G1 (ABCG1) is an intracellular sterol transporter. *Proc Natl Acad Sci U S A* 2011;**108**:19719-19724.
196. Pandzic E, Gelissen IC, Whan R, Barter PJ, Sviridov D, Gaus K, et al. The ATP binding cassette transporter, ABCG1, localizes to cortical actin filaments. *Sci Rep* 2017;**7**:42025.
197. Wiersma H, Nijstad N, de Boer JF, Out R, Hogewerf W, Van Berkel TJ, et al. Lack of Abcg1 results in decreased plasma HDL cholesterol levels and increased biliary cholesterol secretion in mice fed a high cholesterol diet. *Atherosclerosis* 2009;**206**:141-147.
198. Wang X, Collins HL, Ranalletta M, Fuki IV, Billheimer JT, Rothblat GH, et al. Macrophage ABCA1 and ABCG1, but not SR-BI, promote macrophage reverse cholesterol transport in vivo. *J Clin Invest* 2007;**117**:2216-2224.
199. Terasaka N, Yu S, Yvan-Charvet L, Wang N, Mzhavia N, Langlois R, et al. ABCG1 and HDL protect against endothelial dysfunction in mice fed a high-cholesterol diet. *J Clin Invest* 2008;**118**:3701-3713.
200. Westerterp M, Koetsveld J, Yu S, Han S, Li R, Goldberg IJ, et al. Increased atherosclerosis in mice with vascular ATP-binding cassette transporter G1 deficiency--brief report. *Arterioscler Thromb Vasc Biol* 2010;**30**:2103-2105.
201. Whetzel AM, Sturek JM, Nagelin MH, Bolick DT, Gebre AK, Parks JS, et al. ABCG1 deficiency in mice promotes endothelial activation and monocyte-endothelial interactions. *Arterioscler Thromb Vasc Biol* 2010;**30**:809-817.
202. Hirata K, Dichek HL, Cioffi JA, Choi SY, Leeper NJ, Quintana L, et al. Cloning of a unique lipase from endothelial cells extends the lipase gene family. *J Biol Chem* 1999;**274**:14170-14175.
203. Jaye M, Lynch KJ, Krawiec J, Marchadier D, Maugeais C, Doan K, et al. A novel endothelial-derived lipase that modulates HDL metabolism. *Nat Genet* 1999;**21**:424-428.
204. Yu KC, David C, Kadambi S, Stahl A, Hirata K, Ishida T, et al. Endothelial lipase is synthesized by hepatic and aorta endothelial cells and its expression is altered in apoE-deficient mice. *J Lipid Res* 2004;**45**:1614-1623.
205. McCoy MG, Sun GS, Marchadier D, Maugeais C, Glick JM, Rader DJ. Characterization of the lipolytic activity of endothelial lipase. *J Lipid Res* 2002;**43**:921-929.
206. Fuki IV, Blanchard N, Jin W, Marchadier DH, Millar JS, Glick JM, et al. Endogenously produced endothelial lipase enhances binding and cellular processing of plasma lipoproteins via heparan sulfate proteoglycan-mediated pathway. *J Biol Chem* 2003;**278**:34331-34338.

207. Ishida T, Choi S, Kundu RK, Hirata K, Rubin EM, Cooper AD, et al. Endothelial lipase is a major determinant of HDL level. *J Clin Invest* 2003;**111**:347-355.
208. Jin W, Millar JS, Broedl U, Glick JM, Rader DJ. Inhibition of endothelial lipase causes increased HDL cholesterol levels in vivo. *J Clin Invest* 2003;**111**:357-362.
209. Tatematsu S, Francis SA, Natarajan P, Rader DJ, Saghatelian A, Brown JD, et al. Endothelial lipase is a critical determinant of high-density lipoprotein-stimulated sphingosine 1-phosphate-dependent signaling in vascular endothelium. *Arterioscler Thromb Vasc Biol* 2013;**33**:1788-1794.
210. Ross R. Atherosclerosis--an inflammatory disease. *N Engl J Med* 1999;**340**:115-126.
211. Hirata K, Ishida T, Matsushita H, Tsao PS, Quertermous T. Regulated expression of endothelial cell-derived lipase. *Biochem Biophys Res Commun* 2000;**272**:90-93.
212. Yancey PG, Kawashiri MA, Moore R, Glick JM, Williams DL, Connelly MA, et al. In vivo modulation of HDL phospholipid has opposing effects on SR-BI- and ABCA1-mediated cholesterol efflux. *J Lipid Res* 2004;**45**:337-346.
213. Brown RJ, Lagor WR, Sankaranaravanan S, Yasuda T, Quertermous T, Rothblat GH, et al. Impact of combined deficiency of hepatic lipase and endothelial lipase on the metabolism of both high-density lipoproteins and apolipoprotein B-containing lipoproteins. *Circ Res* 2010;**107**:357-364.
214. Qiu G, Hill JS. Endothelial lipase promotes apolipoprotein AI-mediated cholesterol efflux in THP-1 macrophages. *Arterioscler Thromb Vasc Biol* 2009;**29**:84-91.
215. Badellino KO, Wolfe ML, Reilly MP, Rader DJ. Endothelial lipase concentrations are increased in metabolic syndrome and associated with coronary atherosclerosis. *PLoS Med* 2006;**3**:e22.
216. Ko KW, Paul A, Ma K, Li L, Chan L. Endothelial lipase modulates HDL but has no effect on atherosclerosis development in apoE-/- and LDLR-/- mice. *J Lipid Res* 2005;**46**:2586-2594.
217. Ishida T, Choi SY, Kundu RK, Spin J, Yamashita T, Hirata K, et al. Endothelial lipase modulates susceptibility to atherosclerosis in apolipoprotein-E-deficient mice. *J Biol Chem* 2004;**279**:45085-45092.
218. Voight BF, Peloso GM, Orho-Melander M, Frikke-Schmidt R, Barbalic M, Jensen MK, et al. Plasma HDL cholesterol and risk of myocardial infarction: a mendelian randomisation study. *Lancet* 2012;**380**:572-580.
219. Calvo D, Vega MA. Identification, primary structure, and distribution of CLA-1, a novel member of the CD36/LIMPII gene family. *J Biol Chem* 1993;**268**:18929-18935.
220. Pei Y, Chen X, Aboutouk D, Fuller MT, Dadoo O, Yu P, et al. SR-BI in bone marrow derived cells protects mice from diet induced coronary artery atherosclerosis and myocardial infarction. *PLoS One* 2013;**8**:e72492.
221. Acton S, Rigotti A, Landschulz KT, Xu S, Hobbs HH, Krieger M. Identification of scavenger receptor SR-BI as a high density lipoprotein receptor. *Science* 1996;**271**:518-520.
222. Kellner-Weibel G, de La Llera-Moya M, Connelly MA, Stoudt G, Christian AE, Haynes MP, et al. Expression of scavenger receptor BI in COS-7 cells alters cholesterol content and distribution. *Biochemistry* 2000;**39**:221-229.
223. Yancey PG, de la Llera-Moya M, Swarnakar S, Monzo P, Klein SM, Connelly MA, et al. High density lipoprotein phospholipid composition is a major determinant of the bi-directional flux and net movement of cellular free cholesterol mediated by scavenger receptor BI. *J Biol Chem* 2000;**275**:36596-36604.
224. Christison J, Karjalainen A, Brauman J, Bygrave F, Stocker R. Rapid reduction and removal of HDL- but not LDL-associated cholesteryl ester hydroperoxides by rat liver perfused in situ. *Biochem J* 1996;**314 (Pt 3)**:739-742.
225. Van Eck M, Hoekstra M, Hildebrand RB, Yaong Y, Stengel D, Kruijt JK, et al. Increased oxidative stress in scavenger receptor BI knockout mice with dysfunctional HDL. *Arterioscler Thromb Vasc Biol* 2007;**27**:2413-2419.
226. Thacker SG, Rousset X, Esmail S, Zarzour A, Jin X, Collins HL, et al. Increased plasma cholesterol esterification by LCAT reduces diet-induced atherosclerosis in SR-BI knockout mice. *J Lipid Res* 2015;**56**:1282-1295.
227. Linton MF, Tao H, Linton EF, Yancey PG. SR-BI: A Multifunctional Receptor in Cholesterol Homeostasis and Atherosclerosis. *Trends Endocrinol Metab* 2017;**28**:461-472.
228. Connelly MA, de la Llera-Moya M, Monzo P, Yancey PG, Drazul D, Stoudt G, et al. Analysis of chimeric receptors shows that multiple distinct functional activities of scavenger receptor, class B, type I (SR-BI), are localized to the extracellular receptor domain. *Biochemistry* 2001;**40**:5249-5259.
229. Kartz GA, Holme RL, Nicholson K, Sahoo D. SR-BI/CD36 chimeric receptors define extracellular subdomains of SR-BI critical for cholesterol transport. *Biochemistry* 2014;**53**:6173-6182.
230. Neculai D, Schwake M, Ravichandran M, Zunke F, Collins RF, Peters J, et al. Structure of LIMP-2 provides functional insights with implications for SR-BI and CD36. *Nature* 2013;**504**:172-176.

231. Sahoo D, Peng Y, Smith JR, Darlington YF, Connelly MA. Scavenger receptor class B, type I (SR-BI) homo-dimerizes via its C-terminal region: fluorescence resonance energy transfer analysis. *Biochim Biophys Acta* 2007;**1771**:818-829.
232. Gaidukov L, Nager AR, Xu S, Penman M, Krieger M. Glycine dimerization motif in the N-terminal transmembrane domain of the high density lipoprotein receptor SR-BI required for normal receptor oligomerization and lipid transport. *J Biol Chem* 2011;**286**:18452-18464.
233. Zhu W, Saddar S, Seetharam D, Chambliss KL, Longoria C, Silver DL, et al. The scavenger receptor class B type I adaptor protein PDZK1 maintains endothelial monolayer integrity. *Circ Res* 2008;**102**:480-487.
234. Al-Jarallah A, Chen X, Gonzalez L, Trigatti BL. High density lipoprotein stimulated migration of macrophages depends on the scavenger receptor class B, type I, PDZK1 and Akt1 and is blocked by sphingosine 1 phosphate receptor antagonists. *PLoS One* 2014;**9**:e106487.
235. Yesilaltay A, Kocher O, Pal R, Leiva A, Quinones V, Rigotti A, et al. PDZK1 is required for maintaining hepatic scavenger receptor, class B, type I (SR-BI) steady state levels but not its surface localization or function. *J Biol Chem* 2006;**281**:28975-28980.
236. Assanasen C, Mineo C, Seetharam D, Yuhanna IS, Marcel YL, Connelly MA, et al. Cholesterol binding, efflux, and a PDZ-interacting domain of scavenger receptor-BI mediate HDL-initiated signaling. *J Clin Invest* 2005;**115**:969-977.
237. Saddar S, Carriere V, Lee WR, Tanigaki K, Yuhanna IS, Parathath S, et al. Scavenger receptor class B type I is a plasma membrane cholesterol sensor. *Circ Res* 2013;**112**:140-151.
238. Fuller M, Dadoo O, Serkis V, Abutouk D, MacDonald M, Dhingani N, et al. The effects of diet on occlusive coronary artery atherosclerosis and myocardial infarction in scavenger receptor class B, type 1/low-density lipoprotein receptor double knockout mice. *Arterioscler Thromb Vasc Biol* 2014;**34**:2394-2403.
239. Song GJ, Kim SM, Park KH, Kim J, Choi I, Cho KH. SR-BI mediates high density lipoprotein (HDL)-induced anti-inflammatory effect in macrophages. *Biochem Biophys Res Commun* 2015;**457**:112-118.
240. Tao H, Yancey PG, Babaev VR, Blakemore JL, Zhang Y, Ding L, et al. Macrophage SR-BI mediates efferocytosis via Src/PI3K/Rac1 signaling and reduces atherosclerotic lesion necrosis. *J Lipid Res* 2015;**56**:1449-1460.
241. Vaisman BL, Vishnyakova TG, Freeman LA, Amar MJ, Demosky SJ, Liu C, et al. Endothelial Expression of Scavenger Receptor Class B, Type I Protects against Development of Atherosclerosis in Mice. *Biomed Res Int* 2015;**2015**:607120.
242. Lim HY, Thiam CH, Yeo KP, Bisoendial R, Hii CS, McGrath KC, et al. Lymphatic vessels are essential for the removal of cholesterol from peripheral tissues by SR-BI-mediated transport of HDL. *Cell Metab* 2013;**17**:671-684.
243. McGrath KC, Li XH, Puranik R, Liong EC, Tan JT, Dy VM, et al. Role of 3beta-hydroxysteroid-delta 24 reductase in mediating antiinflammatory effects of high-density lipoproteins in endothelial cells. *Arterioscler Thromb Vasc Biol* 2009;**29**:877-882.
244. Yuhanna IS, Zhu Y, Cox BE, Hahner LD, Osborne-Lawrence S, Lu P, et al. High-density lipoprotein binding to scavenger receptor-BI activates endothelial nitric oxide synthase. *Nat Med* 2001;**7**:853-857.
245. Bess E, Fisslthaler B, Fromel T, Fleming I. Nitric oxide-induced activation of the AMP-activated protein kinase alpha2 subunit attenuates IkappaB kinase activity and inflammatory responses in endothelial cells. *PLoS One* 2011;**6**:e20848.
246. Martinez LO, Jacquet S, Esteve JP, Rolland C, Cabezon E, Champagne E, et al. Ectopic beta-chain of ATP synthase is an apolipoprotein A-I receptor in hepatic HDL endocytosis. *Nature* 2003;**421**:75-79.
247. Deckers-Hebestreit G, Altendorf K. The F0F1-type ATP synthases of bacteria: structure and function of the F0 complex. *Annu Rev Microbiol* 1996;**50**:791-824.
248. Stein WD, Lauger P. Kinetic properties of F0F1-ATPases. Theoretical predictions from alternating-site models. *Biophys J* 1990;**57**:255-267.
249. Bae TJ, Kim MS, Kim JW, Kim BW, Choo HJ, Lee JW, et al. Lipid raft proteome reveals ATP synthase complex in the cell surface. *Proteomics* 2004;**4**:3536-3548.
250. Cortes-Hernandez P, Dominguez-Ramirez L, Estrada-Bernal A, Montes-Sanchez DG, Zentella-Dehesa A, de Gomez-Puyou MT, et al. The inhibitor protein of the F1F0-ATP synthase is associated to the external surface of endothelial cells. *Biochem Biophys Res Commun* 2005;**330**:844-849.
251. Arakaki N, Kita T, Shibata H, Higuti T. Cell-surface H+-ATP synthase as a potential molecular target for anti-obesity drugs. *FEBS Lett* 2007;**581**:3405-3409.
252. Martinez-Zaguilan R, Lynch RM, Martinez GM, Gillies RJ. Vacuolar-type H(+)-ATPases are functionally expressed in plasma membranes of human tumor cells. *Am J Physiol* 1993;**265**:C1015-1029.

253. Radojkovic C, Genoux A, Pons V, Combes G, de Jonge H, Champagne E, et al. Stimulation of cell surface F1-ATPase activity by apolipoprotein A-I inhibits endothelial cell apoptosis and promotes proliferation. *Arterioscler Thromb Vasc Biol* 2009;**29**:1125-1130.
254. Gonzalez-Pecchi V, Valdes S, Pons V, Honorato P, Martinez LO, Lamperti L, et al. Apolipoprotein A-I enhances proliferation of human endothelial progenitor cells and promotes angiogenesis through the cell surface ATP synthase. *Microvasc Res* 2015;**98**:9-15.
255. Gent J, Braakman I. Low-density lipoprotein receptor structure and folding. *Cell Mol Life Sci* 2004;**61**:2461-2470.
256. Sudhof TC, Goldstein JL, Brown MS, Russell DW. The LDL receptor gene: a mosaic of exons shared with different proteins. *Science* 1985;**228**:815-822.
257. Goldstein JL, Brown MS. Binding and degradation of low density lipoproteins by cultured human fibroblasts. Comparison of cells from a normal subject and from a patient with homozygous familial hypercholesterolemia. *J Biol Chem* 1974;**249**:5153-5162.
258. Pullinger CR, Hennessy LK, Chatterton JE, Liu W, Love JA, Mendel CM, et al. Familial ligand-defective apolipoprotein B. Identification of a new mutation that decreases LDL receptor binding affinity. *J Clin Invest* 1995;**95**:1225-1234.
259. Chatterton JE, Phillips ML, Curtiss LK, Milne R, Fruchart JC, Schumaker VN. Immunoelectron microscopy of low density lipoproteins yields a ribbon and bow model for the conformation of apolipoprotein B on the lipoprotein surface. *J Lipid Res* 1995;**36**:2027-2037.
260. Innerarity TL, Mahley RW. Enhanced binding by cultured human fibroblasts of apo-E-containing lipoproteins as compared with low density lipoproteins. *Biochemistry* 1978;**17**:1440-1447.
261. Weisgraber KH, Innerarity TL, Mahley RW. Role of lysine residues of plasma lipoproteins in high affinity binding to cell surface receptors on human fibroblasts. *J Biol Chem* 1978;**253**:9053-9062.
262. Anderson RG, Goldstein JL, Brown MS. Localization of low density lipoprotein receptors on plasma membrane of normal human fibroblasts and their absence in cells from a familial hypercholesterolemia homozygote. *Proc Natl Acad Sci U S A* 1976;**73**:2434-2438.
263. Anderson RG, Goldstein JL, Brown MS. A mutation that impairs the ability of lipoprotein receptors to localise in coated pits on the cell surface of human fibroblasts. *Nature* 1977;**270**:695-699.
264. Anderson RG, Brown MS, Goldstein JL. Role of the coated endocytic vesicle in the uptake of receptor-bound low density lipoprotein in human fibroblasts. *Cell* 1977;**10**:351-364.
265. Li Y, Marzolo MP, van Kerkhof P, Strous GJ, Bu G. The YXXL motif, but not the two NPXY motifs, serves as the dominant endocytosis signal for low density lipoprotein receptor-related protein. *J Biol Chem* 2000;**275**:17187-17194.
266. He G, Gupta S, Yi M, Michaely P, Hobbs HH, Cohen JC. ARH is a modular adaptor protein that interacts with the LDL receptor, clathrin, and AP-2. *J Biol Chem* 2002;**277**:44044-44049.
267. Mishra SK, Watkins SC, Traub LM. The autosomal recessive hypercholesterolemia (ARH) protein interfaces directly with the clathrin-coat machinery. *Proc Natl Acad Sci U S A* 2002;**99**:16099-16104.
268. Cohen JC, Kimmel M, Polanski A, Hobbs HH. Molecular mechanisms of autosomal recessive hypercholesterolemia. *Curr Opin Lipidol* 2003;**14**:121-127.
269. Rader DJ, Cohen J, Hobbs HH. Monogenic hypercholesterolemia: new insights in pathogenesis and treatment. *J Clin Invest* 2003;**111**:1795-1803.
270. Wu JH, Peppel K, Nelson CD, Lin FT, Kohout TA, Miller WE, et al. The adaptor protein beta-arrestin2 enhances endocytosis of the low density lipoprotein receptor. *J Biol Chem* 2003;**278**:44238-44245.
271. Morris SM, Cooper JA. Disabled-2 colocalizes with the LDLR in clathrin-coated pits and interacts with AP-2. *Traffic* 2001;**2**:111-123.
272. Mishra SK, Keyel PA, Hawryluk MJ, Agostinelli NR, Watkins SC, Traub LM. Disabled-2 exhibits the properties of a cargo-selective endocytic clathrin adaptor. *EMBO J* 2002;**21**:4915-4926.
273. Brown MS, Anderson RG, Goldstein JL. Recycling receptors: the round-trip itinerary of migrant membrane proteins. *Cell* 1983;**32**:663-667.
274. Burden JJ, Sun XM, Garcia AB, Soutar AK. Sorting motifs in the intracellular domain of the low density lipoprotein receptor interact with a novel domain of sorting nexin-17. *J Biol Chem* 2004;**279**:16237-16245.
275. Bartuzi P, Billadeau DD, Favier R, Rong S, Dekker D, Fedoseienko A, et al. CCC- and WASH-mediated endosomal sorting of LDLR is required for normal clearance of circulating LDL. *Nat Commun* 2016;**7**:10961.
276. Frank PG, Cheung MW, Pavlides S, Llaverias G, Park DS, Lisanti MP. Caveolin-1 and regulation of cellular cholesterol homeostasis. *Am J Physiol Heart Circ Physiol* 2006;**291**:H677-686.
277. Drab M, Verkade P, Elger M, Kasper M, Lohn M, Lauterbach B, et al. Loss of caveolae, vascular dysfunction, and pulmonary defects in caveolin-1 gene-disrupted mice. *Science* 2001;**293**:2449-2452.
278. Frank PG, Lee H, Park DS, Tandon NN, Scherer PE, Lisanti MP. Genetic ablation of caveolin-1 confers protection against atherosclerosis. *Arterioscler Thromb Vasc Biol* 2004;**24**:98-105.

279. Fernandez-Hernando C, Yu J, Davalos A, Prendergast J, Sessa WC. Endothelial-specific overexpression of caveolin-1 accelerates atherosclerosis in apolipoprotein E-deficient mice. *Am J Pathol* 2010;**177**:998-1003.
280. Pavlides S, Gutierrez-Pajares JL, Iturrieta J, Lisanti MP, Frank PG. Endothelial caveolin-1 plays a major role in the development of atherosclerosis. *Cell Tissue Res* 2014;**356**:147-157.
281. Kuzmenko ES, Djafarzadeh S, Cakar ZP, Fiedler K. LDL transcytosis by protein membrane diffusion. *Int J Biochem Cell Biol* 2004;**36**:519-534.
282. Acton SL, Scherer PE, Lodish HF, Krieger M. Expression cloning of SR-BI, a CD36-related class B scavenger receptor. *J Biol Chem* 1994;**269**:21003-21009.
283. Pagler TA, Rhode S, Neuhofer A, Laggner H, Strobl W, Hinterndorfer C, et al. SR-BI-mediated high density lipoprotein (HDL) endocytosis leads to HDL resecretion facilitating cholesterol efflux. *J Biol Chem* 2006;**281**:11193-11204.

2. Sphingosine-1-phosphate receptors S1P1 and S1P3 regulate the transendothelial transport of HDL and LDL antagonistically

Srividya Velagapudi [1,2], Mustafa Yalcinkaya [1,2], Arnold von Eckardstein [1,2,*] and Lucia Rohrer [1,2,*]

***: equal contribution**

[1] Institute of Clinical Chemistry, University and University Hospital of Zurich, Schlieren, 8952, Switzerland;
[2] Competence Center for Integrated Human Physiology, University of Zurich, Zurich, 8057, Switzerland

Author contributions

A.v.E and L.R developed the rationale and concept of the entire study. A.v.E provided the funding. S.V, L.R, A.v.E designed the experiments and interpreted the data. S.V and M.Y performed the experiments as well as statistical data analysis. S.V wrote the first version of this manuscript, which was then revised by input of A.v.E and L.R.

Abstract

Lipoproteins may pass the endothelium by paracellular and transcellular routes. Sphingosine-1-phosphate (S1P) bound by apolipoprotein M (apoM) within HDL promotes closure.of interendothelial junctions. This raises the question, how S1P and its cognate receptors S1P1 and S1P3 regulate the transendothelial transport of lipoproteins. Pre-treatment of HAECs with inhibitors of S1P1 and S1P3 decreased the cellular binding, association and transport of ^{125}I-HDL but increased the binding, association and transport of ^{125}I-LDL. Vice-versa the pre-treatment with S1P receptor agonists increased the specific cellular binding, association and transport of ^{125}I-HDL but decreased binding, association and transcytosis of ^{125}I-LDL. The stimulatory effects of the S1P1 and S1P3 agonists on endothelial binding, association and transport of ^{125}I-HDL were abrogated by silencing of scavenger receptor BI (SR-BI). The stimulatory effect of the S1P1 inhibitor but not of the S1P3 inhibitor on endothelial association and transport of ^{125}I-LDL was decreased by treatment with the fluid-phase inhibitor amiloride. The stimulatory effect of the S1P3 inhibitor on the cellular binding and association of ^{125}I-LDL was inhibited by silencing LDL receptor (LDLR). However, the S1P3 inhibitor continued to promote the transport of ^{125}I-LDL through HAECs with suppressed LDLR or SR-BI. Therefore, the protein mediating transcytosis of ^{125}I-LDL in response to S1P3 inhibition remains to be identified.

Conclusion: S1P1 and S1P3 regulate the transendothelial transport of HDL and LDL in an antagonistic manner making them interesting targets for therapeutic interventions with atherosclerosis.

2.1 Introduction

Sphingosine-1-phosphate (S1P) is an endogenous lipid agonist of five G-protein coupled receptors (GPCRs) termed S1P1, S1P2, S1P3, S1P4 and S1P5. [1]. In the endothelium binding of S1P to the S1P1 or S1P3 receptors promotes the closure of intercellular junctions and hence the maintenance of endothelial barrier [2] . Thereby S1P controls the trafficking of solutes, proteins, and cells between intra- and extravascular compartments [3]. S1P signaling hence contributes to edema and inflammation but is also targeted for treatment of inflammatory diseases such as multiple sclerosis or cancers. Also atherosclerosis can be interpreted as the result of disproportionate fluxes of pro-atherogenic low-density lipoproteins (LDL) and anti-atherogenic high density lipoproteins (HDL) between the blood stream and the arterial wall: According to the response to injury and response to retention hypotheses of atherosclerosis, accumulation of LDL play an important role in the pathogenesis of atherosclerosis [4]. Many protective effects by HDL are exerted in the vascular wall, notably induction of cholesterol efflux from macrophages for reverse cholesterol transport [4, 5]. However, the mechanism by which LDL and HDL are transported from plasma to the subendothelial space is not well understood. Lipoproteins are debated to pass the endothelial barrier in a regulated manner possibly by two routes or processes, either through a transcellular or paracellular routes, either in an active and regulated process or by passive filtration by size and concentration [6, 7]. Our laboratory has previously described the transport of HDL through endothelial cells by mechanisms involving ATP binding cassette transporter ABCG1, scavenger receptor SR-BI, and endothelial lipase (EL), as well as the ectopic-β-ATPase/purinergic receptor axis [8-10]. Receptor-mediated LDL transport across the endothelial cells was shown to be mediated by SR-BI and activin-like kinase 1 (ALK1), rather than by the LDL receptor [11-13]. However, it is not yet known whether the S1P/S1P-receptor axis regulates the transport of LDL and HDL through the endothelial cells. This question is of specific relevance because HDL and LDL transport 60% of plasma S1P due to the presence of the S1P binding lipocalin apoM [14].By studying the effects of pharmacological inhibitors and agonists of S1P1 and S1P3 we found evidence for an important regulatory role of S1P receptors in regulating uptake of LDL and HDL by endothelial cells in an antagonistic manner.

2.2 Materials and Methods

Cell culture

Human aortic endothelial cells (HAECs) from Cell Applications Inc (304-05a), were cultured in endothelial cell basal medium (LONZA Clonetics CC-3156 or ATCC PCS-100-030) with 5% fetal bovine serum (GIBCO), 100U/mL of penicillin and 100µg/mL streptomycin (Sigma-Aldrich), supplemented with singleQuots (LONZA Clonetics CC-4176 or ATCC PCS-100-041, containing hFGF, hVEGF, hIGF-1, hEGF, hydrocortisone, ascorbic acid, heparin) at 37ºC in a humidified 5% CO_2, 95% air incubator.

Lipoprotein Isolation and labeling

LDL ($1.019<d<1.063$ g/mL) and HDL ($1.063<d<1.21$ g/mL) were isolated from fresh human normolipidemic plasma of blood donors by sequential ultracentrifugation as described previously [15, 16]. LDL and HDL were radioiodinated with $Na^{125}I$ by the McFarlane monochloride procedure modified for lipoproteins [16, 17]. Specific activities between 300-900 cpm/ ng of protein were obtained.

Small Interfering RNA Transfection

Endothelial cells were reverse transfected with small interfering RNA (Ambion silencer select, Life technologies) targeted to SR-BI (s2648, s2649, s2650) or LDLR (s224006, s224007, s4) or ACVRL1 (s986, s988) or non-silencing control (4390843) at a final concentration of 5nmol/L using Lipofectamine RNA iMAX transfection reagent (Invitrogen, 13778150) in an antibiotic-free medium. All experiments

were performed 72 hours post-transfection and efficiency of transfection was confirmed with at least two siRNAs against each gene using quantitative RT-PCR and western blotting.

Quantitative real time PCR

Total RNA was isolated using TRI reagent (Sigma T9424) according to the manufacturer's instruction. Genomic DNA was removed by digestion using DNase (Roche) and RNase inhibitor (Ribolock, Thermo Scientific). Reverse transcription was performed using M-MLVRT (Invitrogen, 200U/µL) following the standard protocol as described by the manufacturer. Quantitative PCR was done with Lightcycler FastStart DNA Master SYBR Green I (Roche) using gene specific primers as followed:

SCARB1 (For: CTG TGG GTG AGA TCA TGT GG; Rev: GCC AGA AGT CAA CCT TGC TC),
LDL-R (For: AAGGACACAGCACACAACCA; Rev: CATTTCCTCTGCCAGCAACG),
ACVRL1 (primer sequence) normalized to GAPDH (For: CCC ATG TTC GTC ATG GGT GT; Rev: TGG TCA TGA GTC CTT CCA CGA TA).

Lipoprotein Binding, Cell association and Transport

The methods for the quantification of binding, association and transport of radiolabeled HDL and LDL by endothelial cells have been previously described [5, 11, 13]. All assays were performed in DMEM (Sigma) containing 25mmol/L HEPES and 0.2% BSA instead of serum. Where indicated, cells were pretreated for 30mins at 37 ºC with either S1P1 agonist SEW2871 (Cat No:2284, Tocris, 20 nM) or S1P3 agonist CYM-5541 (Cat No: SML0680, Sigma, 100 nM) or S1P1 inhibitor W146 (Cat No:3602, Tocris, 20 nM) or S1P3 inhibitor TY52156 (Cat No:2404, Axon Medchem, 110 nM). For fluid-phase experiments, cells were treated with fluid-phase inhibitor amiloride (Cat No: A7410, Sigma, 20 µM) for 30 min before S1P1 inhibitor treatment. Following the pharmacological drug treatments, the cells were incubated with 10µg/mL of ^{125}I-HDL or ^{125}I-LDL without (total) or with 40 times excess of non-labeled HDL/ LDL (unspecific) for 1hr at 4 ºC for cellular binding and at 37ºC for association and transport experiments. Specific cellular binding/ association/ transport was calculated by subtracting the values obtained in the presence of excess unlabeled HDL/ LDL (unspecific) from those obtained in the absence of unlabeled HDL/ LDL (total).

Dextran uptake assay

To test fluid-phase particle uptake, cells were incubated with fluorescein isothiocyanate–dextran (FD40S, Sigma, 500 µg/ml) for 1h at 37ºC. Prior to the dextran incubation, cells were pre-treated with amiloride (Cat No: A7410, Sigma, 20 µM) or S1P1 inhibitor W146 (Cat No:3602, Tocris, 20 nM) or S1P3 inhibitor TY52156 (Cat No:2404, Axon Medchem, 110 nM) for 30mins where indicated. Following the dextran incubation, cells were washed twice with Tris-BSA and PBS^{++}. The cells were later lysed in RIPA buffer and the fluorescence was measured using TECAN plate reader with a wavelength range from 495 to 519nm. The fluorescence reads were normalized to the protein using micro BCA protein measurement method.

Inulin permeability

HAECs were cultured on trans-well inserts for 72hours and cells were later treated with indicated pharmacological drug inhibitors as indicated for 30mins. Post-treatments, cells in the apical compartment were incubated with 2 mCi/mL of ^{3}H-inulin, and the filtrated radioactivity was collected in the basolateral compartment after 1 hour [16, 18].

Western Blotting

Endothelial cells were lysed in RIPA buffer (10mmol/L Tris pH 7.4, 150mmol/L NaCl, 1% NP-40, 1% sodium deoxycholate, 0.1% SDS, complete EDTA (Roche)) with protease and phosphotase inhibitors. Equal amounts of protein were separated on SDS-PAGE and trans-blotted onto PVDF membrane (GE Healthcare). Membranes were blocked in appropriate blocking buffer recommended for the antibody

(PBS-T supplemented with 5% milk or BSA) and incubated either for 1hour or overnight on shaker at 4 ºC with primary antibodies at a dilution of 1:1000 in the same blocking buffer. Membranes were incubated for 1hour with HRP-conjugated secondary antibody (Dako) in blocking buffer at a dilution of 1:2500. Membranes were further incubated with chemiluminescence substrate for 1min (Pierce ECL plus, Thermo scientific) and imaged using Fusion Fx (Vilber). As indicated, TATA binding protein was used as loading control with primary antibody at 1:5000 and secondary antibody at 1:10000 dilutions. The silencing efficiencies of SR-BI (NB400-131, Novus) and LDLR (ab52818, Abcam) were evaluated and compared to TATA binding protein (ab51841, Abcam). The phospho-expression of Akt S473 (9271L, CST) was compared to TBP.

Cell surface expression analysis

Biotinylation of intact cells was performed using 20mg/mL EZ-Link sulfo-NHS-S-S-Biotin (Thermo Scientific) in the cold for 1 hour with mild shaking and quenched with ice-cold 50mM Tris pH 7.4. Cells were lysed in RIPA buffer (total cell lysate) and 200-500µg of lysates were incubated with 20µL of BSA-blocked streptavidin beads suspension (GE Healthcare) for 16hours at 4ºC and pelleted by centrifugation; the pellet represents surface proteins. Proteins were dissociated from the pellet by boiling with SDS loading buffer and analyzed by SDS-PAGE and immunoblotted with SR-BI antibody (NB400-131, Novus), LDL-receptor (LDLR, ab52818, Abcam) and TATA binding protein (TBP, ab51841, Abcam) used as intracellular control.

Statistical Analysis

The data sets for all validation experiments were analyzed using the GraphPad Prism 5 software. Comparison between groups was performed using Kruskal-Wallis one-way ANOVA followed by Dunn's post-test. The data was obtained from at least three independent experiments, performed in triplicates or quadruplets. Values are expressed as mean±SEM. $P<0.05$ was regarded as significant.

2.3 Results

S1P1 and S1P3 activation regulates cellular association and transendothelial transport of HDL and LDL antagonistically

HAECs expressed both the S1P1 and S1P3 receptors as analyzed at the mRNA (Figure 2.1A) level. To test which S1P receptor regulates the HDL and LDL uptake by endothelial cells, we treated the cells with S1P receptor agonists or inhibitors for 30mins prior to the assays. The efficacy of the agonist treatments on S1P1 and S1P3 activation was validated by increased phosphorylation of downstream signaling kinase Akt (Figure 2.1B).

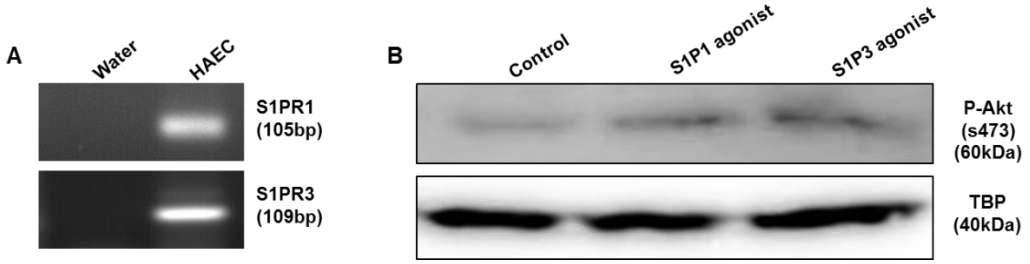

Figure 2.1: Expression and activation of S1P1 and S1P3 in HAECs A, mRNA levels of S1P1 and S1P3 in HAECs were measured by real-time polymerase chain reaction. **B,** HAECs were cultured for 72hours. Cells were then treated with the S1P1 agonist (SEW2871, 20nM), or the S1P3 agonist (CYM5541, 100nM) for 30mins, at 37 ºC as indicated. Cell lysates were analysed by western blotting for phospho Akt (Ser-473) and TATA-binding protein (TBP) was used as a loading control.

Since the S1P/S1P-receptor axis plays an important role in regulating the endothelial barrier function, we tested the permeability of ^{3}H-inulin from apical to basolateral compartments in a trans-well system. Pre-treatment of cells with either S1P agonists or inhibitors did not induce paracellular leakage of ^{3}H-inulin, (Figure 2.2).

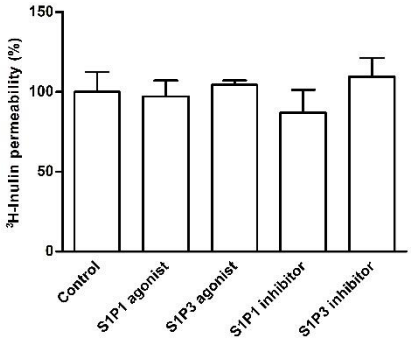

Figure 2.2: S1P1 and S1P3 do not induce the paracellular leakage in HAECs HAECs were cultured for 72hours on trans-well inserts. Cells were then treated with the S1P1 agonist (SEW2871, 20nM), or the S1P3 agonist (CYM5541, 100nM) or the S1P1 inhibitor (W146, 20nM), or the S1P3 inhibitor (TY52156, 110nM) for 30mins, at 37 ºC as indicated. The transport of ^{3}H-Inulin from the apical to basolateral compartment was measured at 37 ºC for 1hour. The results are represented as means±SEM of two independent triplicate experiments (n=2).

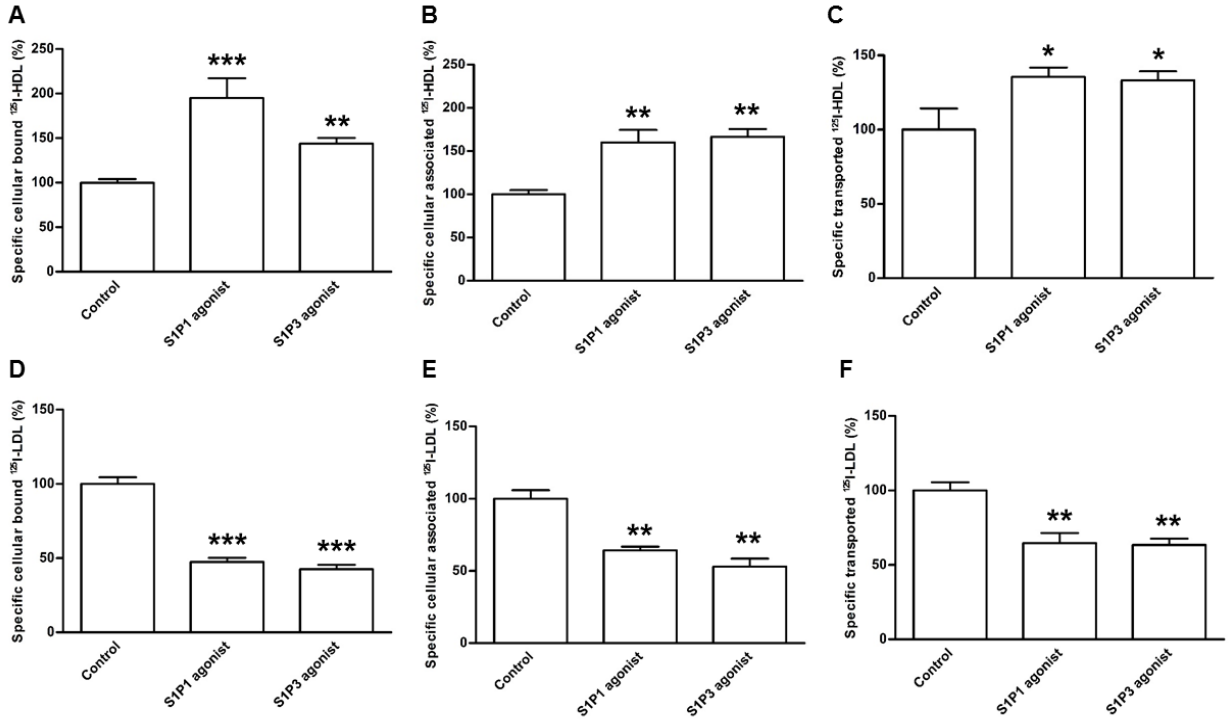

Figure 2.3: S1P1 and S1P3 agonists regulate HDL and LDL binding, association and transendothelial transport in HAECs HAECs were cultured for 72hours. Cells were then treated with S1P1 agonist (SEW2871, 20nM), or S1P3 agonist (CYM5541, 100nM) for 30mins, at 37 ºC as indicated. To study cellular binding, association and transport, HAECs were incubated with 10µg/mL of ^{125}I-HDL or ^{125}I-LDL for 1hour in the absence (total) or in the presence of 40-fold excess of unlabeled HDL and LDL, respectively, to record unspecific interactions. Specific binding, association and transport were calculated by subtracting unspecific values from total values. **A**, Specific binding was measured by incubating cells with ^{125}I-HDL (**A**) or ^{125}I-LDL (**D**) at 4 ºC. To measure specific cell association, cells were incubated with ^{125}I-HDL (**B**) or ^{125}I-LDL (**E**) at 37 ºC. For the measurement of transport, HAECs were cultured on inserts. The transport of ^{125}I-HDL (**C**) and ^{125}I-LDL (**F**) from the apical to basolateral compartment was measured at 37 ºC. The results are represented as means±SEM of three independent triplicate experiments (n=3). ***$P \leq 0.001$, **$P \leq 0.01$, *$P \leq 0.05$.

Treatment of endothelial cells with either S1P1 agonist SEW2871 or S1P3 agonist CYM5541 increased the specific cellular binding of ^{125}I-HDL at 4ºC by 95% and 43%, respectively (Figure 2.3A). Also, treatment with either S1P1 agonist or S1P3 agonist increased the cellular association of ^{125}I-HDL at 37ºC by 60% and 66%, respectively and the transendothelial transport of ^{125}I-HDL from apical to basolateral compartments by 35% and 33%, respectively (Figure 2.3B, C). By contrast, S1P1 or S1P3 agonist treatment decreased the specific cellular binding of ^{125}I-LDL by 47% and 42%, (Figure 2.3D) association by 36% and 47%, respectively (Figure 2.3E) and transendothelial transport of ^{125}I-LDL by 35% and 36%, respectively (Figure 2.3F).

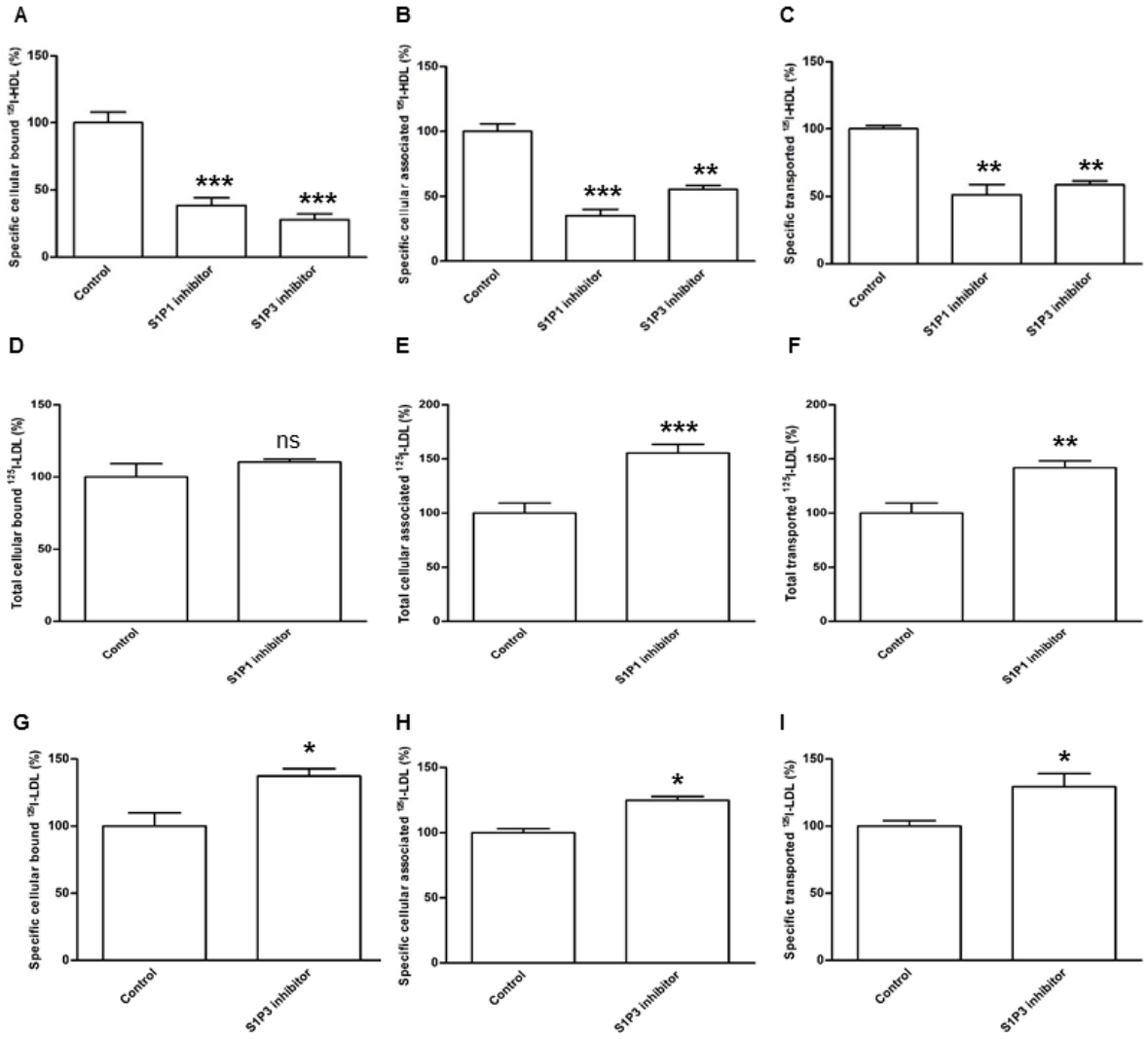

Figure 2.4: S1P1 and S1P3 inhibitors regulate binding, association and transendothelial transport of HDL and LDL in HAECs HAECs were cultured for 72hours. Cells were then treated with the S1P1 inhibitor (W146, 20nM), or the S1P3 inhibitor (TY52156, 110nM) for 30mins, at 37 ºC as indicated. To study cellular binding, association and transport, HAECs were incubated with 10µg/mL of ^{125}I-HDL or ^{125}I-LDL for 1hour in the absence (total) or in the presence of 40-fold excess of unlabeled HDL and LDL, respectively, to record unspecific interactions. Specific binding, association and transport were calculated by subtracting unspecific values from total values. **A**, Binding was measured by incubating cells with ^{125}I-HDL (**A**) or ^{125}I-LDL (**D, G**) at 4 ºC. To measure cell association, cells were incubated with ^{125}I-HDL (**B**) or ^{125}I-LDL (**E, H**) at 37 ºC. For the measurement of transport, HAECs were cultured on inserts. The transport of ^{125}I-HDL (**C**) and ^{125}I-LDL (**F, I**) from the apical to basolateral compartment was measured at 37 ºC. The results are represented as means±SEM of three independent triplicate experiments (n=3). ***$P \leq 0.001$, **$P \leq 0.01$, *$P \leq 0.05$. n.s represents "not significant".

We next determined whether the pharmacological inhibition of the S1P receptors influence the cellular binding, association and transendothelial transport of radioiodinated HDL and LDL in endothelial cells. Cells were pre-treated with pharmacological drug inhibitors against S1P1 or S1P3 for 30mins prior to the assays. Treatment with either the S1P1 inhibitor W146 or the S1P3 inhibitor TY52156 decreased the specific cellular binding of ^{125}I-HDL by 60% and 70% (Figure 2.4A) and cellular association by 65% and 45%, respectively (Figure 2.4B). Treatment of cells with S1P1 or S1P3 inhibitor also decreased the transendothelial transport of ^{125}I-HDL from apical to basolateral compartments by 50% and 42%, respectively (Figure 2.4C). By contrast, treatment of the cells with the S1P1 inhibitor increased total cellular association and transendothelial transport of ^{125}I-LDL by 55% and 42%, respectively but did not affect the cellular binding of ^{125}I-LDL to the endothelial cells (Figure 2.4D-F). However, treatment of HAECs with S1P3 inhibitor increased specific cellular binding of ^{125}I-LDL by 38% (Figure 2.4D) as well as cellular association and transport by 25% and 30%, respectively (Figure 2.4E, F).

Taken together, these results indicate that S1P1 and S1P3 regulate endothelial cellular binding, association as well as transport of HDL and LDL antagonistically.

S1P1 and S1P3 regulate cellular binding, association and transendothelial transport of HDL via SR-BI

We have previously demonstrated that the availability of SR-BI cell surface levels as a crucial factor for the transendothelial transport of HDL[19]. Because of the fast effects of S1P1 and S1P3 agonists on cellular binding, association and transport of ^{125}I-HDL, we hypothesized that S1P1 and S1P3 regulate the availability of SR-BI on the cell surface in HAECs. To test this hypothesis, we performed a cell surface biotinylation experiment. Pre-treatment of HAECs with either S1P1 or S1P3 agonist increased the cell surface SR-BI protein levels compared to the control condition (2.5A). To determine whether S1P1 and S1P3 regulate trans-endothelial transport of HDL through SR-BI, we silenced SR-BI using RNA interference. The knockdown was efficient at the protein level **(**Figure 2.9A**)**. Silencing SR-BI alone significantly decreased ^{125}I-HDL specific cellular binding by 45%, cellular association by 40% and transport by 50%, respectively. Pre-treatment with either the S1P1 or the S1P3 agonist for 30mins did not stimulate the cellular binding or cellular association or transport of ^{125}I-HDL through endothelial cells with suppressed SR-BI (Figure 2.5B-G).

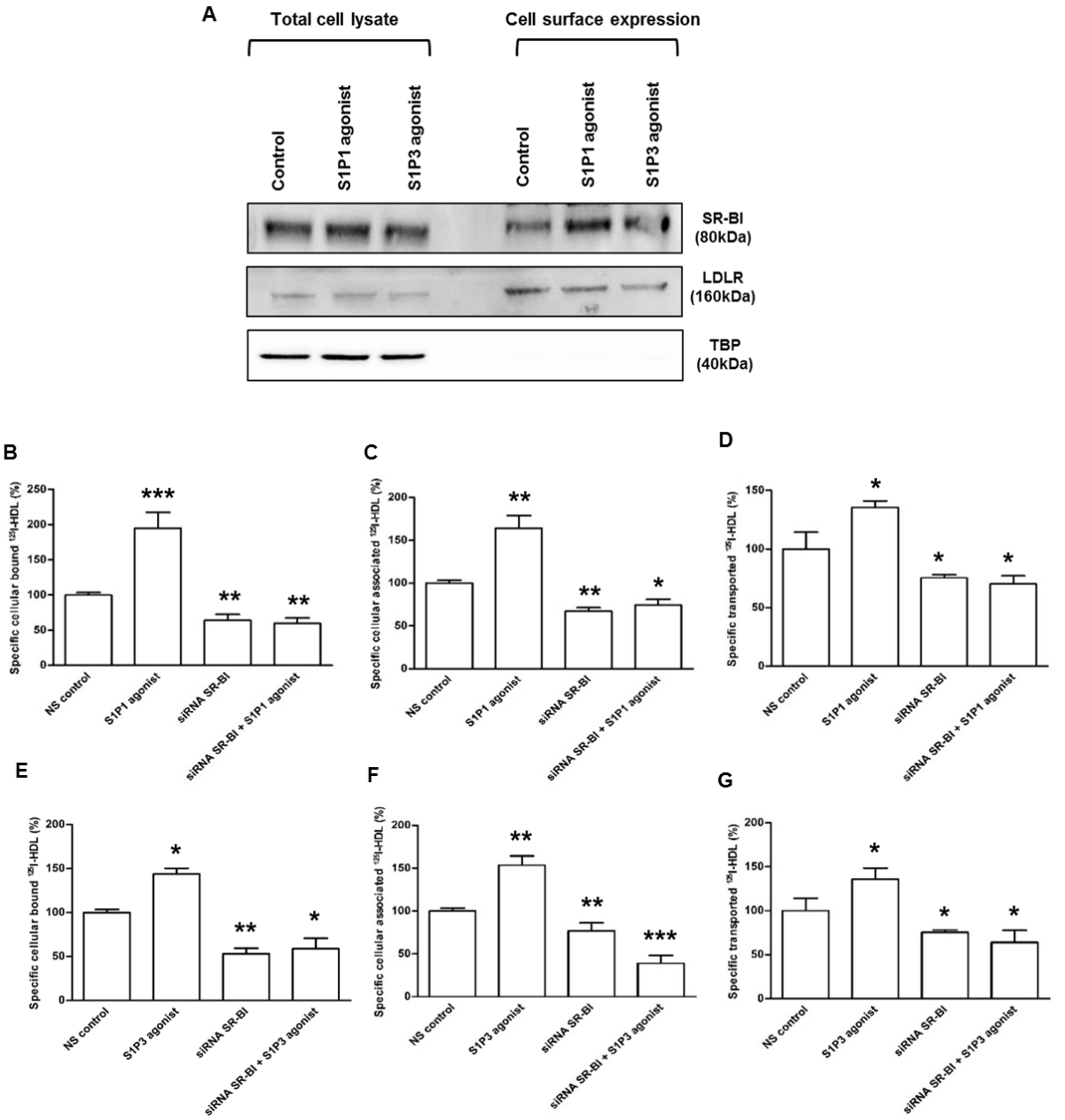

Figure 2.5: S1P1 and S1P3 agonists modulate SR-BI dependent binding, association and transport of HDL by HAECs A, Western blots of SR-BI, LDL-receptor (LDLR) and anti-TATA binding protein (TBP) in total cell lysates (left) and on the cell surface (right). HAECs were cultured for 72hours. Cells were then treated with the S1P1 inhibitor (W146, 20nM), or the S1P3 inhibitor (TY52156, 110nM) for 30mins, at 37 ºC as indicated. The western blot was probed with anti-SR-BI (80 kDa), anti-LDLR (95 kDa and 160 kDa), anti-ABCG1 (90 kDa) as well as anti-endothelial lipase (EL) (60 kDa) and anti- TATA binding protein (TBP) (40 kDa, as control for intracellular protein expression). To study cellular binding, association and transport of ^{125}I-HDL, HAECs were transfected with a specific siRNA against SR-BI or with non-silencing control siRNA (NS control) and assays were performed 72hours post-transfection. Cellular binding of ^{125}I-HDL was measured at 4 ºC by pre-treating cells with the S1P1 agonist (**A**) or the S1P3 agonist (**E**). Cellular association of ^{125}I-HDL was measured at 37 ºC by pre-treating cells with the S1P1 agonist (**C**) or the S1P3 agonist (**F**). For the measurement of transport of ^{125}I-HDL, HAECs were cultured on inserts. The transport of ^{125}I-HDL was measured by pre-treatment with the S1P1 agonist (**D**) or the S1P3 agonist (**G**) from the apical to basolateral compartment was measured at 37 ºC. The results are represented as means±SEM of three independent triplicate experiments (n=3). ***$P \leq 0.001$, **$P \leq 0.01$, *$P \leq 0.05$.

S1P1 regulates cellular association and transendothelial transport of LDL via fluid-phase pathway

As previously described (Figure 2.4D-F), pre-treatment of HAECs with the S1P1 inhibitor did not affect the binding of ^{125}I-LDL by the cells at 4ºC and the presence of excess unlabeled LDL did not decrease

the cellular association and transport of ^{125}I-LDL through the endothelial cells. These phenomena point to fluid-phase uptake (Figure 2.6A, B).

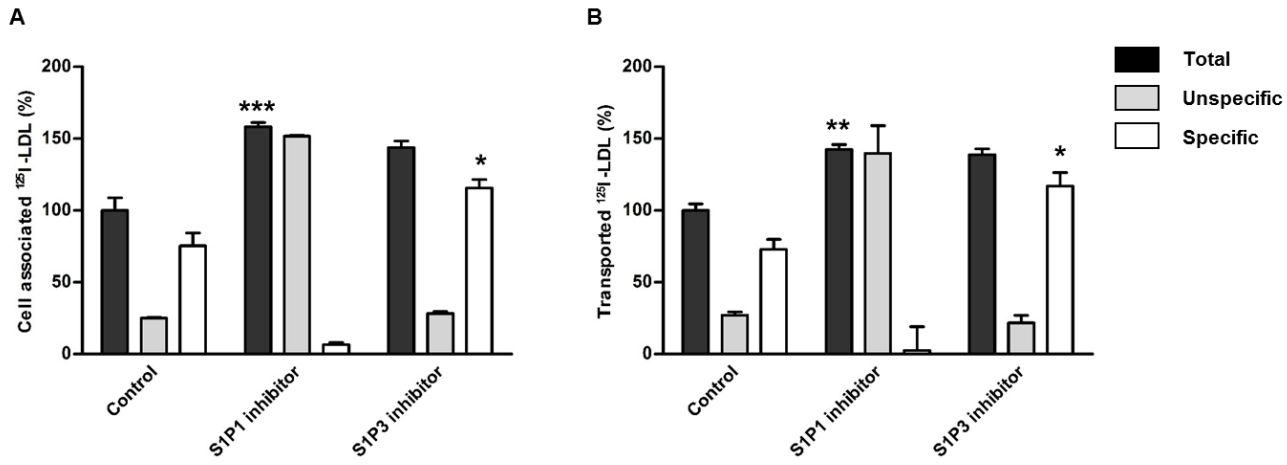

Figure 2.6: S1P1 and S1P3 inhibitors regulate cellular association and transendothelial transport of LDL in HAECs HAECs were cultured for 72hours. Cells were then treated with the S1P1 inhibitor (W146, 20nM), or the S1P3 inhibitor (TY52156, 110nM) for 30mins, at 37 ºC as indicated. To study cellular association and transport, HAECs were incubated with 10µg/mL of ^{125}I-LDL for 1hour in the absence (total) or in the presence of 40-fold excess of unlabeled LDL, respectively, to record unspecific interactions. Specific association and transport were calculated by subtracting unspecific values from total values. **A**, To measure cell association, cells were incubated with ^{125}I-LDL at 37 ºC. **B,** For the measurement of transport, HAECs were cultured on inserts. The transport of ^{125}I-LDL from the apical to basolateral compartment was measured at 37 ºC. The results are represented as means±SEM of three independent triplicate experiments (n=3). ***$P \leq 0.001$, **$P \leq 0.01$, *$P \leq 0.05$.

In line with this hypothesis, pre-treatment of HAECs with the S1P1 inhibitor significantly increased the endothelial uptake of FITC-labeled dextran which is a marker for fluid-phase endocytosis. The uptake of FITC-dextran but not ^{125}I-LDL was markedly decreased by pre-treatment of cells with amiloride, that inhibits Na^+/H^+ channels needed for the induction of fluid-phase trafficking by localized pH shift (Figure 2.7A) [20]. Interestingly, the S1P1 inhibitor failed to stimulate the cellular association and transport of ^{125}I-LDL across the endothelial cells in the presence of amiloride (Figure 2.7B, C). Taken together, these findings indicate that S1P1 inhibitition promotes cellular association and transport of ^{125}I-LDL through fluid-phase. The failure of amiloride to decrease the transport of ^{125}I-LDL in the absence of the S1P1 inhibitor indicates that LDL is also transported by processes that are independent of fluid phase.

S1P3 regulates cellular binding and association of LDL through LDLR but the transendothelial transport of LDL via LDLR and SR-BI independent pathway

Treatment of HAECs with the S1P3 inhibitor significantly increased the specific cellular binding and association of ^{125}I-LDL, indicating a receptor-mediated endocytic pathway (Figure 2.6A, B). To identify how the S1P3 inhibitor promotes the cellular binding and association of ^{125}I-LDL, we silenced LDLR and SR-BI using RNA interference. The knockdown of LDLR (Figure 2.8A) and SR-BI (Figure 2.9A) was efficient at the protein level. Silencing LDLR alone significantly decreased specific cellular binding and association of ^{125}I-LDL by 60% and 70%, respectively. Pre-treatment with the S1P3 inhibitor for 30mins did not stimulate the cellular binding and association of ^{125}I-LDL in the absence of LDLR. Silencing of LDLR had no effect on the transport of ^{125}I-LDL (Figure 2.8B-D). Silencing of SR-BI alone decreased the cellular binding and association of ^{125}I-LDL by 28% and 35%, respectively as well as decreased the transport of ^{125}I-LDL by 26%. However, the stimulatory effect of the S1P3 inhibitor on cellular binding, association and transport of ^{125}I-LDL was unchanged by the RNA interference of SR-BI (Figure 2.9B-D), indicating that the S1P3 inhibitor stimulates transendothelial transport of ^{125}I-LDL independently of SR-BI.

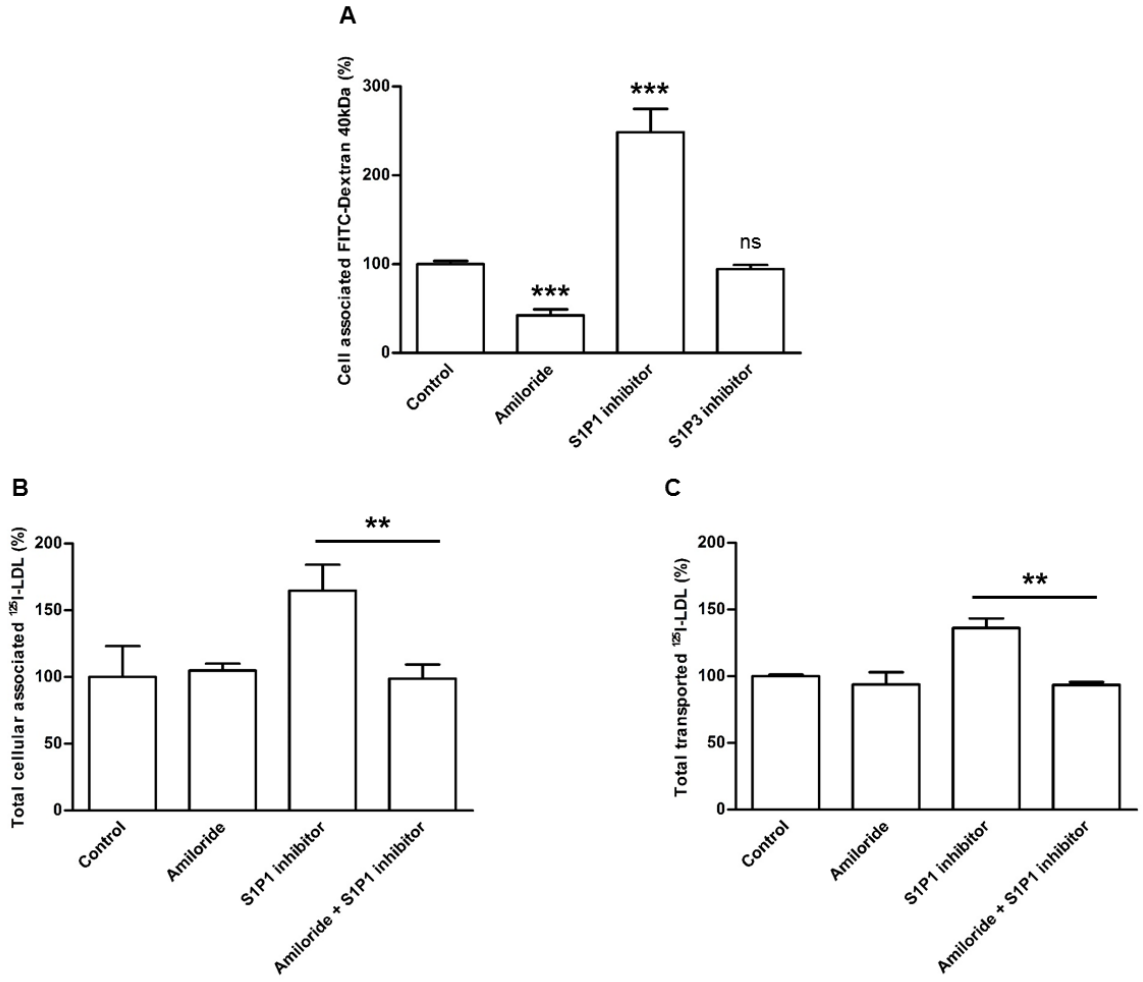

Figure 2.7: S1P1 inhibitor promotes cellular association and transendothelial transport of LDL via fluid-phase in HAECs HAECs were cultured for 72hours. Cells were then treated with amiloride (20 µM) or the S1P1 inhibitor (W146, 20nM) or the S1P3 inhibitor (TY52156, 110nM) for 30mins, at 37 ºC as indicated. **A,** To study cellular association of Dextran, cells were incubated with 1mg/mL of FITC-labeled dextran for 1 hour. **B,** To study cellular association and **C,** transport, HAECs were incubated with 10µg/mL of ^{125}I-LDL for 1hour in the absence (total) or in the presence of 40-fold excess of unlabeled LDL, respectively, to record unspecific interactions. The results are represented as means±SEM of three independent triplicate experiments (n=3). ***$P \leq 0.001$, **$P \leq 0.01$, *$P \leq 0.05$. n.s represents "not significant"

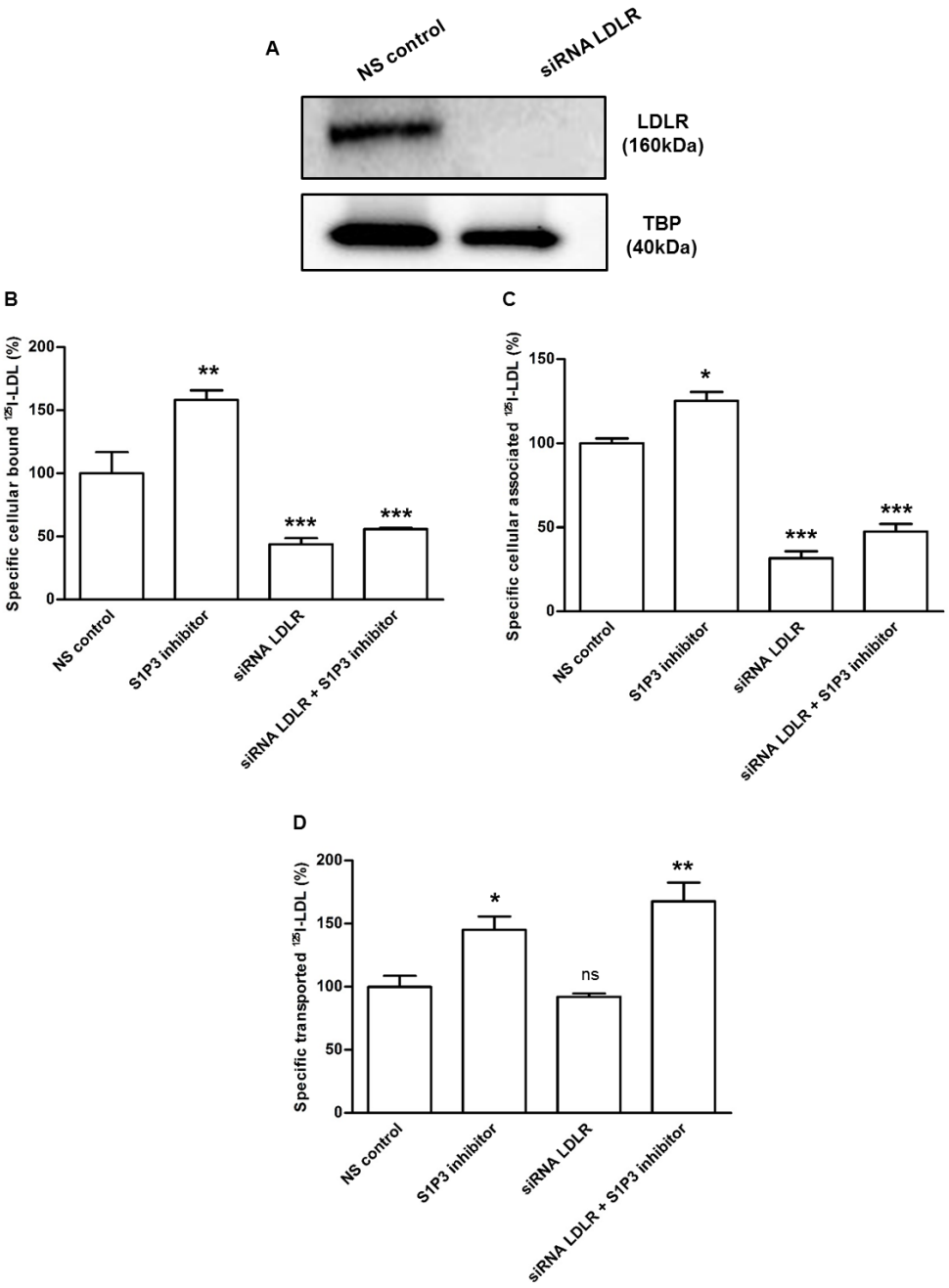

Figure 2.8: S1P3 inhibitor stimulates binding and association but not transport of LDL in HAECs via LDL receptor A, Protein levels of LDLR were measured using western blotting following transfection of endothelial cells with specific siRNAs against LDLR. TATA-binding protein (TBP) was used as a loading control. **B-D,** HAECs were transfected either with siRNA against LDLR or with non-silencing siRNA (NS control) for 72hours. Cells were then treated with the S1P3 inhibitor (TY52156, 110nM) for 30mins, at 37 ºC as indicated. To study cellular binding, association and transport, HAECs were incubated with 10µg/mL of ^{125}I-LDL for 1hour in the absence (total) or in the presence of 40-fold excess of unlabeled HDL and LDL, respectively, to record unspecific interactions. Specific binding, association and transport were calculated by subtracting unspecific values from total values. **B**, Binding was measured by incubating cells with ^{125}I-LDL at 4 ºC. **C,** To measure cell association, cells were incubated with ^{125}I-LDL at 37 ºC. **D,** For the measurement of transport, HAECs were cultured on inserts. The transport of ^{125}I-LDL from the apical to basolateral compartment was measured at 37 ºC. The results are represented as means±SEM of three independent triplicate experiments (n=3). ***$P \leq 0.001$, **$P \leq 0.01$, *$P \leq 0.05$. n.s represents "not significant".

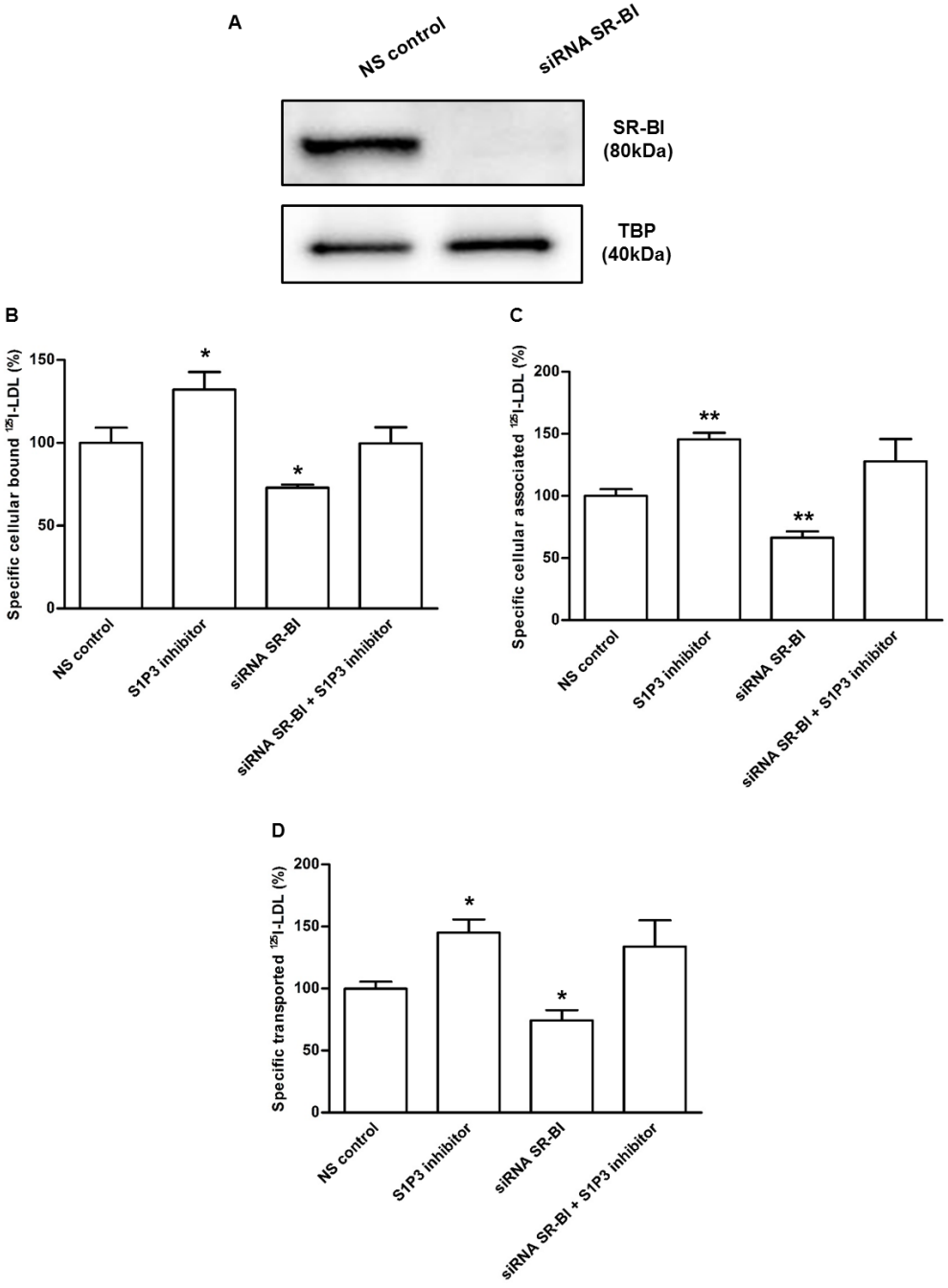

Figure 2.9: S1P3 inhibitor stimulates binding, association and transport of LDL in HAECs independent of SR-BI A, Protein levels of SR-BI were measured using western blotting following transfection of endothelial cells with specific siRNAs against SR-BI. TATA-binding protein (TBP) was used as a loading control. **B-D,** HAECs were transfected either with siRNA against SR-BI or with non-silencing siRNA (NS control) for 72hours. Cells were then treated with the S1P3 inhibitor (TY52156, 110nM) for 30mins, at 37 ºC as indicated. To study cellular binding, association and transport, HAECs were incubated with 10µg/mL of ^{125}I-LDL for 1hour in the absence (total) or in the presence of 40-fold excess of unlabeled HDL and LDL, respectively, to record unspecific interactions. Specific binding, association and transport were calculated by subtracting unspecific values from total values. **B**, Binding was measured by incubating cells with ^{125}I-LDL at 4 ºC. **C,** To measure cell association, cells were incubated with ^{125}I-LDL at 37 ºC. **D,** For the measurement of transport, HAECs were cultured on inserts. The transport of ^{125}I-LDL from the apical to basolateral compartment was measured at 37 ºC. The results are represented as means±SEM of three independent triplicate experiments (n=3). ***$P \leq 0.001$, **$P \leq 0.01$, *$P \leq 0.05$.

2.4 Discussion

It is yet controversial whether transendothelial lipoprotein transport is mediated by specific mechanisms or the result of passive filtration [6, 7]. The antagonistic effects of S1P-receptor agonists and -antagonists on the transendothelial transport of HDL and LDL demonstrated here support the previous notion of our but also other laboratories that the transport of lipoproteins through monolayers of aortic endothelial cells happens in a regulated manner rather than by passive filtration [8-10, 19, 20].

At first sight, our findings of opposite regulation of transendothelial HDL and LDL transport are surprising because S1P is known as an important regulator of intercellular junction closure in the endothelium and because S1P is carried by either lipoprotein. Activation of S1P1, through the G-protein G_i, and S1P3, through activation of G_i, G_q, and $G_{12/13}$, promote cellular motility, vascular maturation, focal contact formation, and decreased permeability through modulation of Rho family GTPases, PI3K/Akt and mitogen activated protein (MAP) kinases [21]. On contrary, inactivation of S1P1 and S1P3 signaling was shown to increase endothelial permeability and to promote edema as well as inflammation[1, 22-24]. Although more moderately, also the decrease of plasma S1P levels in mice which lack the S1P binding protein apoM was associated with impaired endothelial barrier function and the occurrence with edema and exudation of Evan's Blue [25]. However, in our *in vitro* transwell cell culture model we did not observe any differences in the inulin permeability upon treatment with S1P1 or S1P3 inhibitors.

The cellular binding, association and transport of HDL were enhanced upon activation of S1P1 and S1P3 with their respective agonists but reduced in the presence of S1P1 and S1P3 inhibitors. Vice versa, the transport of LDL was inhibited and stimulated by the same agonists and antagonists, respectively, of S1P1 and S1P3. The use of drugs has the limitation of potential off-target effects. The use of S1P dissolved in cell culture medium as the more physiological agonist of S1P receptors did not show any consistent effect on HDL transport (Rohrer et al. *unpublished results*). However, it is important to note that also other activities of S1P on endothelial cells were previously found to depend on the presence of its specific binding protein or chaperone: apoM and HDL-bound S1P but not albumin-bound S1P were reported to inhibit the expression of adhesion molecules and activate endothelial nitric oxide synthase [26-28]. In agreement with both this hypothesis and our results on pharmacological interventions, apoM- and hence S1P-depleted HDL of humans were found to be less effectively bound, internalized and transported by HAECs than complete HDL (Rohrer, Christoffersen et al., *unpublished results*) [25]. Likewise, S1P-poor HDL of *apom* knock-out mice showed reduced binding, association and transport by HAECs compared to HDL from the wild type littermates (Rohrer, Stoffel, Parks et al., *unpublished results*) [29-31]. Conversely, S1P-enriched HDL of mice transgenic for human apoM showed enhanced binding, association and transport (Rohrer, Stoffel, et al., *unpublished results*) [31-33]. Taken together these findings indicate a physiological role of S1P in the regulation transendothelial HDL transport. However, we cannot exclude any additional S1P-independent impact of apoM on the interaction of HDL with endothelial cells, for example binding to a yet unknown apoM receptor, or selection of HDL subclasses, which because of differences in size or composition beyond presence/absence of apoM/S1P are differently interacting with HAECs [34, 35]. Thus, the effects of our pharmacological interferences can be interpreted as being more specific than the findings obtained by the comparative analysis of apoM/S1P-free/poor lipoproteins versus apoM and S1P containing lipoproteins. Despite this limitation, it will be interesting to investigate the transport of apoM-free LDL versus apoM-containing LDL. The feasibility of these experiments is however limited by the lower concentration of apoM and S1P in human LDL as compared to human HDL and even more so by the overall low concentration of LDL in mice. Experiments with mouse LDL will probably only be possible if done on LDL isolated from apoB-overexpressing or LDL-receptor deficient mice crossed with apoM knock-out mice [36].

The opposite effects of S1P-receptor agonists as well S1P-receptor antagonists on transendothelial transport of HDL and LDL can be explained by the activation of several downstream responses [37], which have different impact on receptors, and intracellular itineraries of HDL and LDL. In fact, we found, that the stimulatory effect of both S1P1- and S1P3-receptor agonists on HDL transport involves SR-BI whereas the stimulatory effect of the S1P1- and S1P3-receptor antagonists on LDL transport involved fluid phase uptake and a yet unresolved mechanism, respectively.

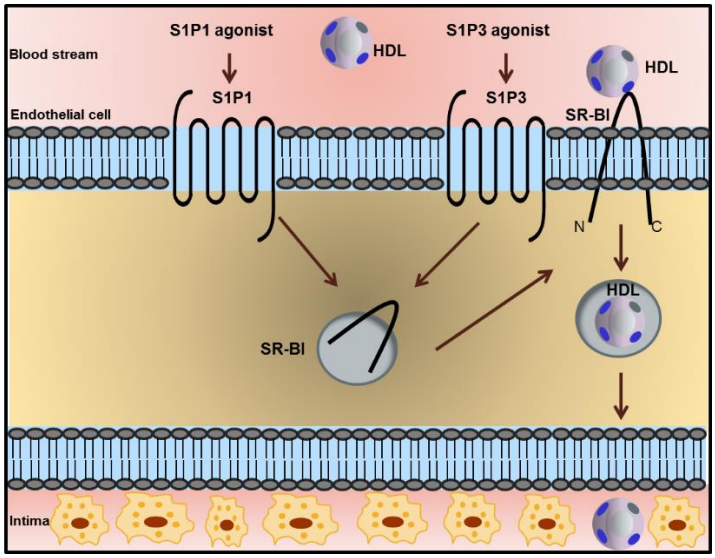

Figure 2.10: S1P1 and S1P3 agonists modulate SR-BI dependent binding, association and transport of HDL by HAECs Both the S1P1 and S1P3 agonists stimulated the translocation of SR-BI to the cell surface, which further increased the cellular binding, association and transport of HDL.

Both S1P1- and S1P3-agonism stimulated the translocation of SR-BI from the intracellular compartments to the cell surface and thereby enhanced the binding of HDL (Figure 2.10). Thus S1P-receptor activation has the same effect as the activation of VEGF receptor 2 by VEGF-A. This may be explained by the fact that activation of either receptor induces Akt phosphorylation [38, 39] which we previously found to mediate the stimulatory effect of VEGF on both SR-BI translocation and binding, uptake and transport of HDL by HAECs [19]. However, SR-BI was previously reported by others and shown by us to mediate binding, association and transport of LDL by HAECs [12, 19]. We also replicated this finding in the present study (Figure 2.9). Therefore, it was surprising that stimulation of both S1P1 and S1P3 rather inhibited transendothelial transport. This discrepancy can be explained by the fact that other receptors and intracellular itineraries overrule the contribution of SR-BI in binding and transport of LDL. In fact, we found two pathways activated by S1P1- or S1P3-antagonists and hence inhibited by S1P1- or S1P3-agonists: Both S1P1 and S1P3 agonist treatment decreased the cell surface expression of the LDL receptor and thereby contributed to the decreased cellular binding and association of LDL. Obviously, the increased cell surface abundance of SR-BI could not compensate for the reduced abundance of the LDL receptor for LDL binding upon activation of S1P1 or S1P3.

The inhibition of S1P1 promoted LDL cellular association and transport through the endothelial cells via fluid-phase. Indirect evidence for this is provided by the increased FITC-dextran uptake and the failure to compete the transport of iodinated LDL with unlabeled LDL in the presence of the S1P1 inhibitor (Figure 2.11). Moreover, the the S1P1 antagonist failed to stimulate LDL transport in the presence of amiloride. However, and interestingly, inhibition of S1P1 did not promote the uptake of HD. In line with this, our lab has previously found neither any effect of amiloride on HDL uptake by HAECs nor any co-localization of FITC-Dextran and fluorescent HDL in HAECs [20]. Moreover, and rather by contrast, inhibition of S1P1 decreased the specific cellular binding, association and transport of HDL through HAECs. This indicates that the SR-BI-dependent internalization of HDL by HAECs overrules any contribution of fluid-phase transport to the transendothelial transport of HDL.

S1P3 inhibition increased the cellular binding, association, and transport of LDL through endothelial cells. By RNA interference, we revealed the involvement of the LDL receptor in the S1P3 inhibitor mediated cellular binding and association of LDL (Figure 2.11). However, and agreement with a previous report [12], silencing of LDLR did not interfere with the transendothelial transport of LDL. Thus, S1P3-stimulated LDL-uptake via the LDL-receptor probably leads to intracellular degradation rather than re-secretion of LDL. Likewise, we ruled out SR-BI as the mediator of enhanced transendothelial LDL transport upon S1P3 inhibition. By contrast, to the S1P1 inhibitor, the S1P3 inhibtor stimulated the transendothelial transport of ioidinated LDL by a mechanism, which could be competed by non-labeled LDL. Thus, we postulate the involvement of a yet unidentified receptor that allows transendothelial LDL transport, for example ALK1 that was recently identified by a genome-wide RNAi-screen as an endothelial LDL binding protein mediating uptake and transcytosis of LDL [13].

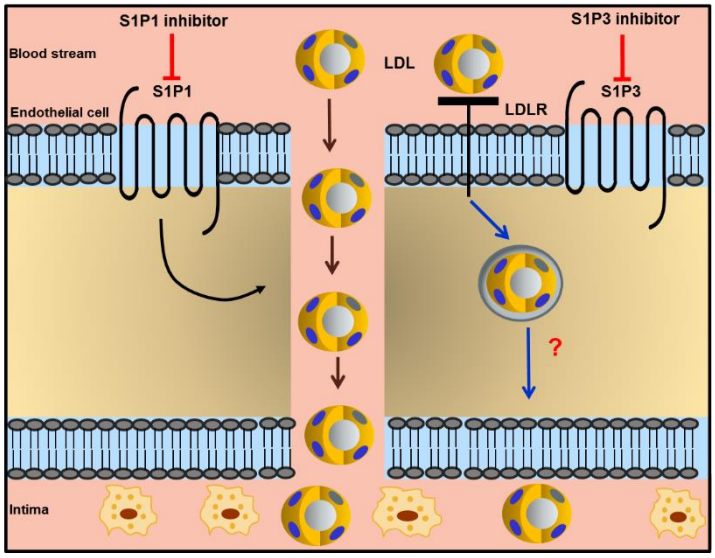

Figure 2.11: S1P1 and S1P3 inhibitors regulate association and transport of LDL by HAECs Both the S1P1 and S1P3 inhibitors stimulated the uptake and transport of LDL. S1P1 inhibitor increased the transport of LDL via fluid-phase transcytosis. S1P3 increased the cellular binding and uptake of LDL through LDL receptor. The candidate protein regulator of LDL transport by S1P3 inhibitor remains unidentified.

In conclusion, we here showed that the S1P1 and S1P3 regulate endothelial binding, uptake and transport of HDL and LDL in an antagonistic manner. By inhibiting the transendothelial transport of pro-atherogenic LDL and promoting the transendothelial transport of potentially anti-atherogenic HDL, S1P and its cognate receptors S1P1 or S1P3 may play an important role in the pathogenesis of atherosclerosis and serve as interesting targets for protection against atherosclerosis. However, any therapeutic interference may need to be endothelium-specific as previous animal experiments on S1P-receptor modulators or knock-out of S1P metabolizing enzymes or S1P receptors yielded controversial findings on the role of S1P in the pathogenesis of atherosclerosis [24, 40-43].

2.5 References

1. Hla T. Signaling and biological actions of sphingosine 1-phosphate. *Pharmacol Res* 2003;**47**:401-407.
2. Wang L, Dudek SM. Regulation of vascular permeability by sphingosine 1-phosphate. *Microvasc Res* 2009;**77**:39-45.
3. Mehta D, Malik AB. Signaling mechanisms regulating endothelial permeability. *Physiol Rev* 2006;**86**:279-367.
4. Schwenke DC, Carew TE. Initiation of atherosclerotic lesions in cholesterol-fed rabbits. II. Selective retention of LDL vs. selective increases in LDL permeability in susceptible sites of arteries. *Arteriosclerosis* 1989;**9**:908-918.
5. Tabas I, Williams KJ, Boren J. Subendothelial lipoprotein retention as the initiating process in atherosclerosis: update and therapeutic implications. *Circulation* 2007;**116**:1832-1844.

6. von Eckardstein A, Rohrer L. HDLs in crises. *Curr Opin Lipidol* 2016;**27**:264-273.
7. Boren J, Williams KJ. The central role of arterial retention of cholesterol-rich apolipoprotein-B-containing lipoproteins in the pathogenesis of atherosclerosis: a triumph of simplicity. *Curr Opin Lipidol* 2016;**27**:473-483.
8. von Eckardstein A, Rohrer L. Transendothelial lipoprotein transport and regulation of endothelial permeability and integrity by lipoproteins. *Curr Opin Lipidol* 2009;**20**:197-205.
9. Michel CC, Nanjee MN, Olszewski WL, Miller NE. LDL and HDL transfer rates across peripheral microvascular endothelium agree with those predicted for passive ultrafiltration in humans. *J Lipid Res* 2015;**56**:122-128.
10. Rohrer L, Ohnsorg PM, Lehner M, Landolt F, Rinninger F, von Eckardstein A. High-density lipoprotein transport through aortic endothelial cells involves scavenger receptor BI and ATP-binding cassette transporter G1. *Circ Res* 2009;**104**:1142-1150.
11. Robert J, Lehner M, Frank S, Perisa D, von Eckardstein A, Rohrer L. Interleukin 6 stimulates endothelial binding and transport of high-density lipoprotein through induction of endothelial lipase. *Arterioscler Thromb Vasc Biol* 2013;**33**:2699-2706.
12. Cavelier C, Ohnsorg PM, Rohrer L, von Eckardstein A. The beta-chain of cell surface F(0)F(1) ATPase modulates apoA-I and HDL transcytosis through aortic endothelial cells. *Arterioscler Thromb Vasc Biol* 2012;**32**:131-139.
13. Vasile E, Simionescu M, Simionescu N. Visualization of the binding, endocytosis, and transcytosis of low-density lipoprotein in the arterial endothelium in situ. *J Cell Biol* 1983;**96**:1677-1689.
14. Armstrong SM, Sugiyama MG, Fung KY, Gao Y, Wang C, Levy AS, et al. A novel assay uncovers an unexpected role for SR-BI in LDL transcytosis. *Cardiovasc Res* 2015;**108**:268-277.
15. Kraehling JR, Chidlow JH, Rajagopal C, Sugiyama MG, Fowler JW, Lee MY, et al. Genome-wide RNAi screen reveals ALK1 mediates LDL uptake and transcytosis in endothelial cells. *Nat Commun* 2016;**7**:13516.
16. Murata N, Sato K, Kon J, Tomura H, Yanagita M, Kuwabara A, et al. Interaction of sphingosine 1-phosphate with plasma components, including lipoproteins, regulates the lipid receptor-mediated actions. *Biochem J* 2000;**352 Pt 3**:809-815.
17. Garcia JG, Liu F, Verin AD, Birukova A, Dechert MA, Gerthoffer WT, et al. Sphingosine 1-phosphate promotes endothelial cell barrier integrity by Edg-dependent cytoskeletal rearrangement. *J Clin Invest* 2001;**108**:689-701.
18. Havel RJ, Eder HA, Bragdon JH. The distribution and chemical composition of ultracentrifugally separated lipoproteins in human serum. *J Clin Invest* 1955;**34**:1345-1353.
19. Rohrer L, Cavelier C, Fuchs S, Schluter MA, Volker W, von Eckardstein A. Binding, internalization and transport of apolipoprotein A-I by vascular endothelial cells. *Biochim Biophys Acta* 2006;**1761**:186-194.
20. Freeman M, Ekkel Y, Rohrer L, Penman M, Freedman NJ, Chisolm GM, et al. Expression of type I and type II bovine scavenger receptors in Chinese hamster ovary cells: lipid droplet accumulation and nonreciprocal cross competition by acetylated and oxidized low density lipoprotein. *Proc Natl Acad Sci U S A* 1991;**88**:4931-4935.
21. Cavelier C, Rohrer L, von Eckardstein A. ATP-Binding cassette transporter A1 modulates apolipoprotein A-I transcytosis through aortic endothelial cells. *Circ Res* 2006;**99**:1060-1066.
22. Velagapudi S, Yalcinkaya M, Piemontese A, Meier R, Norrelykke SF, Perisa D, et al. VEGF-A Regulates Cellular Localization of SR-BI as Well as Transendothelial Transport of HDL but Not LDL. *Arterioscler Thromb Vasc Biol* 2017;**37**:794-803.
23. Perisa D, Rohrer L, Kaech A, von Eckardstein A. Itinerary of high density lipoproteins in endothelial cells. *Biochim Biophys Acta* 2016;**1861**:98-107.
24. McVerry BJ, Garcia JG. Endothelial cell barrier regulation by sphingosine 1-phosphate. *J Cell Biochem* 2004;**92**:1075-1085.
25. Liu F, Verin AD, Wang P, Day R, Wersto RP, Chrest FJ, et al. Differential regulation of sphingosine-1-phosphate- and VEGF-induced endothelial cell chemotaxis. Involvement of G(ialpha2)-linked Rho kinase activity. *Am J Respir Cell Mol Biol* 2001;**24**:711-719.
26. McVerry BJ, Peng X, Hassoun PM, Sammani S, Simon BA, Garcia JG. Sphingosine 1-phosphate reduces vascular leak in murine and canine models of acute lung injury. *Am J Respir Crit Care Med* 2004;**170**:987-993.
27. Keul P, Lucke S, von Wnuck Lipinski K, Bode C, Graler M, Heusch G, et al. Sphingosine-1-phosphate receptor 3 promotes recruitment of monocyte/macrophages in inflammation and atherosclerosis. *Circ Res* 2011;**108**:314-323.
28. Christoffersen C, Obinata H, Kumaraswamy SB, Galvani S, Ahnstrom J, Sevvana M, et al. Endothelium-protective sphingosine-1-phosphate provided by HDL-associated apolipoprotein M. *Proc Natl Acad Sci U S A* 2011;**108**:9613-9618.

29. Blaho VA, Galvani S, Engelbrecht E, Liu C, Swendeman SL, Kono M, et al. HDL-bound sphingosine-1-phosphate restrains lymphopoiesis and neuroinflammation. *Nature* 2015;**523**:342-346.
30. Ruiz M, Frej C, Holmer A, Guo LJ, Tran S, Dahlback B. High-Density Lipoprotein-Associated Apolipoprotein M Limits Endothelial Inflammation by Delivering Sphingosine-1-Phosphate to the Sphingosine-1-Phosphate Receptor 1. *Arterioscler Thromb Vasc Biol* 2017;**37**:118-129.
31. Galvani S, Sanson M, Blaho VA, Swendeman SL, Obinata H, Conger H, et al. HDL-bound sphingosine 1-phosphate acts as a biased agonist for the endothelial cell receptor S1P1 to limit vascular inflammation. *Sci Signal* 2015;**8**:ra79.
32. Liu M, Seo J, Allegood J, Bi X, Zhu X, Boudyguina E, et al. Hepatic apolipoprotein M (apoM) overexpression stimulates formation of larger apoM/sphingosine 1-phosphate-enriched plasma high density lipoprotein. *J Biol Chem* 2014;**289**:2801-2814.
33. Liu M, Allegood J, Zhu X, Seo J, Gebre AK, Boudyguina E, et al. Uncleaved ApoM signal peptide is required for formation of large ApoM/sphingosine 1-phosphate (S1P)-enriched HDL particles. *J Biol Chem* 2015;**290**:7861-7870.
34. Wolfrum C, Poy MN, Stoffel M. Apolipoprotein M is required for prebeta-HDL formation and cholesterol efflux to HDL and protects against atherosclerosis. *Nat Med* 2005;**11**:418-422.
35. Karuna R, Park R, Othman A, Holleboom AG, Motazacker MM, Sutter I, et al. Plasma levels of sphingosine-1-phosphate and apolipoprotein M in patients with monogenic disorders of HDL metabolism. *Atherosclerosis* 2011;**219**:855-863.
36. Sutter I, Park R, Othman A, Rohrer L, Hornemann T, Stoffel M, et al. Apolipoprotein M modulates erythrocyte efflux and tubular reabsorption of sphingosine-1-phosphate. *J Lipid Res* 2014;**55**:1730-1737.
37. Chou CH, Ali SA, Roubey R, Buyon J, Reeves WH. Onset and regulation of anti-lamin B autoantibody production is independent of the level of polyclonal activation. *Autoimmunity* 1991;**8**:297-305.
38. Kontush A, Lindahl M, Lhomme M, Calabresi L, Chapman MJ, Davidson WS. Structure of HDL: particle subclasses and molecular components. *Handb Exp Pharmacol* 2015;**224**:3-51.
39. Christoffersen C, Pedersen TX, Gordts PL, Roebroek AJ, Dahlback B, Nielsen LB. Opposing effects of apolipoprotein m on catabolism of apolipoprotein B-containing lipoproteins and atherosclerosis. *Circ Res* 2010;**106**:1624-1634.
40. Poti F, Simoni M, Nofer JR. Atheroprotective role of high-density lipoprotein (HDL)-associated sphingosine-1-phosphate (S1P). *Cardiovasc Res* 2014;**103**:395-404.
41. Spiegel S, Milstien S. Sphingosine-1-phosphate: an enigmatic signalling lipid. *Nat Rev Mol Cell Biol* 2003;**4**:397-407.
42. Igarashi J, Erwin PA, Dantas AP, Chen H, Michel T. VEGF induces S1P1 receptors in endothelial cells: Implications for cross-talk between sphingolipid and growth factor receptors. *Proc Natl Acad Sci U S A* 2003;**100**:10664-10669.
43. Theilmeier G, Schmidt C, Herrmann J, Keul P, Schafers M, Herrgott I, et al. High-density lipoproteins and their constituent, sphingosine-1-phosphate, directly protect the heart against ischemia/reperfusion injury in vivo via the S1P3 lysophospholipid receptor. *Circulation* 2006;**114**:1403-1409.
44. Nofer JR, Bot M, Brodde M, Taylor PJ, Salm P, Brinkmann V, et al. FTY720, a synthetic sphingosine 1 phosphate analogue, inhibits development of atherosclerosis in low-density lipoprotein receptor-deficient mice. *Circulation* 2007;**115**:501-508.
45. Keul P, Tolle M, Lucke S, von Wnuck Lipinski K, Heusch G, Schuchardt M, et al. The sphingosine-1-phosphate analogue FTY720 reduces atherosclerosis in apolipoprotein E-deficient mice. *Arterioscler Thromb Vasc Biol* 2007;**27**:607-613.
46. Poti F, Gualtieri F, Sacchi S, Weissen-Plenz G, Varga G, Brodde M, et al. KRP-203, sphingosine 1-phosphate receptor type 1 agonist, ameliorates atherosclerosis in LDL-R-/- mice. *Arterioscler Thromb Vasc Biol* 2013;**33**:1505-1512.

3. VEGF-A regulates subcellular localization of scavenger receptor BI and transcytosis of HDL but not LDL in aortic endothelial cells

Srividya Velagapudi [1,2], Mustafa Yalcinkaya [1,2], Antonio Piemontese [1,3], Roger Meier,[4], Simon Flyvbjerg Nørrelykke [4], Damir Perisa [1,2], Andrzej Rzepiela [4], Michael Stebler [4], Szymon Stoma [4], Paolo Zanoni [1,2], Lucia Rohrer [1,2,*], and Arnold von Eckardstein [1,2,*]

***: equal contribution**

[1] Institute of Clinical Chemistry, University and University Hospital of Zurich, Schlieren, 8952, Switzerland;
[2] Competence Center for Integrated Human Physiology, University of Zurich, Zurich, 8057, Switzerland
[3] Department of Pharmacy, University of Parma, Parma, 43124, Italy
[4] Scientific Center for Optical and Electron Microscopy, ETH Zurich, Switzerland

Author contributions

A.v.E and L.R developed the rationale and concept of the entire study. A.v.E provided the funding. S.V, R.M and M.S optimized the high-content kinase inhibitor drug screen protocol. S.V and A.P performed the high-content screen. M.S performed the quality control assessment. S.V and R.M optimized the fluorescence microscope-based image acquisition protocol. R.M, S.F.N and S.S built the image analysis pipeline. S.F.N, A.R and S.S performed the statistical analysis. S.V and M.Y performed the biochemical validation experiments as well as their statistical data analysis. D.P and P.Z contributed to the planning and interpretation of the high-content screen and validation experiments. S.V wrote the first version of this manuscript, which was then revised by input of A.v.E, L.R and other authors.

Abstract

Objective: Low and high-density lipoproteins (LDL and HDL) must pass the endothelial layer to exert pro- and anti-atherogenic activities, respectively, within the vascular wall. However, the rate limiting factors that mediate transendothelial transport of lipoproteins are yet little known. Therefore, we performed a high-throughput screen with kinase drug inhibitors to identify modulators of transendothelial LDL and HDL transport.

Approach and Results: Microscopy based high-content screening was performed by incubating human aortic endothelial cells (HAECs) with 141 kinase inhibiting drugs and fluorescent labeled LDL or HDL. Inhibitors of VEGF receptors (VEGFR) significantly decreased the uptake of HDL but not LDL. Silencing of VEGFR2 significantly decreased cellular binding, association, and transendothelial transport of ^{125}I-HDL but not ^{125}I-LDL. RNA interference with VEGFR1 or VEGFR3 had no effect. Binding, uptake and transport of HDL but not LDL were strongly reduced in the absence of VEGF-A from the cell culture medium and were restored by the addition of VEGF-A. The restoring effect of VEGF-A on endothelial binding, uptake and transport of HDL was abrogated by pharmacological inhibition of PI3K/Akt or p38MAPK as well as silencing of scavenger receptor BI (SR-BI). Moreover, the presence of VEGF-A was found to be a pre-requisite for the localization of SR-BI in the plasma membrane of endothelial cells.

Conclusions: The identification of VEGF as a regulatory factor of transendothelial transport of HDL but not LDL supports the concept that the endothelium is a specific and hence druggable barrier for the entry of lipoproteins into the vascular wall.

3.1 Introduction

Accumulation of low density lipoproteins (LDL) and lipids in the subendothelial matrix and macrophages is crucial in the pathogenesis of atherosclerosis [1]. Conversely, removal of cholesterol from the subendothelial space by cholesterol efflux and subsequent reverse cholesterol transport (RCT) has been postulated to confer protection against atherosclerosis [2]. To reach the subendothelial space, both LDL and HDL have to cross the intact endothelial barrier. It is yet controversial whether transendothelial HDL transport is mediated by specific mechanisms or the result of passive filtration [3, 4]. Our laboratory previously showed that aortic endothelial cells are able to specifically bind, internalize and transport HDL in a saturable and temperature-dependent manner via a non-classical endocytic route involving dynamin and cytosketal networks [5, 6]. We also demonstrated that transcytosis of mature HDL is regulated by ATP binding cassette transporter ABCG1, scavenger receptor SR-BI, and endothelial lipase (EL), as well as the ectopic-β-ATPase/purinergic receptor axis [6-8]. Other laboratories reported that endothelial cells internalize LDL by at least two pathways [3]: The classical one leads to lysosomal degradation and involves clathrin-coated pits and the LDL-receptor [9, 10]. The other non-degrading pathway allows the transendothelial transport of LDL and involves caveolae [11], SR-BI [12] and activin-like kinase 1 (ALK1) [13].

Genome-wide RNA interference studies have shown that both clathrin- and caveolin-dependent endocytosis are regulated by kinases [316]. The kinases regulating the endocytosis of lipoproteins especially by endothelial cells are unknown. To identify such signaling cascades regulating the uptake of LDL and HDL, we performed a microscopy-based high-content screening on human aortic endothelial cells using a kinase inhibitor drug library. Starting with this unbiased strategy, we found evidence for an important regulatory role of vascular endothelial growth factor receptors in regulating uptake of HDL but not LDL by endothelial cells.

3.2 Materials and Methods

Cell culture

Human aortic endothelial cells (HAECs) from Cell Applications Inc (304-05a), were cultured in endothelial cell basal medium (LONZA Clonetics CC-3156 or ATCC PCS-100-030) with 5% fetal bovine serum (GIBCO), 100U/mL of penicillin and 100µg/mL streptomycin (Sigma-Aldrich), supplemented with singleQuots (LONZA Clonetics CC-4176 or ATCC PCS-100-041, containing hFGF, hVEGF, hIGF-1, hEGF, hydrocortisone, ascorbic acid, heparin) hereafter referred to as medium A or singleQuots without VEGF, hereafter referred to as medium B at 37ºC in a humidified 5% CO_2, 95% air incubator. According to the product description by ATCC, medium A contains 5 ng/ml VEGF-A. Lonza does not provide any public information on the VEGF-A content of its medium A. For some experiments (if indicated) we supplemented the VEGF-free medium B with 25 ng/ml VEGF-A (Sigma, V7259)

Lipoprotein Isolation and labeling

LDL ($1.019<d<1.063$ g/mL) and HDL ($1.063<d<1.21$ g/mL) were isolated from fresh human normolipidemic plasma of blood donors by sequential ultracentrifugation as described previously [15, 16]. LDL and HDL were fluorescently labeled with Atto-488 (Atto-Tec, AD 488-35) and Atto-594-NHS-ester dyes, respectively (Atto-Tec, AD 594-35). The reaction was performed at a pH 8.0 adjusted by adding 1M $NaHCO_3$ to obtain a final concentration of 0.1M in dark at room temperature for 1hour. The labeled lipoproteins were separated from free dye by gel filtration chromatography using PD-10 desalting columns (GE healthcare, 170851-01). LDL and HDL were radioiodinated with $Na^{125}I$ by the

McFarlane monochloride procedure modified for lipoproteins [16, 17]. Specific activities between 300-900 cpm/ ng of protein were obtained.

Kinase inhibitor screen

HAECs were seeded in 384 well plates using a washer dispenser (Biotek, EL406) at a density of 1000 cells per well in 80ul of their respective media. The cells were allowed to grow for 72 hours at 37ºC in a humidified 5% CO_2, 95% air incubator. Following culture, cells were treated with 141 drugs encompassing kinase inhibitor library targeting 20 kinases (Table 3.I) or with dimethyl sulfoxide (control-vehicle). For each drug, seven different concentrations were used at a dilution range of 128, 640, 3200, 16000, 80000, 400000, 2000000. After 1 hour of drug treatment, cells were incubated with either fluorescent labeled Atto594-HDL or LDL [RFP (Red fluorescent protein) channel] or medium without any fluorescent labeled lipoprotein (Blank control) for another hour. The cells were later washed with PBS using 384-well head manifold (Biotek, EL406), fixed with 2% paraformaldehyde and nuclei were stained with Hoechst- 33258 (Sigma, 861405). Four compounds, previously reported to interfere with the uptake of lipoproteins into endothelial cells were used as positive control drugs at seven concentrations ranging from 128 ng/ml to 2 mg/ml: Tetrahydrolipstatin (THL) to inhibit endothelial lipase, BLT1 to inhibit SR-BI, colchicine to interfere with the cytoskeleton, and dynasore to interfere with vesicle formation.

Target	Full name of the target
ABL	Abelson murine leukemia viral oncogene homolog 1
ALK	Anaplastic lymphoma kinase
c-Kit	Tyrosine-protein kinase kit or CD117
c-Met	Tyrosine-protein kinase met
EGFR	Epidermal growth factor receptor
FGFR	Fibroblast growth factor receptor
FLT-3	Fms-like tyrosine kinase 3
HER2	Receptor tyrosine-protein kinase erbB-2 or CD340
IGF-1R	Insulin growth factor receptor
VEGFR	Vascular endothelial growth factor receptor
Aurora	Aurora kinase
CDK	Cyclin-dependent kinase
CHK	Check-point kinase
GSK-3	Glycogen synthase kinase-3
JNK	c-Jun N-terminal kinase
JAK/STAT	Janus kinase and signal transducer and activator of transcription proteins
MEK	Mitogen-activated protein kinase kinase
mTOR	Mammalian target of rapamycin
PI3K/AKT	phosphotidyl-inositol 3 kinase/protein kinase B
p38 MAPK	p38 mitogen-activated protein kinase

Table 3.I: List of targets of 141 drug compounds. The drug compounds inhibit a wide range of target kinases, which comprises of both receptor-tyrosine kinases and their downstream signaling kinases.

The assay plates were processed using Molecular Device wide-field fluorescence microscope and nine images per well were acquired with 20X short working distance objective. The primary microscope generated images were analyzed using Cell profiler to segment nuclei in DAPI channel and foci (vesicles) in RFP channel (Figure 3.1).

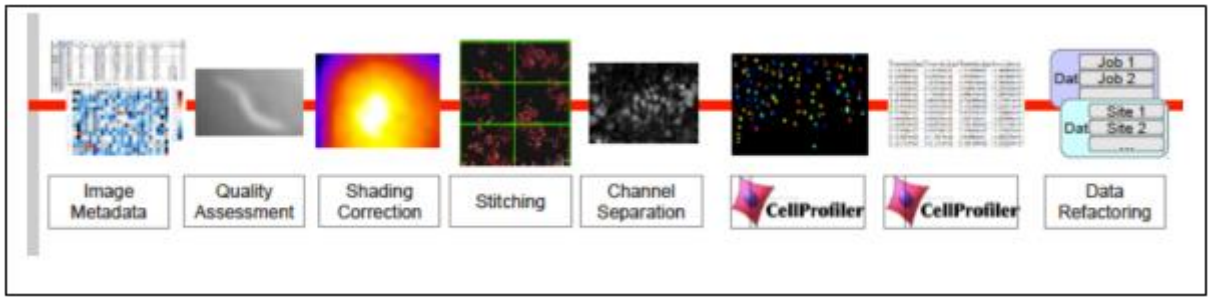

Figure 3.1. Description of the workflow. The microscopy generated images are initially assessed for quality based on the performance of control drug compounds followed by shading correction and dynamic background subtraction. The nine images acquired from each well are stitched together and signal intensities of both DAPI and RFP channel are measured using Cellprofiler.

Image acquisition and analysis

Several hundred features for each cell were extracted – for nucleus, cytoplasm and foci. The raw images had nuclei that were stained many times weaker than the others. For example, in Figure 3.2, a line is drawn connecting a brightly stained nucleus and a weakly stained nucleus to measure the grey values. The difference in the staining intensities across various images was recorded between 5 and 10. The Hoechst stained images were enhanced by taking the 100^{th} root of all intensity values and normalized to the brightest value in each image.

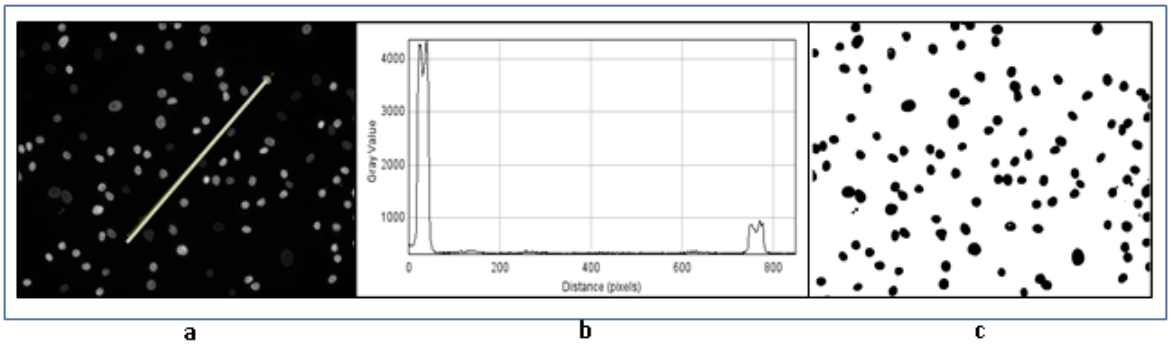

Figure 3.2: Normalization of nuclei – DAPI channel. (a) Staining of nuclei with Hoechst. (b) Difference in staining intensities between two nuclei connected by a line in 5(a). (c) Normalized nuclei staining by enhancing 100^{th} root of all intensity values.

Nuclei were further filtered based on detected shapes to avoid as many artefacts as possible. A two-step segmentation was applied to account for the large variability in Hoechst staining. Segmented nuclei were filtered based on "Solidity measure" with a minimum threshold of 0.93. Solidity measure is potentially a better differentiator of cells with irregular shape versus round cells. It is the ratio of the area of the cell to the enclosed convex hull container. The images in Figure 3.3 show the segmented nuclei and a 30-pixel wide ring around them, overlaid on the RFP channel image. The RFP images were enhanced by taking the square root of all intensity values and normalizing to the brightest value in each image. Three measures in particular were designed to measure the uptake of the fluorescent-labeled HDL/LDL. The number in yellow determines the number of foci detected in the cell (cytoplasm + nucleus). The number in red shows the area-normalised fraction of the intensity in the innermost of three equal-width concentric rings in the cytoplasm; where numbers larger than unity correspond to above cytoplasm-average intensity. The number in cyan is the second component of granularity (resampled at 0.5, radius of structuring element = 1 pixel).

Analysis was done at the well-level, i.e., all cell-level measurements were aggregated before analysis. The aggregation was done using the open-source software KNIME. KNIME was also used to merge the aggregated measurements with the annotation file, containing the names and concentrations of

compounds, the cell type, ligand type. For some measures, such as cell-count, the aggregation method was summation. For most measures, the aggregation method was to calculate the median of all cell values in an image, and then the median of the nine images (there are nine images per well).

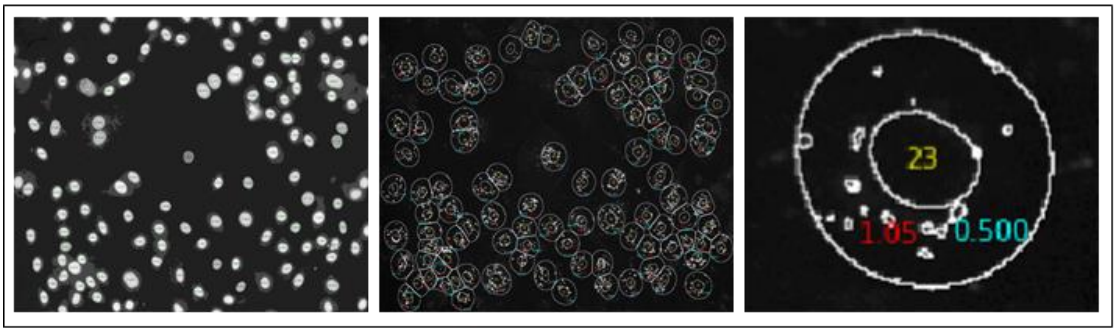

Figure 3.3: Segmentation of nuclei (DAPI) and cytoplasm (RFP channel). (a) Nuclei selected with a threshold solidity measure of 0.93 (b) Segmented nuclei from cytoplasm with HDL containing vesicles (RFP). (c) Measurement of respective signal intensities in DAPI and RFP channels.

To assure quality and limit variance and error, two biological replicate experiments were performed with HAECs. As an indication of reproducibility, the nuclei numbers (Figure 3.4, pink dots = HDL, blue dots = LDL and green dots = no addition of labeled lipoprotein) as well as median foci intensity of Atto 594-labelled LDL and HDL were assessed (Figure 3.5, Plates 1-5 = Run 1 and Plates 6-10 = Run 2) in control vehicle treated wells (dimethyl sulfoxide) per 384-well assay plate and observed negligible variance within and between runs.

Normalization and dose-response curves

Each assay plate was normalised using Genedata Screener (Genedata, Basel, Switzerland) by subtracting and dividing by the value in the blank control wells. This was done for each feature of interest according to the following formula:

$$N(x) = \frac{x - \langle x \rangle}{\langle x \rangle} 100 = \left(\frac{x}{\langle x \rangle} - 1 \right) 100$$

where x is the feature of interest, e.g. cell count, (x) is the median of all blank control wells in the plate, and N(x) is the normalized value in percent. In this example, a value of -100 means that no cells were detected, a value of +100 means that twice as many cells were detected as in the blank control wells.
Post-normalization, the RFP foci per cell values were fitted as a function of drug-concentration in Genedata Screener. The formula used to fit the dose-response data was a logistic function of the Hill Model type.

$$Y(X) = S_\infty + \frac{S_0 - S_\infty}{1 + (X / IC_{50})^{nHill}}$$

where X is the drug concentration, Y is the activity, S_0 is fitted activity level at zero concentration (zero activity), $S\infty$ is fitted activity level at infinite concentration (infinite activity), nHill is the Hill coefficient for the curve which is the measure of the slope at IC_{50}, IC_{50} is the concentration at which the uptake of fluorescent HDL or LDL was inhibited by 50%. The fit parameters were constrained so that $0.5 \leq nHill \leq 4$, $S_0 = 0$, $S_\infty = -100$. Prior to applying the Fisher exact test analysis, the drugs were classified as active based on the possibility to fit Hill model, and the rest of the drugs were assigned as inactive. The only arbitrary feature of this procedure is the choice to fit the logistic model only when the fluorescent signal

drop was more than 50%. The reproducibility of the dose-response curves for foci per cell was assessed by the performance of two independent duplicate experiments.

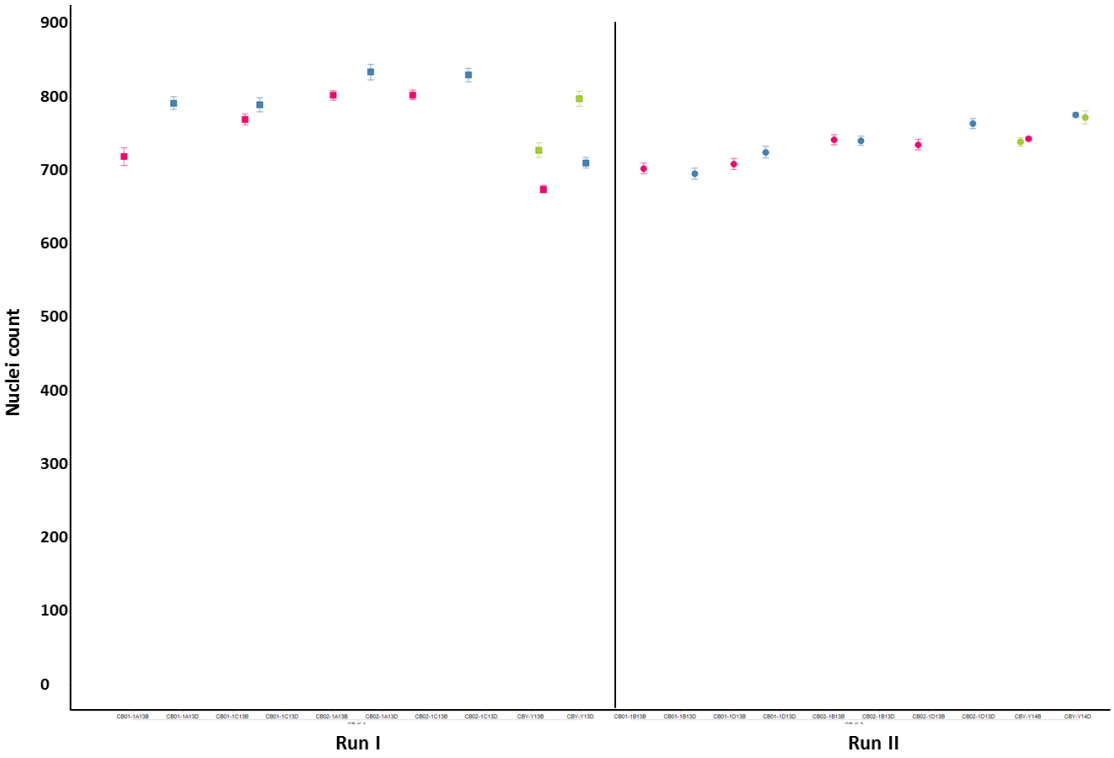

Figure 3.4: Reproducibility of drug screening experiments on the cellular uptake of LDL or HDL by HAECs as reflected by number of nuclei per plate in vehicle treated wells. Each run with one lipoprotein encompassed five plates. Average nuclei numbers (Y-axis) are plotted against screening plates (X-axis). HAECs incubated with fluorescently labeled LDL and HDL represented by blue and pink dots, respectively and vehicle treated wells that did not contain any label (lipoprotein) are represented by green dots.

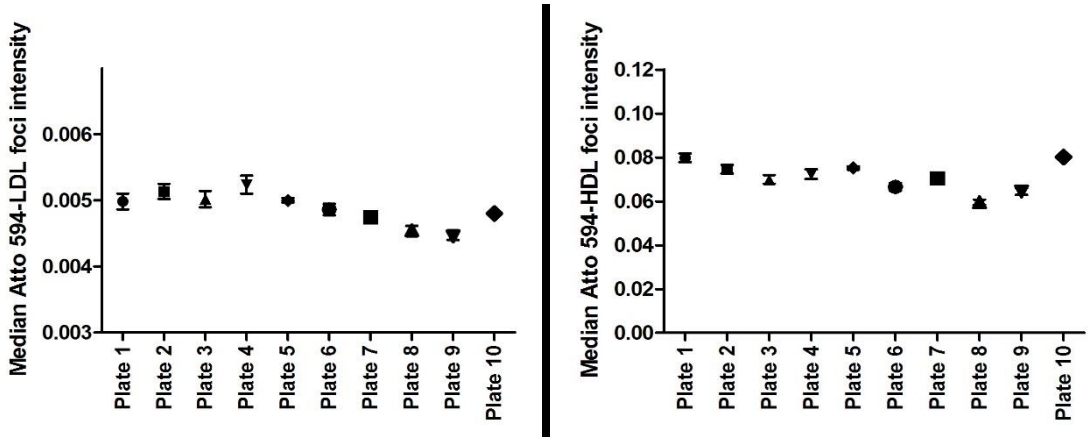

Figure 3.5: Reproducibility of drug screening experiments on the cellular uptake of LDL and HDL by HAECs as reflected by median foci intensity in vehicle treated wells Each run with labeled-lipoprotein (HDL/LDL) encompassed five plates. Median foci intensity of the Atto-labeled lipoprotein (Y-axis) is plotted against screening plates (X-axis). Plates 1-5 represent run 1 and plates 6-10 represent run 2.

To assess the intra- and inter-assay variability after normalization, colchicine dose-response curves (used as positive control drug) for the LDL and HDL median foci intensity feature were generated (Figure 3.6), which did not differ significantly across the two screening runs. For LDL foci intensity, after nonlinear regression analysis, the logIC50 of colchicine was 3.624 (95%CI: 3.060 to 4.188) for run

1 and 3.411 (95%CI: 2.956 to 3.866) for run 2 respectively. For HDL foci intensity, after nonlinear regression analysis, the logIC50 of colchicine was 3.674 (95%CI: 3.139 to 4.208) for run 1 and 3.612 (95%CI: 3.165 to 4.059) for run 2 respectively.

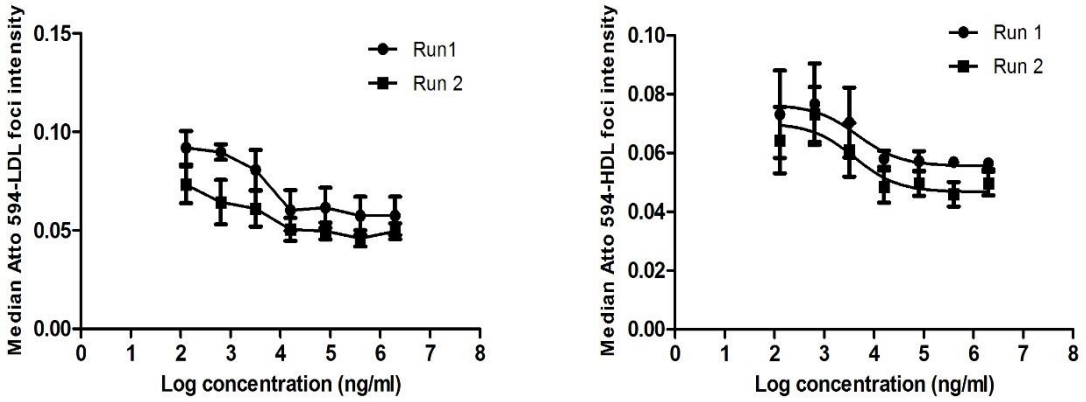

Figure 3.6: Reproducibility of drug screening experiments on the cellular uptake of LDL and HDL by HAECs as reflected by median foci intensity in Colchicine treated wells (positive control) Dose response curves for seven different concentrations of colchicine (X-axis) are plotted against median foci intensity of the Atto-labeled lipoprotein (Y-axis). Data points with circles represent Run 1 and with squares represent Run 2.

For each compound interaction, the amount of downregulation was calculated relative to a control reaction in the presence of vehicle (dimethyl sulfoxide). The analysis of the dose-response data for LDL and HDL uptake by the use of the Hill model identified two and nine drugs, respectively, with a Hill coefficient of 4 which therefore were suspicious of toxicity and hence excluded from further analysis.

Small Interfering RNA Transfection

Endothelial cells were reverse transfected with small interfering RNA (Ambion silencer select, Life technologies) targeted to VEGFR1 (s5287, s5288) or VEGFR2 (s7822, s7824) or VEGFR3 (s5294, s5295) or AKT (s659, s660) or MAPK14 (p38 MAPK) (s3585, s3586) or MAP2K1 & MAPK2K2 (MEK1/2) (s11167, s11170) or SR-BI (s2648, s2649, s2650) or non-silencing control (4390843) at a final concentration of 5nmol/L using Lipofectamine RNA iMAX transfection reagent (Invitrogen, 13778150) in an antibiotic-free medium A or B as indicated. All experiments were performed 72 hours post-transfection and efficiency of transfection was confirmed with at least two siRNAs against each gene using quantitative RT-PCR and western blotting.

Quantitative real time PCR

Total RNA was isolated using TRI reagent (Sigma T9424) according to the manufacturer's instruction. Genomic DNA was removed by digestion using DNase (Roche) and RNase inhibitor (Ribolock, Thermo Scientific). Reverse transcription was performed using M-MLVRT (Invitrogen, 200U/µL) following the standard protocol as described by the manufacturer. Quantitative PCR was done with Lightcycler FastStart DNA Master SYBR Green I (Roche) using gene specific primers as followed:

VEGFR1 (For: CTG AAG GAA GGG AGC TCG TC; Rev: GGC GTG GTG TGC TTA TTT GG), VEGFR2 (For: CGG TCA ACA AAG TCG GGA GA; Rev: CAG TGC ACC ACA AAG ACA CG), VEGFR3 (For: TCC TAC GTG TTC GTG AGA GAC; Rev: CAC CAG GAA GGG GTT GGA AA),SR-BI (For: CTG TGG GTG AGA TCA TGT GG; Rev: GCC AGA AGT CAA CCT TGC TC), normalized to GAPDH (For: CCC ATG TTC GTC ATG GGT GT; Rev: TGG TCA TGA GTC CTT CCA CGA TA).

Wide-field Fluorescence Microscopy for coverslips

Endothelial cells were cultured in medium A or medium B as monolayers on coverslips. After 72hours, cells were subjected to treatment as indicated, followed by incubation with 50µg/mL of Atto594 labeled HDL or Atto488 labeled LDL for 1hour at 37 ºC as previously described [5]. Cells were then washed, fixed with 2% paraformaldehyde and images were acquired on a Zeiss Axiovert 200M.

MTT proliferation assay

Endothelial cells were cultured in medium A or medium B at a density of 10^5 cells per well in a 24 well plate. After 72 hours of culture, the supernatant was removed and cells were washed twice with PBS. The cells were then incubated with 30µL of MTT solution (5mg/ml in PBS,Sigma, M5655) diluted in 270µL of DMEM for 1 hour. The resultant formazan salts were extracted with dimethyl sulfoxide (DMSO) and absorbance intensity was read at 550nm and reference wavelength at 650nm (DMSO). The rate of cell proliferation is calculated relative to the cells cultured in medium A.

Lipoprotein Binding, Cell association and Transport

The methods for the quantification of binding, association and transport of radiolabeled HDL and LDL by endothelial cells have been previously described [6, 16, 18]. All assays were performed in DMEM (Sigma) containing 25mmol/L HEPES and 0.2% BSA instead of serum. Where indicated, cells were pretreated for 30mins at 37 ºC with PI3K inhibitor wortmannin (Sigma, 200nmol/L) or Akt inhibitor MK2206 (Selleckchem, 1µmol/L) or Raf/MEK/ERK inhibitor U0126 (Abcam, 10µmol/L) or p38MAPK inhibitor PD169316 (Calbiochem, 100nmol/L), followed by pre-treatment with VEGF-A_{165} (Sigma, 25ng/ml) for 1hr at 37 ºC. Following treatments, the cells were incubated with 10µg/mL of ^{125}I-HDL/ LDL without (total) or with a 40 time excess of non-labeled HDL/ LDL (unspecific) for 1hr at 4 ºC for cellular binding and at 37ºC for association and transport experiments. Specific cellular binding/ association/ transport was calculated by subtracting the values obtained in the presence of excess unlabeled HDL/ LDL (unspecific) from those obtained in the absence of unlabeled HDL/ LDL (total).

Western Blotting

Endothelial cells were lysed in RIPA buffer (10mmol/L Tris pH 7.4, 150mmol/L NaCl, 1% NP-40, 1% sodium deoxycholate, 0.1% SDS, complete EDTA (Roche)) with protease and phosphotase inhibitors. Equal amounts of protein were separated on SDS-PAGE and trans-blotted onto PVDF membrane (GE Healthcare). Membranes were blocked in appropriate blocking buffer recommended for the antibody (TBS-T supplemented with 5% milk or BSA) and incubated either for 1hour or overnight on shaker at 4 ºC with primary antibodies at a dilution of 1:1000 in the same blocking buffer. Membranes were incubated for 1hour with HRP-conjugated secondary antibody (Dako) in blocking buffer at a dilution of 1:2500. Membranes were further incubated with chemiluminescence substrate for 1min (Pierce ECL plus, Thermo scientific) and imaged using Fusion Fx (Vilber). As indicated Beta-Actin, GAPDH or TATA binding protein was used as loading control with primary antibody at 1:5000 and secondary antibody at 1:10000 dilutions. The silencing efficiencies of VEGFR1 (2893, CST), VEGFR2 (9686, CST) and VEGFR3 (ab27278, Abcam) were evaluated and compared to Beta-Actin (ab8226, Abcam). The expression of SR-BI (NB400-131, Novus) was evaluated and compared to the expression of GAPDH (ab9484, Abcam). The silencing efficiencies of Akt (9272, CST), p38 MAPK (9212, CST) and MEK1/2 (8727, CST) were compared to TATA binding protein (TBP, ab51841, Abcam). The Phospho-expressions of VEGFR2 (3817, CST), Akt S473 (9271, CST), p38 MAPK Thr180/Tyr182 (9211, CST), p44/42 MAPK Thr202/Tyr204 & Thr185/Tyr187 (9106, CST) were compared to the total expression of VEGFR2 (9698, CST), Akt (9272, CST), p38 MAPK (9212, CST) and p44/42 MAPK (4695, CST) respectively.

Cell surface expression analysis

Biotinylation of intact cells was performed using 20mg/mL EZ-Link sulfo-NHS-S-S-Biotin (Thermo Scientific) in the cold for 1 hour with mild shaking and quenched with ice-cold Tris pH 7.4. Cells were lysed in RIPA buffer (total cell lysate) and 200-500µg of lysates were incubated with 20µL of BSA-blocked streptavidin beads suspension (GE Healthcare) for 16hours at 4 ºC and pelleted by centrifugation; the pellet represents surface proteins. Proteins were dissociated from the pellet by boiling with SDS loading buffer and analyzed by SDS-PAGE and immunoblotting with SR-BI antibody (NB400-131, Novus) and LDL receptor (LDLR, ab30532, Abcam), ABCG1 (NB400-132, Novus). TATA binding protein (TBP, ab51841, Abcam) and endothelial lipase (EL, NB400-118, Novus) were used as intracellular and plasma membrane controls.

Statistical Analysis

Probability of finding active and inactive drugs for a given target compared to non-targeting drugs was performed using Fisher exact test analysis. The drugs were pre-classified as active based on their ability to fit the Hill logistic model only when the RFP foci signal dropped more than 50%. The data sets for all validation experiments were analyzed using the GraphPad Prism 5 software. Comparison between groups in follow up biochemical validation experiments was performed using Kruskal-Wallis one-way ANOVA followed by Dunn's post-test. The data was obtained from at least three independent experiments, performed in triplicates or quadruplets. Values are expressed as mean±SEM. $P<0.05$ was regarded as significant.

3.3 Results

Screening of kinase inhibitors

Following culture for 72 hours in 384 well plates at a density of 1000 cells per well, HAECs were treated with 141 kinase inhibiting drugs for one hour at seven different dilutions spanning four orders of magnitude. Thereafter cells were incubated with fluorescent-labeled Atto 594-LDL or Atto 594-HDL for another hour. After washing, fixation and nuclei staining, nine images per well were acquired using a molecular devices widefield microscope. The microscope generated images were processed by Cell profiler to segment nuclei and RFP foci intensity (vesicles) per cell. For each compound interaction, the amount of downregulation was calculated relative to a control reaction in the presence of vehicle (dimethyl sulfoxide). The analysis of the dose-response data for LDL and HDL uptake by the use of the Hill model (see methods) identified two and nine drugs, respectively, with a Hill coefficient of 4 which therefore were suspicious of toxicity and hence excluded from further analysis. The drugs were pre-classified as active based on their ability to fit the Hill logistic model only when the RFP foci signal dropped more than 50%. Finally using Fisher's exact test, we statistically evaluated the probability of finding drugs targeting a kinase that actively decrease the uptake of fluorescent LDL or HDL in the presence of maximal concentration versus non-targeting drugs. After correction of p values for multiple statistical testing, VEGFR emerged as the only target whose inhibition significantly interfered with the HDL uptake by HAECs. However, this analysis did not reveal any target whose inhibition led to a significant and consistent decrease in LDL uptake (Table 3.II).

Target	LDL					HDL				
	n	m	n'	m'	p-value	n	m	n'	m'	p-value
ABL	1	5	26	113	**0.71653**	2	4	51	88	**0.714**
ALK	1	3	26	115	**0.56562**	1	3	52	89	**0.842**
c-Kit	1	6	26	112	**0.77159**	3	4	50	88	**0.505**
c-Met	4	7	23	111	**0.12361**	5	6	48	86	**0.369**
EGFR	3	11	24	107	**0.50494**	8	6	45	86	**0.084**
FGFR	2	4	25	114	**0.31014**	3	3	50	89	**0.383**
FLT-3	0	1	27	117	**1**	0	1	53	91	**1**
HER2	2	5	25	113	**0.38616**	4	3	49	89	**0.221**
IGF-1R	1	0	26	118	**0.18621**	1	0	52	92	**0.366**
VEGFR	9	22	18	96	**0.08137**	18	13	35	79	**0.005**
Aurora	5	10	22	108	**0.11871**	7	8	46	84	**0.278**
CDK	2	6	25	112	**0.45878**	1	7	52	85	**0.977**
CHK	0	1	27	117	**1**	0	1	53	91	**1**
GSK-3	0	3	27	115	**1**	0	3	53	89	**1**
JNK	0	1	27	117	**1**	0	1	53	91	**1**
JAK/STAT	1	3	26	115	**0.56562**	0	4	53	88	**1**
MEK	1	10	26	108	**0.90542**	4	7	49	85	**0.623**
mTOR	0	10	27	108	**1**	1	9	52	83	**0.991**
PI3K/AKT	1	17	26	101	**0.98121**	2	16	51	76	**0.998**
p38 MAPK	2	5	25	113	**0.38616**	2	5	51	87	**0.798**

Table 3.II: Fisher exact test analysis of binary activity signal for uptake of LDL and HDL For each target, Fisher exact test analysis was used to calculate the probability to get more active drugs (m) and less active drugs (n), for a given target, and at the same time less active drugs (m') and more active (n') drugs for non-targets. The drugs were pre-classified as active based on their ability to fit the Hill logistic model only when the RFP foci signal dropped more than 50%. Inhibition of targets with ** $P \leq 0.01$ are interpreted to be more likely than the inhibition of all other targets to decrease the uptake of LDL or HDL. The data were obtained from two replicate experiments.

VEGFR2 regulates endothelial binding, association and transport of HDL but not LDL

We first confirmed the regulatory role of VEGFR in the uptake of HDL by HAECs and to identify the relevant VEGF receptor by a knock-down strategy. HAECs expressed all three VEGF receptors: VEGFR1, VEGFR2 and VEGFR3 as analyzed by qRT-PCR (Figure 3.7A). To test which VEGF receptor was involved in HDL uptake, each of the three VEGF receptors was targeted using RNA interference. Although knock-down was efficient for each VEGFR on the mRNA level (Figure 3.7B) and protein level (Figure 3.7C), only the silencing of VEGFR2 decreased the cellular uptake of fluorescent-labeled Atto594-HDL whereas silencing VEGFR1 and VEGFR3 showed no effect (Left lane of Figure 3.8). These findings were confirmed using radioiodinated HDL, where silencing of

VEGFR2 significantly reduced the specific 4ºC binding of ^{125}I-HDL to ECs by 60% (Figure 3.9A), the specific 37°C cellular association by 80% (Figure 3.9B) and the specific transendothelial transport of ^{125}I-HDL from apical to basal compartment at 37 ºC by 60% (Figure 3.9C). However, neither cellular uptake of fluorescent-labeled Atto488-LDL (Figure 3.8) nor specific cellular binding, association and transendothelial transport of ^{125}I-LDL were affected by silencing of any VEGF receptor (Figure 3.9D-F). Taken together, these results indicate a specific effect of VEGFR2 on endothelial binding and uptake as well as trans-endothelial transport of HDL but not LDL.

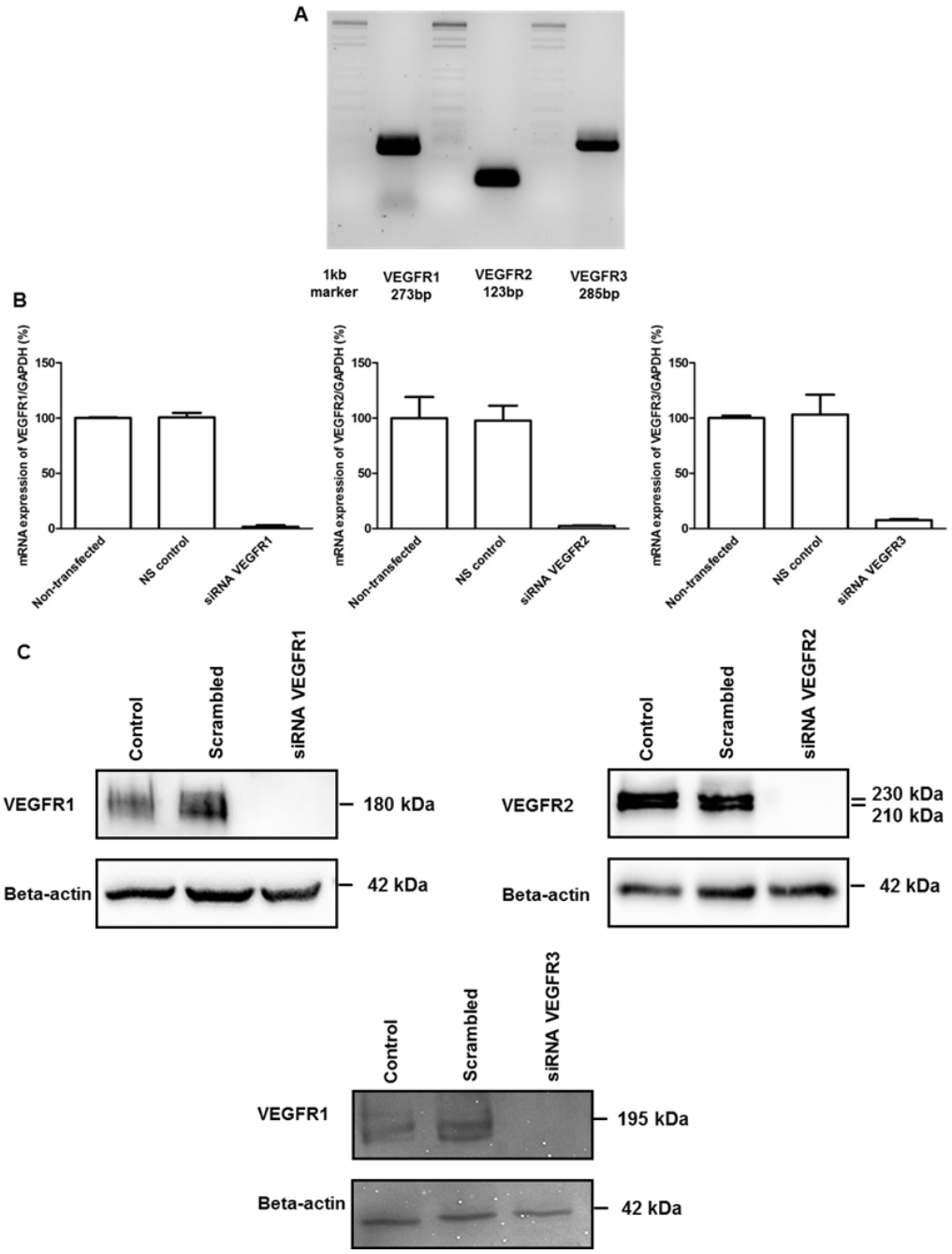

Figure 3.7: Expression of VEGF receptors (A) and efficiency of RNA interference (B, C) A, mRNA levels of VEGFR1, VEGFR2 and VEGFR3 in HAECs were measured by real-time polymerase chain reaction. HAECs were transfected with specific siRNA against VEGFR1, VEGFR2, or VEGFR3 or with non-silencing control siRNA (NS control). Assays were performed 72hours after transfection. Silencing efficiency was analyzed at the **B,** mRNA level using qRT-PCR and **C,** protein level using western blotting. The western blots were probed with antibodies against VEGFR1 (180 kDa), VEGFR2 (210 kDa, 230 kDa) and VEGFR3 (195 kDa) respectively and Beta-actin (42 kDa) was used as the loading control.

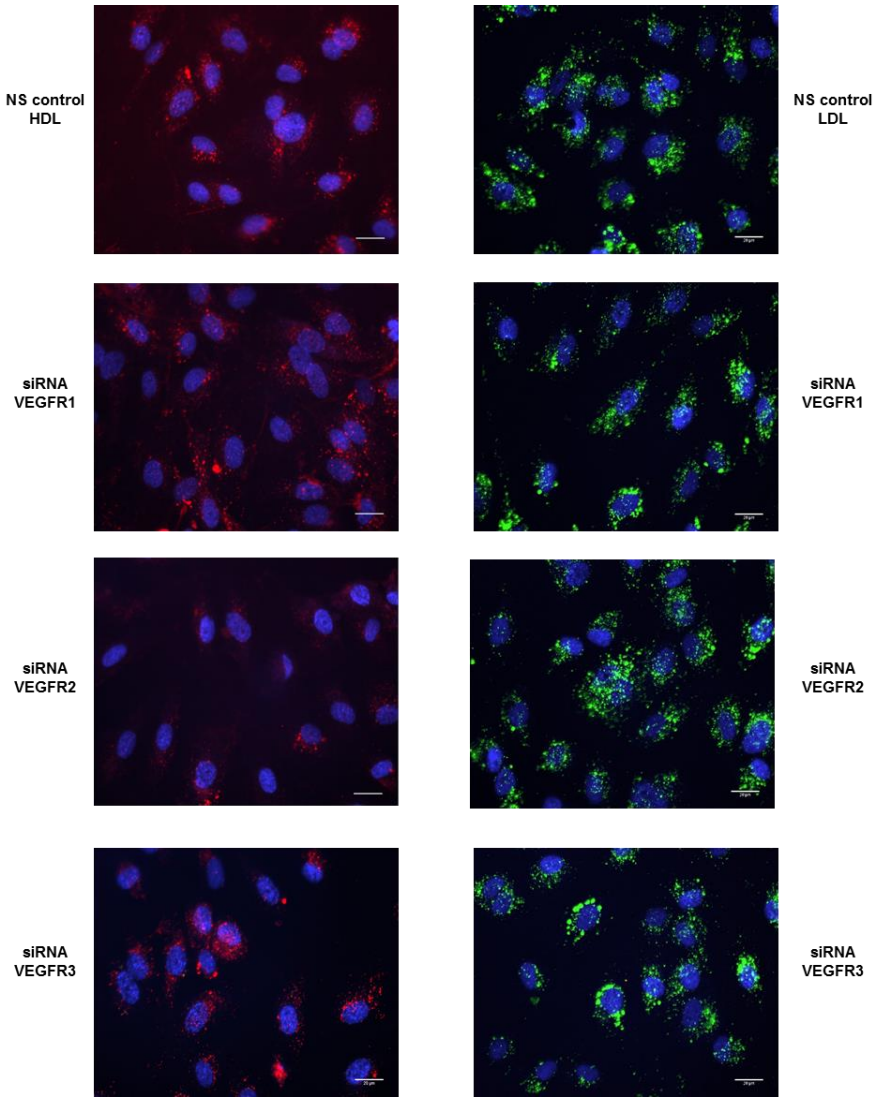

Figure 3.8: Effect of VEGF receptors on the uptake of HDL (left lane) and LDL (right lane) by HAECs HAECs were transfected with a specific siRNA against VEGFR2 or with non-silencing control siRNA (NS control) and fluorescent lipoprotein uptake assay was performed 72hours after transfection. Uptake of Atto594-HDL (red) and Atto488-LDL (green) into transfected endothelial cells was analyzed by wide-field fluorescence microscopy. ECs were incubated with 50ug/ml of Atto594-HDL or 50ug/ml Atto488-LDL for 1hour prior to fixation and nuclei were counterstained with DAPI (blue). Scale bar is 20µM.

VEGF-A regulates endothelial binding, association and transport of HDL but not LDL

Binding of VEGF-A to its receptor VEGFR2 induces conformational changes and receptor dimerization which in turn triggers kinase activation and auto-phosphorylation of tyrosine residues [19]. To investigate whether VEGF-A regulates trans-endothelial transport of HDL, we cultured ECs either in the VEGF-A containing medium A or in the VEGF-A-free medium B. Upon Western blot analysis we found that, HAECs cultured in VEGF-free medium for 72hours, lose phosphorylation of Tyr residues 1054 and 1059 in the major tyrosine kinase catalytic domain of VEGFR2, (Figure 3.10). As shown in the top panel of Figure 3.11, cells cultured in VEGF-free medium for 72 hours decreased the cellular uptake of Atto594-HDL compared to cells cultured in VEGF containing medium (control). Interestingly, pre-treatment of cells cultured in medium B supplemented with 25 ng/ml VEGF-A for 1 hour showed a significant increase in the uptake of Atto594-HDL. Confirming these microscopic findings, pre-treatment of cells for 1hour with VEGF-A significantly increased 4ºC cellular binding of ^{125}I-HDL

(Figure 3.12A) and 37°C cellular association of ^{125}I-HDL (Figure 3.12B) as well as apical-to-basolateral transendothelial transport of ^{125}I-HDL (Figure 3.12C) compared to cells cultured in VEGF-free medium.

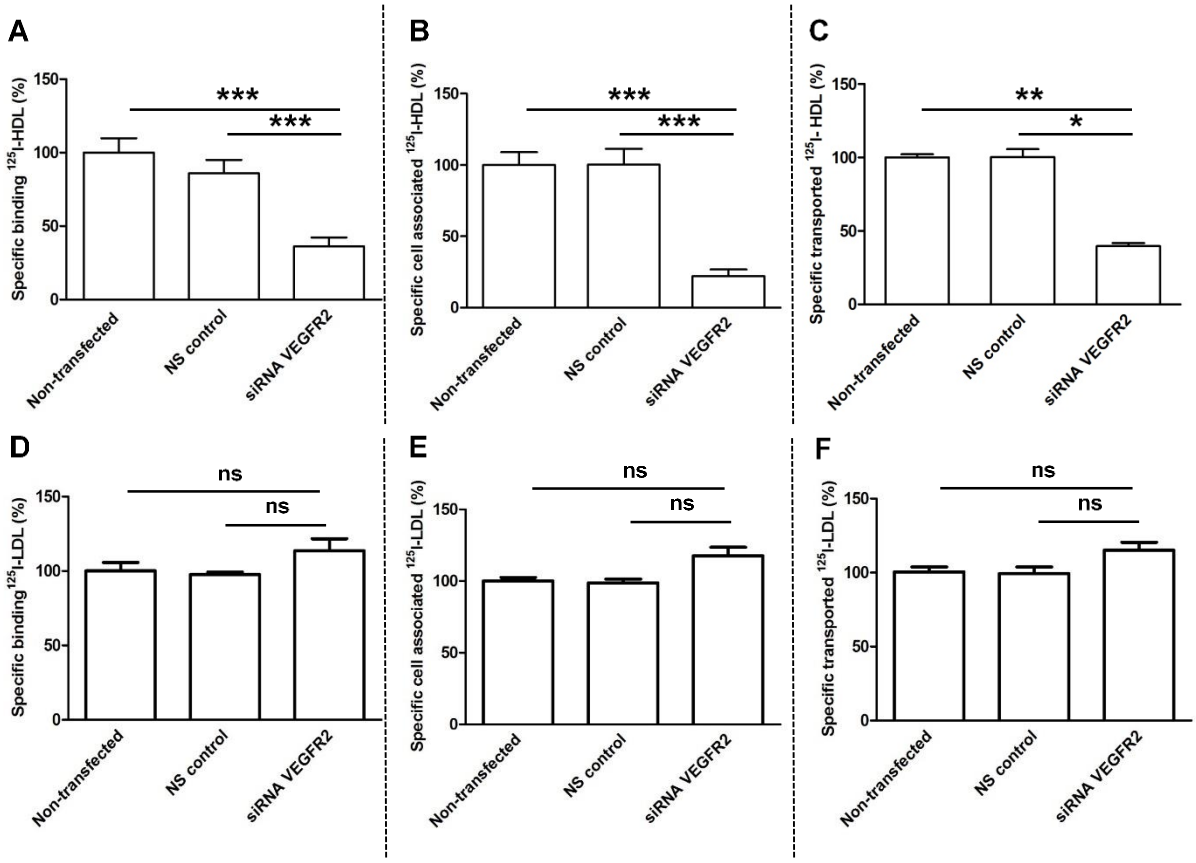

Figure 3.9: VEGFR2 mediates binding, association and transendothelial transport of HDL but not LDL in HAECs HAECs were transfected with a specific siRNA against VEGFR2 or with non-silencing control siRNA (NS control) and assays were performed 72hours after transfection. To study cellular binding, association and transport, transfected ECs were incubated with 10µg/mL of ^{125}I-HDL or ^{125}I-LDL for 1hour in the absence (total) or in the presence of 40-fold excess of unlabeled HDL and LDL, respectively, to record unspecific interactions. Specific binding, association and transport were calculated by subtracting unspecific values from total values. **A**, Specific binding was measured by incubating cells with ^{125}I-HDL (**A**) or ^{125}I-LDL (**D**) at 4 ºC. To measure specific cell association, cells were incubated with ^{125}I-HDL (**B**) or ^{125}I-LDL (**E**) at 37 ºC. For the measrument of transport HAECs were cultured on inserts. The transport of ^{125}I-HDL (**C**) and ^{125}I-LDL (**F**) from the apical to basolateral compartment was measured at 37 ºC. The results are represented as means±SEM of three independent triplicate experiments (n=3). ***$P \leq 0.001$, **$P \leq 0.01$, *$P \leq 0.05$ and ns represents "not significant".

By contrast, cells cultured in VEGF-free medium for 72 hours, did not show any decrease in the uptake of Atto488-LDL compared to the control condition (Bottom lane of Figure 3.11). Likewise, presence, absence or supplementation of VEGF-A had no effect on the cellular binding, association and transport of ^{125}I-LDL (Figures 3.12D-F). Taken together, these results indicate that VEGF-mediated VEGFR2 receptor activation is required for endothelial binding and uptake as well as trans-endothelial transport of HDL but not LDL.

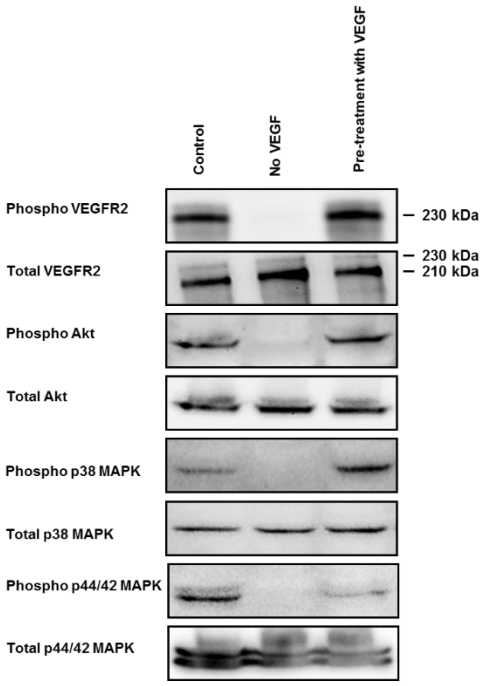

Figure 3.10: Effect of VEGF-A phosphorylation of VEGFR2 and its downstream kinases (A). HAECs were cultured in regular medium containing VEGF-A (control) or in medium free of VEGF-A (no VEGF) for 72hours or cells were pre-treated with 25ng/ml of $VEGF_{165}$ for 1hour prior to protein extraction. **A:** Cell lysates were analysed by western blotting for phospho VEGFR2 (Tyrosine 1054/1059) and total VEGFR2, phospho Akt (Ser-473) and total Akt, phospho p38 MAPK (Thr180/Tyr182) and total p38 MAPK, phospho ERK1/2 (Thr202/Tyr204 & Thr185/Tyr187) and total ERK1/2.

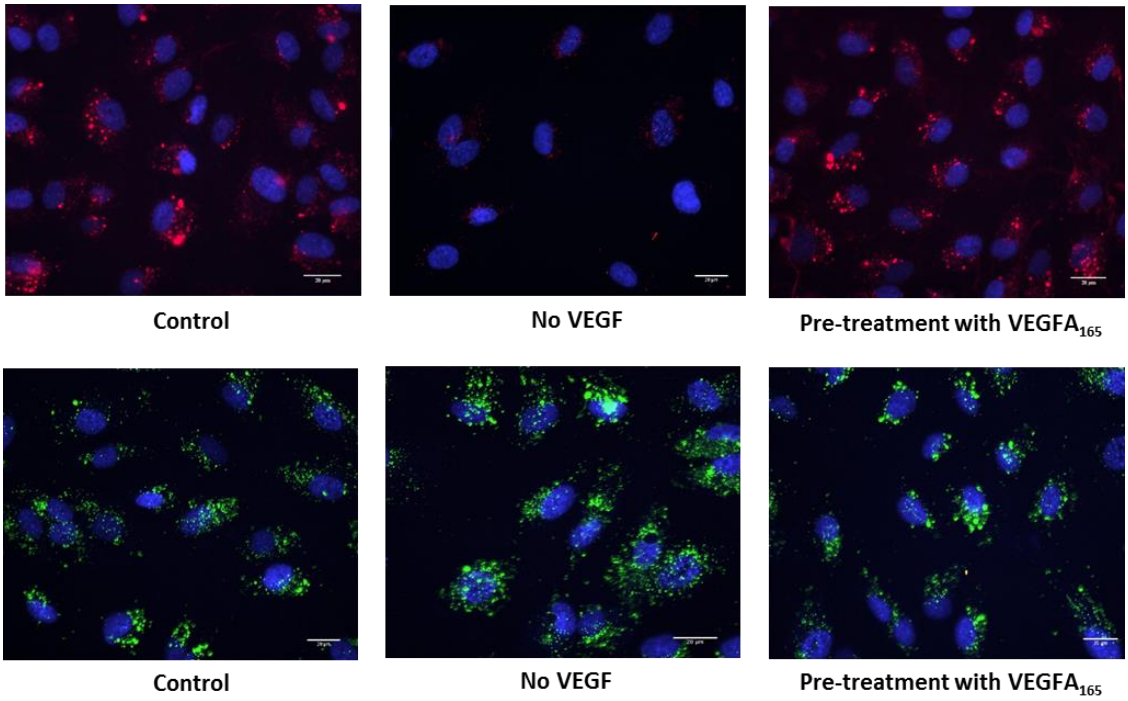

Figure 3.11: Effect of VEGF-A treatment on HDL (left lane) and LDL (right lane) uptake by HAECs HAECs were cultured in the presence of VEGF-A (control) or absence of VEGF-A (no VEGF) for 72hours or cells were pre-treated with 25ng/ml of $VEGF_{165}$ for 1hour prior to the incubation with fluorescent lipoproteins. ECs were incubated with 50ug/ml of Atto594-HDL or Atto488-LDL for 1hour prior to fixation and nuclei were counterstained with DAPI (blue). Uptake of Atto594-HDL (red) and Atto488-LDL (green) in endothelial cells was analyzed by wide-field microscopy. Scale bar is 20µM.

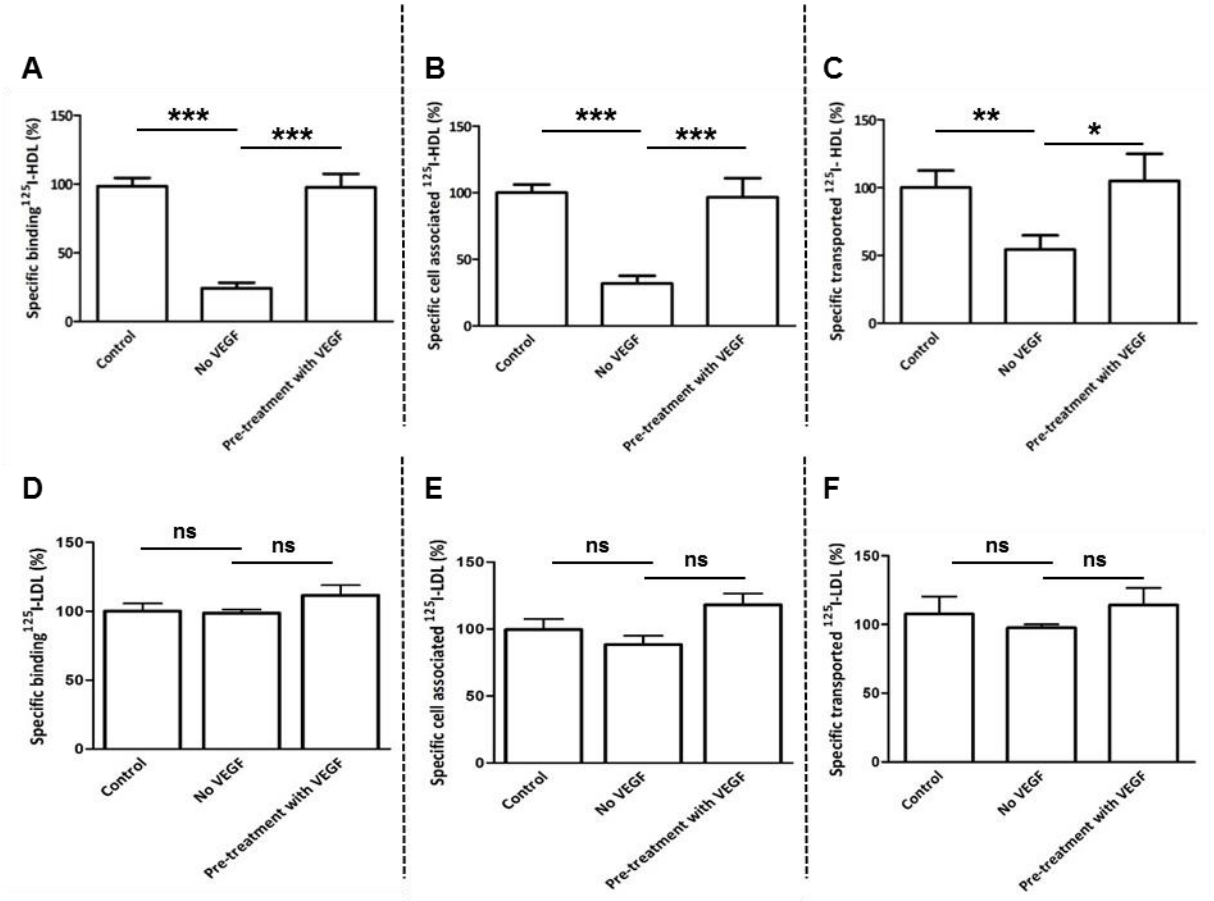

Figure 3.12: Effect of VEGF-A on binding, association and transendothelial transport of HDL and LDL in HAECs HAECs were cultured in medium containing VEGF-A (control) or lacking VEGF-A (no VEGF) for 72hours. Cells were pre-treated with 25ng/mL of VEGF-A_{165} for 1hour prior to the assays if indicated. Specific binding was measured by incubating cells with ^{125}I-HDL (**A**) and ^{125}I-LDL (**D**) at 4 ºC. Specific cell association was analyzed by incubating cells with ^{125}I-HDL (**B**) and ^{125}I-LDL (**E**) at 37 ºC. HAECs were cultured on inserts and transport of ^{125}I-HDL (**C**) and ^{125}I-LDL (**F**) from the apical to basolateral compartment was measured at 37 ºC. The results are represented as mean±SEM of three independent triplicate experiments (n=3). ***$P \leq 0.001$, **$P \leq 0.01$, *$P \leq 0.05$ and ns represents "not significant".

VEGF-A regulates endothelial binding and association of HDL through p38MAPK and PI3K/Akt

We determined whether the knock down of the downstream kinases of VEGF signaling, namely phosphatidyl-inositol 3 kinase (PI3K), p38 mitogen activated protein kinase (p38MAPK), and mitogen-activated protein kinase kinase (MEK) interfere with endothelial binding and association of HDL. The knockdown was found efficient for each kinase on the protein level (Figure 3.13). Western blot analysis revealed that residue Ser473 of Akt (the downstream kinase targeted by PI3K), residues Thr180 and Tyr182 of p38 MAPK as well as residues Thr202, Tyr204, Thr185, and Tyr187 of p44/42 MAPK (ERK1/2, which is a common kinase target of MEK1 & MEK2) were phosphorylated in the presence but not in the absence of VEGF (Figure 3.10). Silencing of either Akt or p38 MAPK or MEK1/2 decreased the cellular binding and association of ^{125}I-HDL. However, VEGF-A treatment restored the cellular binding and association of ^{125}I-HDL by endothelial cells lacking MEK1/2 but not by endothelial cells lacking Akt or p38 MAPK. (Figure 3.14A & B). Taken together, these results show that VEGF-induced binding and association of HDL depends on the activation of PI3K/Akt and p38MAPK but independent of the MEK/ERK pathway. Interestingly, endothelial binding or cell association of ^{125}I-LDL was not affected by silencing of Akt but significantly decreased by silencing of p38 MAPK and MEK (Figure 3.15A&B).

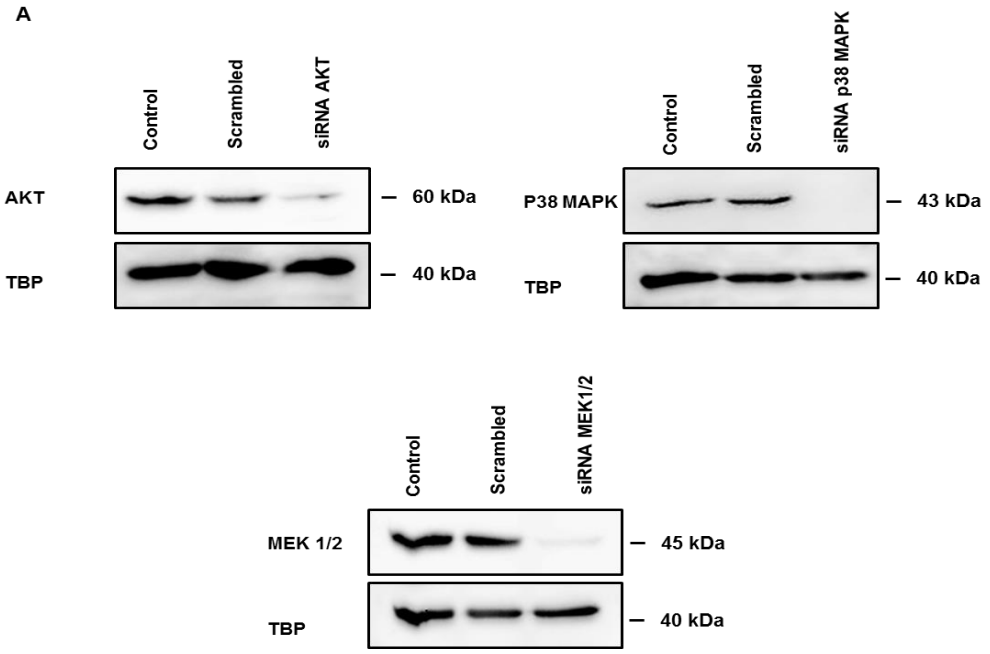

Figure 3.13: Silencing efficiency of AKT, p38 MAPK and MEK1/2 Protein levels of Akt, p38 MAPK and MEK1/2 were measured using western blotting following transfection of ECs with specific siRNAs against AKT, MAPK14 (p38 MAPK), MAP2K1/MAP2K2 (MEK1/2). TATA-binding protein (TBP) was used as a loading control.

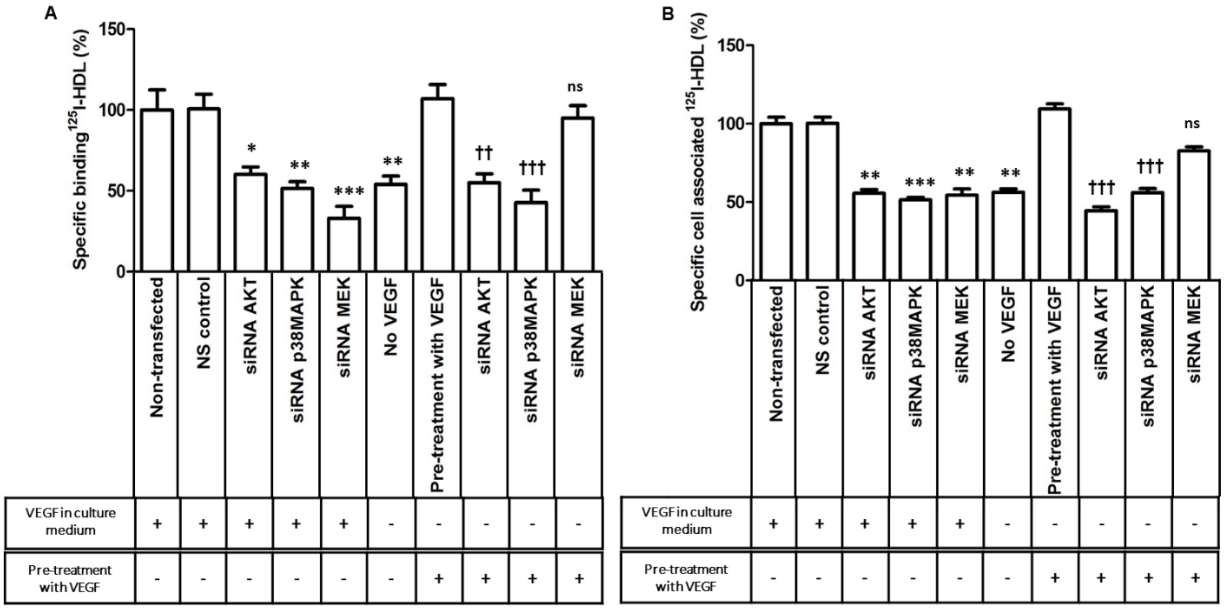

Figure 3.14: VEGF-A regulates HDL binding and association through PI3K/Akt and p38 MAPK HAECs were transfected with specific siRNA against AKT or MAPK14 (p38 MAPK) or MAP2K1/MAP2K2 (MEK1/2) or with non-silencing control (NS control) siRNA in the presence or absence of VEGF-A containing medium and assays were performed 72hours post-transfection. **A**, Specific binding was measured by incubating cells with ^{125}I-HDL at 4 ºC. **B**, Specific cell association was analyzed by incubating cells with ^{125}I-HDL at 37 ºC. The results are represented as mean±SEM and three independent triplicate experiments (n=3). ***$P \leq 0.001$, **$P \leq 0.01$, *$P \leq 0.05$. †††$P \leq 0.001$, ††$P \leq 0.01$, †$P \leq 0.05$ and ns represents "not significant".

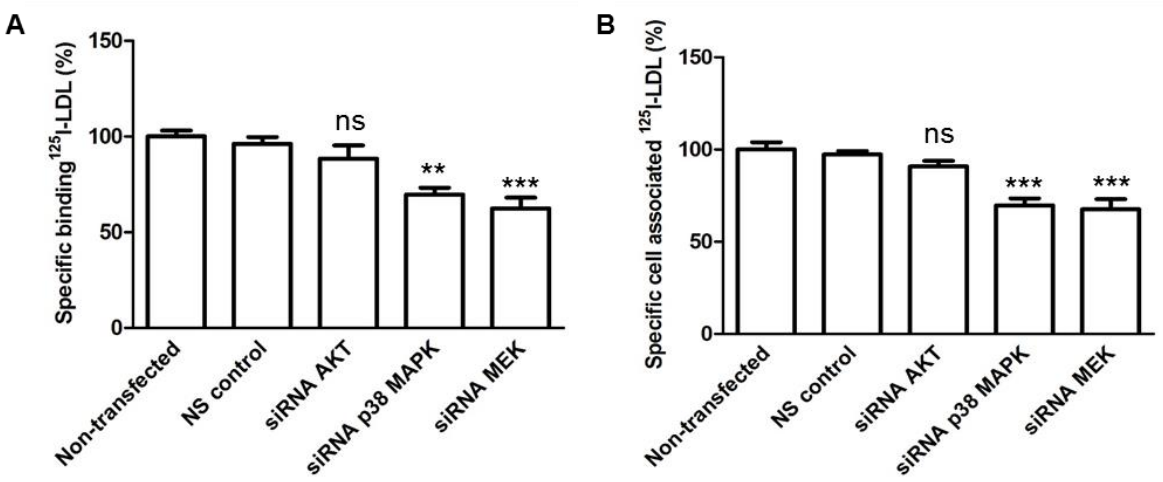

Figure 3.15: Binding and association of ^{125}I-LDL through p38 MAPK and MEK1/2 HAECs were transfected with specific siRNA against AKT or MAPK14 (p38 MAPK) or MAP2K1/MAP2K2 (MEK1/2) or with non-silencing control (NS control) siRNA in the presence of VEGF-A containing medium and assays were performed 72hours post-transfection. **A**, Specific binding was measured by incubating cells with ^{125}I-LDL at 4 ºC. **B**, Specific cell association was analyzed by incubating cells with ^{125}I-LDL at 37 ºC. The results are represented as mean±SEM and three independent triplicate experiments (n=3). ***$P\leq$ 0.001, **$P\leq$ 0.01, *$P\leq$ 0.05 and ns represents "not significant".

VEGF-A regulates binding, association and transport of HDL via SR-BI

We have previously demonstrated that SR-BI, ABCG1 and EL regulate binding and trans-endothelial transport of HDL. Because of the fast effects of VEGF-A on cellular binding, association and transport of ^{125}I-HDL, we hypothesized that VEGF-A regulates the availability of one of these HDL interacting proteins on the cell surface in HAECs. To test this hypothesis, we performed a cell surface biotinylation experiment. HAECs cultured in the VEGF-free cell culture medium did not show any SR-BI on the cell surface. Pre-treatment with VEGF-A restored the expression of cell surface SR-BI. By contrast the presence or absence of VEGF-A had no effect on the cell surface expression of LDLR, ABCG1, or EL. (Figure 3.16). To determine whether VEGF-A regulated HDL trans-endothelial transport through SR-BI, we silenced SR-BI using RNA interference. The knockdown was efficient at the mRNA (Figure 3.17A) and protein levels (Figure 3.17B). Silencing SR-BI alone significantly decreased ^{125}I-HDL cellular binding and association by 50-55% and transport by 60%, respectively. Pre-treatment with VEGF-A for 1hour did not restore the cellular binding, association and transport of ^{125}I-HDL inhibited by suppression of SR-BI (Figure 3.18A-C).

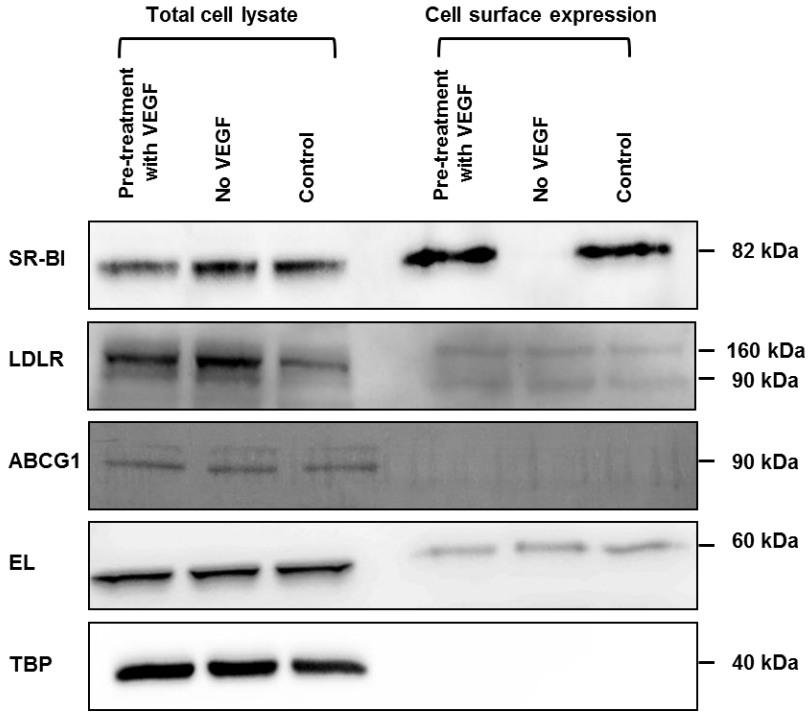

Figure 3.16: VEGF-A regulates cell surface expression of SR-BI Western blots of SR-BI, LDL-receptor, ATP binding cassette transporter ABCG1, endothelial lipase (EL), and anti-TATA binding protein (TBP) in total cell lysates (left) and on the cell surface (right). HAECs were cultured in the presence or absence of VEGF for 72hours and cells were then pre-treated with 25ng/mL of $VEGF_{165}$ for 1hour if indicated. The western blot was probed with anti-SR-BI (82 kDa), anti-LDLR (95 kDa and 160 kDa), anti-ABCG1 (90 kDa) as well as anti-endothelial lipase (EL) (60 kDa) and anti- TATA binding protein (TBP) (40 kDa, as control for intracellular protein expression).

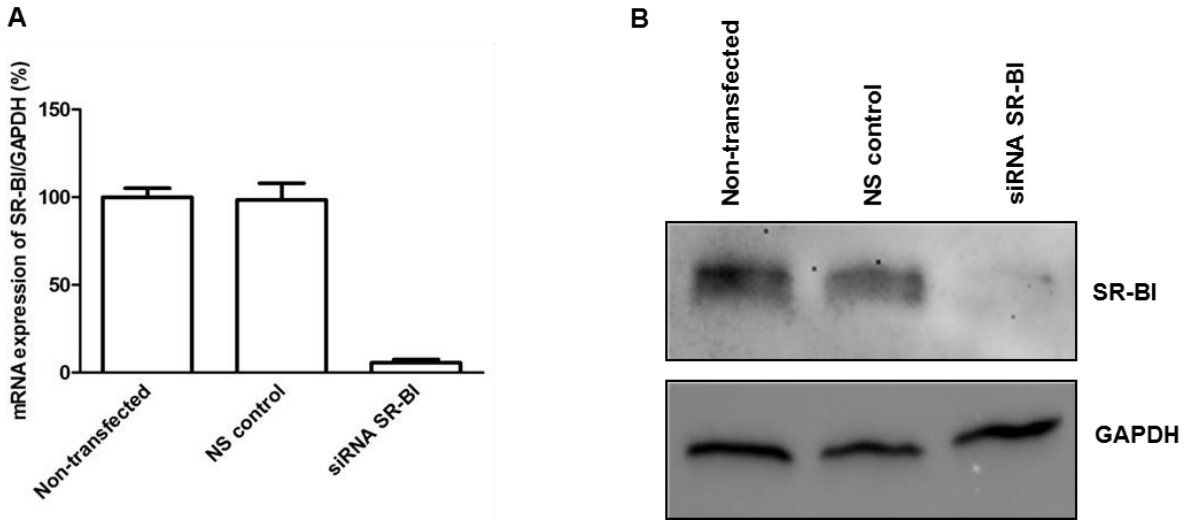

Figure 3.17: Efficiency of silencing SR-BI A, mRNA levels of SR-BI were analyzed following transfection of ECs with specific siRNAs against SR-BI. GAPDH was used as a housekeeping control. **B**, SR-BI (82 kDa) protein expression levels measured by western blotting, GAPDH (38 kDa) used as loading control.

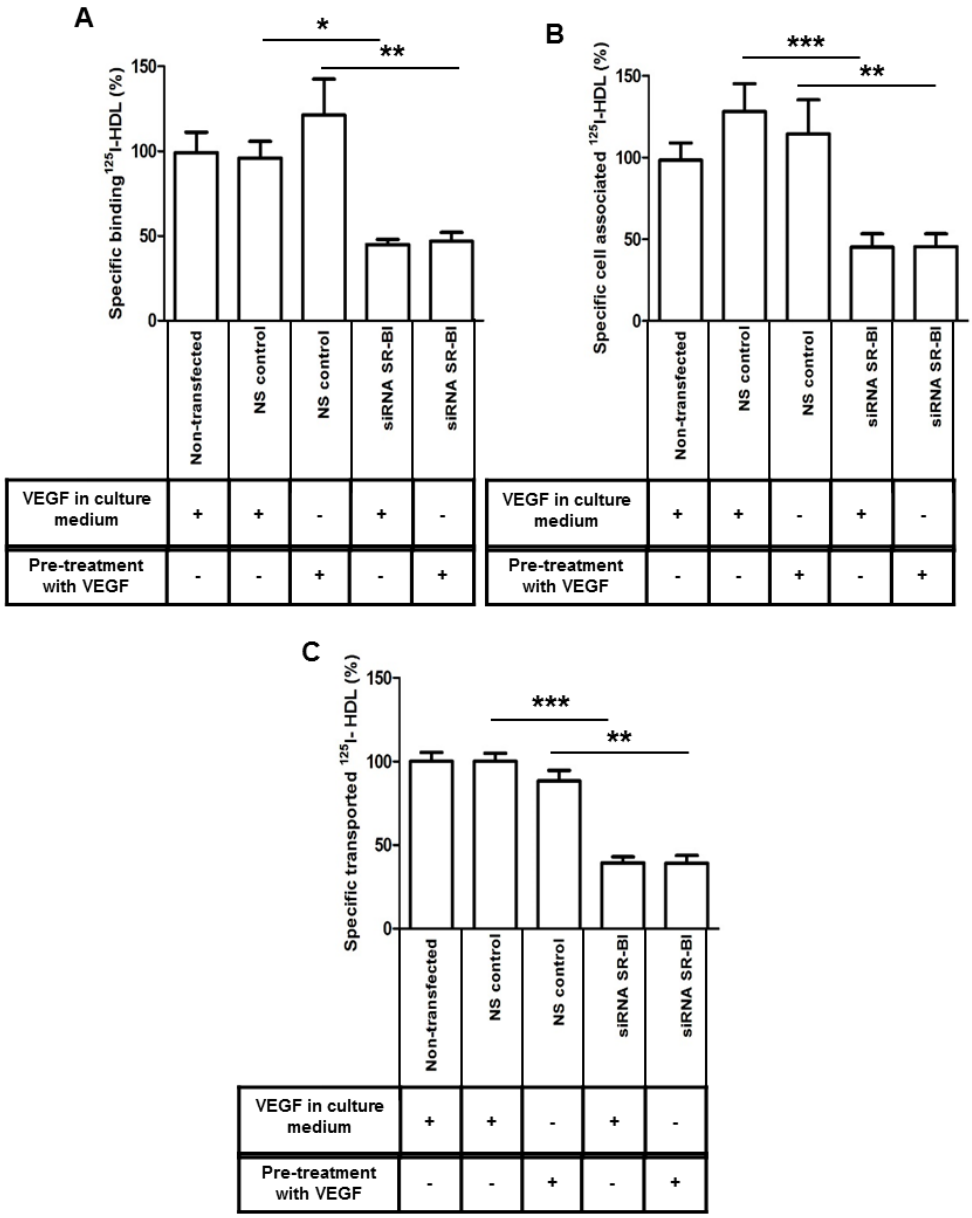

Figure 3.18: VEGF-A modulates SR-BI dependent binding, association and transport of HDL by HAECs HAECs were transfected with a specific siRNA against SR-BI or with non-silencing control siRNA (NS control) in the presence or absence of VEGF-A containing medium and assays were performed 72hours post-transfection. **A**, Specific binding was measured by incubating cells with ^{125}I-HDL at 4 ºC. **B**, Specific cell association was analyzed by incubating cells with ^{125}I-HDL at 37 ºC. **C**, ECs were cultured on inserts and transport of ^{125}I-HDL from the apical to basolateral compartment was measured at 37 ºC. The results are represented as mean±SEM of three independent triplicate experiments (n=3). ***$P \leq 0.001$, **$P \leq 0.01$, *$P \leq 0.05$.

3.4 Discussion

We previously reported that bovine aortic endothelial cells bind, internalize and transport HDL in a specific process dependent on SR-BI, ABCG1 [6], EL [7], and ectopic beta-ATPase [8]. Here we show that human aortic endothelial cells (HAECs) also bind, internalize and transport HDL as well as LDL. Using a high-content drug screening approach we identified VEGF-A/VEGFR2 signaling as a rate-limiting factor for the cell surface abundance of SR-BI and, as a consequence, regulator of uptake and transport of HDL by HAECs (Figure 3.19). Interestingly, VEGF-A and VEGFR2 had no effect on endothelial binding, uptake and transport of LDL.

VEGFs are important regulators of both vasculogenesis and angiogenesis in the adult [20]. In mammals, the VEGF family encompasses five different isoforms namely, VEGF-A, -B, -C, and -D as well as placenta growth factor

(PLGF). These ligands bind to three VEGF receptors - VEGFR1, VEGFR2, and VEGFR3 - in an overlapping pattern. VEGF-A, VEGF-B, and PLGF bind to VEGFR1 [21-23]; VEGF-A binds to VEGFR2 [24]; VEGF-C and VEGF-D bind to VEGFR3 [25, 26]. Among VEGF-A receptors, VEGFR1 has the highest affinity and acts as a negative regulator by sequestering VEGF-A from binding to VEGFR2 [27], hence VEGFR2 is the key receptor mediating most of the cellular effects of VEGF-A in endothelial cells. In accordance with this, our results show that RNA interference with VEGFR2 but not with VEGFR1 decrease HDL uptake (Figure 3.8). Our data show some analogy with those reported by Lim et al. and Martel et al, who observed improved lymphatic function and transport of HDL after VEGF-C treatment in mice [28, 29]

Binding of VEGF-A induces conformational changes and dimerization of VEGFR2 which in turn triggers kinase activation, tyrosine phosphorylation of the dimerized VEGFR2 and subsequent phosphorylation of SH2-containing intracellular signaling proteins, including phospholipase C-γ1 (PLCγ1), Src family tyrosine kinases, and phosphatidylinositol 3-kinase (PI3K) and Ras GTPase-activating protein residues of Ras-Raf-MEK-MAPK pathway [30-33]. VEGF was also shown to induce actin remodeling through activation of CDC42 and p38MAPK [34]. Both by pharmacological inhibition and RNA interference we revealed the involvement of PI3K/Akt, p38MAPK, and the Ras-Raf-MEK pathway in binding and uptake of HDL (Figure 3.14). However, the inhibition of the Ras-Raf-MEK pathway but not the inhibition of PI3K/Akt and p38MAPK could be overcome by VEGF stimulation. Thus, VEGF regulates the interaction of HDL with endothelial cells by activating PI3K/Akt and p38MAPK but not the Ras-Raf-MEK pathway. PI3K is known to be involved in endosomal membrane trafficking [35, 36] and its inhibition by wortmannin in polarized cells affects early trafficking in the endocytic pathway as well as inward vesicularization for the formation of multivesicular bodies in the later stages [37]. For example, PI3K was shown to mediate the stimulatory effect of insulin on the cell surface translocation of the glucose transporter-4 (GLUT-4) [36, 38]. It has also been shown in hepatocytes, that insulin regulates the cell surface expression of SR-BI and selective lipid uptake dependent on PI3K activation [39]. VEGF-A is known to stimulate actin reorganization, which in turn contributes to HDL uptake [5], and cell migration depending on activation of p38MAPK but not ERK1/2 MAP kinase [40, 41]. Thus it will be interesting to identify agonists beyond VEGF that regulate the endothelial binding, uptake and transport of HDL by activating the MEK pathway. In this regard, it is also important to note our finding that RNA interference with MEK but not with Akt inhibited the binding and association of LDL with endothelial cells (Figure 3.15).

We found that in HAECs, VEGF-A is required for the translocation of SR-BI from intracellular compartments to the cell surface which in turn facilitates the binding, uptake and transport of HDL (Figure 3.16 & 3.18). Similarly the cell-surface translocation of SR-BI is enhanced by insulin in hepatocytes [39] and by both insulin and angiotensin-II in adipocytes [42].In hepatocytes, cell surface expression of SR-BI was shown to be dependent on PDZK1 [43] which is a tissue specific adaptor protein with 4 PDZ domains. However, in our hands interference with PDZK1 did not limit the binding of HDL (*data not shown*) indirectly confirming that in endothelial cells targeting of SR-BI to the plasma membrane does not depend on PDZK1 [44].

SR-BI has been shown to be involved in the protective effects of HDL on the endothelium, namely angiogenesis, migration, activation of endothelial nitric oxide synthase, and monocyte adhesion [45]. Recent studies have shown the association of enhanced expression of SR-BI expression in endothelial cells with decreased atherosclerosis in mice [46]. Thus, the requirement of VEGF on maintaining cell

surface expression of SR-BI may have vascular effects beyond regulating transendothelial lipoprotein transport.

HDL was previously reported to enhance hypoxia-induced angiogenesis by stimulating the expression of VEGF and VEGFR2 in endothelial cells by a mechanism involving SR-BI [47, 48]. It thus appears that in endothelial cells, HDL and SR-BI are both upstream regulators and downstream targets of the VEGF/VEGFR2 system.

We confirmed previous reports [3, 10-13] that endothelial cells internalize and transcytose LDL. We also confirmed the previous report of Armstrong et al. [12] that this process involves SR-BI (*Velagapudi, Rohrer, von Eckardstein; unpublished observations*). However, despite regulating the cell surface abundance of SR-BI, VEGF does not regulate the transendothelial transport of LDL. Neither the interference with the VEGF receptors by drugs or RNAi, nor the removal or addition of VEGF had any significant effect on the binding, uptake or transport of LDL by HAECs. These lipoprotein-specific effects of VEGF on the processing of HDL and LDL by HAECs indicate the existence of additional regulators and routes of transendothelial transport, for example ALK1 which was recently identified by a genome-wide RNAi-screen as an endothelial LDL binding protein mediating uptake and transcytosis of LDL [13].

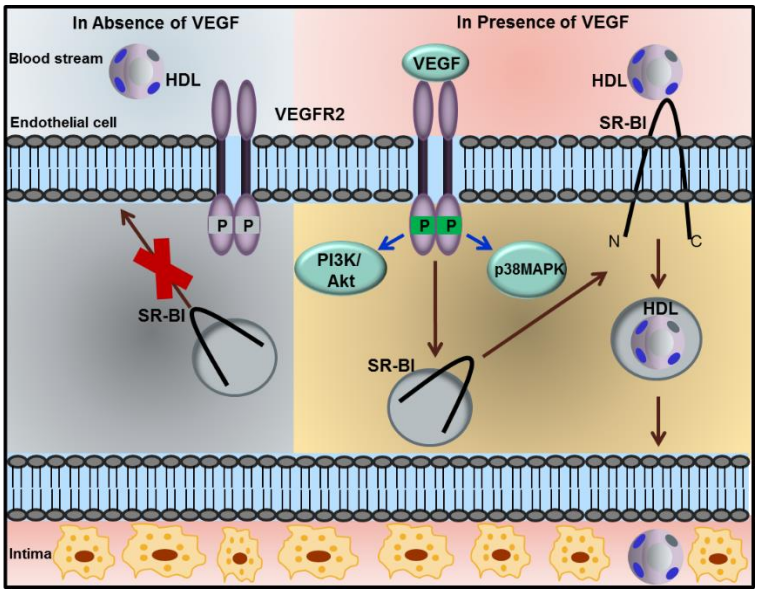

Figure 3.19: VEGF-A modulates SR-BI dependent binding, association and transport of HDL by HAECs
The VEGF-A/VEGFR2 regulates endothelial binding, uptake and transport of HDL through PI3K/Akt and p38 MAPK and, as the final result, cell surface expression of SR-BI.

From a more general perspective, our findings provide further evidence that transendothelial lipoprotein transport occurs by regulated processes [3, 6-8, 12, 13] rather than passive filtration [4]. Dys-regulated transendothelial lipoprotein transport may influence the pathogenesis of atherosclerosis beyond plasma levels of LDL and HDL. In fact, it was recently shown in LDL receptor deficient mice that acute lowering of LDL-cholesterol with anti-ApoB antisense oligonucleotides rapidly reduces the permeability of the aortic endothelium for LDL and causes regression of atherosclerosis independently of LDL pool size [49]. It is less obvious how changes in arterial permeability for HDL may affect atherosclerosis. At first sight, increased availability of HDL in the subendothelium will be protective, for example by enhancing cholesterol efflux from macrophage foam cells. However, this will only be effective if HDL also leave the arterial wall to conclude reverse cholesterol transport. Disturbed egress of HDL from the arterial wall, potentially via the lymphatics [29], will lead to the accumulation of HDL

in the arterial wall. These particles will be eventually oxidized and become dysfunctional [50, 51] and thereby promote rather than inhibit cholesterol accumulation and hence atherosclerosis.

In conclusion, we here showed that the VEGF-A/VEGFR2 regulates endothelial binding, uptake and transport of HDL through PI3K/Akt and p38 MAPK and, as the final result, cell surface expression of SR-BI. Thereby VEGF-A may play an important regulatory role for the vascular protective effects of HDL as well as reverse cholesterol transport.

3.5 References

1. Boren J, Williams KJ. The central role of arterial retention of cholesterol-rich apolipoprotein-B-containing lipoproteins in the pathogenesis of atherosclerosis: a triumph of simplicity. *Curr Opin Lipidol* 2016;**27**:473-483.
2. von Eckardstein A, Rohrer L. HDLs in crises. *Curr Opin Lipidol* 2016;**27**:264-273.
3. von Eckardstein A, Rohrer L. Transendothelial lipoprotein transport and regulation of endothelial permeability and integrity by lipoproteins. *Curr Opin Lipidol* 2009;**20**:197-205.
4. Michel CC, Nanjee MN, Olszewski WL, Miller NE. LDL and HDL transfer rates across peripheral microvascular endothelium agree with those predicted for passive ultrafiltration in humans. *J Lipid Res* 2015;**56**:122-128.
5. Perisa D, Rohrer L, Kaech A, von Eckardstein A. Itinerary of high density lipoproteins in endothelial cells. *Biochim Biophys Acta* 2016;**1861**:98-107.
6. Rohrer L, Ohnsorg PM, Lehner M, Landolt F, Rinninger F, von Eckardstein A. High-density lipoprotein transport through aortic endothelial cells involves scavenger receptor BI and ATP-binding cassette transporter G1. *Circ Res* 2009;**104**:1142-1150.
7. Robert J, Lehner M, Frank S, Perisa D, von Eckardstein A, Rohrer L. Interleukin 6 stimulates endothelial binding and transport of high-density lipoprotein through induction of endothelial lipase. *Arterioscler Thromb Vasc Biol* 2013;**33**:2699-2706.
8. Cavelier C, Ohnsorg PM, Rohrer L, von Eckardstein A. The beta-chain of cell surface F(0)F(1) ATPase modulates apoA-I and HDL transcytosis through aortic endothelial cells. *Arterioscler Thromb Vasc Biol* 2012;**32**:131-139.
9. Goldstein JL, Brown MS. The LDL receptor. *Arterioscler Thromb Vasc Biol* 2009;**29**:431-438.
10. Vasile E, Simionescu M, Simionescu N. Visualization of the binding, endocytosis, and transcytosis of low-density lipoprotein in the arterial endothelium in situ. *J Cell Biol* 1983;**96**:1677-1689.
11. Pavlides S, Gutierrez-Pajares JL, Iturrieta J, Lisanti MP, Frank PG. Endothelial caveolin-1 plays a major role in the development of atherosclerosis. *Cell Tissue Res* 2014;**356**:147-157.
12. Armstrong SM, Sugiyama MG, Fung KY, Gao Y, Wang C, Levy AS, et al. A novel assay uncovers an unexpected role for SR-BI in LDL transcytosis. *Cardiovasc Res* 2015;**108**:268-277.
13. Kraehling JR, Chidlow JH, Rajagopal C, Sugiyama MG, Fowler JW, Lee MY, et al. Genome-wide RNAi screen reveals ALK1 mediates LDL uptake and transcytosis in endothelial cells. *Nat Commun* 2016;**7**:13516.
14. Pelkmans L, Fava E, Grabner H, Hannus M, Habermann B, Krausz E, et al. Genome-wide analysis of human kinases in clathrin- and caveolae/raft-mediated endocytosis. *Nature* 2005;**436**:78-86.
15. Havel RJ, Eder HA, Bragdon JH. The distribution and chemical composition of ultracentrifugally separated lipoproteins in human serum. *J Clin Invest* 1955;**34**:1345-1353.
16. Rohrer L, Cavelier C, Fuchs S, Schluter MA, Volker W, von Eckardstein A. Binding, internalization and transport of apolipoprotein A-I by vascular endothelial cells. *Biochim Biophys Acta* 2006;**1761**:186-194.
17. Freeman M, Ekkel Y, Rohrer L, Penman M, Freedman NJ, Chisolm GM, et al. Expression of type I and type II bovine scavenger receptors in Chinese hamster ovary cells: lipid droplet accumulation and nonreciprocal cross competition by acetylated and oxidized low density lipoprotein. *Proc Natl Acad Sci U S A* 1991;**88**:4931-4935.
18. Cavelier C, Rohrer L, von Eckardstein A. ATP-Binding cassette transporter A1 modulates apolipoprotein A-I transcytosis through aortic endothelial cells. *Circ Res* 2006;**99**:1060-1066.

19. Lu D, Kussie P, Pytowski B, Persaud K, Bohlen P, Witte L, et al. Identification of the residues in the extracellular region of KDR important for interaction with vascular endothelial growth factor and neutralizing anti-KDR antibodies. *J Biol Chem* 2000;**275**:14321-14330.
20. Millauer B, Wizigmann-Voos S, Schnurch H, Martinez R, Moller NP, Risau W, et al. High affinity VEGF binding and developmental expression suggest Flk-1 as a major regulator of vasculogenesis and angiogenesis. *Cell* 1993;**72**:835-846.
21. Quinn TP, Peters KG, De Vries C, Ferrara N, Williams LT. Fetal liver kinase 1 is a receptor for vascular endothelial growth factor and is selectively expressed in vascular endothelium. *Proc Natl Acad Sci U S A* 1993;**90**:7533-7537.
22. Olofsson B, Korpelainen E, Pepper MS, Mandriota SJ, Aase K, Kumar V, et al. Vascular endothelial growth factor B (VEGF-B) binds to VEGF receptor-1 and regulates plasminogen activator activity in endothelial cells. *Proc Natl Acad Sci U S A* 1998;**95**:11709-11714.
23. Park JE, Chen HH, Winer J, Houck KA, Ferrara N. Placenta growth factor. Potentiation of vascular endothelial growth factor bioactivity, in vitro and in vivo, and high affinity binding to Flt-1 but not to Flk-1/KDR. *J Biol Chem* 1994;**269**:25646-25654.
24. Terman BI, Dougher-Vermazen M, Carrion ME, Dimitrov D, Armellino DC, Gospodarowicz D, et al. Identification of the KDR tyrosine kinase as a receptor for vascular endothelial cell growth factor. *Biochem Biophys Res Commun* 1992;**187**:1579-1586.
25. Joukov V, Pajusola K, Kaipainen A, Chilov D, Lahtinen I, Kukk E, et al. A novel vascular endothelial growth factor, VEGF-C, is a ligand for the Flt4 (VEGFR-3) and KDR (VEGFR-2) receptor tyrosine kinases. *EMBO J* 1996;**15**:290-298.
26. Achen MG, Jeltsch M, Kukk E, Makinen T, Vitali A, Wilks AF, et al. Vascular endothelial growth factor D (VEGF-D) is a ligand for the tyrosine kinases VEGF receptor 2 (Flk1) and VEGF receptor 3 (Flt4). *Proc Natl Acad Sci U S A* 1998;**95**:548-553.
27. Kappas NC, Zeng G, Chappell JC, Kearney JB, Hazarika S, Kallianos KG, et al. The VEGF receptor Flt-1 spatially modulates Flk-1 signaling and blood vessel branching. *J Cell Biol* 2008;**181**:847-858.
28. Lim HY, Thiam CH, Yeo KP, Bisoendial R, Hii CS, McGrath KC, et al. Lymphatic vessels are essential for the removal of cholesterol from peripheral tissues by SR-BI-mediated transport of HDL. *Cell Metab* 2013;**17**:671-684.
29. Martel C, Li W, Fulp B, Platt AM, Gautier EL, Westerterp M, et al. Lymphatic vasculature mediates macrophage reverse cholesterol transport in mice. *J Clin Invest* 2013;**123**:1571-1579.
30. Waltenberger J, Claesson-Welsh L, Siegbahn A, Shibuya M, Heldin CH. Different signal transduction properties of KDR and Flt1, two receptors for vascular endothelial growth factor. *J Biol Chem* 1994;**269**:26988-26995.
31. Takahashi T, Shibuya M. The 230 kDa mature form of KDR/Flk-1 (VEGF receptor-2) activates the PLC-gamma pathway and partially induces mitotic signals in NIH3T3 fibroblasts. *Oncogene* 1997;**14**:2079-2089.
32. Igarashi K, Isohara T, Kato T, Shigeta K, Yamano T, Uno I. Tyrosine 1213 of Flt-1 is a major binding site of Nck and SHP-2. *Biochem Biophys Res Commun* 1998;**246**:95-99.
33. Guo D, Jia Q, Song HY, Warren RS, Donner DB. Vascular endothelial cell growth factor promotes tyrosine phosphorylation of mediators of signal transduction that contain SH2 domains. Association with endothelial cell proliferation. *J Biol Chem* 1995;**270**:6729-6733.
34. Lamalice L, Houle F, Jourdan G, Huot J. Phosphorylation of tyrosine 1214 on VEGFR2 is required for VEGF-induced activation of Cdc42 upstream of SAPK2/p38. *Oncogene* 2004;**23**:434-445.
35. Backer JM. Phosphoinositide 3-kinases and the regulation of vesicular trafficking. *Mol Cell Biol Res Commun* 2000;**3**:193-204.
36. Corvera S. Phosphatidylinositol 3-kinase and the control of endosome dynamics: new players defined by structural motifs. *Traffic* 2001;**2**:859-866.
37. Hansen SH, Olsson A, Casanova JE. Wortmannin, an inhibitor of phosphoinositide 3-kinase, inhibits transcytosis in polarized epithelial cells. *J Biol Chem* 1995;**270**:28425-28432.
38. van Dam EM, Govers R, James DE. Akt activation is required at a late stage of insulin-induced GLUT4 translocation to the plasma membrane. *Mol Endocrinol* 2005;**19**:1067-1077.

39. Shetty S, Eckhardt ER, Post SR, van der Westhuyzen DR. Phosphatidylinositol-3-kinase regulates scavenger receptor class B type I subcellular localization and selective lipid uptake in hepatocytes. *Arterioscler Thromb Vasc Biol* 2006;**26**:2125-2131.
40. Rousseau S, Houle F, Kotanides H, Witte L, Waltenberger J, Landry J, et al. Vascular endothelial growth factor (VEGF)-driven actin-based motility is mediated by VEGFR2 and requires concerted activation of stress-activated protein kinase 2 (SAPK2/p38) and geldanamycin-sensitive phosphorylation of focal adhesion kinase. *J Biol Chem* 2000;**275**:10661-10672.
41. Rousseau S, Houle F, Landry J, Huot J. p38 MAP kinase activation by vascular endothelial growth factor mediates actin reorganization and cell migration in human endothelial cells. *Oncogene* 1997;**15**:2169-2177.
42. Tondu AL, Robichon C, Yvan-Charvet L, Donne N, Le Liepvre X, Hajduch E, et al. Insulin and angiotensin II induce the translocation of scavenger receptor class B, type I from intracellular sites to the plasma membrane of adipocytes. *J Biol Chem* 2005;**280**:33536-33540.
43. Silver DL. A carboxyl-terminal PDZ-interacting domain of scavenger receptor B, type I is essential for cell surface expression in liver. *J Biol Chem* 2002;**277**:34042-34047.
44. Zhu W, Saddar S, Seetharam D, Chambliss KL, Longoria C, Silver DL, et al. The scavenger receptor class B type I adaptor protein PDZK1 maintains endothelial monolayer integrity. *Circ Res* 2008;**102**:480-487.
45. Trigatti BL, Krieger M, Rigotti A. Influence of the HDL receptor SR-BI on lipoprotein metabolism and atherosclerosis. *Arterioscler Thromb Vasc Biol* 2003;**23**:1732-1738.
46. Vaisman BL, Vishnyakova TG, Freeman LA, Amar MJ, Demosky SJ, Liu C, et al. Endothelial Expression of Scavenger Receptor Class B, Type I Protects against Development of Atherosclerosis in Mice. *Biomed Res Int* 2015;**2015**:607120.
47. Tan JT, Prosser HC, Dunn LL, Vanags LZ, Ridiandries A, Tsatralis T, et al. High-Density Lipoproteins Rescue Diabetes-Impaired Angiogenesis via Scavenger Receptor Class B Type I. *Diabetes* 2016;**65**:3091-3103.
48. Prosser HC, Tan JT, Dunn LL, Patel S, Vanags LZ, Bao S, et al. Multifunctional regulation of angiogenesis by high-density lipoproteins. *Cardiovasc Res* 2014;**101**:145-154.
49. Bartels ED, Christoffersen C, Lindholm MW, Nielsen LB. Altered metabolism of LDL in the arterial wall precedes atherosclerosis regression. *Circ Res* 2015;**117**:933-942.
50. Huang Y, DiDonato JA, Levison BS, Schmitt D, Li L, Wu Y, et al. An abundant dysfunctional apolipoprotein A1 in human atheroma. *Nat Med* 2014;**20**:193-203.
51. DiDonato JA, Aulak K, Huang Y, Wagner M, Gerstenecker G, Topbas C, et al. Site-specific nitration of apolipoprotein A-I at tyrosine 166 is both abundant within human atherosclerotic plaque and dysfunctional. *J Biol Chem* 2014;**289**:10276-10292.

4. Cytoplasmic accumulation of lipoproteins is induced by VHL/HIF pathway activation in clear-cell renal cell carcinoma

Srividya Velagapudi[1,3], Peter Schraml[2], Mustafa Yalcinkaya[1,3], Lucia Rohrer[1,3], Holger Moch[2,*], and Arnold von Eckardstein[1,3*]

***: equal contribution**

Institute of Clinical Chemistry[1] and Department of Pathology and Molecular Pathology[2], University of Zurich and University Hospital of Zurich, Switzerland
[3] Competence Center for Integrated Human Physiology, University of Zurich, Switzerland

Author contributions

A.v.E. and H.M. developed the rationale and concept of the entire study and provided funding. H.M and P.S designed and performed the human ccRCC tissue micro array experiments as well as their statistical analysis and interpretation. S.V, L.R, A.vE designed the *in vitro* experiments and interpreted the data. S.V and M.Y performed the *in vitro* experiments as well as statistical data analysis. S.V. and A.v.E. wrote the first version of the manuscript which was then revised by input of P.S, L.R, and H.M.

Abstract

Background: Most clear cell renal cell carcinoma (ccRCC) are characterized by VHL inactivation. ccRCC tumor cells have typically clear cytoplasm partly due to lipid accumulation. We investigated (apo)lipoproteins and their receptor, the scavenger receptor BI (SR-BI) in primary human renal tumors and in RCC cell lines.

Methods: ApoA-I, apoB and SR-BI were analyzed in 356 RCCs by immunohistochemistry as well as in von Hippel-Lindau (VHL) gene defective RCC cell line 786-O and a stably transfected VHL re-expressing derivative (786-O-VHL). In addition, uptake of radio-iodinated HDL or LDL was measured.

Results: ApoA-I, apoB, and SR-BI expression showed significant associations with clear cell RCC subtype, markers of HIF-1α activity, high tumor stage, differentiation grade, and better survival. Neither 786-O nor 786-O-VHL expressed apoA-I and apoB. 786-O cells showed enhanced VEGF and SR-BI expression compared to 786-O-VHL. ^{125}I-LDL and ^{125}I-HDL up-take was significantly higher in 786-O than 786-VHL cells. Uptake of ^{125}I-LDL into 786-VHL was strongly increased by pretreatment with VEGF, whereas blocking of SR-BI with neutralizing antibodies significantly reduced the uptake of ^{125}I-LDL into 786-O as well as into VEGF stimulated 786-VHL. Unlike 786-O-VHL and normal renal tubular cells, 786-O did not degrade ^{125}I-LDL.

Conclusion: Lipid metabolic reprogramming with cholesterol accumulation is caused by enhanced uptake of LDL and HDL via SR-BI into a non-degrading cytoplasmic compartment. VHL inactivation induces cell surface translocation of SR-BI by activating VEGF in a HIF-1α dependent manner. These data are important for novel treatments targeting lipid and cholesterol dependence of renal cancer cells.

4.1 Introduction

Clear cell renal cell carcinoma (ccRCC) is the most common adult kidney cancer subtype [1], followed by papillary, chromophobe and translocation RCC. Classification of these renal cell carcinoma (RCC) subtypes is based on histologically predominant cytoplasmic features (clear cell RCC), characteristic staining (chromophobe RCC), architectural features (papillary RCC) or specific molecular alterations (translocation RCC) (Figure 4.1). ccRCC, received its name from the microscopic appearance upon staining of formalin fixed and paraffin embedded (FFPE) sections with hematoxylin-eosin [2]. The clear appearance of the cytoplasm is due to the accumulation of glycogen and lipids that are dissolved during routine processing with deparaffinization of FFPE sections using xylene and ethanol. The most prominent lipid stored in renal tumor cells is cholesterol, largely in the esterified form [3]. Various cancer cell lines can show lipid and cholesterol avidity, which is due to either increasing the uptake of exogenous lipids and lipoproteins or over activating their endogenous synthesis. The mechanisms for cholesterol accumulation in ccRCC cells is not well understood. Three principle pathways have to be considered, two of which have been ruled out previously, namely excessive cholesterol synthesis by the finding of decreased rather than increased activity of the rate limiting enzyme HMG-CoA reductase [4] as well as abnormal cholesterol efflux [3]. The third explanation is most likely, namely excessive uptake of cholesterol from plasma lipoproteins beyond the capacity of utilization and processing. However, neither the lipoprotein classes nor the receptors and cellular pathways involved are as yet understood.

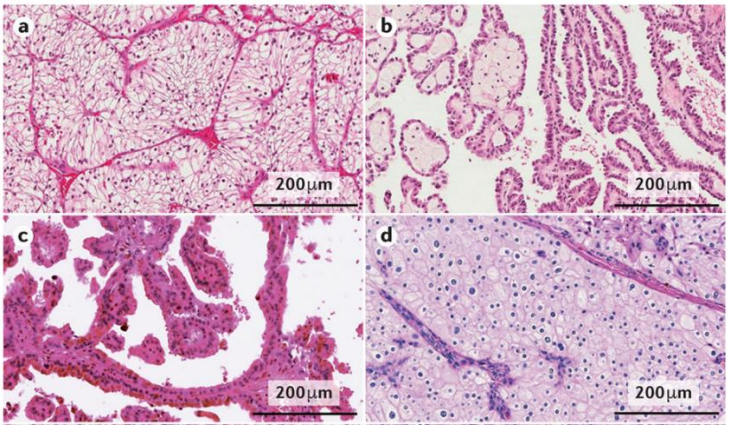

Figure 4.1: Distinct subtypes of renal cell carcinoma Histology of most common RCC subtypes: **A**, Clear cell RCC – cells with lipid rich ample cytoplasm. **B**, Type 1 Papillary RCC – small basophilic cells with scarce cytoplasm, organized in a spindle-shaped pattern, in a single layer of cells surrounding the basal membrane. **C,** Type 2 Papillary RCC – cells organized in a spindle-shaped pattern with papillae covered by cells with abundant eosinophilic granular cytoplasm with prominent nucleoli. **D:** Chromophobe RCC – large pale cells with reticulated cytoplasm and perinuclear halos [5].

Malignantly transformed renal cancer lacks the low-density lipoprotein receptor (LDLR), which is the main entry route for exogenous cholesterol into the majority of cells including many tumor cells [6]. In contrast, the expression of the very low-density lipoprotein receptor (VLDLR) was found increased in ccRCC compared to the normal kidney tissue [7]. Scavenger receptor-BI (SR-BI) is also abundantly expressed in ccRCC [7] and known to mediate selective lipid uptake from both high-density lipoproteins (HDL) and low-density lipoproteins (LDL) [8-11].

We have previously found that the cell surface abundance of SR-BI in endothelial cells is regulated by vascular endothelial growth factor (VEGF). Interestingly, VEGF activity is increased in the majority of ccRCC [12-14] due to the constitutive activation of hypoxia-inducible factor 1 alpha (HIF1α) by somatic mutations in the von Hippel-Lindau (*VHL*) tumor suppressor gene. The VHL protein is a component of

the E3-ubiquitin ligase complex that ubiquitylates HIF-1α and HIF-2α for proteasome-mediated degradation [15]. Thus, the loss of *VHL* function leads to HIF-α stabilization despite an adequately oxygenated tissue microenvironment, which in turn results in uncontrolled activation of HIF- target genes that regulate erythropoiesis (erythropoietin), angiogenesis (VEGF), glycolysis (glucose transporters and glycolytic pathway enzymes), and apoptosis (BNIP3)[16-20]. Therefore, we investigated the hypothesis that the lipid accumulation in ccRCC results from the enhanced uptake of HDL and LDL due to increased HIF-1α and hence VEGF activity. To this end we combined immunohistochemical studies in human renal tumors with experiments in two ccRCC cell lines differing by pVHL activity.

4.2 Materials and Methods

Patients, Tissue microarray Construction and Immunohistochemistry

RCC patients were identified from the database of the Institute of Pathology and Molecular Pathology, University Hospital Zurich, Switzerland. All RCCs were histologically re-evaluated by one pathologist (H.M.) and selected on the basis of hematoxylin and eosin-stained tissue sections. The patient cohort and the construction of tissue microarrays (TMA) of RCC were previously described [21 22]. Tumors were staged and histologically classified according to the World Health Organization classification [23]. Overall survival data were obtained by the Cancer Registry of the Canton Zurich. The clinical and pathologic parameters of the tumors on the TMA are summarized in Table 4.I. For some cases there was no information available. This study was approved by the local commission of ethics (KEK-ZH no. 2011-0072/4). TMA sections (2.5 μm) were transferred to glass slides followed by immunohistochemical analysis according to the Ventana (Tucson, AZ, USA) automat protocols listed in Table 4.II. apoA-I (1:1000 dilution, 600-101-109, Rockland), apoB (1:200 dilution, ab20737, Abcam), SR-BI (1:200 dilution, NB400-131, Novus), CD34 (Pre-diluted, 790-2927, Ventana Roche), HIF-1α (1:400 dilution, ab16066, Abcam), CA9 (1:6000 dilution, ab15086, Abcam), Glut1 (1:1000 dilution, 07-1401, Millipore). The staining intensities were classified as absent (0), weak (1), moderate (2), and strong (3). For detailed analysis, TMAs were scanned using the NanoZoomer Digital Slide Scanner (Hamamatsu Photonics K.K.).

Cell culture

The ccRCC-derived 786-O cells which lack functional pVHL were supplied by American Type Culture Collection (ATCC) and cultured in RPMI-1640 (Sigma, R8758) with 10% fetal bovine serum (Gibco) and 100U/mL of penicillin and 100μg/mL streptomycin (Sigma-Aldrich). Stable transfectant of 786-O re-expressing pVHL-isoform 30 (786-O-VHL) was provided by Prof. Dr. Wilhelm Krek (ETH, Zurich), generated as described[24] and cultured using the same conditions as mentioned for 786-O. 0.5 mg/mL of G418 (Gibco, 10131) was used as selection antibiotic. Both cell lines were authenticated by authentication service of Microsynth (Balgach, Switzerland) and were previously used by our group in different studies [25, 26].

Lipoprotein Isolation and labeling

LDL (1.019<d<1.063 g/mL) and HDL (1.063<d<1.21 g/mL) were isolated from fresh human normolipidemic plasma of blood donors by sequential ultracentrifugation as described previously [27, 28]. LDL and HDL were radioiodinated with $Na^{125}I$ by the McFarlane monochloride procedure modified for lipoproteins [28, 29]. Specific activities between 300-900 cpm/ng of protein were obtained.

Lipoprotein cell association and degradation assays

All assays were performed in RPMI-1640 (Sigma) containing 25mmol/L HEPES and 0.2% BSA instead of serum. Where indicated, cells were pre-treated with Sorafenib Tosylate (Selleckchem, 90nM) or Sunitinib Malate (Selleckchem, 80nM) for 30 minutes or with VEGF-A (Sigma, 25ng/ml) or anti-SR-

BI neutralizing antibody (1:500, Novus NB400-113) or anti-IgG control (1:500, Santa Cruz-2027) for 1hr at 37 ºC. Following treatments, the cells were incubated with 10µg/mL of ^{125}I-HDL or ^{125}I-LDL in the absence or presence of a 40 times excess of non-labeled HDL and LDL respectively for 1hr at 37ºC for association experiments. For the degradation experiments, the cells and the medium alone (Blank condition) were incubated with 15µg/mL of ^{125}I-HDL or ^{125}I-LDL in the absence or presence of a 40 times excess of non-labeled HDL and LDL respectively. After 4 hours of incubation at 37 °C, the amount of ^{125}I-HDL or 125I-LDL degradation products released into the medium were measured. To distinguish the cellular degradation products (amino acid bound radioactivity) from the free radioactivity in the supernatant after TCA precipitation, the supernatant was oxidized by hydrogen peroxide and the free iodine extracted by trichloromethane. The radioactivity of the water phase containing the cellular degradation products was measured using a Perkin Elmer γ-counter The counts in the medium alone condition which are due to the presence of small amounts of acid-soluble ^{125}I-tyrosine are subtracted from all conditions to correct for background [30]. Specific cellular association or degradation were calculated by subtracting the values obtained in the presence of excess unlabeled HDL or LDL (unspecific) from those obtained in the absence of unlabeled HDL and LDL (total) respectively.

Clinical parameters	Patients (%)
RCC subtype	
Clear-cell	264
Papillary type I	24
Papillary type II	24
Chromophobe	15
Oncocytoma	19
Other	8
pT stage*	
1	102
2	26
3	128
4	7
ISUP grading*	
1	5
2	68
3	89
4	101
Sex*	
Women	96
Men	168
Events*	
Censor	133
Death	107

Table 4.I: Clinicopathological characteristics of patients and tumors The clinical and pathological characteristics of patient cohort are summarized here. *clear cell RCC only.

Real-time polymerase chain reaction

Total RNA was isolated using TRI reagent (Sigma T9424) according to the manufacturer's instruction. Genomic DNA was removed by digestion using DNase (Roche) and RNase inhibitor (Ribolock, Thermo Scientific). Reverse transcription was performed using M-MLVRT (Invitrogen, 200U/µL) following the standard protocol as described by the manufacturer. Quantitative PCR was done with Lightcycler FastStart DNA Master SYBR Green I (Roche) using gene specific primers as followed:

APOA1 (For: ATGAAAGCTGCGGTGCTG; Rev: AGGTCCTTCACTCGATCCCA)

APOB (For: TGCCTCTCCTGGGTGTTCTA; Rev: CCCGAAGGCTGAAATGGTCT)

VEGF (For: CTGTCTAATGCCCTGGAGCC; Rev: ACGCGAGTCTGTGTTTTTGC)

LDL-R (For: AAGGACACAGCACACAACCA; Rev: CATTTCCTCTGCCAGCAACG)

SCARB1 (For: CTGTGGGTGAGATCATGTGG; Rev: GCCAGAAGTCAACCTTGCTC)

BNIP3 (For: GGAAGATGATATTGAAAGAAGGAAAG, Rev: CGCCTTCCAATATAGATCCCC)

SLC2A1 (For: ACTGTCGTGTCGCTGTTTG, Rev: CCAGGACCCACTTCAAAGAA)

PDK1 (For: CACGCTGGGTAATGAGGATT, Rev: GGAGGTCTCAACACGAGGT)

CAIX (For: GGGTGTCATCTGGACTGTGTT, Rev: CTTCTGTGCTGCCTTCTCATC)

VEGFR1 (For: CTGAAGGAAGGGAGCTCGTC, Rev: GGCGTGGTGTGCTTATTTGG)

VEGFR2 (For: CGGTCAACAAAGTCGGGAGA, Rev: CAGTGCACCACAAAGACACG)

VEGFR3 (For: TCCTACGTGTTCGTGAGAGAC, Rev: CACCAGGAAGGGGTTGGAAA)

NRP1 (For: AGGACAGAGACTGCAAGTATGAC, Rev: AACATTCAGGACCTCTCTTGA)

GAPDH (For: CCCATGTTCGTCATGGGTGT; Rev: TGGTCATGAGTCCTTCCACGA TA).

Antibody	Supplier	Clone	Species	Automat	Dilution	Pre-incubation	Incubation time
Apo-Al	Rockland	600-101-109	goat polyclonal	Ventana Discovery	1:1000	CC1 32min	44min
ApoB	Abcam	Ab20737	rabbit polyclonal	Ventana Discovery	1:200	CC1 32min	60min
SR-BI	Novus	NB400-131	goat polyclonal	Ventana Discovery	1:200	CC1 64min	60min
Glut1	Millipore	07-1401	rabbit polyclonal	Ventana Discovery	1:1000	CC1 32min	44min
HIF-1α	Abcam	Ab16066	mouse monoclonal	Leica Bond	1:400	H2(60)	30min
CD34	Ventana Roche	790-2927	mouse monoclonal	Ventana Ultra	pre-diluted	CC1 16min	32min
CA9	Abcam	Ab15086	rabbit polyclonal	Leica Bond	1:6000	H2(30) 95°C	30min

Table 4.II: Immunohistochemistry protocol The table represents the list of the antibodies and the protocol used to perform immunostaining on RCC tissue microarrays.

Small interfering RNA transfection

786-O and 786-O-VHL cells were reverse transfected with small interfering RNA (Ambion silencer select, Life technologies) targeted to LDLR (s224006, s224007, s4) or NRP1 (s16844, s16843) or non-silencing control (4390843) at a final concentration of 5nmol/L using Lipofectamine RNA iMAX transfection reagent (Invitrogen, 13778150) in an antibiotic-free RPMI medium. All experiments were performed 72 hours post-transfection and efficiency of transfection was confirmed with at two siRNAs against each gene using qRT-PCR.

Western Blotting

Cells were lysed in RIPA buffer (10mmol/L Tris pH 7.4, 150mmol/L NaCl, 1% NP-40, 1% sodium deoxycholate, 0.1% SDS, complete EDTA (Roche)) with protease inhibitors (Roche). Equal amounts of protein were separated on SDS-PAGE and trans-blotted onto PVDF membrane (GE Healthcare). Membranes were blocked in appropriate blocking buffer recommended for the antibody (TBS-T supplemented with 5% milk) and incubated overnight on a shaker at 4 ºC with primary antibodies in the same blocking buffer. Membranes were incubated for 1hour with an HRP-conjugated secondary antibody (Dako) in the blocking buffer. Membranes were further incubated with chemiluminescence substrate for 1min (Pierce ECL plus, Thermo scientific) and imaged using Fusion Fx (Vilber). The expression of apoA-I (1:1000, 600-101-109, Rockland), apoB (1:250, ab20737, Abcam), LDLR (1:1000, ab30532, Abcam), SR-BI (1:1000, Novus, NB400-131) were evaluated and compared to the expression of either TATA binding protein (1:1000, TBP, ab51841, Abcam) or Na^+/K^+- ATPase (1:200, SC-21712, Santa Cruz) which were used as loading control.

Cell surface expression analysis

Biotinylation of intact cells was performed using 20mg/mL EZ-Link sulfo-NHS-S-S-Biotin (Thermo Scientific) in the cold for 1 hour with mild shaking and quenched with ice-cold 50mM Tris pH 7.4. Cells were lysed in RIPA buffer (total cell lysate) and 200-500µg of lysates were incubated with 20µL of BSA-blocked streptavidin beads suspension (GE Healthcare) for 16hours at 4 ºC and pelleted by centrifugation; the pellet represents surface proteins. Proteins were dissociated from the pellet by boiling with SDS loading buffer and analyzed by SDS-PAGE and immunoblotted with SR-BI antibody (NB400-131, Novus) and TATA binding protein (TBP, ab51841, Abcam) used as intracellular control.

Statistical Analysis

Contingency table analysis and Pearson's chi-square tests were used to analyze the associations between protein expression patterns and clinical parameters. Overall survival rates were determined according to the Kaplan–
Meier method and analyzed for statistical differences using a log rank test. The data sets for all *in vitro* experiments were analyzed using the GraphPad Prism 5 software. Comparison between groups in experiments was performed using t-test or Kruskal-Wallis test followed by Dunn's comparison between groups. Values are expressed as mean±SEM. $P<0.05$ was regarded as significant.

4.3 Results

Lipoprotein and apolipoprotein expression and pathological parameters

Immunostaining was performed on RCC tissue microarrays (TMA) for the major apolipoproteins of HDL and LDL, apolipoprotein A-I (apoA-I) and apolipoprotein B (apoB) respectively (Figures 4.2A and B), as well as receptor scavenger receptor BI (SR-BI, Figure 4.2C). Based on the staining intensities, expression levels in tumors were graded from 0 to 3 for apoA-I and SR-BI expression, and from 0 to 2 for apoB expression as staining intensities were generally lower. Immunoreactivity with anti-apoA-I or anti SR-BI antibodies but not immunoreactivity with anti-apoB antibodies significantly differentiated ccRCC from papillary RCC. The 175 ccRCCs showed significantly stronger immunoreactivity against apoA-I and SR-BI than papillary RCC (Table 4.III).

Strong cytoplasmic apoA-I and membranous SR-BI expression (staining intensity 2 and 3) was seen in approximately 75% and 56% of ccRCC, whereas, only 16% of ccRCC (staining intensity 2) showed strong cytoplasmic apoB expression. Of note, apoA-I and apoB expression were significantly correlated ($P < 0.001$) but not with SR-BI positivity (Table 4.III).

We next evaluated the associations of the lipoprotein immunoreactivities in ccRCC with tumor stage (pT) and tumor grade. pT1/pT2 tumor stage represent organ confined and pT3/pT4 represent late stage metastasizing tumors. By this definition, only anti-apoB-immunoreactivity was significantly associated with tumor stage (Table 4.III, $p = 0.0371$). Four nuclear grades ranging from 1 to 4 were defined and showed significant associations with the immunoreactivity of apoA-I ($P = 0.025$) and apoB ($P = 0.0006$) but not SR-BI (Table 4.III). The higher the grade the less likely the tumors were immunoreactive against anti-apoA-I or anti-apoB antibodies.

Expression of apolipoproteins, SR-BI, and VHL downstream targets

The protein encoded by the VHL gene, von Hippel–Lindau protein, acts as an adaptor protein to recruit various effectors to target proteins. Therefore, we statistically evaluated the associations of lipoprotein immunoreactivity with markers of VHL downstream targets (Table 4.III), namely microvessel density recorded by CD34 abundance, nuclear abundance of HIF1α, and the protein abundance of HIF-1α targets CA9 and GLUT1. Interestingly, the immunoreactivity for apoA-I showed significant positive associations with each of the four markers (CD34: $P < 0.001$; HIF1a: $P = 0.0078$; CA9: $P = 0.0272$; GLUT1: $P = 0.0175$). By contrast, SR-BI immunoreactivity showed no significant association with any marker. ApoB immunoreactivity was significantly and positively associated with microvessel density ($P = 0.0197$) and nuclear HIF-1α staining ($P = 0.0049$).

Measured features	apoA-I	apoB	SR-BI
apoA-I	-	0.0001	n.s
apoB	0.0001	-	n.s
SR-BI	n.s	n.s	-
ISUP grade	0.025	0.0006	n.s
Tumor stage	n.s	0.037	n.s
Microvessel density (CD34)	0.0001	0.0197	n.s
HIF-1α	0.0078	0.0049	n.s
CA9	0.0272	n.s	n.s
GLUT1	0.0175	n.s	n.s

Table 4.III Correlation of apoA-I, apoB and SR-BI expression with different measured features: Correlation analysis between ccRCC tumor tissue microarray sections immunostained for apoA-I, apoB ,SR-BI and different pathological parameters as well as HIF-target proteins. The values in the table represents the P value, n.s means No significance.

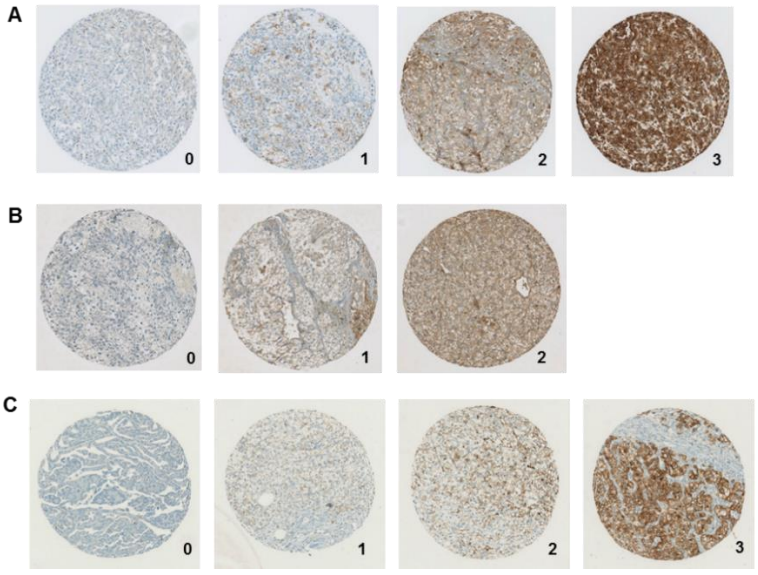

Figure 4.2: Apolipoprotein and SR-BI expression in renal cell carcinoma TMA Immunostaining of **A**, apoA-I **B**, apoB and **C**, SR-BI of human tissue microarrays. The grading from 0-3 represents the staining intensity from negative to the strongest.

Lipoprotein and apolipoprotein expression and patient survival

Finally, we used the Kaplan-Meier method and log-rank test to evaluate the associations of apoA-I, apoB and SR-BI immunoreactivity with overall survival. Stronger immunoreactivity of apoA-I, apoB, and SR-BI are associated with better survival (Figure 4.3A-C), but, this association was significant for anti-apoA-I expression only (p-Value = 0.0407, Figure 4.3A). However also this association lost statistical significance upon multivariate analysis taking into account tumor stage and grade.

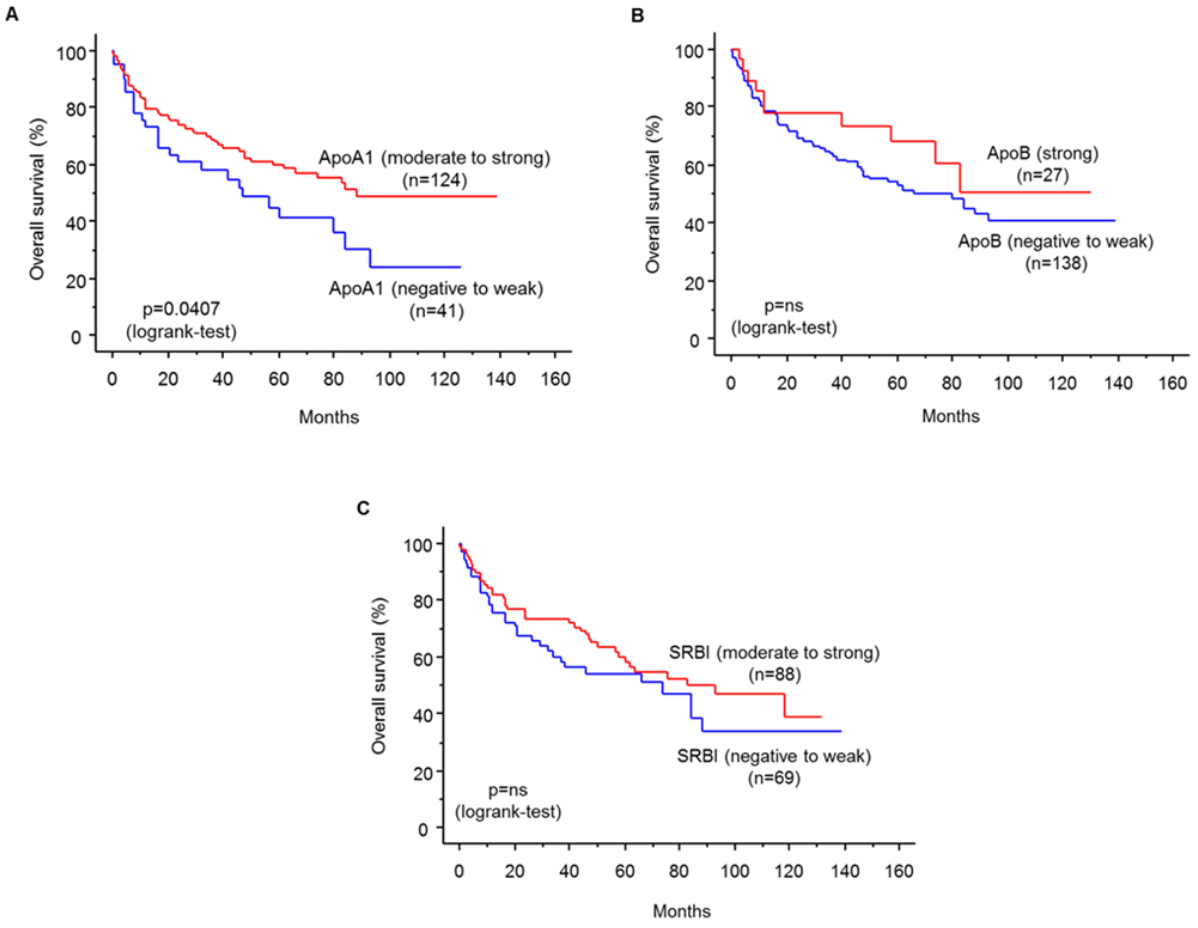

Figure 4.3 Kaplan-Meier curves depicting overall survival (OS) according to differential expression of apolipoproteins and SR-BI in ccRCC tissue microarray sections A, Kaplan-Meier analysis of OS of apoA-I immunoreactivity, **B**, Kaplan-Meier analysis of OS of apoB immunoreactivity and C, Kaplan-Meier analysis of OS of SR-BI immunoreactivity.

Lipoprotein RNA expression in ccRCC cell lines

APOA1 and APOB transcripts were seen in hepatocellular derived carcinoma cells, Huh7 (positive control) but neither in 786-O cells which lacks functional VHL nor in 786-O cells which are stably transfected with wild-type VHL (786-O-VHL), nor in human aortic endothelial cells (HAECs) that served as the negative control (Figure 4.4A and 4.4B). Western blot analysis of the ccRCC cell lines neither revealed any ApoA-I nor ApoB protein expression (Figure 4.4C,D).

To test the hypothesis that apolipoprotein accumulation in ccRCC is caused by excessive lipoprotein uptake, 786-O as well as HAECs were incubated with radio-iodinated HDL or LDL at 37°C for 1 hour [14]. Compared to HAECs, the cellular association of ^{125}I-HDL in 786-O cells was very low (Figure 4.5A) whereas the cellular association of ^{125}I-LDL was very high (Figure 4.5B).

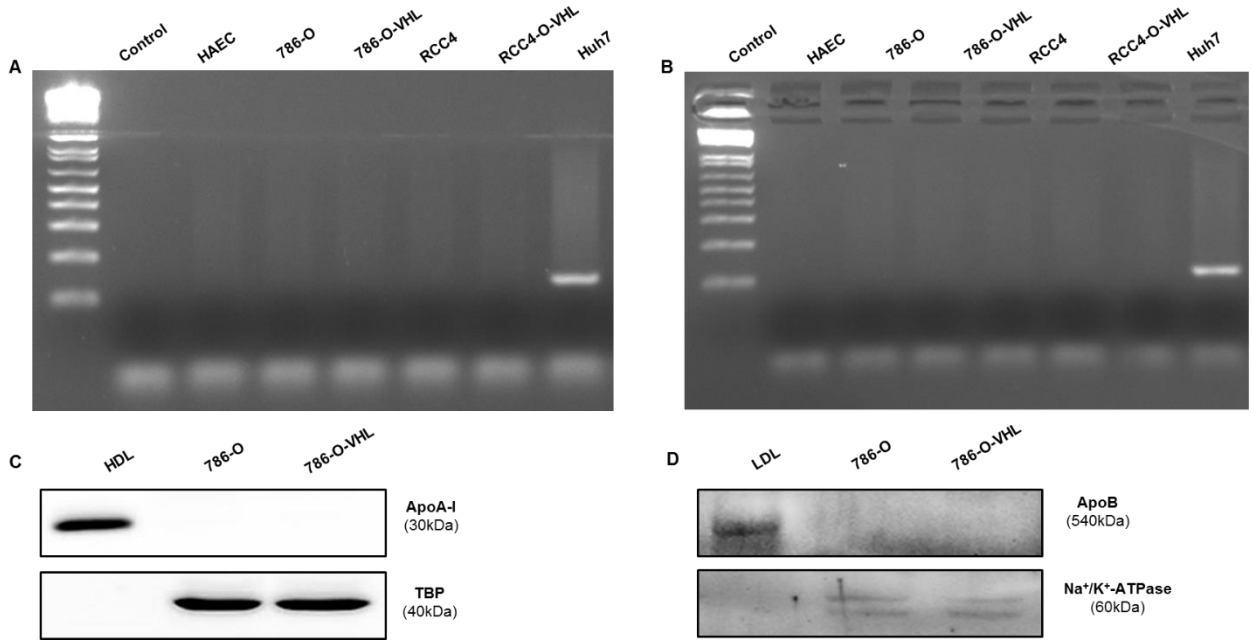

Figure 4.4: mRNA and protein expression of apolipoproteins in renal carcinoma 786-O cells mRNA levels of APOA1 (113bp, **A**) and APOB (111bp, **B**) were measured by real-time polymerase chain reaction in 786-O cells compared to Huh7 and HAECs (used as positive and negative controls respectively). The control reaction was carried out in the presence of water. Also included were 786-O-VHL transfected cells and RCC4 and RCC4-VHL transfected cells (RCC4 represents another renal-cell carcinoma cell line model). Western blot analysis of ApoA-I (**C**) and apoB (**D**) in 786-O and 786-VHL cells compared to HDL (**C**) and LDL (**D**), respectively, as the positive controls. The western blots were probed with anti-ApoA-I (30kDa), anti-ApoB (540 kDa), and anti-TATA binding protein (TBP, 40kDa), anti-Na^+/K^+-ATPase (60kDa) were used as loading controls.

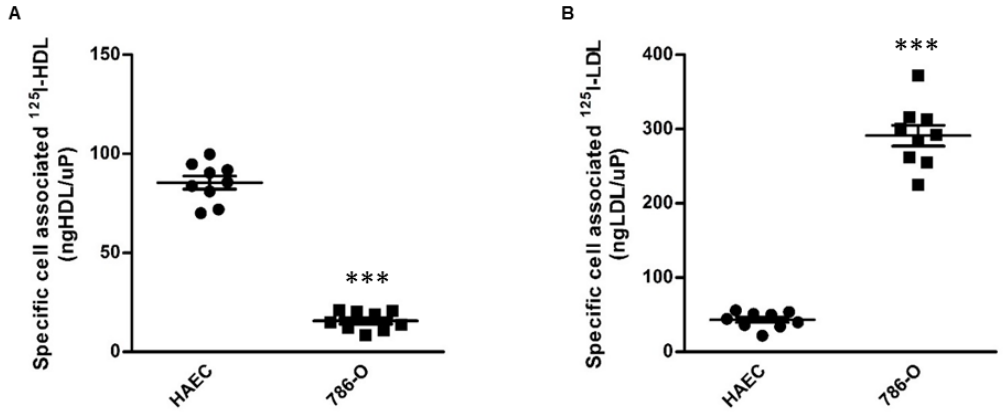

Figure 4.5: Radioiodinated lipoprotein cellular association in renal carcinoma 786-O cells To study cellular association, HAECs and 786-O cells were incubated with 10µg/mL of **A**, ^{125}I-HDL or **B**, ^{125}I-LDL for 1 hour in the absence (total) or in the presence of 40-fold excess of unlabeled HDL or LDL (unspecific). Specific association was calculated by subtracting unspecific values from total values. The results are represented as mean±SEM of three independent triplicate experiments. ***$P \leq 0.001$.

Loss of VHL function enhances the uptake but inhibits the degradation of LDL

To investigate the involvement of VHL in regulating the cellular association of radioiodinated lipoproteins, we compared 786-O cells with 786-O-VHL cells. Parental 786-O cells showed higher mRNA expression of the HIF-1α responsive genes VEGF, BNIP3, PDK1 and SLC2A1 (Figure 4.6A-E) compared to the 786-VHL cells.

The 786-VHL cells showed decreased cellular association of both ^{125}I-HDL and ^{125}I-LDL compared to the parental 786-O cells. Interestingly, pre-treatment with VEGF for 1 hour increased the specific cellular association of ^{125}I-HDL as well as ^{125}I-LDL in 786-O-VHL cells but had no effect in 786-O cells (Figure 4.7A & B). Pre-treatment of 786-O cells with VEGF receptor inhibitors for 30 minutes decreased specific cellular association of both ^{125}I-HDL and ^{125}I-LDL but had no effect in 786-O-VHL cells (Figure 4.8A-D).

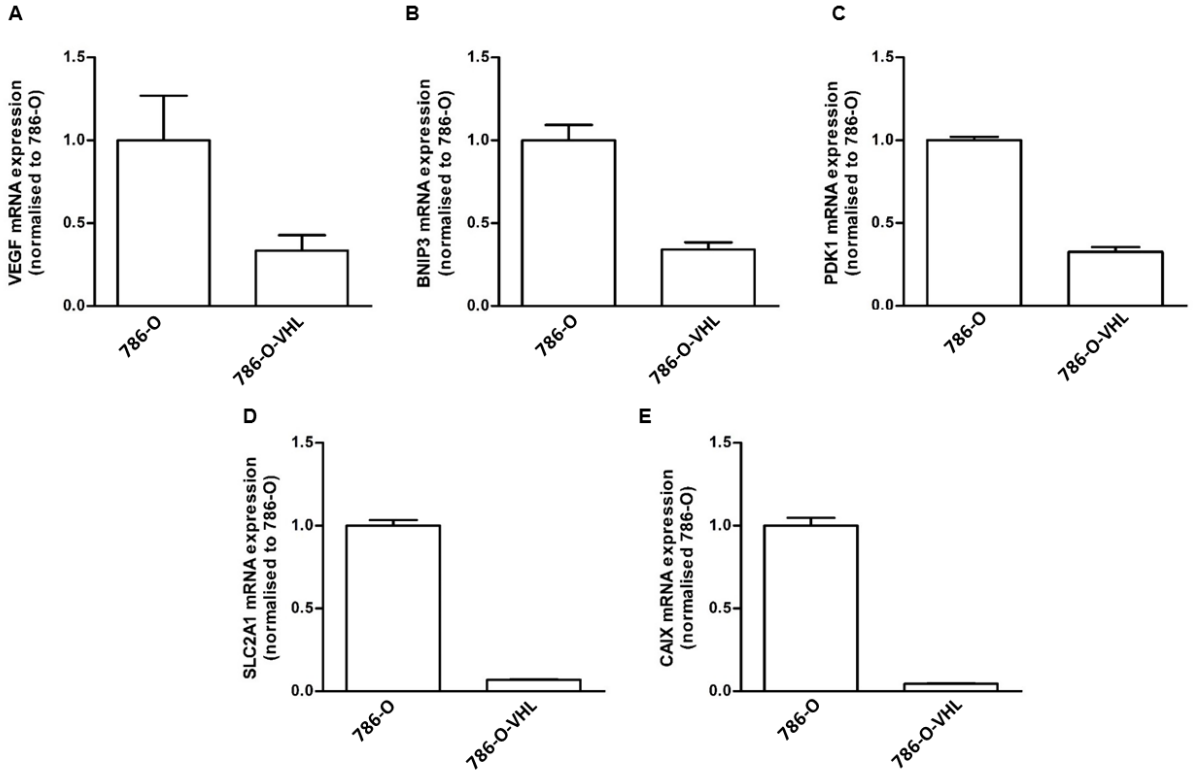

Figure 4.6: mRNA expression of HIF-1*α* target genes in ccRCC cells Quantification of **A**, VEGF mRNA **B,** BNIP3 mRNA **C,** PDK1 mRNA and **D,** SLC2A1 mRNA (GLUT1) **E,** CAIX mRNA. GAPDH was used a house keeping control gene.

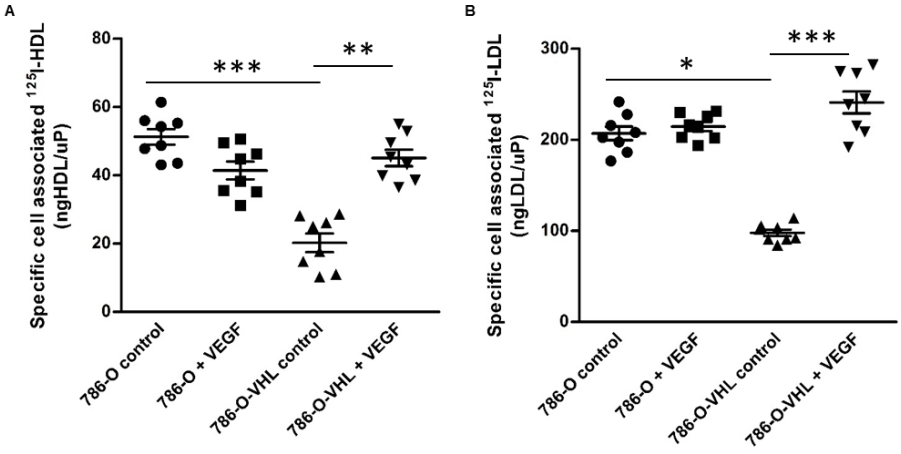

Figure 4.7: VHL promotes cellular association of ^{125}I-HDL and ^{125}I-LDL in renal carcinoma 786-O cells 786-O and 786-VHL cells were pre-treated with 25ng/ml of VEGF for 1 hour prior to assays as indicated, followed by incubation with 10µg/mL of **A,** ^{125}I-HDL or **B,** ^{125}I-LDL at 37 ºC for 1hour in the absence (total) or in the presence of 40-fold excess of unlabeled HDL or LDL (unspecific). Specific cellular association was calculated by subtracting unspecific values from total values. The results are represented as mean±SEM of three independent triplicate experiments. ***$P \leq 0.001$, **$P \leq 0.01$, *$P \leq 0.05$.

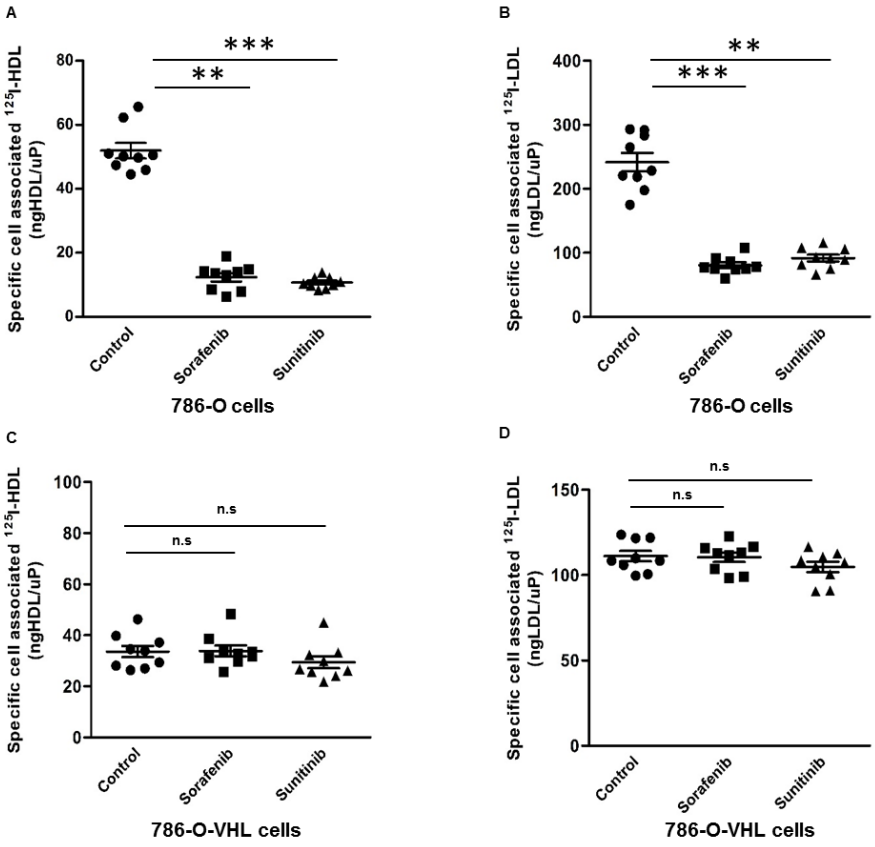

Figure 4.8: Receptor tyrosine kinases promote cellular association of ^{125}I-HDL and ^{125}I-LDL in renal carcinoma 786-O cells 786-O and 786-O-VHL cells were pre-treated with either Sorafenib (90nM) or Sunitinib (80nM) for 30 minutes prior to assays as indicated, followed by incubation with 10µg/mL of ^{125}I-HDL or ^{125}I-LDL. 786-O cells incubated with **A,** ^{125}I-HDL **B,** ^{125}I-LDL. 786-O-VHL cells incubated with **C,** ^{125}I-HDL **D**, ^{125}I-LDL at 37 ºC for 1hour in the absence (total) or in the presence of 40-fold excess of unlabeled HDL or LDL (unspecific). Specific cellular association was calculated by subtracting unspecific values from total values. The results are represented as mean±SEM of three independent experiments. ***$P\leq 0.001$, **$P\leq 0.01$, *$P\leq 0.05$, "n.s" represents no significance.

Interestingly, both the ccRCC cell lines expressed neither VEGFR1 nor VEGFR2 nor VEGFR3, but expressed neuropilin-1 (NRP1) which is a co-receptor of VEGFR (Figure 4.9). The 786-O cells showed higher expression of NRP1 compared to the 786-VHL cells (Figure 4.10A). To test whether NRP1 is involved in the regulation of cellular association of radioiodinated lipoproteins, we targeted NRP1 using RNA interference and validated the knock-down efficiency at the mRNA level (Figure 4.10B, C). Silencing NRP1 decreased the specific cellular association of ^{125}I-HDL as well as ^{125}I-LDL in both 786-O and 786-O-VHL cells. Interestingly, pre-treatment with VEGF for 1hour stimulated the specific cellular association of neither ^{125}I-HDL nor ^{125}I-LDL in 786-VHL cells in which NRP1 was knocked-down (Figure 4.11A-D).

786-O-VHL cells showed considerable degradation of ^{125}I-LDL similar to the hepatocyte cell line Huh7 and healthy kidney cell line HK-2 cells. By contrast, degradation of ^{125}I-LDL was strongly reduced in the parental 786-O cells, which lack functional VHL (Figure 4.12A&B). There was no detectable degradation of cell-associated ^{125}I-HDL in either of the ccRCC cell lines (Data not shown). Together, these results indicate that the loss of VHL function increases the lipoprotein uptake in ccRCC into a non-degrading compartment.

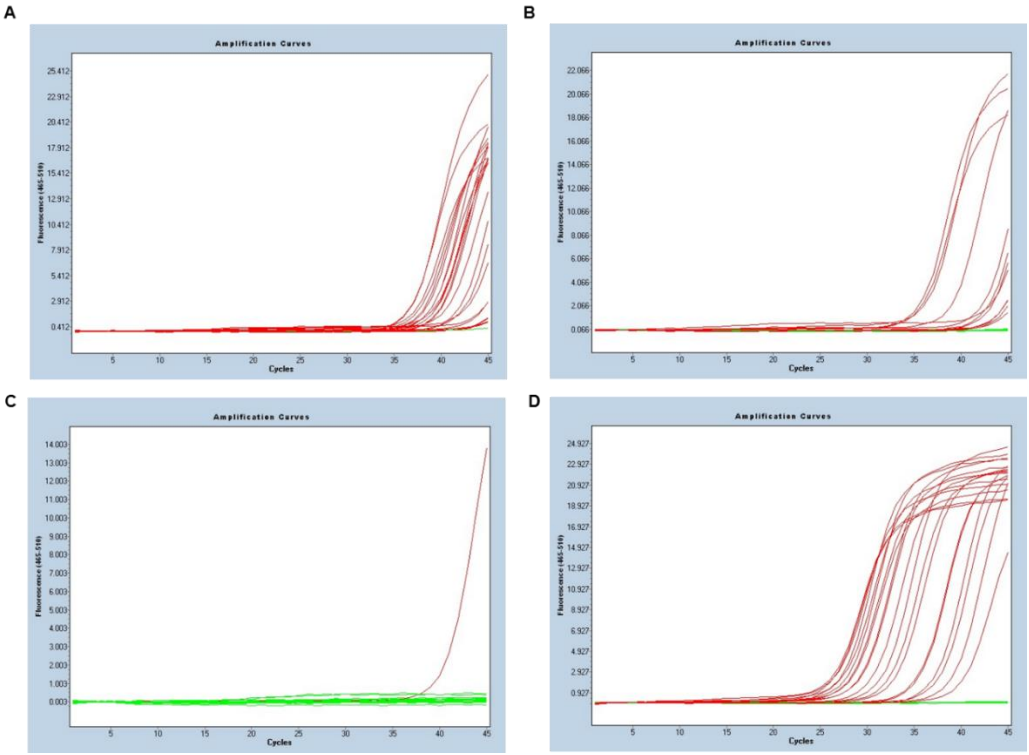

Figure 4.9 qRT-PCR expression of VEGF receptors and NRP1 in ccRCC cells Amplication curves of PCR products of **A**, VEGFR1 **B,** VEGFR2 **C,** VEGFR3 **D,** NRP1 in 786-O and 786-O-VHL cells.

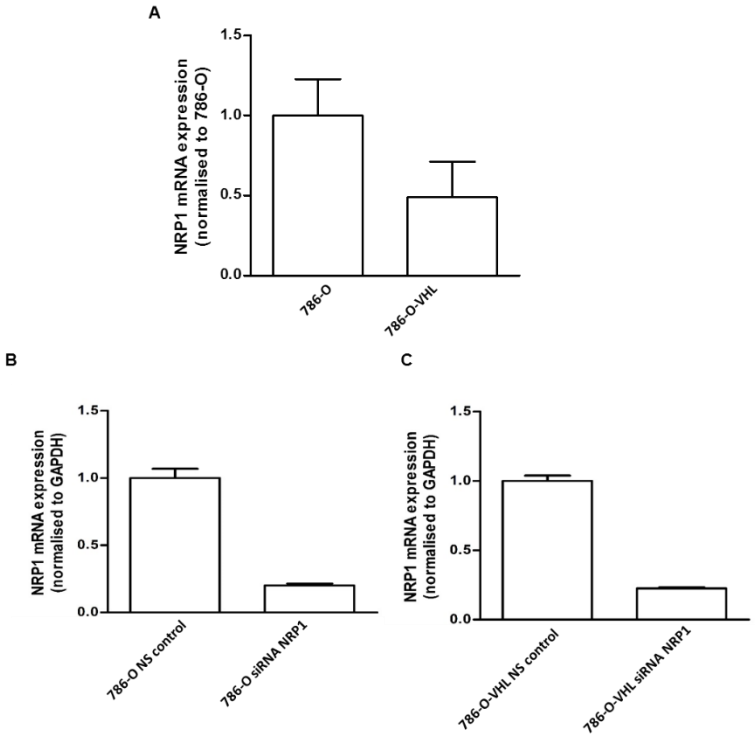

Figure 4.10: qRT-PCR expression of NRP1 and efficiency of NRP1 RNA interference in ccRCC cells A, Quantification of NRP1 mRNA expression. GAPDH was used as a house keeping control gene. **B,** 786-O **C,** 786-O-VHL cells were transfected with a specific siRNA against NRP1 or with non-silencing control siRNA (NS control) and silencing efficiency was analyzed at mRNA level using qRT-PCR after 72hours of transfection.

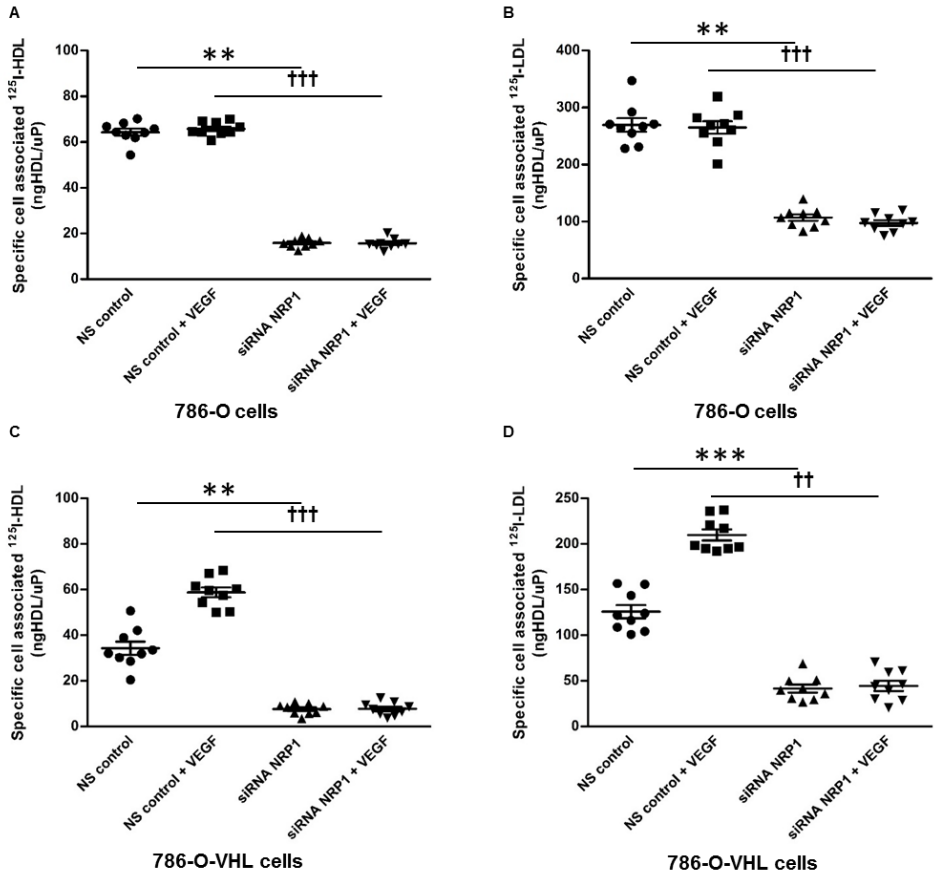

Figure 4.11: NRP1 promotes cellular association of ^{125}I-HDL and ^{125}I-LDL in renal carcinoma 786-O cells 786-O and 786-O-VHL cells were transfected with specific siRNA against NRP1 or with non-silencing control siRNA (NS control). After 72hours of transfection, the cells were pre-treated with 25ng/ml of VEGF for 1 hour prior to assays as indicated, followed by incubation with 10µg/mL of ^{125}I-HDL or ^{125}I-LDL. 786-O cells incubated with **A,** ^{125}I-HDL **B,** ^{125}I-LDL. 786-O-VHL cells incubated with **C,** ^{125}I-HDL **D,** ^{125}I-LDL at 37 ºC for 1hour in the absence (total) or in the presence of 40-fold excess of unlabeled HDL or LDL (unspecific). Specific cellular association was calculated by subtracting unspecific values from total values. The results are represented as mean±SEM of three independent experiments. ***$P \leq 0.001$, **$P \leq 0.01$, *$P \leq 0.05$, †††$P \leq 0.001$ ††$P \leq 0.01$, †$P \leq 0.05$.

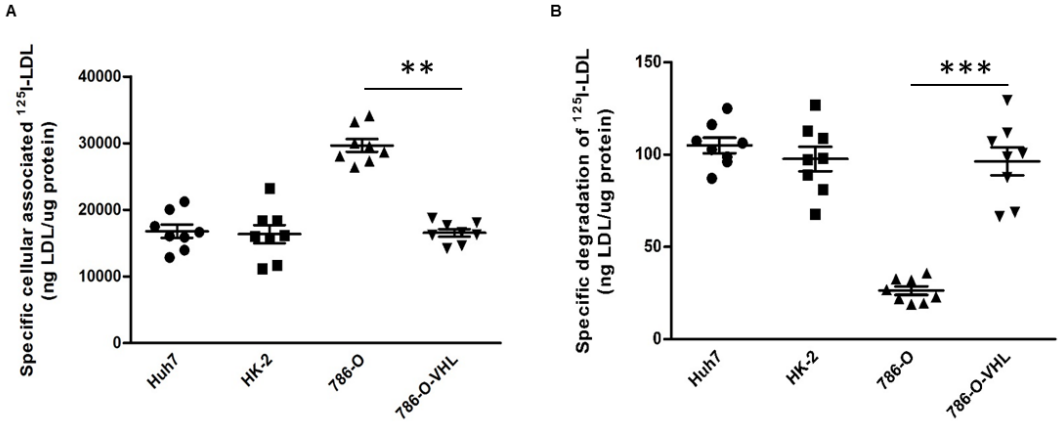

Figure 4.12: Degradation of ^{125}I-LDL in renal carcinoma 786-O cells Cells were incubated with 15µg/mL of ^{125}I-LDL at 37 ºC for 4 hours in the absence (total) or in the presence of 40-fold excess of unlabeled LDL (unspecific). **A,** The adhered cells were processed to analyze cellular association. **B,** The supernatant was collected and processed to analyze the degradation of ^{125}I-LDL as described in the methods section. Specific values were calculated by subtracting unspecific values from total values. The specific degradation was calculated by normalizing to the specific cellular uptake. The results are represented as mean±SEM of three independent experiments, with significance determined by unpaired *t* test. ***$P \leq 0.001$, **$P \leq 0.01$.

SR-BI mediates cellular association and binding of ^{125}I-LDL in ccRCC

We next aimed to unravel the receptor which enhances the lipoprotein uptake by ccRCC cells. We first assessed the expression of two candidate receptors, LDLR and SR-BI. We found lower expression of LDLR in the 786-O cells compared to 786-VHL and HK-2. In addition, the presence of several lower molecular weight anti-LDLR-immunoreactive bands cell lines suggests that the two ccRCC cell lines degrade the LDL receptor more extensively compared to the HK-2 cells (Figure 4.13A). To test whether LDLR mediates the cellular uptake of LDL in ccRCC cells, the LDLR was targeted using RNA interference. Although the knockdown efficiently suppressed protein abundance of LDLR, it did not affect the cellular uptake of ^{125}I-LDL (Figure 4.13 B,C). This finding is in agreement with a previous report [6], but in contrast to the enhanced uptake of LDL by 786-O cells.

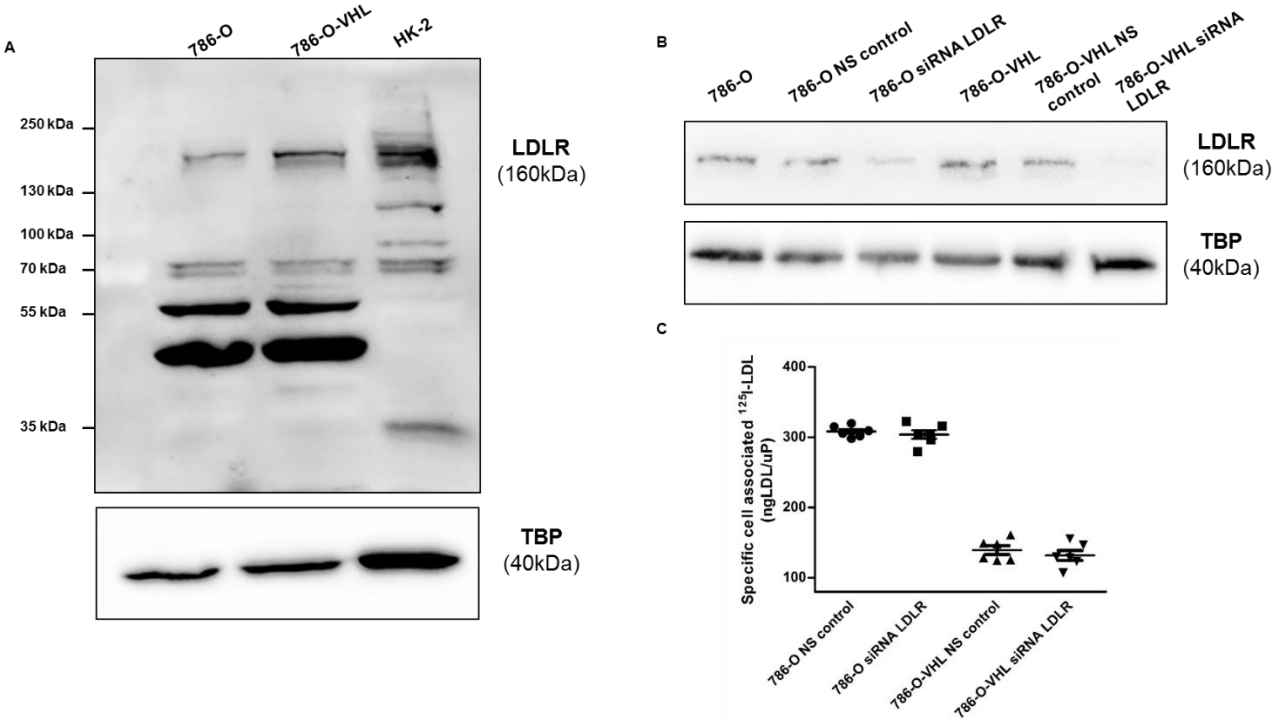

Figure 4.13: Cellular uptake of ^{125}I-LDL in ccRCC is independent of LDLR A, Western blot analysis of LDLR and TATA-binding protein (TBP) in 786-O and 786-O-VHL cells compared to healthy kidney cells (HK-2). The mature glycosylated LDLR is 160kDa while the degradation product is between 55-35kDa. 786-O and 786-O-VHL were transfected with siRNA against LDLR or with non-silencing control siRNA (NS control). **B,** The silencing efficiency was analyzed 72 hours post-transfection at the protein level using western blotting. The western blots were probed with anti-LDLR (160kDa) and anti-TBP (40kDa, used as a loading control). **C,** Specific cell association was analyzed by incubating ccRCC cells with ^{125}I-LDL at 37 ºC for 1hour.

Total lysates of 786-O and 786-VHL cells did not differ in SR-BI protein levels. However, cell-surface biotinylation revealed strongly increased expression of SR-BI on the cell surface of parental 786-O cells compared to that of 786-VHL cells (Figure 4.14A). To test whether the cellular association of lipoproteins in renal carcinoma cells involves SR-BI, we incubated the cells with an SR-BI neutralizing antibody. In both 786-O and 786-VHL cells the specific cellular association of ^{125}I-HDL as well as ^{125}I-LDL was significantly decreased in the presence of the neutralizing antibody (Figures 4.14 B,C). Taken together, these results indicate that the uptake of HDL and LDL by ccRCC cells is dependent on the cell-surface expression of SR-BI.

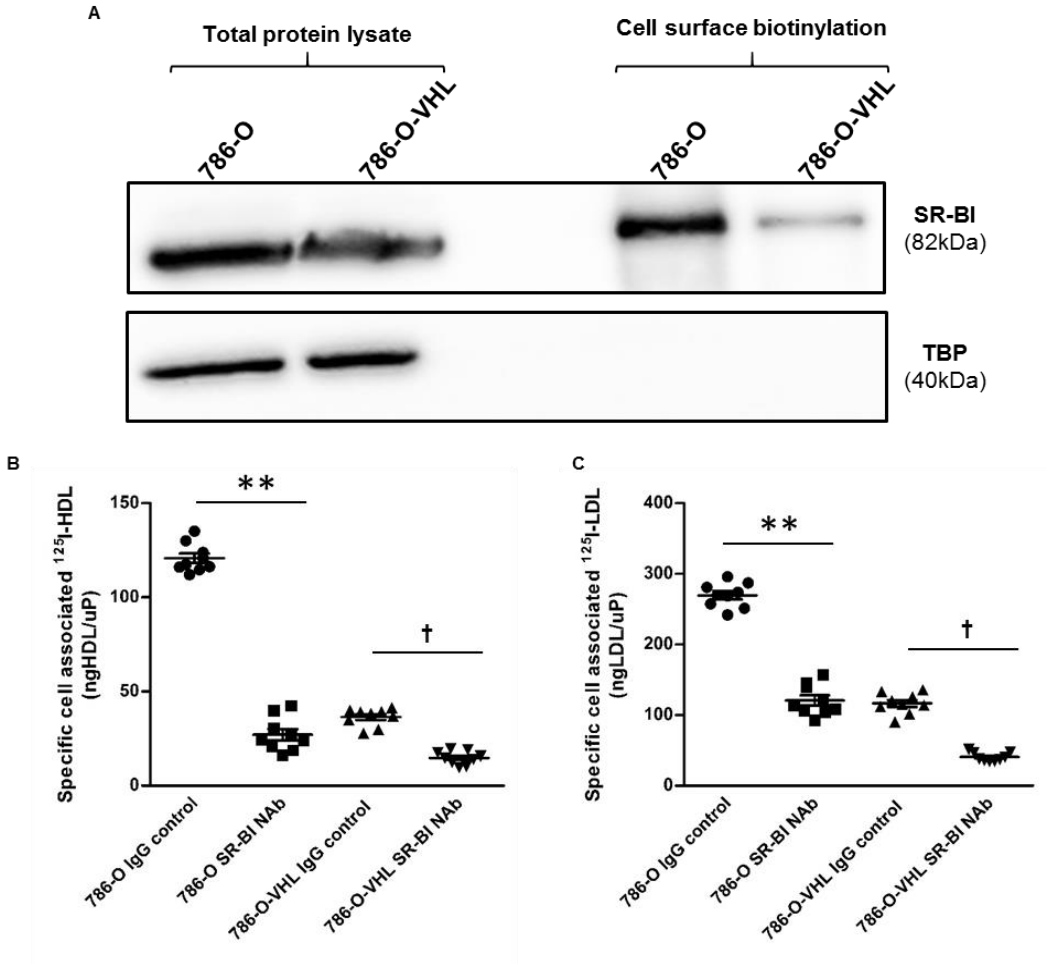

Figure 4.14: SR-BI mediates cellular association of ^{125}I-HDL and ^{125}I-LDL in ccRCC cells A, Cell surface expression of SR-BI in renal carcinoma cells. Western blot analysis of SR-BI and TATA-binding protein (TBP) in total cell lysates (left) and on the cell surface (right) in 786-O and 786-O-VHL cells. The western blots were probed with anti-SR-BI (82kDa) and anti-TBP (40kDa, used as a control for intracellular protein expression). 786-O and 786-O-VHL cells were pre-treated with 25ng/ml of VEGF for 1 hour prior to assays, followed by incubation with 10µg/mL of **B,** ^{125}I-HDL or **C,** ^{125}I-LDL for 1hour in the absence (total) or in the presence of 40-fold excess of unlabeled HDL or LDL (unspecific) at 37 ºC. Specific association was calculated by subtracting unspecific values from total values. The results are represented as mean±SEM of three independent experiments. ***$P\leq$ 0.001, **$P\leq$ 0.01, *$P\leq$ 0.05, †††$P\leq$ 0.001 ††$P\leq$ 0.01, †$P\leq$ 0.05. IgG control represents isotype control and anti-SR-BI Nab represents treatment with SR-BI neutralizing antibody.

4.4 Discussion

In this study, we identified a mechanism of intracellular lipid accumulation by enhanced uptake of LDL and HDL via SR-BI in clear cell RCC. The identification of immunoreactivity for apoA-I and apoB in ccRCC but not or less so in other renal tumors provides strong evidence that this lipid storage is characteristic for ccRCC, which is characterized by VHL inactivation and consecutive HIF activation. Of note, the maintained apoA-I and apoB immunoreactivity suggests that the lipoproteins are not or only partially degraded. In line with this, we found that the ccRCC cell line 786-0 does not produce any apoB and apoA-I but readily takes up LDL and – to much lesser extent - HDL, however without degrading them.

The intracellular storage of LDL is very unusual because the internalization of LDL into other cells, notably hepatocytes, macrophages but also renal mesangial or tubular cells, is followed by degradation [30-32]. Most cells internalize LDL via the LDL-receptor into clathrin-coated pits [33, 34]. LDL is then trafficked into an endosomal/lysosomal route, depending on the presence or absence of PCSK9 either

together or separated from the receptor [35, 36]. The apoB moiety and cholesteryl esters of LDL are hydrolysed by lysosomal proteases and acid lipases respectively [37-39]. Internalisation of apoB-containing lipoproteins by other members of the LDL receptor family, for example LRP1, LRP2, or the VLDL receptor into a broad variety of cells is also followed by lysosomal degradation of both their proteins and lipids [40]. Interestingly, the VLDL receptor was previously reported to be up-regulated in ccRCC and to promote lipid uptake into ccRCC cells. However, this study only recorded the uptake of lipoprotein-derived lipids rather than the lipoproteins' protein moiety [7]. Likewise macrophages degrade modified LDL internalized by class A scavenger receptors [41]. In hepatocytes and macrophages but also other cells, any cholesteryl ester storage in lipid droplets results from the re-esterification of cholesterol in the ER after transfer from the lysosomes [42]. The intracellular storage of endocytosed holoparticles hence appears to be a specific finding in ccRCC cells.

The most likely reason for this atypical behavior of ccRCC cells is the involvement of SR-BI rather than the LDL-receptor in LDL internalization. We found strong immunoreactivity of SR-BI in ccRCC but not in other renal tumors. Also other scientists have previously reported strong expression of SR-BI in ccRCC [7]. We also confirmed the findings of others, that ccRCC cell lines strongly express SR-BI but much less so the LDL receptor [6, 7]. We here extend these previous findings by showing that the inhibition of SR-BI but not the interference with LDLR prevents the uptake of LDL as well as HDL into ccRCC cells (Figure 4.13 and 4.14). The mechanism by which SR-BI promotes cellular lipoprotein uptake is not clear: SR-BI is traditionally regarded as a receptor which binds HDL as well as LDL and provides bidirectional fluxes of cholesterol from these lipoproteins into cells or from the plasma membrane to the lipoprotein depending on the concentration gradient [8, 12]. However, several examples have been reported where ablation or blockage of SR-BI also inhibited the uptake of lipoproteins. Notably vascular endothelial cells were reported by our and other laboratories to internalize and transcytose HDL and LDL in an SR-BI dependent manner [13, 43]. However, it is not clear whether SR-BI or one of its splice variants directly serve as an endocytic receptor [44, 45] or whether SR-BI only enables other pathways of endocytosis. Such indirect effects of SR-BI may include the activation of other receptors by altering the cholesterol distribution within the plasma membrane or signaling via its PDZ domain [46]. SR-BI mediated endocytosis of HDL and LDL into endothelial cells is followed by re-secretion and hence allows transcytosis of lipoproteins, for example from the blood stream into the arterial wall or into the brain as well as from the extravascular tissue into the lymph [47]. This raises the question whether ccRCC cells not only fail to degrade but also to re-secrete the internalized lipoproteins.

VEGF signaling activated by loss of VHL function appears to be the reason for the enhanced SR-BI mediated uptake of HDL and LDL into ccRCC cells: Compared to wild type VHL expressing 786-O-VHL cells, VHL lacking 786-O cells show increased expression of VEGF among other HIF-1α target genes, increased cell surface expression of SR-BI (Figure 4.14A), and increased uptake of both LDL and HDL (Figure 4.5A&B). The uptake of both HDL and LDL was enhanced in 786-O-VHL cells by pre-treatment with VEGF (Figure 4.7A&B) but lowered in 786-O cells by VEGFR inhibitors (Figure 4.8A-D). These findings are in line with the previous report of HIF-1α -dependent lipid uptake into ccRCC [7]. They are in line with our previous observation in HAECs where VEGF promoted the translocation of SR-BI to the cell membrane as well as the uptake and transcytosis of HDL [14]. In this regard it is noteworthy to reconcile the significant correlation of VHL/HIF-1α downstream targets (Glut1, CAIX and high microvessel density) with immunoreactivity of both apoA-I and apoB in our study, suggesting that increased apoA-I and apoB levels are a consequence of VHL/HIF-1α signaling activation. Activated VEGF signaling in ccRCC due to increased HIF-1α activity may enhance lipoprotein uptake into the tumor not only by direct actions on tumor cells but also indirectly by promoting their transport from the circulation into the tumor tissue. VEGF is known to activate the downstream signaling by binding to VEGF receptors [48]. However, we did not detect the expression of any of the three VEGF receptors in the ccRCC cells (Figure 4.9). Importantly, in line with previous

findings [49], we detected higher expression of NRP1 in the VHL lacking 786-O cells compared to the wild type VHL expressing 786-O-VHL cells. Upon binding of VEGF NRP1 elicits angiogenesis and tumorigenesis both dependently and independently of VEGF receptors[45]. The enhanced uptake of HDL and LDL in 786-O-VHL cells by pre-treatment with VEGF was abrogated by the suppression of NRP1 (Figure 4.11). Altogether, our findings identify a novel role of NRP1 in the cholesterol accumulation of ccRCC.

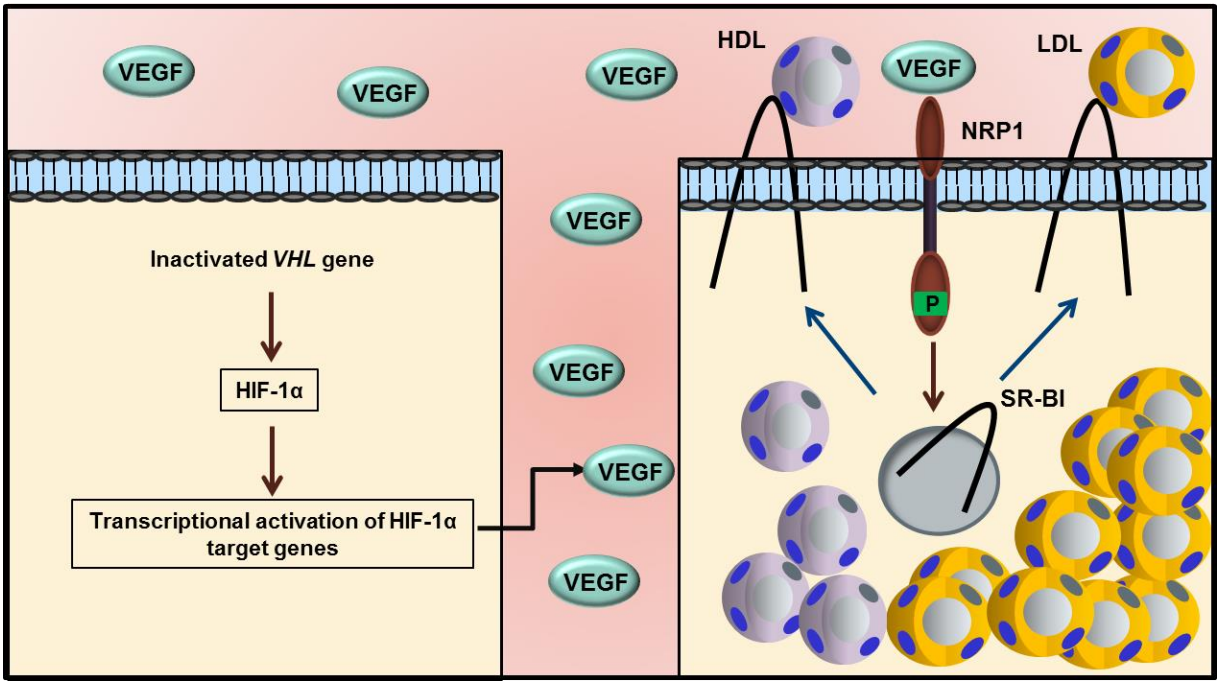

Figure 4.15: Loss of VHL promotes uptake of HDL and LDL in renal cell carcinoma cells In clear cell renal cell carcinoma, somatic mutations in VHL and subsequent HIF-1α activation induce the expression of VEGF. VEGF further induces the cell surface translocation of SR-BI, thereby promoting the excessive uptake and accumulation of HDL and LDL in ccRCC cells.

Our observations provide plausible explanation for the origin of cholesteryl ester accumulation in ccRCC. However, they do not allow any conclusion whether or not enhanced lipoprotein uptake into ccRCC has any impact on the clinical course of this disease. Excessive lipids and cholesterol in cancer cells are considered as markers of cancer aggressiveness [50].In our study. In line with this, immunoreactivity for apoA-I, apoB, or SR-BI was associated with the differentiation of renal carcinomas into ccRCC as well as with tumor grade (apoB) or tumor stage (apoB and SR-BI). However, expression of apoB or SR-BI showed no association with prognosis. Rather by contrast apoA-I immunoreactivity was an indicator of better survival but this association did not remain significant after adjustment for tumor stage and grade. Previously, in a study of 100 Chinese patients, SR-BI expression was associated with the prognosis of ccRCC [51]. We did not replicate this observation in our larger cohort of 172 patients. However, it is important to note, that in our in vitro experiments the cell surface expression of SR-BI rather than the total SR-BI content was depending on VHL and VEGF. The semi-quantitative scoring immunostaining intensity does however not discriminate between the larger pool of intracellular SR-BI and the smaller pool of cell surface SR-BI. Interestingly, genome-wide association studies identified a borderline significant association of the rs4765623 polymorphism in SCARB1 with ccRCC susceptibility [52] indicating some pathogenic role of SR-BI in ccRCC.

Our data are important for the understanding of lipid metabolic reprogramming as a hallmark of cancer. Exacerbated glucose uptake and glycolysis utilization leading to increased lactate production (Warburg effect) is one of the first adaptive events of the cancer cells [53, 54]. However, cancer cells also rely on

glutamine consumption, which provides carbon needed for amino-acid, nucleotide and lipid biosynthesis [54, 55]. Importantly, alterations in lipid- and cholesterol-associated pathways are now regarded as potential targets in cancer therapy [50]. Drugs targeting lipid and cholesterol dependencies, modulating lipid raft components to induce cell death signaling as well as drugs targeting lipid mediators of tumor-stroma interactions are tested in preclinical trials [50].

In conclusion, we identified SR-BI mediated intracellular accumulation of intact lipoproteins as the likely origin of cholesterol accumulation and the characteristic clear cytoplasm of ccRCC. VEGF induced SR-BI cell surface translocation may be the underlying mechanism.

4.5 References

1. Frew IJ, Moch H. A clearer view of the molecular complexity of clear cell renal cell carcinoma. *Annu Rev Pathol* 2015;**10**:263-289.
2. Lopez JI. Renal tumors with clear cells. A review. *Pathol Res Pract* 2013;**209**:137-146.
3. Gebhard RL, Clayman RV, Prigge WF, Figenshau R, Staley NA, Reesey C, et al. Abnormal cholesterol metabolism in renal clear cell carcinoma. *J Lipid Res* 1987;**28**:1177-1184.
4. Wiley MH, Howton MM, Siperstein MD. The quantitative role of the kidneys in the in vivo metabolism of mevalonate. *J Biol Chem* 1977;**252**:548-554.
5. Hsieh JJ, Purdue MP, Signoretti S, Swanton C, Albiges L, Schmidinger M, et al. Renal cell carcinoma. *Nat Rev Dis Primers* 2017;**3**:17009.
6. Clayman RV, Bilhartz LE, Spady DK, Buja LM, Dietschy JM. Low density lipoprotein-receptor activity is lost in vivo in malignantly transformed renal tissue. *FEBS Lett* 1986;**196**:87-90.
7. Sundelin JP, Stahlman M, Lundqvist A, Levin M, Parini P, Johansson ME, et al. Increased expression of the very low-density lipoprotein receptor mediates lipid accumulation in clear-cell renal cell carcinoma. *PLoS One* 2012;**7**:e48694.
8. Pagler TA, Rhode S, Neuhofer A, Laggner H, Strobl W, Hinterndorfer C, et al. SR-BI-mediated high density lipoprotein (HDL) endocytosis leads to HDL resecretion facilitating cholesterol efflux. *J Biol Chem* 2006;**281**:11193-11204.
9. Acton S, Rigotti A, Landschulz KT, Xu S, Hobbs HH, Krieger M. Identification of scavenger receptor SR-BI as a high density lipoprotein receptor. *Science* 1996;**271**:518-520.
10. Stangl H, Cao G, Wyne KL, Hobbs HH. Scavenger receptor, class B, type I-dependent stimulation of cholesterol esterification by high density lipoproteins, low density lipoproteins, and nonlipoprotein cholesterol. *J Biol Chem* 1998;**273**:31002-31008.
11. Swarnakar S, Temel RE, Connelly MA, Azhar S, Williams DL. Scavenger receptor class B, type I, mediates selective uptake of low density lipoprotein cholesteryl ester. *J Biol Chem* 1999;**274**:29733-29739.
12. Acton SL, Scherer PE, Lodish HF, Krieger M. Expression cloning of SR-BI, a CD36-related class B scavenger receptor. *J Biol Chem* 1994;**269**:21003-21009.
13. Armstrong SM, Sugiyama MG, Fung KY, Gao Y, Wang C, Levy AS, et al. A novel assay uncovers an unexpected role for SR-BI in LDL transcytosis. *Cardiovasc Res* 2015;**108**:268-277.
14. Velagapudi S, Yalcinkaya M, Piemontese A, Meier R, Norrelykke SF, Perisa D, et al. VEGF-A Regulates Cellular Localization of SR-BI as Well as Transendothelial Transport of HDL but Not LDL. *Arterioscler Thromb Vasc Biol* 2017.
15. Masson N, Ratcliffe PJ. Hypoxia signaling pathways in cancer metabolism: the importance of co-selecting interconnected physiological pathways. *Cancer Metab* 2014;**2**:3.
16. Hakimi AA, Reznik E, Lee CH, Creighton CJ, Brannon AR, Luna A, et al. An Integrated Metabolic Atlas of Clear Cell Renal Cell Carcinoma. *Cancer Cell* 2016;**29**:104-116.
17. Wiesener MS, Munchenhagen PM, Berger I, Morgan NV, Roigas J, Schwiertz A, et al. Constitutive activation of hypoxia-inducible genes related to overexpression of hypoxia-inducible factor-1alpha in clear cell renal carcinomas. *Cancer Res* 2001;**61**:5215-5222.
18. Haase VH. Regulation of erythropoiesis by hypoxia-inducible factors. *Blood Rev* 2013;**27**:41-53.
19. Chan DA, Sutphin PD, Nguyen P, Turcotte S, Lai EW, Banh A, et al. Targeting GLUT1 and the Warburg effect in renal cell carcinoma by chemical synthetic lethality. *Sci Transl Med* 2011;**3**:94ra70.
20. Greijer AE, van der Wall E. The role of hypoxia inducible factor 1 (HIF-1) in hypoxia induced apoptosis. *J Clin Pathol* 2004;**57**:1009-1014.
21. Kononen J, Bubendorf L, Kallioniemi A, Barlund M, Schraml P, Leighton S, et al. Tissue microarrays for high-throughput molecular profiling of tumor specimens. *Nat Med* 1998;**4**:844-847.

22. Beleut M, Zimmermann P, Baudis M, Bruni N, Buhlmann P, Laule O, et al. Integrative genome-wide expression profiling identifies three distinct molecular subgroups of renal cell carcinoma with different patient outcome. *BMC Cancer* 2012;**12**:310.
23. Humphrey PA, Moch H, Cubilla AL, Ulbright TM, Reuter VE. The 2016 WHO Classification of Tumours of the Urinary System and Male Genital Organs-Part B: Prostate and Bladder Tumours. *Eur Urol* 2016;**70**:106-119.
24. Hergovich A, Lisztwan J, Barry R, Ballschmieter P, Krek W. Regulation of microtubule stability by the von Hippel-Lindau tumour suppressor protein pVHL. *Nat Cell Biol* 2003;**5**:64-70.
25. Ruf M, Mittmann C, Nowicka AM, Hartmann A, Hermanns T, Poyet C, et al. pVHL/HIF-regulated CD70 expression is associated with infiltration of CD27+ lymphocytes and increased serum levels of soluble CD27 in clear cell renal cell carcinoma. *Clin Cancer Res* 2015;**21**:889-898.
26. Casagrande S, Ruf M, Rechsteiner M, Morra L, Brun-Schmid S, von Teichman A, et al. The protein tyrosine phosphatase receptor type J is regulated by the pVHL-HIF axis in clear cell renal cell carcinoma. *J Pathol* 2013;**229**:525-534.
27. Havel RJ, Eder HA, Bragdon JH. The distribution and chemical composition of ultracentrifugally separated lipoproteins in human serum. *J Clin Invest* 1955;**34**:1345-1353.
28. Rohrer L, Cavelier C, Fuchs S, Schluter MA, Volker W, von Eckardstein A. Binding, internalization and transport of apolipoprotein A-I by vascular endothelial cells. *Biochim Biophys Acta* 2006;**1761**:186-194.
29. Freeman M, Ekkel Y, Rohrer L, Penman M, Freedman NJ, Chisolm GM, et al. Expression of type I and type II bovine scavenger receptors in Chinese hamster ovary cells: lipid droplet accumulation and nonreciprocal cross competition by acetylated and oxidized low density lipoprotein. *Proc Natl Acad Sci U S A* 1991;**88**:4931-4935.
30. Goldstein JL, Brunschede GY, Brown MS. Inhibition of proteolytic degradation of low density lipoprotein in human fibroblasts by chloroquine, concanavalin A, and Triton WR 1339. *J Biol Chem* 1975;**250**:7854-7862.
31. Keidar S, Brook GJ, Rosenblat M, Fuhrman B, Dankner G, Aviram M. Involvement of the macrophage low density lipoprotein receptor-binding domains in the uptake of oxidized low density lipoprotein. *Arterioscler Thromb* 1992;**12**:484-493.
32. Ong AC, Moorhead JF. Tubular lipidosis: epiphenomenon or pathogenetic lesion in human renal disease? *Kidney Int* 1994;**45**:753-762.
33. Goldstein JL, Brown MS. The LDL receptor. *Arterioscler Thromb Vasc Biol* 2009;**29**:431-438.
34. Chen WJ, Goldstein JL, Brown MS. NPXY, a sequence often found in cytoplasmic tails, is required for coated pit-mediated internalization of the low density lipoprotein receptor. *J Biol Chem* 1990;**265**:3116-3123.
35. Davis CG, Goldstein JL, Sudhof TC, Anderson RG, Russell DW, Brown MS. Acid-dependent ligand dissociation and recycling of LDL receptor mediated by growth factor homology region. *Nature* 1987;**326**:760-765.
36. Lambert G, Sjouke B, Choque B, Kastelein JJ, Hovingh GK. The PCSK9 decade. *J Lipid Res* 2012;**53**:2515-2524.
37. Skrzydlewski Z, Worowski K. Degradation of low-density lipoproteins (LDL) and LDL - protamine complexes by lysosomal protease. *Acta Biol Acad Sci Hung* 1978;**29**:19-22.
38. Linke M, Gordon RE, Brillard M, Lecaille F, Lalmanach G, Bromme D. Degradation of apolipoprotein B-100 by lysosomal cysteine cathepsins. *Biol Chem* 2006;**387**:1295-1303.
39. Goldstein JL, Dana SE, Faust JR, Beaudet AL, Brown MS. Role of lysosomal acid lipase in the metabolism of plasma low density lipoprotein. Observations in cultured fibroblasts from a patient with cholesteryl ester storage disease. *J Biol Chem* 1975;**250**:8487-8495.
40. Go GW, Mani A. Low-density lipoprotein receptor (LDLR) family orchestrates cholesterol homeostasis. *Yale J Biol Med* 2012;**85**:19-28.
41. Sun B, Boyanovsky BB, Connelly MA, Shridas P, van der Westhuyzen DR, Webb NR. Distinct mechanisms for OxLDL uptake and cellular trafficking by class B scavenger receptors CD36 and SR-BI. *J Lipid Res* 2007;**48**:2560-2570.
42. Soccio RE, Breslow JL. Intracellular cholesterol transport. *Arterioscler Thromb Vasc Biol* 2004;**24**:1150-1160.
43. Rohrer L, Ohnsorg PM, Lehner M, Landolt F, Rinninger F, von Eckardstein A. High-density lipoprotein transport through aortic endothelial cells involves scavenger receptor BI and ATP-binding cassette transporter G1. *Circ Res* 2009;**104**:1142-1150.
44. Eckhardt ER, Cai L, Sun B, Webb NR, van der Westhuyzen DR. High density lipoprotein uptake by scavenger receptor SR-BII. *J Biol Chem* 2004;**279**:14372-14381.

45. Eckhardt ER, Cai L, Shetty S, Zhao Z, Szanto A, Webb NR, et al. High density lipoprotein endocytosis by scavenger receptor SR-BII is clathrin-dependent and requires a carboxyl-terminal dileucine motif. *J Biol Chem* 2006;**281**:4348-4353.
46. Saddar S, Mineo C, Shaul PW. Signaling by the high-affinity HDL receptor scavenger receptor B type I. *Arterioscler Thromb Vasc Biol* 2010;**30**:144-150.
47. Lim HY, Thiam CH, Yeo KP, Bisoendial R, Hii CS, McGrath KC, et al. Lymphatic vessels are essential for the removal of cholesterol from peripheral tissues by SR-BI-mediated transport of HDL. *Cell Metab* 2013;**17**:671-684.
48. Zachary I, Gliki G. Signaling transduction mechanisms mediating biological actions of the vascular endothelial growth factor family. *Cardiovasc Res* 2001;**49**:568-581.
49. Cao Y, Wang L, Nandy D, Zhang Y, Basu A, Radisky D, et al. Neuropilin-1 upholds dedifferentiation and propagation phenotypes of renal cell carcinoma cells by activating Akt and sonic hedgehog axes. *Cancer Res* 2008;**68**:8667-8672.
50. Beloribi-Djefaflia S, Vasseur S, Guillaumond F. Lipid metabolic reprogramming in cancer cells. *Oncogenesis* 2016;**5**:e189.
51. Xu G, Lou N, Xu Y, Shi H, Ruan H, Xiao W, et al. Diagnostic and prognostic value of scavenger receptor class B type 1 in clear cell renal cell carcinoma. *Tumour Biol* 2017;**39**:1010428317699110.
52. Pospiech E, Ligeza J, Wilk W, Golas A, Jaszczynski J, Stelmach A, et al. Variants of SCARB1 and VDR Involved in Complex Genetic Interactions May Be Implicated in the Genetic Susceptibility to Clear Cell Renal Cell Carcinoma. *Biomed Res Int* 2015;**2015**:860405.
53. Ying H, Kimmelman AC, Lyssiotis CA, Hua S, Chu GC, Fletcher-Sananikone E, et al. Oncogenic Kras maintains pancreatic tumors through regulation of anabolic glucose metabolism. *Cell* 2012;**149**:656-670.
54. Gaglio D, Metallo CM, Gameiro PA, Hiller K, Danna LS, Balestrieri C, et al. Oncogenic K-Ras decouples glucose and glutamine metabolism to support cancer cell growth. *Mol Syst Biol* 2011;**7**:523.
55. Son J, Lyssiotis CA, Ying H, Wang X, Hua S, Ligorio M, et al. Glutamine supports pancreatic cancer growth through a KRAS-regulated metabolic pathway. *Nature* 2013;**496**:101-105.

5. Conclusion and discussion

Atherosclerosis remains the major cause of mortality and morbidity in the world. According to the response to injury and response to retention theories, the accumulation of apoB containing lipoproteins within the vascular wall play a crucial role in the pathogenesis of atherosclerosis [1]. HDL have to enter and leave the arterial wall to play their presumed anti-atherogenic role in reverse cholesterol transport [2]. Imbalance in the influx and efflux of the lipoproteins across the arterial wall hence is an important determinant of disease susceptibility. Hence, identifying the factors involved in the lipoprotein transport through the endothelial cells will give a better understanding of the development and progression of the disease, which will help to design novel therapeutic targets [3, 4]. Therefore, in this thesis we aimed to identify the receptors and signalling kinase cascades involved in regulating the transport of the lipoproteins across the endothelium. Based on hypothesis-driven and hypothesis-free approaches we found that S1P/S1PR and VEGF/VEGFR axes contribute to the regulation of the lipoprotein transport through the endothelium.

Activation of S1P1 and S1P3 as well as VEGFR2 with their respective agonists stimulated the translocation of SR-BI from cytosol to the plasma membrane, thereby increasing the cellular binding, uptake and transport of HDL through the endothelial cells (Figure 5.1). The activation of the S1P1 and the S1P3 receptors activates intracellular signaling pathways encompassing trimeric G-proteins (G_i, G_q, and $G_{12/13}$) and other signalling molecules including small G proteins Rac1 and Rho, PI3K/Akt and mitogen activated protein kinases[5]. The Rho GTPases regulate actin cytoskeletal architecture and cell polarity. Actin cytoskeleton plays a role in apical and basolateral vesicular trafficking in polarized cells. Rho GTPases and Rac1 regulate actin dynamics as well as endocytic trafficking pathway by modulating PI3K, respectively [6]. Therefore, it will be interesting to investigate whether the S1P1 and S1P3 mediated HDL endocytosis and transport is dependent on the activation of Rho/Rac GTPases.

Binding of VEGF-A induces conformational changes and dimerization of VEGFR2 which in turn triggers kinase activation, tyrosine phosphorylation of the dimerized VEGFR2 and subsequent phosphorylation of SH2-containing intracellular signaling proteins, including phospholipase C-γ1 (PLCγ1), Src family tyrosine kinases, and phosphatidylinositol 3-kinase (PI3K) and GTPase-activating protein residues of Ras, Raf, MEK and MAPK [7-10]. By both pharmacological inhibition and RNA interference, we revealed the involvement of PI3K/Akt, p38MAPK, and the Ras-Raf-MEK pathway in binding and uptake of HDL. However, the inhibition of the Ras-Raf-MEK pathway but not the inhibition of PI3K/Akt and p38MAPK could be overcome by VEGF stimulation. Thus, VEGF regulates the interaction of HDL with endothelial cells by activating PI3K/Akt and p38MAPK but not the Ras-Raf-MEK pathway. Thus, it will be interesting to identify agonists beyond VEGF that regulate the endothelial binding, uptake and transport of HDL by activating the MEK/ERK pathway. Since, S1P1 and S1P3 were previously shown to activate the MEK/ERK pathway, it will be interesting to study its involvement in S1P1 and S1P3 dependent regulation of endothelial cellular binding, uptake and transport of HDL. It has been previously shown that VEGF promotes the activation of S1P1 receptor and its downstream signaling kinases such as PI3K/Akt and members of mitogen-activated protein kinase family (MAPK) [11, 12]. We also found that PI3K/Akt and p38 MAPK are involved in the VEGF-mediated cellular binding and uptake of HDL. Therefore, it will be interesting to investigate the role of cross-talk between S1P/S1PR and VEGF/VEGFR2 in the regulation of transendothelial transport of HDL.

Interestingly and in contrast to the effects of S1P on HDL transport, we found that treatment of endothelial cells with either the S1P1 or the S1P3 agonists decrease the cellular binding, uptake and transport of LDL through HAECs. Moreover, the inhibition of both S1P1 and S1P3 increased the transendothelial transport of LDL through different mechanisms. The S1P1 inhibitor was found to enhance the total cellular uptake and transport of LDL through fluid-phase (Figure 5.1). Pre-treatment

of cells with a fluid-phase uptake inhibitor decreased the total cellular uptake and transport of LDL stimulated by the S1P1 inhibitor. The treatment of endothelial cells with the S1P3 inhibitor increased the cellular binding and uptake of LDL through LDLR and transport independent of both LDLR and SR-BI. We confirmed previous reports that endothelial cells internalize and transcytose LDL in a process involving SR-BI [13]. Interestingly, VEGF-A and VEGFR2 had no effect on binding, uptake and transport of LDL in HAECs. However, despite regulating the cell surface abundance of SR-BI, neither S1P nor VEGF regulate the transendothelial transport of LDL. These lipoprotein-specific effects of S1P/S1P1 & S1P3 and VEGF/VEGFR2 on the processing of HDL and LDL by HAECs indicate the existence of additional regulators and routes of transendothelial transport, for example ALK1 which was recently identified by a genome-wide RNAi-screen as an endothelial LDL binding protein mediating uptake and transport of LDL [14].

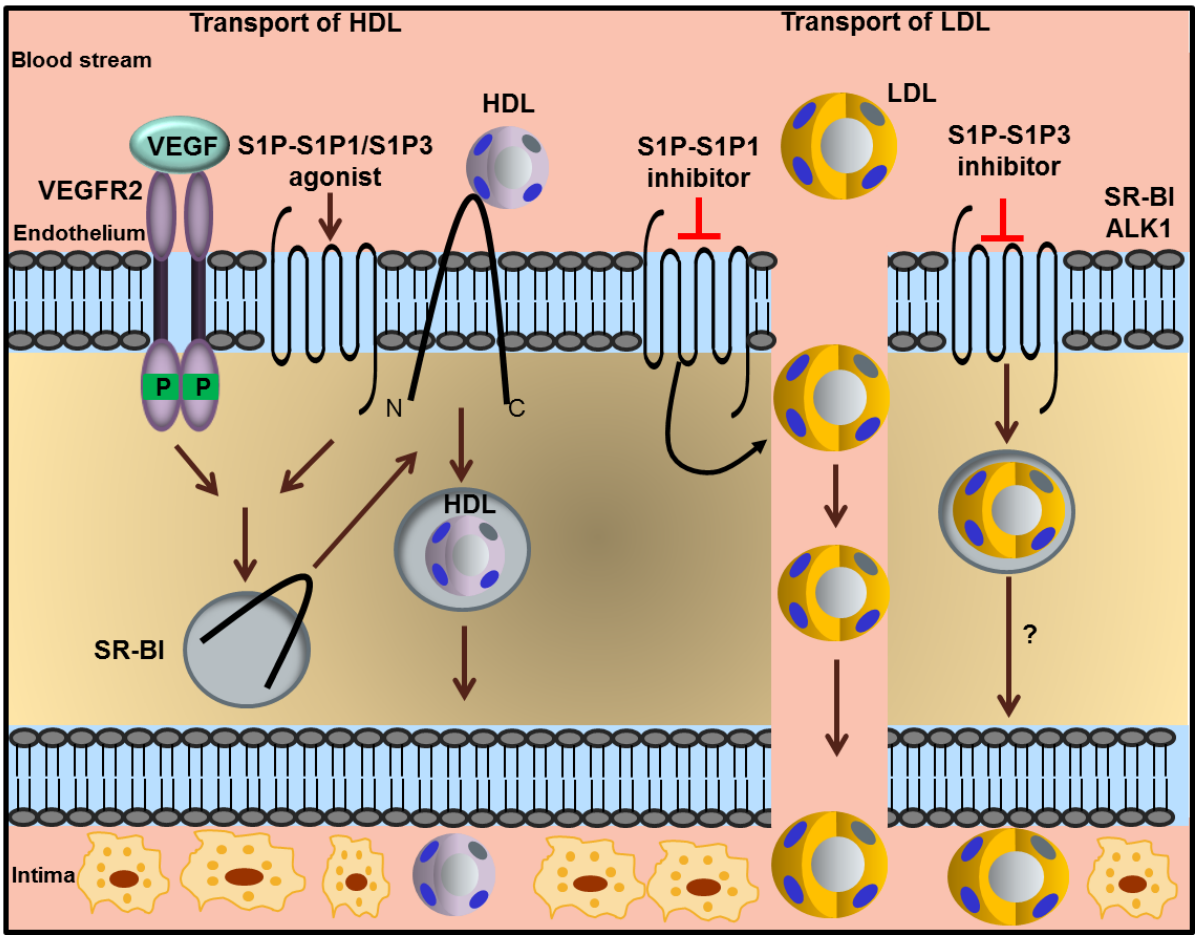

Figure 5.1: Rate-limiting factors involved in the regulation of HDL transport by HAECs Activation of S1P1 and S1P3 receptors as well as VEGFR2 with their respective agonists stimulated the translocation of SR-BI to the cell surface, which further increased the transport of HDL across the endothelial cells. The transport of LDL is increased in the presence of S1P1 inhibitor through fluid-phase. The mechanism through which S1P3 inhibitor increased the transport of LDL through the endothelial cells remains unknown.

Finally, we tried to translate our findings on the regulation of transendothelial lipoprotein transport into the elucidation of pathomechanisms in human disease. In clear cell renal cell carcinoma (ccRCC) somatic mutations in VHL and subsequent HIF-1α activation induce the expression of VEGF. Thereby, we identified VEGF as the driver of LDL and HDL accumulation in ccRCC again by promoting the SR-BI abundance in the cell membrane. (Figure 4.15). Moreover, our findings in ccRCC raise the question whether SR-BI is a therapeutic target in clear-cell renal cell carcinoma. We also found that treatment of ccRCC cells with the inhibitors against VEGF receptors or NRP1 decreased the uptake of HDL as well

as LDL. In view of our findings on the upregulation of HDL transport in endothelial cells, this mechanism may not only happen in tumor cells but also in the microvasculature of ccRCC. Infact, we found significant correlation between apoA-I and apoB expression and CD34 expression of the microvasculature marker. Interestingly, treatment of mice with renal cell carcinoma with neutralizing antibody against S1P has been shown to increase their sensitivity to sunitinib treatment, which inhibits VEGF tyrosine kinase receptors [15]. Therefore, it will be interesting to study the cross-talk between S1P/S1PR and VEGF/NRP1 with respect to the transport of lipoproteins into the tumor cells or through the vasculature of ccRCC.

In conclusion, the identification of S1P/S1PR and VEGF/VEGFR signaling cascade in regulating the transport of HDL and LDL through HAECs helped to advance our understanding of lipoprotein accumulation in both atherosclerosis and in specific cancer namely, ccRCC. The analogous findings provide another example of shared pathomechanisms between the two most frequent causes of death, namely cardiovascular diseases (CVD) and cancer [16].

References

1. Boren J, Williams KJ. The central role of arterial retention of cholesterol-rich apolipoprotein-B-containing lipoproteins in the pathogenesis of atherosclerosis: a triumph of simplicity. *Curr Opin Lipidol* 2016;**27**:473-483.
2. von Eckardstein A, Rohrer L. HDLs in crises. *Curr Opin Lipidol* 2016;**27**:264-273.
3. von Eckardstein A, Rohrer L. Transendothelial lipoprotein transport and regulation of endothelial permeability and integrity by lipoproteins. *Curr Opin Lipidol* 2009;**20**:197-205.
4. Michel CC, Nanjee MN, Olszewski WL, Miller NE. LDL and HDL transfer rates across peripheral microvascular endothelium agree with those predicted for passive ultrafiltration in humans. *J Lipid Res* 2015;**56**:122-128.
5. Spiegel S, Milstien S. The outs and the ins of sphingosine-1-phosphate in immunity. *Nat Rev Immunol* 2011;**11**:403-415.
6. Chi X, Wang S, Huang Y, Stamnes M, Chen JL. Roles of rho GTPases in intracellular transport and cellular transformation. *Int J Mol Sci* 2013;**14**:7089-7108.
7. Waltenberger J, Claesson-Welsh L, Siegbahn A, Shibuya M, Heldin CH. Different signal transduction properties of KDR and Flt1, two receptors for vascular endothelial growth factor. *J Biol Chem* 1994;**269**:26988-26995.
8. Takahashi T, Shibuya M. The 230 kDa mature form of KDR/Flk-1 (VEGF receptor-2) activates the PLC-gamma pathway and partially induces mitotic signals in NIH3T3 fibroblasts. *Oncogene* 1997;**14**:2079-2089.
9. Igarashi K, Isohara T, Kato T, Shigeta K, Yamano T, Uno I. Tyrosine 1213 of Flt-1 is a major binding site of Nck and SHP-2. *Biochem Biophys Res Commun* 1998;**246**:95-99.
10. Guo D, Jia Q, Song HY, Warren RS, Donner DB. Vascular endothelial cell growth factor promotes tyrosine phosphorylation of mediators of signal transduction that contain SH2 domains. Association with endothelial cell proliferation. *J Biol Chem* 1995;**270**:6729-6733.
11. Spiegel S, Milstien S. Sphingosine-1-phosphate: an enigmatic signalling lipid. *Nat Rev Mol Cell Biol* 2003;**4**:397-407.
12. Igarashi J, Erwin PA, Dantas AP, Chen H, Michel T. VEGF induces S1P1 receptors in endothelial cells: Implications for cross-talk between sphingolipid and growth factor receptors. *Proc Natl Acad Sci U S A* 2003;**100**:10664-10669.
13. Armstrong SM, Sugiyama MG, Fung KY, Gao Y, Wang C, Levy AS, et al. A novel assay uncovers an unexpected role for SR-BI in LDL transcytosis. *Cardiovasc Res* 2015;**108**:268-277.
14. Kraehling JR, Chidlow JH, Rajagopal C, Sugiyama MG, Fowler JW, Lee MY, et al. Genome-wide RNAi screen reveals ALK1 mediates LDL uptake and transcytosis in endothelial cells. *Nat Commun* 2016;**7**:13516.
15. Zhang L, Wang X, Bullock AJ, Callea M, Shah H, Song J, et al. Anti-S1P Antibody as a Novel Therapeutic Strategy for VEGFR TKI-Resistant Renal Cancer. *Clin Cancer Res* 2015;**21**:1925-1934.
16. Koene RJ, Prizment AE, Blaes A, Konety SH. Shared Risk Factors in Cardiovascular Disease and Cancer. *Circulation* 2016;**133**:1104-1114.

Acknowledgments

This thesis was performed in the Institute of Clinical Chemistry at the University Hospital of Zürich. It has been possible due to the help, support and guidance of several people and it is a great pleasure of mine to thank them all for their contribution to this work.

Firstly, I am immensely grateful to my direct supervisor Dr. Lucia Rohrer for her constant support and guidance in both scientific and technical matters. She would encourage me by providing the freedom to work independently, while always being available for discussions when I was faced with any complexities. I learnt a lot from these constant interactions with her, where she would act as a great sounding board, allowing me to tap into her wealth of experience in the field of lipoproteins. This work would not have been possible without her support and for that, I am very thankful to her.

I am deeply thankful to Professor Dr. Arnold von Eckardstein for giving me the opportunity to work in his group, for his supervision and for his advice whenever needed. His guidance has played an important role in my work and I am grateful for that. Special thanks to him for always taking the time to review, correct and improve all scientific content created by me, including this manuscript.

I would like to thank my thesis committee, Professor Zhihong Yang and Professor Urs Greber for guiding me over the last four years on this project.

I sincerely thank Professor Dr. Holger Moch and Dr. Peter Schraml for their enriching collaboration and for opening a window into the field of cancer biology for me.

I am deeply indebted to my colleagues in the Institute of Clinical Chemistry. This thesis has become possible in no small measure, due to the great atmosphere in the laboratory, where we share a great friendship, both within work and beyond. I would like to thank Silvija for her excellent technical help and for her contribution in making the lab an efficient workplace. Special thanks to Damir, Rahel and Jerome for patiently teaching me techniques in my early days with the lab. I am grateful to Antonio for his enthusiastic and optimistic support during my screening experiments. I am thankful to Paolo and Mustafa for our various scientific collaborations and discussions. I offer my thanks to Katrin, Anton and Grigorios for their help and support. I sincerely appreciate the great working relationship I had with other current and former members of the Institute of Clinical Chemistry: Prof. Hornemann, Heiko, Hans, Maryam, Wijstke, Alaa, Andrea, Reda, Irina, Iryna, Assem, Saranya, Regula, Yu, Museer, and Gergely.

I would express my thanks to Sonja Bernhard and Christine Genne for their tireless support in all administrative affairs. I would also like to thank the imMed program for giving me the opportunity as part of the program.

My special thanks to Dr. Roger Meier of Scientific Center for Optical and Electron Microscopy (SCOPEM, ETH) for his excellent support during the screening experiments. Special thanks to the entire team at SCOPEM for teaching me microscopy techniques and image analysis. I would like to thank Simon for patiently explaining various statistical techniques to me. I would also like to thank the group of Dr. Gabor Csucs: Mike, Szymon, Andrzej, Miriam for their technical support.

I would like to thank my parents, Uma and Sarma, and my sister Divya, who have always been supportive and a constant source of motivation to me. They encouraged my decision to move to Switzerland to pursue my scientific endeavors, even if that meant they would see less of me. I am also thankful to my husband, Karun, for being a constant supportive companion.

Curriculum Vitae

Personal Details

Name: Srividya Velagapudi

Date of birth: 02.06.1989

Nationality: Indian

Education

Mar'13 – present **Ph.D. student**
Institute of Clinical Chemistry, University Hospital of Zurich, Switzerland
In the group of Prof.Dr.med Arnold von Eckardstein and Dr.Lucia Rohrer

Apr'12 – Feb'13 **Research Assistant**
Department of Plant Biology, University of Fribourg, Switzerland
In the group of Dr.Didier Reinhardt

Sep'10 – Mar'12 **Master in Biology** - Option Biochemistry
University of Fribourg, Switzerland
Master's thesis under the guidance of Prof.Dr.Zhihong Yang
Laboratory of Vascular Biology, Department of Medicine
University of Fribourg, Switzerland

Aug'06 – Jun'09 **Bachelor in Science**
Osmania University, India
Majors in Biotechnology, Biochemistry and Chemistry

Work Experience

Mar'16 – present **Co-editor** – open access book featuring expert views on 'Signal Transduction'
DeGruyter medicine

Jul'13 – present **Assistant editor**
DeGruyter medicine

Jun'09 – Feb'10 **Technology & Process Management Analyst**
Deloitte Consulting, India

Publications

Velagapudi S, Yalcinkaya M, Piemontese A, Meier R, Nørrelykke SF, Perisa D, Rzepiela A, Stebler M, Stoma S, Zanoni P, Rohrer L, von Eckardstein A. **VEGF-A regulates cellular localization of SR-BI as well as transendothelial transport of HDL but not LDL.** Arterioscler Thromb Vasc Biol. 2017 May;37(5):794-803.

Lautenbach N, Müntener M, Zanoni P, Saleh L, Saba K, Umbehr M, **Velagapudi S**, Hof D, Sulser T, Wild PJ, von Eckardstein A, Poyet C. **Prevalence and causes of abnormal PSA recovery.** Clin Chem Lab Med. 2017 Aug.

Sutter I, **Velagapudi S**, Othman A, Riwanto M, Manz J, Rohrer L, Rentsch K, Hornemann T, Landmesser U, von Eckardstein A. **Plasmalogens of high-density lipoproteins (HDL) are associated with coronary artery disease and anti-apoptotic activity of HDL.** Atherosclerosis. 2015 Aug; 241(2):539-46.

Yepuri G, **Velagapudi S*,** Xiong Y, Rajapakse AG, Montani JP, Ming XF, Yang Z. **Positive crosstalk between arginase-II and S6K1 in vascular endothelial inflammation and aging.** Aging Cell. 2012 Dec;11(6):1005-16. (*Equal Contribution)

Srividya Velagapudi, Peter Schraml, Mustafa Yalcinkaya, Lucia Rohrer, Holger Moch, and Arnold von Eckardstein. **Cytoplasmic accumulation of lipoproteins is induced by VHL/HIF pathway activation in clear-cell renal cell carcinoma.** (In preparation)

Conference Presentations

58th International Conference on Bioscience of Lipids, Zurich, 2017 – 'Sphingosine-1-phosphate and its receptors S1P1 and S1P3 regulate the transendothelial transport of HDL and LDL antagonistically'

40th European Lipoprotein Club, Tutzing, 2017 – 'Sphingosine-1-phosphate and its receptors S1P1 and S1P3 regulate the transendothelial transport of HDL and LDL antagonistically'

85th European Atherosclerosis Society Congress, Prague, 2017 – 'VEGF-A regulates subcellular localization of scavenger receptor bi and transcytosis of high-density lipoproteins but not low-density lipoproteins in aortic endothelial cells'

39th European Lipoprotein Club, 2016 - 'A High-throughput screening of kinase inhibitors identifies a regulatory role of VEGF signalling for transendothelial transport of HDL'

84th European Atherosclerosis Society Congress, 2016 - 'A High-throughput screening of kinase inhibitors identifies a regulatory role of VEGF signalling for transendothelial transport of HDL'

Annual meeting of Swiss physiological society, 2011 – 'Arginase-II increases vascular endothelial adhesion molecule expression through eNOS-uncoupling in senescent endothelial cells'